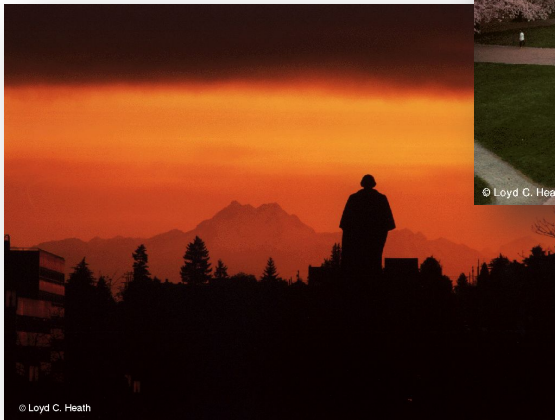




Northwest 2023 BIOMECHANICS Symposium

May 19-20, 2023
University of Washington
Seattle, WA

W
UNIVERSITY *of*
WASHINGTON



**An American Society of Biomechanics
Regional Meeting**

 **ASB** American Society
of Biomechanics
FOUNDED IN 1977



Northwest 2023 BIOMECHANICS Symposium

GOLD SPONSORS

CLIMB

Center for Limb Loss and MoBility

W

COLLEGE OF ENGINEERING
UNIVERSITY of WASHINGTON

ASB American Society
of Biomechanics
FOUNDED IN 1977

W

MECHANICAL ENGINEERING
UNIVERSITY of WASHINGTON

SILVER SPONSORS

DELSYS

THEIA
Markerless

Waters™ | **TA**
Instruments



BERTEC

Tekscan

ProtoKinetics
The **New** Standard in Gait Analysis

XSENSOR

BRONZE SPONSORS

novel 


KISTLER

AMTI
FORCE AND MOTION

**Advanced
SOLUTIONS**
LIFE SCIENCES

Student Presentation Awards Sponsored By:

 **mea
forensic**



Northwest 2023 BIOMECHANICS Symposium

Symposium Program

Friday, May 19, 2023: Alder Commons

1:00 - 1:30 pm	Registration
1:30 - 1:45 pm	Welcoming Remarks
1:45 - 3:00 pm	Podium Session: Human Development and Aging
3:00– 3:30 pm	Round-table Discussion (refreshments)
3:30 – 4:45 pm	Podium Session: Posture, Balance, and Falls
4:45 – 5:45 pm	Poster Session A
<i>Sponsored by the Mechanical Engineering Department of the University of Washington</i>	
6:30 – 9:00 pm	Dinner & Games (Husky Union Building (HUB))

Saturday, May 20, 2023: Alder Commons

8:00 – 8:30 am	Continental Breakfast
8:30 – 10:00 am	Podium Session: Running
10:00 – 11:00 am	Poster Session B
<i>Sponsored by the College on Engineering at the University of Washington</i>	
11:00 – 12:00 pm	ASB Keynote Address – David Nuckley
<i>Sponsored by the American Society of Biomechanics</i>	
12:00 – 1:15 pm	Lunch
1:15 – 2:30 pm	Podium Session: Sports and Performance
2:30 – 3:00 pm	Round-table Discussion (refreshments)
3:00 – 4:00 pm	Podium Session: Gait
4:00 – 4:15 pm	Awards and Closing Remarks

NWBS Keynote Address

David Nuckley

"Spine Biomechanics Research at the Intersection of Academe and Industry"



David Nuckley received his Bachelor's degree in Bioengineering from Syracuse University (1995) and his Ph.D. in Bioengineering from the University of Washington (2002). Dr. Nuckley was on faculty at the University of Washington (Research Assistant Professor 2002-2007) and the University of Minnesota (Assistant Professor 2008-2013) before moving to work in Industry for Zimmer (2013-2016) and now Stryker's Spine Division (2016-present). Dr. Nuckley's research focuses on the basic and clinically applied biomechanics of the spine. His research spans developmental through aging changes to the spine and includes experiments utilizing benchtop models, cadavers, human subjects, and computational simulations. He has performed NIH, CDC, and NHTSA funded research and has been part of the development of 4 spine medical device systems for the treatment of spinal disorders. David currently serves on the ORS Spine Section board and the ASTM Spine Committee, driving research within Industry.

Session Sponsor: American Society of Biomechanics

ASB 2023 Annual Meeting

August 8 – 11, 2023 • Knoxville, Tennessee

<https://asbweb.org/asb-2023/>



Podium Session 1: Human Development and Aging

Friday, May 19
1:45 - 3:00 pm

Moderators: Erin Mannen and JJ Hannigan

THE EFFECTS OF WEAKNESS, CONTRACTURE, AND ALTERED CONTROL ON WALKING ENERGETICS DURING CROUCH GAIT

Elijah C. Kuska and Katherine M. Steele

EFFECTS OF SPINAL STIMULATION AND INTERVAL TREADMILL TRAINING ON MOTOR CONTROL IN CHILDREN WITH CEREBRAL PALSY

Victoria M. Landrum, Charlotte D. Caskey, Siddhi Shrivastav, Kristie Bjornson, Chet T. Moritz, Katherine M. Steele

BONE DENSITY CHANGES ASSOCIATED WITH LUMBAR SPONDYLOLISTHESIS

Brandon Khoo, Celeste Tavoraro, Scott Telfer

QUANTIFYING TODDLER EXPLORATION WITH POWERED MOBILITY IN SEATED AND STANDING POSTURES

Zaino NL, Ingraham KA, Hoffman ME, Feldner HA, Steele KM

MECHANICAL ENVIRONMENT AFFECTS MUSCLE UTILIZATION DURING INFANT ROLLING

Danielle N. Siegel, Safeer F. Siddicky, Wyatt D. Davis, and Erin M. Mannen

THE EFFECTS OF WEAKNESS, CONTRACTURE, AND ALTERED CONTROL ON WALKING ENERGETICS DURING CROUCH GAIT

Elijah C. Kuska¹, Katherine M. Steele¹

¹Department of Mechanical Engineering, University of Washington, Seattle, WA
email: kuskael@uw.edu

INTRODUCTION

Cerebral palsy is the result of a neurologic injury at or near the time of birth that results in altered motor control. Individuals with CP often develop secondary, musculoskeletal impairments like weakness and contracture. Interactions between neuromuscular impairments impart complex restrictions on gait which are difficult to understand experimentally, limiting treatment efficacy. For example, individuals with CP consume on average 2x the energy of their non-disabled peers when walking; however, we remain unable to improve energy consumption [1]. Furthermore, CP is a heterogenous populations which further limits our understanding of factors that impact energy and treatment efficacy.

Machine learning (ML) enables parsing of complex interactions within heterogenous populations, but requires Big Data. Musculoskeletal modelling and simulation offer a non-resource intensive way to rapidly evaluate hypothetical relationships and generate synthetic data which can be used to inform ML algorithms [2]. However, these methods have yet to be combined to examine energetics during gait.

The purpose of this study was to investigate the effects of neuromuscular impairments on walking energetics in CP.

METHODS

We utilized a previously developed 2D sagittal-plane musculoskeletal model and direct collocation framework [3] to generate tracking simulations of common gait patterns in CP—moderate and severe crouch—and nondisabled (ND) gait [4]. Simulations of each gait pattern were perturbed by altering control, weakness, and contracture. Altered control was simulated by reducing the number of muscle synergies controlling each leg from 8 (individual muscle control or IMC) to 5 and 3: fewer synergies reflect reduced control complexity which is associated with worse function in CP [5]. Weakness was simulated by reducing a muscle's maximum isometric force and contracture was simulated by reducing a muscle's tendon slack length; both were imposed in muscles commonly affected in CP. Altered control and weakness or contracture were simulated combinatorial and the severity of each was increased while the simulation minimized deviations from the desired gait pattern and cost of transport (CoT).

A Bayesian Additive Regression Trees (BART) model predicted resultant CoT values from simulated neuromuscular impairments and enabled us to parse the simulated impairments accumulated local effects (ALEs) on CoT [6]. Greater effects indicate impairments that were major drivers of CoT. Then, by comparing crouch to ND gait, we elicit advantages and disadvantages of walking in crouch in the presence of various neuromuscular impairments

RESULTS AND DISCUSSION

Simulations closely tracked crouch and ND kinematics and BART accurately predicted CoT for all gait patterns.

Almost all simulated neuromuscular impairments had a larger impact on CoT during ND gait than crouch gait (Figure 1), highlighting possible advantages of walking in crouch. Vasti weakness had a larger effect on CoT as crouch severity increased; likely stemming from the increased demand placed on, and the reduced capacity of, the knee extensors when walking in crouch. Thus, addressing vasti weakness in crouch may be an effective way to reduced CoT. Surprisingly, control complexity had a smaller effect on CoT relative to the other simulated neuromuscular impairments which contrasts common clinical assumptions [7].

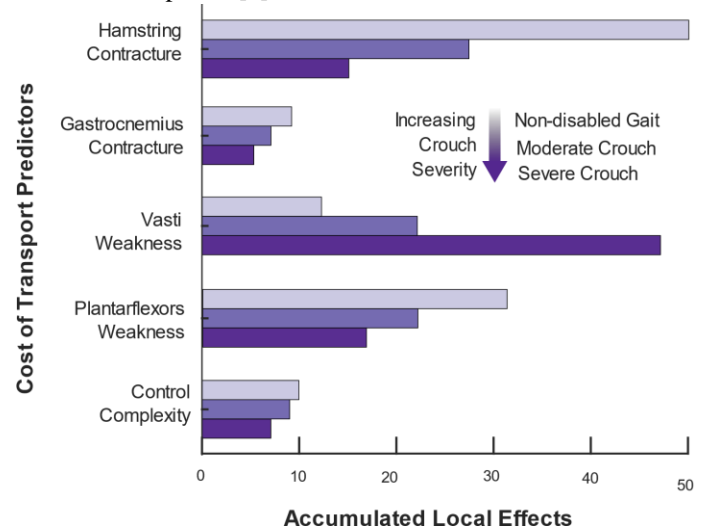


Figure 1: Accumulated local effects of neuromuscular impairments on cost of transport (CoT) during non-disabled and crouch gait.

CONCLUSIONS

By informing machine learning with synthetic data generated from modelling and simulation we probed and identified mechanisms contributing to elevated energetics during gait. We demonstrated that altered gait patterns, like crouch—typically considered inefficient—may reduce the effect of neuromuscular impairments, highlighting potential advantages of common gait patterns in CP. Similar work extended to patient-specific data could improve the efficacy of neurorehabilitation by identifying neuromuscular impairments that have large effects on CoT.

REFERENCES

1. Ries et al. (2018), *Hum. Mov. Sci.* **57**.
2. Renani et al. (2021), *Sensors* **21**.
3. Mehrabi et al. (2019), *J. Biomech* **90**.
4. Rozumalski et al. (2009), *Gait Posture* **30**.
5. Schwartz et al. (2016), *Dev Med Child Neurol* **58**.
6. Chipman et al. (2010) *Ann App Stat* **4**.
7. Gill et al. (2023), *medRxiv*.

ACKNOWLEDGEMENTS

This work was supported by NIH Award R01NS091056

EFFECTS OF SPINAL STIMULATION AND INTERVAL TREADMILL TRAINING ON MOTOR CONTROL IN CHILDREN WITH CEREBRAL PALSY

Victoria M. Landrum¹, Charlotte D. Caskey¹, Siddhi Shrivastav^{1,2}, Kristie Bjornson^{1,2}, Chet T. Moritz¹, Katherine M. Steele¹

¹University of Washington, ²Seattle Children's Research Institute, Seattle, WA USA

email: vlandrum@uw.edu

INTRODUCTION

Cerebral palsy (CP) is caused by a brain injury around the time of birth and alters motor function and muscle activation patterns. When compared to their nondisabled peers, individuals with CP often use a smaller number of muscle groups, called synergies, that are activated for cyclical tasks like walking [1, 2]. Prior research has theorized that the use of fewer muscle synergies during walking is due to a simplified motor control strategy that adversely impacts movement. The total variance accounted for by one synergy ($tVAF_1$) can be used to describe control complexity, and higher values of $tVAF_1$ indicate that fewer synergies are needed to describe muscle activity. Task-specific training, such as short-burst interval locomotor treadmill training (SBLTT), and transcutaneous spinal cord stimulation (tSCS) are potential ways to improve motor control [3]. SBLTT consists of 30-minutes of treadmill walking with alternating 30-second intervals of slow and fast speeds. Pairing these interventions together may promote natural reorganization of the central nervous system, known as neuroplasticity, and have a positive impact on coordination of limb movement [4], leading to a decrease in $tVAF_1$.

The goal of this research was to quantify the effects of SBLTT and SBLTT+tSCS on motor control. We hypothesized that $tVAF_1$ would decrease as a result of both interventions but would have a larger reduction after SBLTT+tSCS.

METHODS

The participants in this study were Participant A: 4-year-old male, Gross Motor Function Classification System (GMFCS) Level I, spastic diplegia and Participant B: 10-year-old male, GMFCS Level II with spastic diplegia. The participants received 24 sessions each of SBLTT and SBLTT+tSCS delivered using a SCONE device (SpineX Inc, Los Angeles, CA) across 8-10 weeks, with a washout period between the interventions. Motion capture (Mocap) and electromyography (EMG) data was collected using Qualisys Track Manager (Qualisys AB, Göteborg, Sweden) at 120 Hz and Delsys Trigno Sensors (Delsys, Natick, MA) at 2000 Hz. EMG sensors were placed bilaterally on the legs to record activity in the rectus femoris, vastus medialis, biceps femoris, tibialis anterior, and gastrocnemius muscles. The collected data are from barefoot overground self-selected walking pace on a 10-meter walkway.

EMG data was segmented into gait cycles collected from the Mocap data using a custom MATLAB (Mathworks, Inc., Natick MA) script and filtered through a high and low-pass filter of 20 Hz and 10 Hz, respectively, rectified, and normalized to the 95th percentile. Gait cycles with EMG recordings outside two standard deviations of each study time point average were considered outliers and not included in the analysis. Non-negative matrix factorization (NNMF) was used to quantify $tVAF_1$ [1, 2].

RESULTS AND DISCUSSION

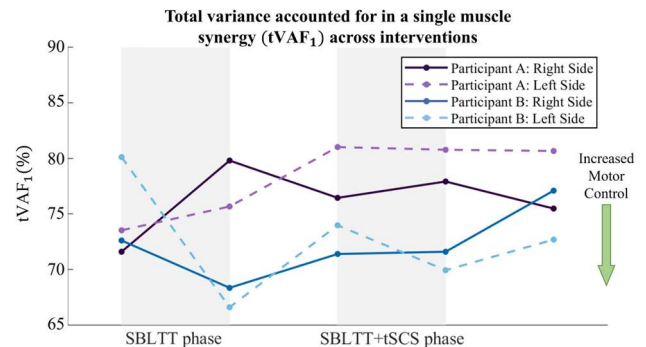


Figure 1: Both participant's $tVAF_1$ during intervention (gray) and no intervention (white) periods. Each point on the graph represents the calculated $tVAF_1$ at that time in the study.

For Participant A, SBLTT showed increases between 2-8.5% in $tVAF_1$ (Figure 1). SBLTT+tSCS resulted in an increase of 1.47% right side $tVAF_1$ and decrease of 0.24% left side $tVAF_1$ (Figure 1). For Participant B, SBLTT showed changes in both left and right $tVAF_1$, with decreases between 4-13.5% (Figure 1). SBLTT+tSCS showed a smaller amount of change in $tVAF_1$, with a decrease of 4.04% in the left side and increase of 0.20% in the right side (Figure 1). For both participants, the changes in $tVAF_1$ were larger during SBLTT, with smaller or no changes resulting from SBLTT+tSCS. The direction of these changes (i.e., a decrease or increase in $tVAF_1$) was not consistent between participants, however, the participant with a higher GMFCS level maintained or decreased $tVAF_1$ during both interventions and increased when there was no intervention.

CONCLUSION

These outcomes are indicative of individualized responses in neuromuscular control as a result of both interventions. While $tVAF_1$ can help quantify control complexity, it can also reflect competing changes in motor control and muscle tone that may explain these results. The tSCS phase also resulted in reductions in spasticity for both participants. Reductions in spasticity from other interventions have been shown [5] to increase $tVAF_1$ as spasticity can increase variability in muscle activity, reducing $tVAF_1$. Combining these analyses with changes in EMG during physical exams and other tasks will help extract how these novel interventions may influence motor control in CP.

REFERENCES

1. L. H. Ting, et al. *Cell Press* **86**, 2015.
2. K. M. Steele, et al. *Dev. Med. and Child Neuro.* **57**, 2015.
3. K. Bjornson, et al. *Pediatr. Phys. Ther.* **87**, 2007.
4. V. R. Edgerton, et al. *Front Neurosci.* **15**, 2021.
5. B. R. Shuman, et al. *Neuroeng. Rehabil.* **16**, 2019.

ACKNOWLEDGEMENTS

SCH CP Research Pilot Study Fund 2020 Award

BONE DENSITY CHANGES ASSOCIATED WITH LUMBAR SPONDYLOLISTHESIS

Khoo, B¹, Tavalaro C¹ and Telfer, S^{1,2,3}

Departments of ¹Orthopaedics and Sports Medicine, and ²Mechanical Engineering, University of Washington

³RR&D Center of Excellence, Department of Veterans Affairs, Seattle, WA USA

email: telfers@uw.edu

INTRODUCTION

Degenerative spondylolisthesis is a common spinal pathology with prevalence reaching 25%–43% in women and 19%–31% in men over 65 years [1]. Most often presenting as an anterior displacement of one of the lumbar vertebrae, this condition can cause significant pain and may require surgery to reduce nerve compression and, if there is instability, spinal fusion to prevent further damage.

Clinical measurements of bone density, such as DEXA scores, have been found to be poor predictors of the local bone quality variability seen within the bones of the spine, and thus are of limited utility for surgical planning of deformity correction and fracture repair in these bones. Recently however, researchers have found that measurements derived from standard clinical computed tomography (CT) scans, taken as part of normal patient care, can provide detailed information on bone quality across the anatomy. This is referred to as opportunistic quantitative CT (QCT) and has been suggested to be a rapid and effective screening tool to identify those at risk of fragility fractures. Providing this type of detailed local bone quality information for the lumbar spine in cases of spondylolisthesis could assist spine surgeons in optimizing the design of the repair procedure by identifying areas of relatively high and low bone density.

In this study, we hypothesized that anterolisthesis, Cobb angle, age, and sex would be associated with regional cortical bone density.

METHODS

Spinal CT scans from 50 adult patients with spondylolisthesis along with relevant details from medical records were obtained, as well as matched controls with no spinal deformity. L4 and L5 vertebrae were segmented from the CT data and 3D models produced. A set of 16 anatomical landmarks were identified on each bone model by two operators and their positions averaged. Based on a single, randomly chosen template bone, these landmarks were then used to generate a total of 5,000 anatomically matched points on each surface model for cortical bone analysis. This process is described in more detail elsewhere [2]. Equivalent density values were obtained and mapped to the model voxels using a detailed set of asynchronous calibration measurements.

A linear regression model was produced for each point defined on the vertebrae ($\alpha = 0.05$, adjusted for false discovery rate). Density was modeled as the dependent variable. Anterolisthesis, L4-L5 Cobb angle, age and sex were modeled as independent variables. To visualize changes in the cortical bone, the predicted density values for each point on the surface were mapped to a color scale (Figure 1A) and these color values applied to the surface model.

RESULTS AND DISCUSSION

Changes in cortical bone density with age for males and females are shown in Figure 1. Across the entirety of the L4 and L5 vertebrae, the mean loss of BMD was found to be 4.1 mg/cc per year (SD 1.4 mg/cc) for females vs 3.2 mg/cc per year (SD 1.1 mg/cc) for males, with several areas showing several times greater rates of BMD loss per year. Several regions also showed significant sex-related changes in BMD.

No systematic effects on bone density were found for Cobb angle or amount of anterolisthesis, however several distinct regions within the bones were significantly affected (Figure 1C). This demonstrates the utility of our approach and allows us to better understand the effects these deformities have on regional bone density.

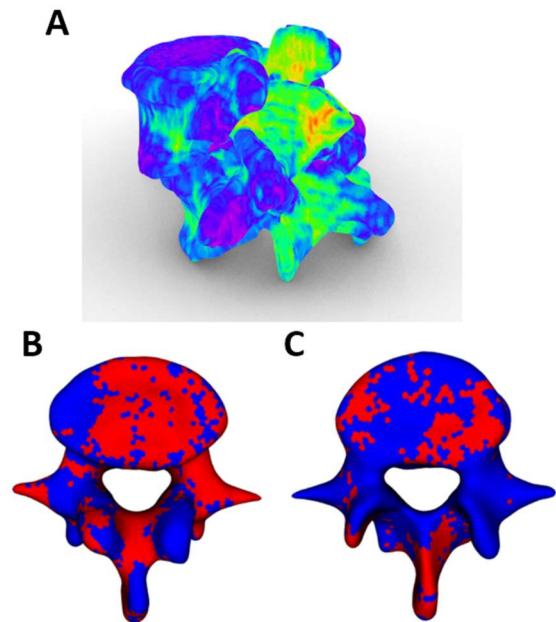


Figure 1: A) L4 and L5 with density mapped to colors (blue lower, red higher); B) areas significantly affected by age highlighted in red; C) areas significantly affected by amount of anterolisthesis highlighted in red

CONCLUSIONS

Regional changes in bone density were found to be associated with both anatomical and demographic variables. Spinal procedures used to treat spondylolisthesis may take advantage of patient-specific BMD mapping from opportunistic QCT may contribute to the development of new fracture fixation techniques as well as provide improved outcomes.

REFERENCES

1. Wang et al. *J Orthop Translat* **11**, 39-52, 2017.
2. Telfer et al. *J Orthop Res* **39**, 485-92.

QUANTIFYING TODDLER EXPLORATION WITH POWERED MOBILITY IN SEATED AND STANDING POSTURES

Zaino, NL^{1,4}, Ingraham, KA^{2,4}, Hoffman, ME^{1,4}, Feldner HA^{3,4}, and Steele, KM^{1,4}

Departments of ¹Mechanical Engineering, ²Electrical and Computer Engineering, and ³Rehabilitation Medicine, ⁴Center for Research and Education on Accessible Technology and Experiences, University of Washington, Seattle, WA USA

email: nzaino@uw.edu, web: <https://steelelab.me.uw.edu/>

INTRODUCTION

For many toddlers with mobility disabilities, access to developmentally appropriate mobility technology is crucial to facilitate self-initiated movement, exploration, and social engagement. Delayed early mobility can initiate a cascade of effects across multiple developmental domains [1]. The Permobil Explorer Mini (EM) is the first FDA-cleared pediatric mobility device specifically designed for children 12-36 months old [2].

METHODS

Six children (Table 1) and their parent(s) participated in 4 visits where they drove the EM in an enriched play environment in two postures. The joystick-controlled device has a 360° turn radius and has five speeds. The EM saddle seat and tray height were changed so the knees were bent at a 90-degree angle in a seated posture and when in the standing posture, the knees were straightened, and the feet were more under the hips. Each visit consisted of two 15-minute play sessions. We developed a custom sensor-suite that integrates with the EM and included joystick tracking, wheel encoders to accurately calculate distance traveled, and four compact compression load cells to measure loading from the child's legs on the footplate.

Table 1: Participant Characteristics

	Age (mo)	Sex	Weight (kg)	Disability type	Mobility at study entry
P01	14	M	9.9	Neurological	Sitting
P02	16	M	10.1	Orthopedic	Cruising
P03	21	M	8.7	Neurological	Sitting
P04	24	F	9.9	Neurological	Walking
P05	28	M	10.7	Cerebral palsy	Rolling
P06	18	F	11.3	Cerebral palsy	Rolling

RESULTS AND DISCUSSION

Across all play sessions, the participants traveled between 2.4 and 190.0 meters (range) and activated the joystick an average of 658 time (range: 103-1305). The average time of each joystick activation was 0.7 seconds and 93% of activations were short bursts of less than 1 second. The longest joystick activations were between 36 and 266 seconds, often correlating to spinning or continuously driving. Primary joystick activation direction was different for each participant. For P03 (28%), P05 (37%), and P06 (29%) the most common direction was backward, while P01 (57%), P02 (30%), and P04 (30%) primarily drove forward. This preference in direction may relate to motor control and which motion was easiest to control the joystick instead of a preference in driving direction.

On average, participants drove shorter distances in the standing posture (1.96 m per minute) than in the seated posture (2.14 m per minute) (Figure 1). However, the average number of driving

bouts in standing was 187% greater compared to the seated sessions. The average maximum loading through the base of the device was 52.3% and 48.3% of bodyweight for seated and standing sessions, respectively.

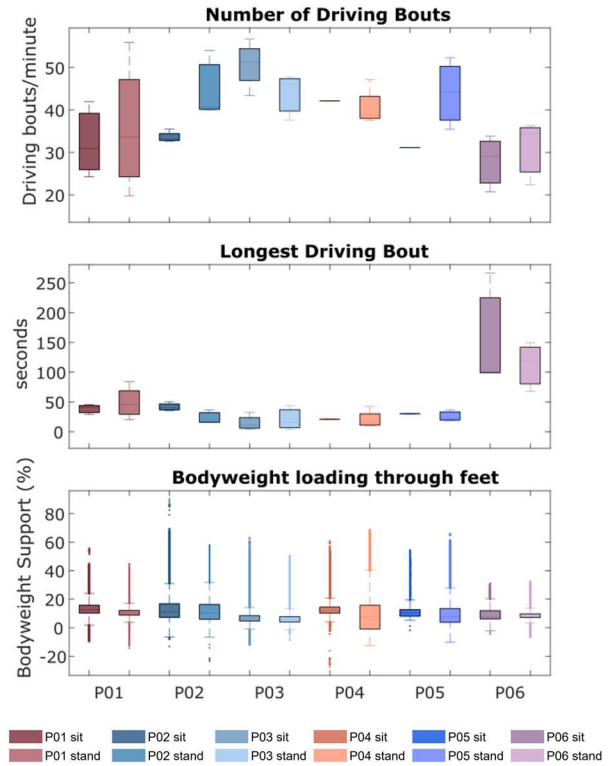


Figure 1: Navigation and bodyweight support differences in seated and standing posture.

CONCLUSIONS

We successfully quantified toddler exploration in both seated and standing postures while using the EM by investigating how they learn to activate the joystick and navigate through space in multiple play sessions. Participants supported a similar percentage of their bodyweight in both seated and standing postures likely due to the design and positioning in the postures. This finding suggests that children continued to put a large proportion of the bodyweight through the saddle seat in both postures. Quantifying how children learn to engage with their environment with powered mobility will help inform the future design and control of these devices to support play and development.

REFERENCES

1. Feldner H, et al. *Disabil Rehabil Assist Technol* **11**, 89-102, 2006.
2. Plummer T, et al. *Phys Occup Ther Pediatr* **41**, 192-208, 2021.

MECHANICAL ENVIRONMENT AFFECTS MUSCLE UTILIZATION DURING INFANT ROLLING

Danielle N. Siegel¹, Safeer F. Siddicky^{1,2}, Wyatt D. Davis¹, and Erin M. Mannen¹

¹Biomedical Engineering Doctoral Program, Boise State University, Boise, ID ²University of Texas at Austin, Austin, TX
email: daniellesiegel@u.boisestate.edu

INTRODUCTION

Rolling is a key motor skill and an important developmental milestone for infants. To achieve a roll, infants must use whole-body, goal-oriented movements that take them from a supine to prone position [1]. Previous research has found that musculoskeletal and motor development of infants is largely affected by their experience, including their environment [2]. In addition, research studying infants lying prone and supine found that muscle activity is significantly different at inclines compared to the flat surface [3]. With infants spending a considerable amount of time in inclined environments, it is important to understand how an infant's muscle utilization and thus motor development and milestone achievements are affected by an incline. Therefore, the purpose of this study is to characterize the muscle activation of infant rolling in different mechanical environments.

METHODS

Twenty-nine healthy infants (6.7±0.6 months, 13F) participated in this IRB-approved study. The infants first laid supine on a flat playmat and then in four different device configurations, in a random order, for 5 minutes or until a complete supine to prone roll was achieved. The four device configurations, designed to represent common commercial infant products, had seatback angles of 0°, 10°, 18°, or 28°. The 0° configuration had a base angle of 0°, while the other three configurations had a base angle of 15° (Figure 2A). Surface electromyography (EMG) electrodes (Delsys, 2000Hz) recorded muscle activity from the erector spinae (ES), hamstrings (HAM), abdominal muscles (AB), and quadriceps (QUAD) as shown in Figure 1A.

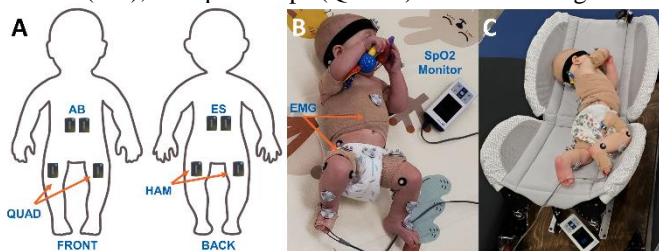


Figure 1: (A) EMG Placement, (B) experimental setup on flat surface, and (C) infant rolling in 18° seatback configuration.

The EMG signals were filtered [3] and normalized to a 5-second resting period for each rolling movement, defined as the supine to lateral rotation of the torso. This data was represented as a percentage of each rolling movement completed and categorized by muscle group and the testing condition. The mean EMG value for each muscle group was calculated at each time point throughout the rolling movement for each condition. The mean magnitudes were then normalized to the maximum mean value on the flat surface for each muscle group. Each rolling movement was divided into three sections beginning (0-24% of the rolling movement complete), middle (25-74%), and end (75-100%). The mean muscle activation was taken for each muscle group for each section, and for the entirety of the roll. A repeated-measures ANOVA (Tukey post-hoc test) determined

statistical differences between mean muscle activation and mechanical environment at different sections of the rolling movements (SPSS Inc., v.26).

RESULTS AND DISCUSSION

A total of 234 rolling movements were observed throughout this study. For the 10°, 18°, and 28° seatback configurations, the ES were found to have significantly higher activation and the AB significantly lower activation over the entire rolling movement when compared to the flat surface (Figure 2B,D-F). A previous study found that during prone lying on different inclined surfaces the converse occurred, confirming our results since the AB and ES muscles are antagonist pairs [3]. For the 0° configuration, there was significantly higher HAM and QUAD muscle activation compared to the flat surface over the entire rolling movement (Figure 2B,C). This indicates that infants interact with the device to achieve a roll.

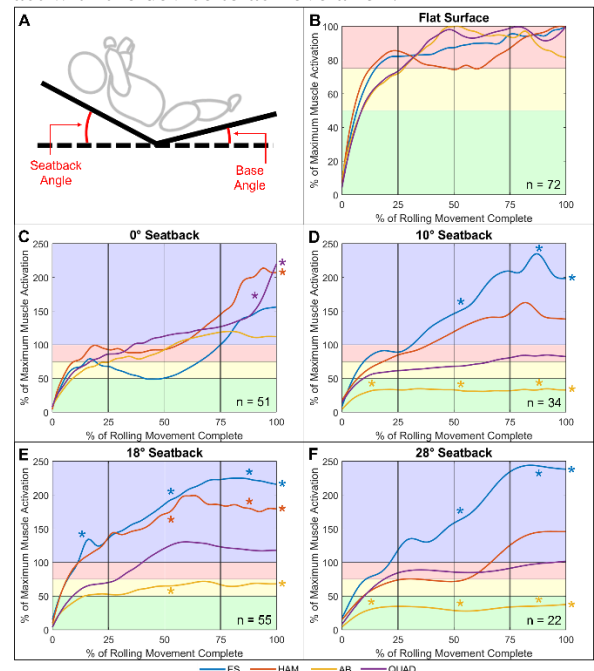


Figure 2: (A) Diagram of device and (B-F) muscle activation patterns for each condition where an asterisk (*) represents a significant difference ($p<0.05$) compared to the flat surface.

CONCLUSIONS

Our results indicate that infants utilize different coordinated muscle activation patterns to achieve a roll, based on the mechanical environment. This information could be used to inform the juvenile products industry.

ACKNOWLEDGEMENTS

We thank Iron Mountains LLC for their support of our study.

REFERENCES

- [1] Richter RR, et al. *Phys Ther*, 1989. [2] Hadders-Algra M. *Neuro & Bio Rev*, 2018. [3] Wang J, et al. *J Biomech*, 2021.

Podium Session 2: Posture, Balance, and Falls

Friday, May 19
3:30 - 4:45 pm

Moderators: Kat Steele and Peter Crompton

DEVELOPMENT OF AN AUTOMATED FRAMEWORK FOR A TINYML-BASED FALL DETECTION SYSTEM

Mojtaba Mohasel, Lindsey Molina, Shane R. Wurdeman, Richard R. Neptune, Corey A. Pew

WHEELED WALKER USERS FALL SIDEWAYS AND BACKWARDS DURING TURNS AND TRANSFERS

Kimberly Nickerson, Kailey Diaz, Brittney Muir

DIFFERENT NEUROCOGNITIVE CONTROLS MODULATE OBSTACLE AVOIDANCE THROUGH PREGNANCY

Pegah Jamali, Kameron M. Kinkade, Asher Ericson, Ben Tyler, Shikha Prashad, Robert D. Catena

INVESTIGATING THE RELATIONSHIP BETWEEN LEG STRENGTH, MOBILITY, AND CENTER OF PRESSURE BALANCE IN OLDER ADULTS

Maya Holmen, Filip Fullerton, Katie Butte, Dale Cannavan

A BIOMECHANICAL CASE STUDY: NON-LINEAR RESPONSE OF THE PELVIS DURING A SIDEWAYS FALL IMPACT

E. Bliven, A. Fung, A. Baker, B. Helgason, P. Guy, P. Crompton

Development of an Automated Framework for a TinyML-Based Fall Detection System

Mojtaba Mohasel¹, Lindsey Molina², Shane R. Wurdeman³, Richard R. Neptune², Corey A. Pew¹

¹Department of Mechanical and Industrial Engineering, Montana State University, Bozeman, MT

²Walker Department of Mechanical Engineering, The University of Texas at Austin, Austin, TX

³Clinical and Scientific Affairs, Hanger Clinic, Austin, TX

Email: *Corey.Pew@montana.edu

Introduction

Falls pose a significant risk of injury and even mortality for individuals with lower limb amputations [1]. Although fall detection devices can objectively track fall incidence, they often have limited memory and low power. Therefore, many previous studies have relied on simple machine learning (ML) algorithms, which can suffer from high false alarms and low detection rates [2]. In contrast, deep learning (DL) models have the potential to reduce false alarms by automatically learning features from input data using neural networks. However, designing a TinyML [3] model architecture (i.e., to be run on low-power, small footprint devices) that achieves a high detection rate relies on multiple interdependent variables, making manual configuration challenging. This study aims to automate both ML and DL workflows and optimize their performance, thereby enabling the development of an efficient TinyML system.

Methods

Data was collected from 35 individuals, 30 intact controls (model training) and 5 lower limb amputees (model testing). Two inertial measurement unit sensors [4] placed on the anterior of each shank measured acceleration and angular velocity in the x, y, and z directions. Participants navigated a laboratory course that involved a range of activities of daily living (ADL) and controlled falling movements.

Data was highly imbalanced, with 98.3% ADL versus 1.7% falls, requiring appropriate methods and metric (F-score) for training and model comparison. RUSBoost [5] and Easy Ensemble [6] are designed for imbalanced data and represent ML models. For DL, a one-dimensional Convolutional Neural Network (CNN) has shown high accuracy on time series data [2]. CNNs extract features from input data with convolutional layers, allowing parallel processing and faster inference time compared to similar deep models. The final model was designed to be implemented on an ESP32 processor with onboard memory of 512 KB. Automation utilized a weighted sum approach [7] with F-beta score and the number of inference operations as objectives, and memory capacity as a constraint. ML classifier data was segmented into windows of 15 consecutive samples based on hardware restrictions. Optimal performance of models considered several hyperparameters including the number of estimators, maximum depth of trees, minimum sample leaves, minimum number of samples required to split a node, the cost-complexity parameter (ccp_alpha), sampling strategy, and window size. A Bayesian optimization method [8] and 10-fold cross-validation techniques were employed to tune the hyperparameters and determine the optimal combination that yielded the highest F-beta score while minimizing the number of inference operations.

CNN data was segmented into fixed windows of 100 consecutive samples, representing the duration of a fall or ADL. A weighting method by percent of sample count was utilized to handle the class imbalance [9]. Hyperparameters including the number of convolutional, pooling, and dropout layers, as well as their order, filter size, number of fully connected layers, and number of neurons were fine-tuned using Bayesian

optimization. The developed neural architecture search approach simultaneously scales all dimensions of the network (width, depth, and resolution) and constructs architectures that use memory below 512 KB.

Results and Discussion

Table 1: Comparison of developed models. Best performance bolded.

Model	RUSboost		EasyEnsemble		CNN	
Class	Fall	ADL	Fall	ADL	Fall	ADL
Recall	91%	79%	81%	93%	97%	98%
Precision	6%	100%	15%	100%	43%	100%
F-score	87%		95%		98%	
Run-time	18 KB		27KB		228 KB	

The CNN model outperformed in all metrics except run time size (Table 1). The RUSboost model ranked second in fall detection with a 91% recall, but with a high false alarms rate (6% precision). The EasyEnsemble model lowered the false alarm rate but at the expense of misclassifying fall incidence (81% recall). The success of the CNN model can be attributed to three factors: 1) CNN employs time domain features to distinguish between falls and ADLs, whereas the raw data was directly used in the other models as generating features for traditional ML models was not feasible in real time due to the hardware constraint of our ESP32, 2) availability of 7 million samples for training favors deep models more, and 3) the weighting method utilized for CNN is effective for high imbalance ratios.

Conclusion

This study presents a novel automated framework that uses multi-objective optimization to train ML and DL models. It facilitates the deployment of these models on hardware with limited resources, which is ideal for settings where resources are constrained. The framework also addresses the persistent challenge of class imbalance in fall detection studies.

Prior research [2] developed a CNN architecture for TinyML, achieving a 96% recall rate without class imbalance, indicating our present work meets or exceeds previous methods. Building upon this work, the proposed automated framework can export TinyML with high detection rates without requiring tedious manual model tuning. Our CNN model can provide clinicians with accurate and objective information about patient falls, enabling them to develop appropriate interventions and prosthetic prescriptions to improve patient care and safety.

Acknowledgements

Funding provided by OPORP Grant W81XWH-20-1-0164. The authors thank Bryce Billings from Hanger Clinic for feedback on this work.

References

- 1) Miller et al., Arch. Phys. Med. Rehab. 82(2001).
- 2) Salah et al, Int. J. Elect. Comp. Eng. 12, no. 4(2022).
- 3) Warden p et al, O'Reilly media 2016
- 4) Choi, A et al, IEEE TNSRE 30 (2022)
- 5) Seiffert et al, IEEE T-Systems, 1(2009)
- 6) Liu et al, IEEE IBSIC, (2009)
- 7) Kim et al, SMO, 29 (2005)
- 8) Wu et al, J. Electron. Sci. Technol.17 (1) 2019
- 9) King et al., Political Analysis 9 (2) 2001.

WHEELED WALKER USERS FALL SIDEWAYS AND BACKWARDS DURING TURNS AND TRANSFERS

Nickerson, KA^{1,2}, Diaz, K^{1,2}, Muir, BC^{1,2}

¹RR&D Center for Limb Loss and MoBility (CLiMB), Department of Veterans Affairs, Seattle, WA

²Department of Mechanical Engineering, University of Washington, Seattle, WA

email: kanick@uw.edu, web: <https://www.amputation.research.va.gov/>

INTRODUCTION

In individuals over the age of 65, falls are the leading cause of fatal and nonfatal injuries with 30% of this population falling each year [1][2]. Walkers are common mobility aids prescribed to reduce fall risk, however, the role of walkers in risk reduction is limited as walker users and non-users alike experience similar fall incidence rates [3]. Improvement to clinical user device training is often suggested as a method to reduce falls with walkers. However, modified training regimens may not be applicable to many walker users who self-obtain the devices commercially or receive them from family, friends, or long-term care facility staff rather than from medical professionals who provide user training [4]. The limited access to device training suggests that fall mitigation efforts should address device deficiencies in addition to training deficiencies. Walker deficits remain largely unknown, therefore the purpose of this study was to identify the common circumstances of falls in older adult walker users and the associated deficits in walker designs.

METHODS

41 videos from a public data set capturing real-life falls of walker users in two retirement facilities were reviewed independently by two researchers [5]. For each video, the circumstances leading up to the fall were evaluated. Qualitative codes were established to describe three fall mechanism categories: walker type (two-wheeled walker or rollator), fall direction (forward, backward, or sideways), and activity at the time of the fall (forward walking, turning, standing, transferring from standing to sitting on the walker's seat or stationary chair, transferring from sitting on the walker's seat to standing, transferring to an upright position after bending over, collapsing the walker's seat, misuse of walker or walker not used). The researchers coded each video separately, compared codes, and then came to a consensus through discussion and video review following any discrepancies. Falls with the activity at the time of fall coded as "misuse of walker" (n=5) or "walker not used" (n=2) were excluded from further analysis. For the remaining 34 falls, a frequency analysis was performed to assess the frequency of falls associated with each combination of walker type, fall direction, and activity at the time of fall. Combinations with high-frequency rates were identified as common fall scenarios.

RESULTS AND DISCUSSION

Of falls that occurred during two-wheeled walker use (n=7), users mostly fell sideways while turning (Table 1). Turning with a two-wheeled walker is often reported as a difficult maneuver [6]. Due to the fixed nature of the front wheels, users frequently pick up the walker to complete a turn, reducing their base of support and lateral stability. Since turning may be necessary for the safe navigation of many environments, improvement to the turning functionalities of two-wheeled walkers is needed to mitigate sideways falls.

Table 1: Percentages of falls involving two-wheeled walkers by activity and fall direction

Activity	Fall Direction			Total
	Forwards	Backwards	Sideways	
Turning	0	0	43	43
Walking	14	0	0	14
Standing	0	14	0	14
Transferring	0	29	0	29
Collapsing seat	0	0	0	0
Total	14	43	43	100

Of falls that occurred during rollator use (n=27), users primarily fell backwards during transfer activities (Table 2). The percentage of backward falls was 16 % higher in rollator users than in two-wheeled walker users, while the percentage of sideways falls was 17% lower for rollator users. Compared to two-wheeled walkers, the implementation of two fixed back wheels and rotatable front wheels in rollators may improve mediolateral maneuverability but at a cost to anteroposterior stability. Backward falls with rollators were often a result of individuals neglecting to lock the wheels while transferring. These findings emphasize the need for a more accessible, easily controlled braking mechanism. The challenges users may face in engaging rollator brakes should be further investigated.

Table 2: Percentages of falls involving rollators by activity and fall direction

Activity	Fall Direction			Total
	Forwards	Backwards	Sideways	
Turning	0	11	15	26
Walking	7	0	7	15
Standing	7	0	4	11
Transferring	0	44	0	44
Collapsing seat	0	4	0	4
Total	15	59	26	100

CONCLUSIONS

The use of two-wheeled walkers and rollators do not completely mitigate fall risk in older adults. The poor maneuverability, lateral stability, and braking mechanisms of these devices contributed to falls in our study. These results may be used to inform the design of an improved walker that specifically addresses current walker deficiencies, ultimately reducing the number of falls that occur while using wheeled walkers.

REFERENCES

1. Bergen et al. (2016), *MMWR Morb Mortal Wkly Rep* **63**(37).
2. Hartholt et al. (2011), *J Trauma – Inj, Inf, Crit Care* **71**(3).
3. Gell et al. (2015), *J Am Ger Soc* **63**(5).
4. Sloot and Komisar (2022), *Gait & Posture* **97**.
5. Robinovitch et al. Databrary (2018).
6. Lindemann et al. (2016), *Aging Clin & Exp Res* **28**(2).

DIFFERENT NEUROCOGNITIVE CONTROLS MODULATE OBSTACLE AVOIDANCE THROUGH PREGNANCY

Pegah Jamali, Kameron M. Kinkade, Asher Ericson, Ben Tyler, Shikha Prashad, Robert D. Catena

Gait and Posture Biomechanics Lab, Washington State University, Pullman WA USA

email: Pegah.Jamali@wsu.edu web: <https://labs.wsu.edu/biomechanics/>

Introduction

Understanding why 25% of pregnant women fall will have clinical impacts on the health of pregnant women and their fetuses. Anthropometric changes during pregnancy only partially ($r < 0.5$) account for balance deficits [1]. Attention, joint position sense, and perception of the environment are required to prevent trips and potential falls, so their change through pregnancy may explain some of the fall rate increase. The goal of this research was to understand how the changes to these neurocognitive processes affect obstacle avoidance through gestation.

Methods

Seventeen pregnant participants were tested five times in 6-week intervals, between 13 to 37 weeks of gestation. Participants walked an obstacle course (OC) at a self-selected speed (Fig. 1). The two obstacles in the middle and the bottom left were set to 10% body height and the three other obstacles were randomly set to 5%, 7.5%, and 12.5% of body height. We calculated minimum distances and crossing heights over middle obstacles for leading and trailing feet. Participants performed an attentional network test (ANT) which assessed alerting, spatial orienting, and conflict resolution components of attention. The obstacle perception (OP) task asked participants to match their foot height to the height of a 10% body height obstacle in eyes closed and open conditions. The joint position sense (JPS) task asked participants to actively match hip and knee joint angles to passively created joint angles.



Figure 1: View from the start of the obstacle course. Six obstacles spaced 3 m apart. Participants walk the right side (12 m) to the end of the walkway, come back on the left side, and repeat for 2 minutes.

Results and Discussion

In the OC task, leading and trailing foot crossing heights significantly reduced between week 13 and 31 of pregnancy ($p < 0.02$), indicating that the risk of obstacle contacts increases during this time (Fig. 2). Pregnant participants also lifted their foot to a height less than the obstacle height in the 2nd trimester ($p = 0.012$) in the OP task.

Around week 19 of pregnancy, leading foot crossing height was correlated with OP variables, ($R^2 = 0.753$, $p = 0.001$). About week 31, leading and trailing foot crossing heights were correlated with the alerting aspect of attention ($R^2 = 0.512$, $p = 0.002$ and $R^2 = 0.572$, $p < 0.001$, respectively).

Minimum leading foot distance was correlated with OP and JPS variables around week 19 of pregnancy ($R^2 = 0.455$, $p = 0.004$ and $R^2 = 0.266$, $p = 0.041$ respectively) with more dependency on OP.

However, in the early 3rd trimester, the alerting attention network became important for modulating obstacle crossing and then perception again (Fig. 3).

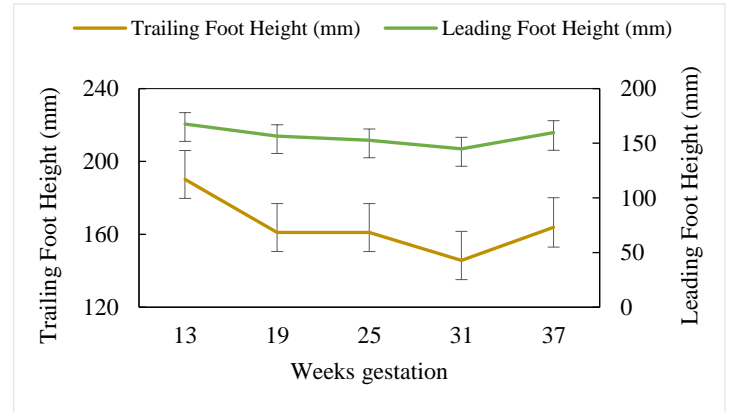


Figure 2: Leading and trailing foot crossing heights over the obstacle (0 mm represents obstacle height).

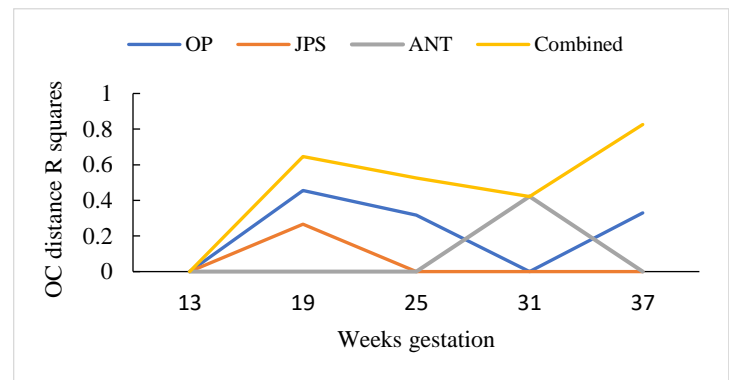


Figure 3: Correlation of each neurocognitive component (OP, JPS, ANT) and all components "Combined" with OC distance (the minimum leading foot distance from the 10% obstacles while performing OC task).

Conclusions

Increased number of falls in 2nd and 3rd trimesters of pregnancy [2] may be correlated with reduced perception of the environment, with additional contributions of joint position sense and attention at various stages. Increased reliance on attention and perception during 3rd trimester may compensate for reduced joint position sense during this time. However, since OC performance seems to degrade when attention has the largest correlation, this may indicate reliance on attention as a poorer controller for obstacle avoidance. The correlation to the combination of neurocognitive processes also increases over time, indicating a possible reliance in overall cognition to make up for greater obstacle avoidance challenge or the fear of tripping.

Acknowledgments

ASB funded this project (JFR Award)

References

1. Catena et al. (2019). J Applied Biomechanics.
2. Dunning et al. (2010). Matern Child Health J.

Investigating the Relationship Between Leg Strength, Mobility, and Center of Pressure Balance in Older Adults

Holmen, M, Fullerton, F, Butte, K & Cannavan, D

Departments of Health and Human Performance, Seattle Pacific University

email: holmenm@spu.edu and fullertonf@spu.edu web: <https://depts.washington.edu/nwbs/2023/index.htm>

INTRODUCTION

There is a current global fall crisis in older adults. Thus, discovering objective ways to measure and improve balance to decrease fall risk is crucial. Leg strength and mobility are pertinent in muscle utilization and muscle control for balance. Therefore, the primary purpose of this study was to examine the relationship between leg strength and balance in older adults. The secondary purpose was to examine the relationship between mobility and balance. With the information gathered from this study, there will be further insight into how to improve and prevent the current fall crisis for older adults.

METHODS

This cross-sectional study consisted of one data collection session for each participant lasting about 30 minutes. Participants (N = 33) were recruited via email and in-person at a community senior center and elderly apartment complex. Demographics, balance, leg strength, and mobility were measured via survey, Balance Tracking System (BTrackS), 30-second chair sit-to-stand, and 8-foot-up-and-go, respectively (1,2). The BTrackS is an innovative portable force plate measuring Center of Pressure (COP) that has been validated in older adults and produces Fall Risk Percentiles based on COP measure, gender, and age (1; Figure 1). Data were uploaded to SPSS for analyses. Independent sample t-tests were used to measure differences in leg strength and mobility between those with ≥ 75 percentile of CoP measure compared with those that were < 75 percentile.

RESULTS AND DISCUSSION

There was a statistically significant difference between the higher-performing balance group and the lower-performing balance group when comparing leg strength using the measure of the 30-second chair stand ($p < 0.045$). This difference was also clinically meaningful as those with better balance performed nearly 3 more chair stands (Table 1). Further, there was a statistically significant difference between balance groups and agility ($p < 0.039$) between the balance groups, showing those with better balance had better (faster agility). This difference was also clinically meaningful showing nearly 2 seconds faster on their 8-ft up-and-go. Thus, this study supports that those with better leg strength and agility have more stable objective COP, resulting in better balance and reduced fall risk.



Figure 1. BTrackS board for balance measure.

Table 1. Independent samples t-tests between balance categories and Means and Standard Deviations for measures

	≥ 75 ile Balance (n=18)	< 75 ile Balance (n=15)	p-value
Leg Strength (chair stand #)	15.0 (± 13)	12.5 (± 5)	0.045
Agility (8 ft up and go second)	5.84 (± 1.57)	7.60 (± 3.61)	0.039

CONCLUSIONS

This study helps fill the gaps in the literature since there have been few studies done on the correlation of balance and leg strength specifically using an affordable, effective force plate such as BTrackS (1). This research can inform future interventions to target factors such as leg strength and agility to help decrease fall risk. Further, future clinical settings may want to incorporate BTrackS regular measures to evaluate fall risk.

REFERENCES

1. Goble D. The BTrackS balance test is a valid predictor of older adult falling. *Balancing Tracking System Inc.* 2018.
2. Jones CJ, Rikli RE. Measuring functional fitness of older adults. *The of Active Aging.* 2002;24-30.

A BIOMECHANICAL CASE STUDY: NON-LINEAR RESPONSE OF THE PELVIS DURING A SIDEWAYS FALL IMPACT

Bliven, EB¹, Fung, A³, Baker, A³, Helgason, B³, Guy², and Crompton, PA¹

School of Biomedical Engineering¹ and Department of Orthopaedics², University of British Columbia, Canada

³Institute for Biomechanics, ETH Zürich, Zürich, Switzerland

email: emily.bliven@ubc.ca

INTRODUCTION

Hip fracture, in the geriatric context, is prevalent and often leads to catastrophic levels of disability. One approach towards mitigating hip fracture risk is prophylactic strengthening of the vulnerable femur with an orthopaedic augmentation. The efficacy of such augmentations has been investigated in biomechanics studies that simulate a sideways fall from standing, which is how most hip fractures occur. However, these studies lack sufficient representation of the pelvis, a critical medial boundary condition for the femur during sideways falls. Understanding the breadth of pelvic biomechanics in this loading mode is one key to designing effective augmentation approaches.

The objective of this work is to describe one complex case of cadaveric pelvis failure and deformation captured in an augmented specimen during a simulated sideways fall impact and explore the potential implications for future injury prevention approaches.

METHODS

The donated specimen in this case study was a 63-year-old female. The cadaveric femur-pelvis construct was cast in a mold of ballistic gel shaped to represent their soft tissue. The femur that was impacted was augmented with a commercially available intramedullary nail. The specimen was subjected to an inertia-driven sideways fall impact using a previously-developed inverted pendulum simulator (Figure 1) [1]. We collected impact force-time data, pelvic marker deformations (using high speed videography), and x-ray video of the impact. The biplanar x-ray system included two each of x-ray sources, image intensifiers, and high-speed cameras.

RESULTS AND DISCUSSION

Post-fall inspection of the specimen revealed damage to the pelvis at the superior pubic ramus on the impacting side, and no evidence of hip fracture. Analysis of pelvic marker deformation at the impacting pelvic brim and pubic symphysis showed large deformations initiating shortly after the peak surface impact force of 3.58 kN (Figure 1).

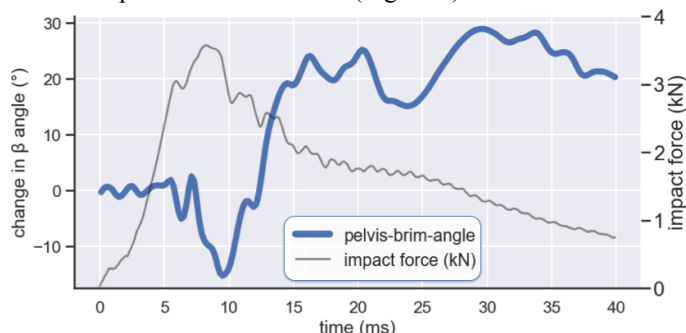


Figure 1: Impact force and change in pelvis-brim angle on the impacting side of the pelvis plotted over impact time.

Observation of the x-ray video confirmed this (Figure 2), displaying an S-shaped deformation pattern propagating along the superior pubic ramus on the impacting side throughout the fall event.

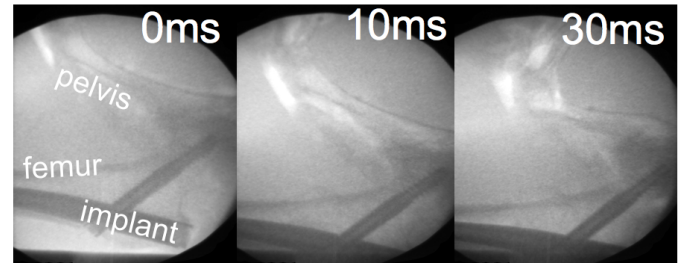


Figure 2: X-ray video frames showing pelvis deformations on the impacting side over 30ms of the impact.

The deformations and bending observed in this pelvis (8.3 mm and 37°, respectively) without displaced fracture are consistent with dynamic buckling, a force response has been previously documented in other parts of the human body like the cervical spine [2]. Our findings expand on other work characterizing the non-linearity of the pelvis under lower forces [3], highlighting the high apparent stiffness of the pelvis at high loads. This is further enhanced by offering the real-time visualization of this phenomenon as it occurs within a biofidelic soft tissue surrogate.

CONCLUSIONS

Classifying pelvic response and fracture potential is imperative when investigating prophylactic femoral augmentations. Pelvic fractures are preferred to femur fracture as a clinical outcome in falls because they are associated with far less operative morbidity and possibly mortality. However, to optimize femoral augmentation systems, any increased likelihood of pelvic fracture associated with augmenting the femur must be assessed. This case study demonstrates the high tolerance of the pelvis to extreme deformations at high rates, with the ability to sustain only a nondisplaced and relatively small fracture. Understanding the biomechanics of such injurious events is essential for advancing effective treatment and prevention strategies.

REFERENCES

1. Fleps I, et al. *PLoS ONE* **13**, e0201096, 2018.
2. Nightingale RW, et al. *SAE Technical Paper Series*, 973344, 1997.
3. Laing AC, and Robinovitch SN. *J Biomech* **43**, 1898-1904, 2010.

ACKNOWLEDGEMENTS

The authors would like to thank Jade Levine for her invaluable assistance in conducting the fall experiment.

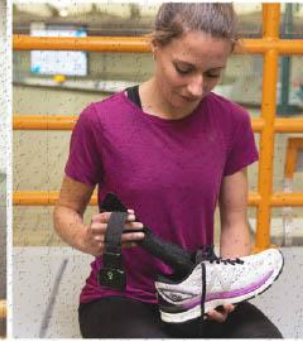
XSENSOR

Augment Research with real-time motion data captured in real-world scenarios

Our plantar pressure and gait measurement system enables lab-quality biomechanical and human performance data capture and analysis — without compromising natural motion.



***Intelligent Insoles
featured in Trail Running
Research Study***



xsensor.com

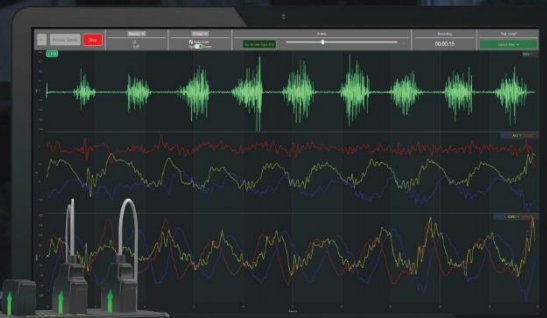
ADVANCED EMG TOOLS FOR RESEARCH APPLICATIONS



PROUD SPONSOR OF THE
**NORTHWEST BIOMECHANICS
SYMPOSIUM 2023**



 **DELSYS®**



Podium Session 3: Running

Saturday, May 20
8:30 - 10:00 am

Moderators: Calvin Kuo and Ravi Balasubramanian

ANKLE KINEMATICS OF SELF-SELECTED MAXIMAL AND TRADITIONAL SHOE RUNNERS

Traut, AG. Hannigan, JJ. Bartel, L. Burr, B. Pollard, CD.

EFFECT OF GRADED RUNNING ON LOWER EXTREMITY JOINT WORK ASYMMETRY

Rachel Robinson, Seth Donahue, Aida Chebbi, Michael Hahn

RUN MECHANICS IN INDIVIDUALS WITH RESOLVED PLANTAR FASCIITIS VERSUS NO HISTORY OF PLANTAR FASCIITIS

Lukas Krumpal, Nickolai J.P. Martonick, Joshua P. Bailey

INFLUENCE OF SHOE CUSHIONING ON SKELETAL AND MUSCULAR CONTRIBUTIONS TO LEG STIFFNESS PRE AND POST LONG HILLY RUN

Ashlyn Baird and James Becker

COMPARING PEAK ANTERIOR-POSTERIOR GROUND REACTION FORCES BETWEEN RECREATIONAL RUNNERS IN MAXIMAL AND TRADITIONAL SHOES

Lily Bartel, Andrew Traut, Bethany Burr, Christine Pollard, JJ Hannigan

A BIOMECHANICAL COMPARISON OF "SUPER" SPIKES TO A TRADITIONAL TRACK SPIKE IN COMPETITIVE LONG DISTANCE FEMALE RUNNERS

Christina Geisler and JJ Hannigan

Development of an Automated Framework for a TinyML-Based Fall Detection System

Mojtaba Mohasel¹, Lindsey Molina², Shane R. Wurdeman³, Richard R. Neptune², Corey A. Pew¹

¹Department of Mechanical and Industrial Engineering, Montana State University, Bozeman, MT

²Walker Department of Mechanical Engineering, The University of Texas at Austin, Austin, TX

³Clinical and Scientific Affairs, Hanger Clinic, Austin, TX

Email: *Corey.Pew@montana.edu

Introduction

Falls pose a significant risk of injury and even mortality for individuals with lower limb amputations [1]. Although fall detection devices can objectively track fall incidence, they often have limited memory and low power. Therefore, many previous studies have relied on simple machine learning (ML) algorithms, which can suffer from high false alarms and low detection rates [2]. In contrast, deep learning (DL) models have the potential to reduce false alarms by automatically learning features from input data using neural networks. However, designing a TinyML [3] model architecture (i.e., to be run on low-power, small footprint devices) that achieves a high detection rate relies on multiple interdependent variables, making manual configuration challenging. This study aims to automate both ML and DL workflows and optimize their performance, thereby enabling the development of an efficient TinyML system.

Methods

Data was collected from 35 individuals, 30 intact controls (model training) and 5 lower limb amputees (model testing). Two inertial measurement unit sensors [4] placed on the anterior of each shank measured acceleration and angular velocity in the x, y, and z directions. Participants navigated a laboratory course that involved a range of activities of daily living (ADL) and controlled falling movements.

Data was highly imbalanced, with 98.3% ADL versus 1.7% falls, requiring appropriate methods and metric (F-score) for training and model comparison. RUSBoost [5] and Easy Ensemble [6] are designed for imbalanced data and represent ML models. For DL, a one-dimensional Convolutional Neural Network (CNN) has shown high accuracy on time series data [2]. CNNs extract features from input data with convolutional layers, allowing parallel processing and faster inference time compared to similar deep models. The final model was designed to be implemented on an ESP32 processor with onboard memory of 512 KB. Automation utilized a weighted sum approach [7] with F-beta score and the number of inference operations as objectives, and memory capacity as a constraint. ML classifier data was segmented into windows of 15 consecutive samples based on hardware restrictions. Optimal performance of models considered several hyperparameters including the number of estimators, maximum depth of trees, minimum sample leaves, minimum number of samples required to split a node, the cost-complexity parameter (ccp_alpha), sampling strategy, and window size. A Bayesian optimization method [8] and 10-fold cross-validation techniques were employed to tune the hyperparameters and determine the optimal combination that yielded the highest F-beta score while minimizing the number of inference operations.

CNN data was segmented into fixed windows of 100 consecutive samples, representing the duration of a fall or ADL. A weighting method by percent of sample count was utilized to handle the class imbalance [9]. Hyperparameters including the number of convolutional, pooling, and dropout layers, as well as their order, filter size, number of fully connected layers, and number of neurons were fine-tuned using Bayesian

optimization. The developed neural architecture search approach simultaneously scales all dimensions of the network (width, depth, and resolution) and constructs architectures that use memory below 512 KB.

Results and Discussion

Table 1: Comparison of developed models. Best performance bolded.

Model	RUSboost		EasyEnsemble		CNN	
Class	Fall	ADL	Fall	ADL	Fall	ADL
Recall	91%	79%	81%	93%	97%	98%
Precision	6%	100%	15%	100%	43%	100%
F-score	87%		95%		98%	
Run-time	18 KB		27KB		228 KB	

The CNN model outperformed in all metrics except run time size (Table 1). The RUSboost model ranked second in fall detection with a 91% recall, but with a high false alarms rate (6% precision). The EasyEnsemble model lowered the false alarm rate but at the expense of misclassifying fall incidence (81% recall). The success of the CNN model can be attributed to three factors: 1) CNN employs time domain features to distinguish between falls and ADLs, whereas the raw data was directly used in the other models as generating features for traditional ML models was not feasible in real time due to the hardware constraint of our ESP32, 2) availability of 7 million samples for training favors deep models more, and 3) the weighting method utilized for CNN is effective for high imbalance ratios.

Conclusion

This study presents a novel automated framework that uses multi-objective optimization to train ML and DL models. It facilitates the deployment of these models on hardware with limited resources, which is ideal for settings where resources are constrained. The framework also addresses the persistent challenge of class imbalance in fall detection studies.

Prior research [2] developed a CNN architecture for TinyML, achieving a 96% recall rate without class imbalance, indicating our present work meets or exceeds previous methods. Building upon this work, the proposed automated framework can export TinyML with high detection rates without requiring tedious manual model tuning. Our CNN model can provide clinicians with accurate and objective information about patient falls, enabling them to develop appropriate interventions and prosthetic prescriptions to improve patient care and safety.

Acknowledgements

Funding provided by OPORP Grant W81XWH-20-1-0164. The authors thank Bryce Billings from Hanger Clinic for feedback on this work.

References

- 1) Miller et al., Arch. Phys. Med. Rehab. 82(2001).
- 2) Salah et al, Int. J. Elect. Comp. Eng. 12, no. 4(2022).
- 3) Warden p et al, O'Reilly media 2016
- 4) Choi, A et al, IEEE TNSRE 30 (2022)
- 5) Seiffert et al, IEEE T-Systems, 1(2009)
- 6) Liu et al, IEEE IBSIC, (2009)
- 7) Kim et al, SMO, 29 (2005)
- 8) Wu et al, J. Electron. Sci. Technol.17 (1) 2019
- 9) King et al., Political Analysis 9 (2) 2001.

WHEELED WALKER USERS FALL SIDEWAYS AND BACKWARDS DURING TURNS AND TRANSFERS

Nickerson, KA^{1,2}, Diaz, K^{1,2}, Muir, BC^{1,2}

¹RR&D Center for Limb Loss and MoBility (CLiMB), Department of Veterans Affairs, Seattle, WA

²Department of Mechanical Engineering, University of Washington, Seattle, WA

email: kanick@uw.edu, web: <https://www.amputation.research.va.gov/>

INTRODUCTION

In individuals over the age of 65, falls are the leading cause of fatal and nonfatal injuries with 30% of this population falling each year [1][2]. Walkers are common mobility aids prescribed to reduce fall risk, however, the role of walkers in risk reduction is limited as walker users and non-users alike experience similar fall incidence rates [3]. Improvement to clinical user device training is often suggested as a method to reduce falls with walkers. However, modified training regimens may not be applicable to many walker users who self-obtain the devices commercially or receive them from family, friends, or long-term care facility staff rather than from medical professionals who provide user training [4]. The limited access to device training suggests that fall mitigation efforts should address device deficiencies in addition to training deficiencies. Walker deficits remain largely unknown, therefore the purpose of this study was to identify the common circumstances of falls in older adult walker users and the associated deficits in walker designs.

METHODS

41 videos from a public data set capturing real-life falls of walker users in two retirement facilities were reviewed independently by two researchers [5]. For each video, the circumstances leading up to the fall were evaluated. Qualitative codes were established to describe three fall mechanism categories: walker type (two-wheeled walker or rollator), fall direction (forward, backward, or sideways), and activity at the time of the fall (forward walking, turning, standing, transferring from standing to sitting on the walker's seat or stationary chair, transferring from sitting on the walker's seat to standing, transferring to an upright position after bending over, collapsing the walker's seat, misuse of walker or walker not used). The researchers coded each video separately, compared codes, and then came to a consensus through discussion and video review following any discrepancies. Falls with the activity at the time of fall coded as "misuse of walker" (n=5) or "walker not used" (n=2) were excluded from further analysis. For the remaining 34 falls, a frequency analysis was performed to assess the frequency of falls associated with each combination of walker type, fall direction, and activity at the time of fall. Combinations with high-frequency rates were identified as common fall scenarios.

RESULTS AND DISCUSSION

Of falls that occurred during two-wheeled walker use (n=7), users mostly fell sideways while turning (Table 1). Turning with a two-wheeled walker is often reported as a difficult maneuver [6]. Due to the fixed nature of the front wheels, users frequently pick up the walker to complete a turn, reducing their base of support and lateral stability. Since turning may be necessary for the safe navigation of many environments, improvement to the turning functionalities of two-wheeled walkers is needed to mitigate sideways falls.

Table 1: Percentages of falls involving two-wheeled walkers by activity and fall direction

Activity	Fall Direction			Total
	Forwards	Backwards	Sideways	
Turning	0	0	43	43
Walking	14	0	0	14
Standing	0	14	0	14
Transferring	0	29	0	29
Collapsing seat	0	0	0	0
Total	14	43	43	100

Of falls that occurred during rollator use (n=27), users primarily fell backwards during transfer activities (Table 2). The percentage of backward falls was 16 % higher in rollator users than in two-wheeled walker users, while the percentage of sideways falls was 17% lower for rollator users. Compared to two-wheeled walkers, the implementation of two fixed back wheels and rotatable front wheels in rollators may improve mediolateral maneuverability but at a cost to anteroposterior stability. Backward falls with rollators were often a result of individuals neglecting to lock the wheels while transferring. These findings emphasize the need for a more accessible, easily controlled braking mechanism. The challenges users may face in engaging rollator brakes should be further investigated.

Table 2: Percentages of falls involving rollators by activity and fall direction

Activity	Fall Direction			Total
	Forwards	Backwards	Sideways	
Turning	0	11	15	26
Walking	7	0	7	15
Standing	7	0	4	11
Transferring	0	44	0	44
Collapsing seat	0	4	0	4
Total	15	59	26	100

CONCLUSIONS

The use of two-wheeled walkers and rollators do not completely mitigate fall risk in older adults. The poor maneuverability, lateral stability, and braking mechanisms of these devices contributed to falls in our study. These results may be used to inform the design of an improved walker that specifically addresses current walker deficiencies, ultimately reducing the number of falls that occur while using wheeled walkers.

REFERENCES

1. Bergen et al. (2016), *MMWR Morb Mortal Wkly Rep* **63**(37).
2. Hartholt et al. (2011), *J Trauma – Inj, Inf, Crit Care* **71**(3).
3. Gell et al. (2015), *J Am Ger Soc* **63**(5).
4. Sloot and Komisar (2022), *Gait & Posture* **97**.
5. Robinovitch et al. Databrary (2018).
6. Lindemann et al. (2016), *Aging Clin & Exp Res* **28**(2).

DIFFERENT NEUROCOGNITIVE CONTROLS MODULATE OBSTACLE AVOIDANCE THROUGH PREGNANCY

Pegah Jamali, Kameron M. Kinkade, Asher Ericson, Ben Tyler, Shikha Prashad, Robert D. Catena

Gait and Posture Biomechanics Lab, Washington State University, Pullman WA USA

email: Pegah.Jamali@wsu.edu web: <https://labs.wsu.edu/biomechanics/>

Introduction

Understanding why 25% of pregnant women fall will have clinical impacts on the health of pregnant women and their fetuses. Anthropometric changes during pregnancy only partially ($r < 0.5$) account for balance deficits [1]. Attention, joint position sense, and perception of the environment are required to prevent trips and potential falls, so their change through pregnancy may explain some of the fall rate increase. The goal of this research was to understand how the changes to these neurocognitive processes affect obstacle avoidance through gestation.

Methods

Seventeen pregnant participants were tested five times in 6-week intervals, between 13 to 37 weeks of gestation. Participants walked an obstacle course (OC) at a self-selected speed (Fig. 1). The two obstacles in the middle and the bottom left were set to 10% body height and the three other obstacles were randomly set to 5%, 7.5%, and 12.5% of body height. We calculated minimum distances and crossing heights over middle obstacles for leading and trailing feet. Participants performed an attentional network test (ANT) which assessed alerting, spatial orienting, and conflict resolution components of attention. The obstacle perception (OP) task asked participants to match their foot height to the height of a 10% body height obstacle in eyes closed and open conditions. The joint position sense (JPS) task asked participants to actively match hip and knee joint angles to passively created joint angles.



Figure 1: View from the start of the obstacle course. Six obstacles spaced 3 m apart. Participants walk the right side (12 m) to the end of the walkway, come back on the left side, and repeat for 2 minutes.

Results and Discussion

In the OC task, leading and trailing foot crossing heights significantly reduced between week 13 and 31 of pregnancy ($p < 0.02$), indicating that the risk of obstacle contacts increases during this time (Fig. 2). Pregnant participants also lifted their foot to a height less than the obstacle height in the 2nd trimester ($p = 0.012$) in the OP task.

Around week 19 of pregnancy, leading foot crossing height was correlated with OP variables, ($R^2 = 0.753$, $p = 0.001$). About week 31, leading and trailing foot crossing heights were correlated with the alerting aspect of attention ($R^2 = 0.512$, $p = 0.002$ and $R^2 = 0.572$, $p < 0.001$, respectively).

Minimum leading foot distance was correlated with OP and JPS variables around week 19 of pregnancy ($R^2 = 0.455$, $p = 0.004$ and $R^2 = 0.266$, $p = 0.041$ respectively) with more dependency on OP.

However, in the early 3rd trimester, the alerting attention network became important for modulating obstacle crossing and then perception again (Fig. 3).

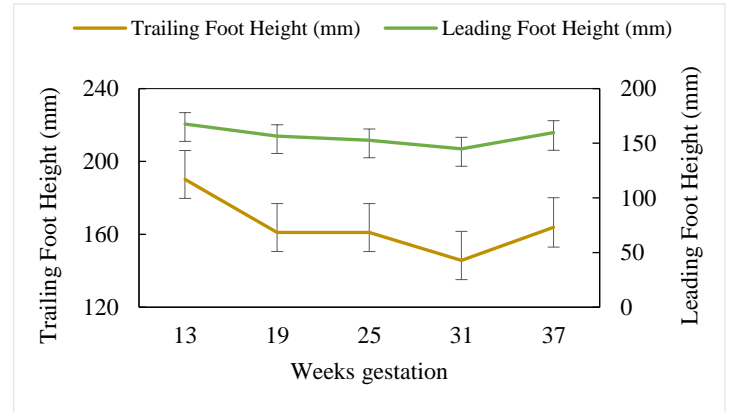


Figure 2: Leading and trailing foot crossing heights over the obstacle (0 mm represents obstacle height).

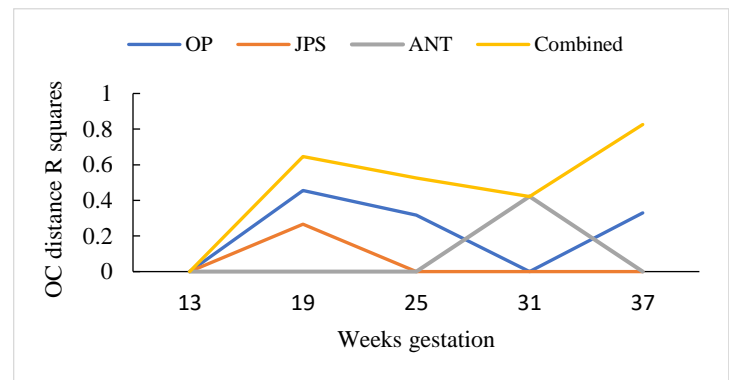


Figure 3: Correlation of each neurocognitive component (OP, JPS, ANT) and all components "Combined" with OC distance (the minimum leading foot distance from the 10% obstacles while performing OC task).

Conclusions

Increased number of falls in 2nd and 3rd trimesters of pregnancy [2] may be correlated with reduced perception of the environment, with additional contributions of joint position sense and attention at various stages. Increased reliance on attention and perception during 3rd trimester may compensate for reduced joint position sense during this time. However, since OC performance seems to degrade when attention has the largest correlation, this may indicate reliance on attention as a poorer controller for obstacle avoidance. The correlation to the combination of neurocognitive processes also increases over time, indicating a possible reliance in overall cognition to make up for greater obstacle avoidance challenge or the fear of tripping.

Acknowledgments

ASB funded this project (JFR Award)

References

1. Catena et al. (2019). J Applied Biomechanics.
2. Dunning et al. (2010). Matern Child Health J.

Investigating the Relationship Between Leg Strength, Mobility, and Center of Pressure Balance in Older Adults

Holmen, M, Fullerton, F, Butte, K & Cannavan, D

Departments of Health and Human Performance, Seattle Pacific University

email: holmenm@spu.edu and fullertonf@spu.edu web: <https://depts.washington.edu/nwbs/2023/index.htm>

INTRODUCTION

There is a current global fall crisis in older adults. Thus, discovering objective ways to measure and improve balance to decrease fall risk is crucial. Leg strength and mobility are pertinent in muscle utilization and muscle control for balance. Therefore, the primary purpose of this study was to examine the relationship between leg strength and balance in older adults. The secondary purpose was to examine the relationship between mobility and balance. With the information gathered from this study, there will be further insight into how to improve and prevent the current fall crisis for older adults.

METHODS

This cross-sectional study consisted of one data collection session for each participant lasting about 30 minutes. Participants (N = 33) were recruited via email and in-person at a community senior center and elderly apartment complex. Demographics, balance, leg strength, and mobility were measured via survey, Balance Tracking System (BTrackS), 30-second chair sit-to-stand, and 8-foot-up-and-go, respectively (1,2). The BTrackS is an innovative portable force plate measuring Center of Pressure (COP) that has been validated in older adults and produces Fall Risk Percentiles based on COP measure, gender, and age (1; Figure 1). Data were uploaded to SPSS for analyses. Independent sample t-tests were used to measure differences in leg strength and mobility between those with ≥ 75 percentile of CoP measure compared with those that were < 75 percentile.

RESULTS AND DISCUSSION

There was a statistically significant difference between the higher-performing balance group and the lower-performing balance group when comparing leg strength using the measure of the 30-second chair stand ($p < 0.045$). This difference was also clinically meaningful as those with better balance performed nearly 3 more chair stands (Table 1). Further, there was a statistically significant difference between balance groups and agility ($p < 0.039$) between the balance groups, showing those with better balance had better (faster agility). This difference was also clinically meaningful showing nearly 2 seconds faster on their 8-ft up-and-go. Thus, this study supports that those with better leg strength and agility have more stable objective COP, resulting in better balance and reduced fall risk.



Figure 1. BTrackS board for balance measure.

Table 1. Independent samples t-tests between balance categories and Means and Standard Deviations for measures

	≥ 75 ile Balance (n=18)	< 75 ile Balance (n=15)	p-value
Leg Strength (chair stand #)	15.0 (± 13)	12.5 (± 5)	0.045
Agility (8 ft up and go second)	5.84 (± 1.57)	7.60 (± 3.61)	0.039

CONCLUSIONS

This study helps fill the gaps in the literature since there have been few studies done on the correlation of balance and leg strength specifically using an affordable, effective force plate such as BTrackS (1). This research can inform future interventions to target factors such as leg strength and agility to help decrease fall risk. Further, future clinical settings may want to incorporate BTrackS regular measures to evaluate fall risk.

REFERENCES

1. Goble D. The BTrackS balance test is a valid predictor of older adult falling. *Balancing Tracking System Inc.* 2018.
2. Jones CJ, Rikli RE. Measuring functional fitness of older adults. *The of Active Aging.* 2002;24-30.

A BIOMECHANICAL CASE STUDY: NON-LINEAR RESPONSE OF THE PELVIS DURING A SIDEWAYS FALL IMPACT

Bliven, EB¹, Fung, A³, Baker, A³, Helgason, B³, Guy², and Crompton, PA¹

School of Biomedical Engineering¹ and Department of Orthopaedics², University of British Columbia, Canada

³Institute for Biomechanics, ETH Zürich, Zürich, Switzerland

email: emily.bliven@ubc.ca

INTRODUCTION

Hip fracture, in the geriatric context, is prevalent and often leads to catastrophic levels of disability. One approach towards mitigating hip fracture risk is prophylactic strengthening of the vulnerable femur with an orthopaedic augmentation. The efficacy of such augmentations has been investigated in biomechanics studies that simulate a sideways fall from standing, which is how most hip fractures occur. However, these studies lack sufficient representation of the pelvis, a critical medial boundary condition for the femur during sideways falls. Understanding the breadth of pelvic biomechanics in this loading mode is one key to designing effective augmentation approaches.

The objective of this work is to describe one complex case of cadaveric pelvis failure and deformation captured in an augmented specimen during a simulated sideways fall impact and explore the potential implications for future injury prevention approaches.

METHODS

The donated specimen in this case study was a 63-year-old female. The cadaveric femur-pelvis construct was cast in a mold of ballistic gel shaped to represent their soft tissue. The femur that was impacted was augmented with a commercially available intramedullary nail. The specimen was subjected to an inertia-driven sideways fall impact using a previously-developed inverted pendulum simulator (Figure 1) [1]. We collected impact force-time data, pelvic marker deformations (using high speed videography), and x-ray video of the impact. The biplanar x-ray system included two each of x-ray sources, image intensifiers, and high-speed cameras.

RESULTS AND DISCUSSION

Post-fall inspection of the specimen revealed damage to the pelvis at the superior pubic ramus on the impacting side, and no evidence of hip fracture. Analysis of pelvic marker deformation at the impacting pelvic brim and pubic symphysis showed large deformations initiating shortly after the peak surface impact force of 3.58 kN (Figure 1).

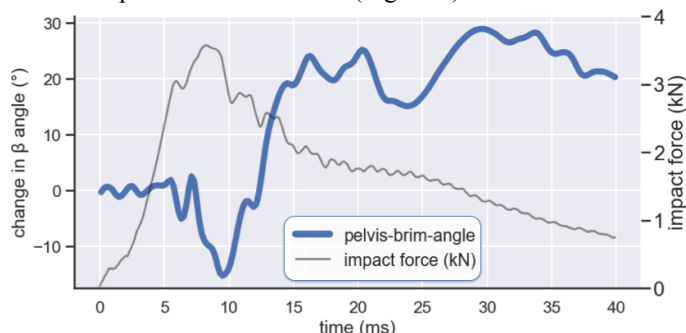


Figure 1: Impact force and change in pelvis-brim angle on the impacting side of the pelvis plotted over impact time.

Observation of the x-ray video confirmed this (Figure 2), displaying an S-shaped deformation pattern propagating along the superior pubic ramus on the impacting side throughout the fall event.

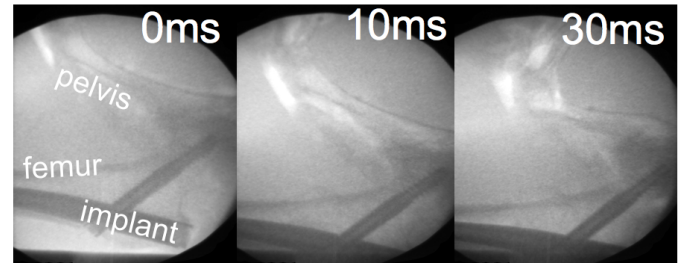


Figure 2: X-ray video frames showing pelvis deformations on the impacting side over 30ms of the impact.

The deformations and bending observed in this pelvis (8.3 mm and 37°, respectively) without displaced fracture are consistent with dynamic buckling, a force response has been previously documented in other parts of the human body like the cervical spine [2]. Our findings expand on other work characterizing the non-linearity of the pelvis under lower forces [3], highlighting the high apparent stiffness of the pelvis at high loads. This is further enhanced by offering the real-time visualization of this phenomenon as it occurs within a biofidelic soft tissue surrogate.

CONCLUSIONS

Classifying pelvic response and fracture potential is imperative when investigating prophylactic femoral augmentations. Pelvic fractures are preferred to femur fracture as a clinical outcome in falls because they are associated with far less operative morbidity and possibly mortality. However, to optimize femoral augmentation systems, any increased likelihood of pelvic fracture associated with augmenting the femur must be assessed. This case study demonstrates the high tolerance of the pelvis to extreme deformations at high rates, with the ability to sustain only a nondisplaced and relatively small fracture. Understanding the biomechanics of such injurious events is essential for advancing effective treatment and prevention strategies.

REFERENCES

1. Fleps I, et al. *PLoS ONE* **13**, e0201096, 2018.
2. Nightingale RW, et al. *SAE Technical Paper Series*, 973344, 1997.
3. Laing AC, and Robinovitch SN. *J Biomech* **43**, 1898-1904, 2010.

ACKNOWLEDGEMENTS

The authors would like to thank Jade Levine for her invaluable assistance in conducting the fall experiment.

Podium Session 4: Sports and Performance

Saturday, May 20
1:15 - 2:30 pm

Moderators: Kayla Fewster and Corey Pew

UPPER LIMB MOVEMENT IN VIRTUAL AND REAL-WORLD ENVIRONMENTS

Spitzley, KA, Hoffman, Z, Perlman, SE, Karduna, AR

THE EFFECTS OF SUBSCAPULARIS TRIGGER POINT RELEASE ON ROTATOR CUFF FUNCTION

Nathan Allas, Liana Castaneda, Jared Hubbell, Katie Butte, and Dale Cannavan

SEX DIFFERENCES IN PLANTAR PRESSURE DISTRIBUTION IN SOCCER PLAYERS AFTER FATIGUE

Aymeric Feyfant, Emily Karolidis, Michael Hahn

BIOMECHANICAL CONTRIBUTORS TO HEAD IMPACT DURING FALLS IN MOUNTAIN BIKING

Rickie Ma, Sukhman Gosal, Gary Mann, Stephen Robinovitch

A LOOK AT KINEMATIC METRICS IN BOTH HALVES OF PLAYER GAMES IN WOMEN'S SOCCER

Suliat Yakubu and Calvin Kuo

UPPER LIMB MOVEMENT IN VIRTUAL AND REAL-WORLD ENVIRONMENTS

Spitzley, KA, Hoffman, Z, Perlman, SE, Karduna, AR
Department of Human Physiology, University of Oregon
email: kspitzle@uoregon.edu, web: karduna.uoregon.edu

INTRODUCTION

Virtual reality (VR) systems are being introduced to train surgeons, provide clinical and in-home health care, and teach sensorimotor skills. Each of these uses rely on translation of sensorimotor skills between VR and the real-world (RW). However, neuroimaging studies and long-held concepts of visual processing call to question the translational capacity between virtual and real sensory environments [1]. Further evidence of altered movement patterns and unintended aftereffects of sensorimotor training in virtual environments highlight the potential limitations of deploying VR as a substitute for RW training [2-3].

To apply VR safely and effectively, it is important to understand the performance of sensorimotor tasks in both VR and RW environments. This study analyzed upper limb kinematics and muscle activity during a visually guided reaching task in VR and RW environments. It was hypothesized that a) Reaching movements in VR would be slower, less smooth, and less direct than movements in RW and b) Muscle activity would peak higher and more often in VR than in RW.

METHODS

Forty-six participants were recruited to perform a reaching task to visual targets in RW and VR environments. Participants were randomly assigned to one of two groups. Group 1 ($n = 23$) performed three blocks of the task in RW followed by one block in VR. Group 2 ($n = 23$) performed three blocks of the task in VR followed by one block in RW.

In the RW, visual reaching targets were presented using a LED board. In VR, the laboratory space was modelled, and the virtual LED board presented targets. An HTC VIVE Pro Eye headset and v3.0 Trackers displayed the virtual environment and

captured position and orientation of the trunk, arm, and wrist segments. Electrical activity of the Biceps Brachii, Anterior Deltoid, and Upper Trapezius muscles were captured through the Delsys Trigno EMG system. Customized Arduino, Unity, and LabVIEW programs facilitated communication between and data output from the light board, VR, and EMG systems.

Endpoint speed, trajectory error, and movement phase metrics were calculated using the wrist position as an endpoint. EMG peaks were detected from RMS rectified and smoothed signals. All processing and analyses were completed using a custom MATLAB program. One way repeated-measures ANOVAs ($\alpha = 0.05$) were used to determine differences between testing blocks (B1-B4) within each group (Table 1).

RESULTS AND DISCUSSION

Participants took no less time to respond to the visual signal or to reach the target, nor did they follow a less accurate movement trajectory in VR than in RW. At the mean and peak, participants moved more slowly throughout the entire movement in VR than they did in RW. Overall, participant's EMG activity peaked more in VR than in RW.

The proposed hypotheses were partially confirmed, some differences in upper limb movements are seen between RW and VR environments. Further investigation is underway to fully understand the performance of this sensorimotor task in VR and RW environments.

REFERENCES

1. L. Beck et al. *Cyberpsychology, Behav. Soc. Netw.* **13**, 211-215, 2010
2. S. Ikbali Afsar et al. *J. Stroke Cerebrovasc. Dis.* **27**, 3473-3478, 2018
3. E. A. Keshner et al. *J. Neuroeng. Rehabil.* **16**, 1-15, 2019

Table 1: Significant differences are annotated using superscripts with [^] indicating a higher value and ^v indicating a lower value.

Group 1) Mean endpoint velocity - lower in B1 than B2 and B3, and lower in B4 than in any other block. Peak endpoint velocity - lower in B1 than in B2, and lower in B4 than in B2 and B3. EMG Peak Count: Bicep - B1 and B4 were both higher than B2 and B3, but not different from each other. Anterior Deltoid - B4 was higher than B2 and B3, but not different from B1. Upper Trapezius - B1 was higher than B2, but no different from any other block.

Group 2) Mean and peak endpoint velocity - lower in B1 than in any other block and higher in B4 than in any other block. EMG Peak Count: Bicep - B1 was higher than all other blocks and B4 was lower than all other blocks. Anterior Deltoid - blocks were all different from each other, with B1 being highest, decreasing each block, and B4 being the lowest. Upper Trapezius - B1 was higher than all other blocks and B4 was lower than all other blocks.

	Group 1				Group 2			
	B1 – RW	B2 – RW	B3 – RW	B4 – VR	B1 – VR	B2 – VR	B3 – VR	B4 – RW
Mean Endpoint Speed [m/s]	0.65±0.11 ^v	0.69±0.12	0.69±0.13	0.60±0.11 ^{vv}	0.57±0.08 ^v	0.62±0.08	0.62±0.08	0.68±0.09 [^]
Peak Endpoint Speed [m/s]	1.63±0.25 ^v	1.71±0.31	1.70±0.32	1.56±0.32 ^v	1.46±0.21 ^v	1.53±0.21	1.56±0.22	1.65±0.24 [^]
Bicep EMG Peaks [count]	3.6±0.2 [^]	3.0±0.5	3.0±0.7	3.4±0.8 [^]	3.9±0.8 [^]	3.4±0.6	3.4±0.6	3.0±0.6 ^v
A.Delt EMG Peaks [count]	3.6±0.8	3.4±0.8	3.3±0.9	3.9±1.2 [^]	4.5±0.9 ^{^^}	3.8±0.6 ^{^^}	3.6±0.6 [^]	3.2±0.1 ^v
U.Trap EMG peaks [count]	3.8±1.3 [^]	3.4±1.1	3.5±1.2	3.6±1.2	3.8±0.7 [^]	3.3±0.6	3.2±0.6	2.9±0.6 ^v

THE EFFECTS OF SUBSCAPULARIS TRIGGER POINT RELEASE ON ROTATOR CUFF FUNCTION

Allas, N¹, Castaneda, L¹, Hubbell, J¹, Butte, K¹, and Cannavan, D¹

Department of ¹Health and Human Performance, Seattle Pacific University

Email: hubbellj@spu.edu , web: SPU HHP Website

INTRODUCTION

The subscapularis is a primary agonist for shoulder internal rotation (IR). A tight subscapularis causes reciprocal inhibition in antagonistic muscles during external rotation (ER). Myofascial release (MFR) is a method to remove muscular restrictions in the muscle allowing it to return to normal function. Scapular mobilization with MFR is effective to improve pain, range of motion (ROM) and function in subjects with chronic frozen shoulder [2]. However, there are limited studies examining reciprocal inhibition caused by the subscapularis in regards to force production and ROM. The purpose of this study was to examine the effects of subscapularis MFR on torque production and ROM of the internal and external rotator cuff muscles.

METHODS

Participants (male, $n = 13$; female, $n = 13$; Age = 20.96 (± 1.11) yrs) were randomly assigned to either an MFR intervention group ($n = 14$) or a control group ($n = 12$). All participants completed ROM and torque measures on an isokinetic dynamometer (Biodex). Immediately after the Biodex assessment, they completed a MFR to the subscapularis, or they rested for 5-minutes. Then, measures were performed again (post). For the MFR, a 90 second passive MFR was achieved through pressure in the anterior plane past the latissimus dorsi and onto the anterior portion of the scapula. ROM measures were analyzed with Kinovea. A RMANOVA was used to compare the main effects for group, time and the group*time interaction for torque and ROM for IR and ER.

RESULTS AND DISCUSSION

RMANOVA showed no statistical changes for torque for ER or IR ($p > 0.05$) after the myofascial release. However, there was a significant interaction for external ROM ($p < 0.02$), showing a significant increase in ROM for the MFR intervention and no change for the control (Table 1; Figure 1). Further, there was a main effect for time for both groups for IR ROM, with no significant interaction, showing both groups significantly increased their IR ROM (Figure 2). While external ROM showed a strong effectiveness for the intervention, internal ROM did not see the same significance between the two groups (see Figure 2). There are multiple reasons that torque did not experience significance. The first reason could be due to a proprioceptive neuromuscular facilitation stretch applied to the subscapularis during the ER contraction on the dynamometer. Another reason may be the young age demographic providing less frequency of reciprocal inhibition upon the shoulder.

CONCLUSION

Although there was no change in torque production, this study supports the use of MFR to increase ROM for shoulder external rotation. MFR on the subscapularis will allow a

functional rotator cuff to produce optimal ROM which may reduce the chance of shoulder pathologies such as obstetric brachial plexus paralysis [1]. The reason for lack of change in torque production is unclear, but it may be due to a lack of reintroducing motor control post MFR. A reduction in persistent inward current would have determined reduced synaptic output with a reduction in the force output of muscles. Future studies may want to examine a more diverse group with higher sample size.

REFERENCES

1. Naoum E, et al. *Journal of Children's Orthopedics* **5**, 339-344, 2015.
2. Sinha U, et al. *International Journal of Health Sciences and Research* **4**, 2019

Table 1

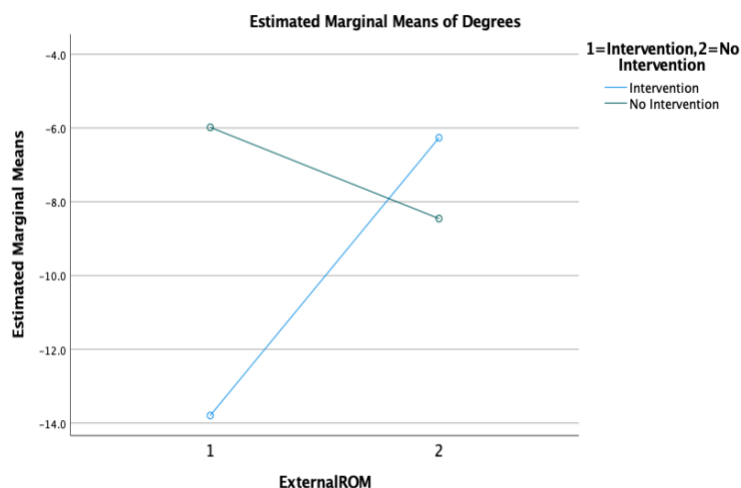
Means and Standard Deviations of External (ER) and Internal (IR) Range of Motion (Degrees)

Time	Intervention	Control
Pre-ER	-13.79(± 16.12)*	-5.98(± 8.10)
Post-ER	-6.26(± 10.82)*	-8.46(± 7.46)
P-value	.02	.22
Pre-IR	50.10(± 14.37)	47.29(± 8.93)
Post-IR	57.96(± 14.85)	52.26(± 15.74)

Note. *Indicates significance from our RMANOVA testing.

Figure 1

Estimated Marginal Means of Degrees for External ROM



SEX DIFFERENCES IN PLANTAR PRESSURE DISTRIBUTION IN SOCCER PLAYERS AFTER FATIGUE

Feyfant, A¹, Karolidis, E¹ and Hahn, M¹

¹Department of Human Physiology, University of Oregon, Eugene, Oregon

email: aymericf@uoregon.edu

INTRODUCTION

Soccer is a sport with repeated bouts of intense physical demand, subjecting players to systemic fatigue progression over the course of play. Fatigue results in decrements to performance, limiting the distance covered by sprinting and high intensity running after the first half of play [1]. The manifestation of fatigue has been shown to differ between sex; females typically demonstrate greater resistance to fatigue than males, including during sprinting tasks [2]. Sprinting mechanics also differ between sexes during maximal velocity [3].

Plantar pressure distribution has been used to examine how force, contact time, and relative load change during sprinting in response to fatigue [4]. Despite sex-based differences in fatigue manifestation, studies into the effects of fatigue in cleated sports are often generalized to male athletes. The purpose of this study is to examine sex differences in plantar pressure in soccer players before and after systemic fatigue.

METHODS

Three college soccer players (two male, one female, n = 20 in progress) performed a fatigue protocol in a turf fieldhouse, in accordance with IRB approval. Footwear was standardized across participants (adidas Predator Edge.2). Novel Pedar-X pressure insoles (Pedar, Munich, Germany, sampled at 100 Hz) were inserted in place of the sock liner and calibrated to the athlete. Plantar pressure data were recorded during the warm-up and at the end of the fatigue protocol. Athletes performed a warm-up, progressing from light jogging to speed work, culminating in a maximal effort 50-meter sprint. Data during this sprint were representative of the pre-fatigue condition. Following the warm-up, athletes performed a modified Gauntlet test which is a validated assessment of aerobic fitness [5]. Data were recorded during the final stage of this protocol (a maximal effort 100-meter sprint), representing a fatigued state.

To represent the maximal velocity phase of sprinting, the last two steps of each trial were removed, and the last three remaining left and right steps were analyzed. Plantar pressure data were analyzed by anatomical regions: medial heel (MH), lateral heel (LH), medial midfoot (MM), lateral midfoot (LM), medial forefoot (MF), central forefoot (CF), lateral forefoot (LF), hallux, and lesser toes (LT). The MH and LH were excluded from analysis due to minimal observed contact. The

force-time integral (FTI) was calculated for each region, and peak pressure was determined for the whole foot. Regional FTI were compared across fatigue states and sex. Due to limited sample size, only descriptive statistics are reported.

RESULTS AND DISCUSSION

Increased FTI was observed in the LF and the whole foot and decreased FTI was observed in the LT post-fatigue, in both males and females (Table 1). In males, FTI increased in the hallux, MF, and CF, and was unchanged in the MM and LM post-fatigue. In females, FTI was unchanged in the hallux, decreased in the MF and CF, and increased in the MM and LM post-fatigue. Total FTI was greater in females both pre- and post-fatigue. Peak pressure was consistently observed in the hallux across sex and fatigue condition; sample data is shown in Figure 1.

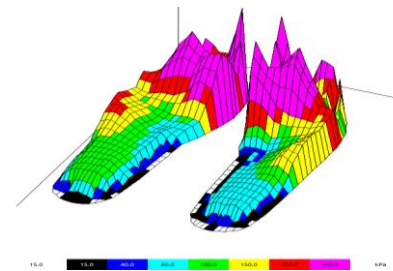


Figure 1: Visualization of peak pressure distribution.

CONCLUSIONS

Initial results suggest sex differences in sprinting mechanics due to fatigue, with females showing FTI increases in the midfoot and males showing FTI increases in the MF and CF.

ACKNOWLEDGEMENTS

This work was supported by the Wu Tsai Human Performance Alliance and the Joe and Clara Tsai Foundation. Footwear was generously donated by adidas.

REFERENCES

1. Mohr M, et al. *J Sports Sci* **21**, 519-528, 2003.
2. Hunter S. *Cold Spring Harb Perspect Med* **8**, a029728, 2018.
3. Debaere S, et al. *J Strength Cond Res* **27**, 116-124, 2013.
4. Girard, O et al. *Eur J Appl Physiol* **111**, 2547-2555, 2011.
5. Burnsed-Torres ML, et al. *J Strength Cond Res* **36**, 386-391, 2022.

Table 1: Sex differences in force-time integral during the maximal velocity phase by foot region.

Force-Time Integral (%BW*s)	Foot Region							
	Hallux	LT	MF	CF	LF	MM	LM	Whole Foot
Male								
Pre-fatigue	4.2 ± 0.28	4.9 ± 0.66	5.4 ± 1.29	5.4 ± 0.88	3.4 ± 0.42	0.9 ± 0.25	3.0 ± 0.87	28.6 ± 2.22
Post-fatigue	4.3 ± 0.29	4.6 ± 0.43	5.8 ± 1.76	6.0 ± 1.42	3.6 ± 0.55	0.9 ± 0.08	3.0 ± 0.61	28.8 ± 2.37
Female								
Pre-fatigue	2.3 ± 0.21	3.8 ± 0.11	4.0 ± 1.20	5.2 ± 0.38	3.7 ± 0.58	1.3 ± 0.11	4.1 ± 0.35	30.1 ± 0.76
Post-fatigue	2.3 ± 0.29	3.6 ± 0.45	3.4 ± 0.40	5.1 ± 0.20	4.0 ± 0.46	1.5 ± 0.38	4.6 ± 0.42	31.0 ± 0.37

BIOMECHANICAL CONTRIBUTORS TO HEAD IMPACT DURING FALLS IN MOUNTAIN BIKING

Ma, Rickie; Gosal, Sukhman; Mann, Gary; Robinovitch, Stephen

Departments of Biomedical Physiology & Kinesiology, Simon Fraser University, Burnaby, BC, Canada

INTRODUCTION

Mountain biking (MTB) is a popular recreational activity associated with a high risk for falls and fall-related injuries [1], including concussion and more severe forms of traumatic brain injury (TBI). Risk for TBI during a fall depends on whether impact occurs to the head [1]. A barrier to prevention is the lack of understanding on the types of falls in MTB that are most likely to result in head impact. We analyzed video footage of real-life falls in MTB to identify the intrinsic, situational, and environmental factors that influence risk for head impact in falls.

METHODS

We accessed publicly available falls in MTB posted to the Pinkbike website. We contacted 974 video posters to inquire about the rider's sex, gender, age, and riding experience, of which 147 provided this information. Video analysis was done by trained raters using a structured questionnaire to classify whether impact occurred to the head (and other body sites), situational and environment factors, activity, causes of imbalance, and safe landing responses. The questionnaire was coded in DataVyu (v1.5.3), and refined by experts to assess content validity [2], and through measures of inter-rater reliability between individual raters. Nominal logistic regression (JMP v16) was used to analyze whether the probability of head impact depended on characteristics of the rider and characteristics of the fall.

RESULTS AND DISCUSSION

Participants captured included 138 men, 8 women, and 1 non-binary. Their mean age was 26.7 years (SD 12.0) and mean MTB experience was 6.8 years (SD 7.0). 84 of the 147 falls occurred while performing jumps. The head was impacted in 53.1% of falls. The probability for head impact was higher for falls caused by wheel slippage and forward tilting of the bike, but did not depend on speed or the height of the fall. The probability for head impact was lower for falls where riders dismounted or stepped, but did not depend on upper limb bracing or rolling. There was a trend towards sideways falls having a lower risk for head impact. The probability of head impact did not associate with age, gender, sex, or experience.

While previous studies have examined the circumstances of specifically injuries in MTB, our study extends the literature by examining the factors that separate falls that cause head impact, from those that do not. Our results support previous findings on the high risks posed by falling forwards over the handlebar, and falls due to loss of traction [3]. Surprisingly, speed and fall height were not predictive, perhaps reflecting modulation of these factors based on safe landing abilities [4].

Factors in Head Impact from an MTB Fall

Factor	P-value	Odds ratio (95% CI)
Age (1 year increase)	0.127	0.97 (0.93 – 1.01)
Sex (male)	0.821	0.69 (0.10 - 4.52)
Gender (men)	0.821	2.27 (0.10 – 4.52)
MTB experience (1 year increase)	0.567	0.98 (0.93 – 1.05)
Jump (vs non-jump fall)	0.654	1.26 (0.45 – 3.43)
Wheel slippage	0.043	3.59 (1.44 – 8.95)
Forward tilting of bike	0.045	4.03 (0.95 – 17.19)
Initial direction of fall - sideways	0.068	0.23 (0.04 – 1.17)
Fast speed	0.327	1.75 (0.56 – 5.47)
High height	0.593	0.77 (0.30 – 3.30)
Steep grade	0.295	1.37 (0.40 – 4.71)
Abrupt deceleration	0.306	0.59 (0.21 – 1.63)
Rider loss of contact	0.590	1.34 (0.46 – 3.90)
Reach to Grasp	0.041	16.45 (0.65 – 412.9)
Dismounted	0.008	0.07 (0.007 – 0.77)
Stepping	0.047	0.37 (0.13 – 1.00)
Upper limb bracing	0.204	0.56 (0.23 - 1.38)
Rolling	0.770	1.17 (0.41 – 3.28)

CONCLUSION

More than half of falls in MTB posted to Pinkbike involved head impact. The probability for head impact depended on loss of traction, forward falling, and protective responses in dismounting and stepping. There was no effect of age, experience, sex, or gender on probability of head impact. Our study reveals new insights on how riders respond to falls to avoid head impact.

REFERENCES

- [1] Carmont MR. Mountain biking injuries: a review. *Br Med Bull* 2008; 85: 101-12
- [2] Polit, Denise F, and Cheryl Tatano Beck. "The content validity index: are you sure you know what's being reported? Critique and recommendations." *Research in nursing & health* vol. 29,5 (2006): 489-97.
- [3] Chow TK, Kronisch RL. Mechanisms of Injury in Competitive Off-Road Bicycling. *Wilderness and Environmental Medicine* (2002)., 13, 27-30.
- [4] Moon, Yaejin, and Jacob J Sosnoff. "Safe Landing Strategies During a Fall: Systematic Review and Meta-Analysis." *Archives of physical medicine and rehabilitation* vol. 98,4 (2017): 783-794

A LOOK AT KINEMATIC METRICS IN BOTH HALVES OF PLAYER GAMES IN WOMEN'S SOCCER

Yakubu, S., Kuo, C.

School of Biomedical Engineering, University of British Columbia

email: suliati16@student.ubc.ca, web: <https://humbl.bme.ubc.ca/>

INTRODUCTION

Soccer has a relatively high injury rate compared to other contact sports, including volleyball, basketball, field hockey and rugby [1]. As players progress through the game, the effects of fatigue, including depletion of glycogen stores and hypohydration, may affect the mental and physical abilities of the athletes. Though some studies have reported a higher injury incidence rate in the second half than the first [2], others have reported no significant difference [3]. Rather than looking at injury risk directly, there may be value in looking at the changes in the kinematics of play, especially those relevant to injury. Lateral accelerations, frontal plane and horizontal plane angular accelerations are associated with movements with an increased risk of injury, such as cutting and pivoting. Therefore, this abstract takes a preliminary look at IMU data collected during game play, to investigate whether a change in the kinematics of play can be observed between halves.

METHODS

A single IMU (ICM 20649), sampling at 1000Hz was deployed to 15 female collegiate soccer players over 254 player events (including 46 player games and 208 player practices) at the University of British Columbia during the Fall 2022 season. The sensor was securely mounted between the shoulder blades of each player using hypoallergenic tape. Participants then proceeded to play as normal. This analysis consisted of games where players were on the pitch for at least 68 minutes, signifying games where athletes were in play for at least half of each half of play, numbering 13 player games. Full 6-degree-of-freedom linear acceleration and angular velocity was recorded.

Data processing was performed using MATLAB R2021b software (The Mathworks Inc., Natick, MA, USA). Signals were processed using a zero-lag 2nd order low-pass Butterworth filter with cut-off 100 Hz. A customized peak-detection method on the anteroposterior axis was used to identify foot strikes with peak magnitude $>25\text{m/s}^2$. Peak mediolateral accelerations, frontal plane angular accelerations, and horizontal plane angular accelerations were assessed in the first and second halves of game play. The median peak acceleration and the standard deviation of the distribution of peak accelerations per player game was used to assess the change between game halves. A one-sided paired Wilcoxon rank-sum test was performed on the median peak acceleration and the standard deviation to assess change between game halves.

RESULTS AND DISCUSSION

The aim of this preliminary analysis was to determine whether the median peak acceleration of high-impact foot strikes would change between the first and second halves of game play. The hypothesis was that the median peak value of these impacts would be higher in the second half of play. A significant increase ($n=13$) in the peak median angular acceleration was observed in the frontal ($p=0.0007$) and horizontal ($p=0.0081$) planes from the first to the second half of player games (Figure

1). A significant increase in the standard deviation in the horizontal plane ($p=0.0024$) was also observed. All other metrics reported insignificant change between halves.

The increase in the magnitude of the frontal and horizontal plane peaks could suggest that players are increasing the intensity with which they perform these bending and twisting motions. The increase in the standard deviation of the peaks horizontal plane could suggest increased variation in the way that movements are executed.

To better understand these metrics in the context of active game play, future analyses should divide each half into 3 portions, for 6 portions total. This is in line with work done by Rahnama et al [3], which reports that injury risk is highest during the first 15 minutes of each half. In addition, as more data is collected in future seasons, this analysis should be repeated with a larger sample size. Lastly, to assess the validity of the associations made, video analysis is being performed, so that future work in a similar vein can be stratified based on the activities being performed.

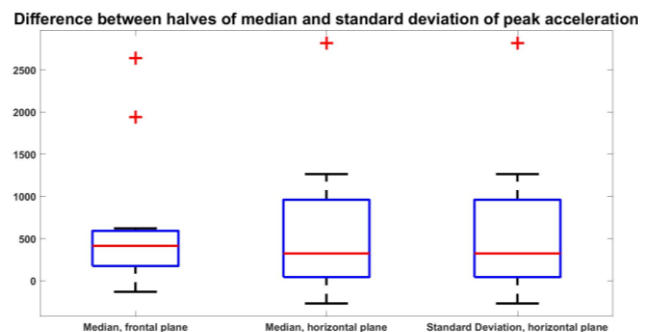


Figure 1: The differences between the medians of the peak accelerations in the second and the first half, and the standard deviation of the horizontal plane are greater than zero, indicating an increasing in the respective value between halves.

CONCLUSIONS

Based on this preliminary analysis, the angular acceleration in the frontal and horizontal planes may prove relevant for determining quantitative metrics that are likely to change between the first and second halves of game play, which could indicate the value of looking at these metrics with respect to movements with an increased risk of injury.

REFERENCES

1. Wong P and Hong Y. *Br J Sports Md* **39**, 473–482, 2005.
2. Hawkins, RD and Fuller, CW. *Br J Sports Md* **33**, 196-203, 1999.
3. Rahnama N, et al. *Br J Sports Md* **36**, 354-359, 2002.

ACKNOWLEDGEMENTS

We would like to acknowledge the UBC Women's Soccer team and coaching team for their enthusiasm towards sports research.

Podium Session 5: Gait

Saturday, May 20
3:00 - 4:00 pm

Moderators: Michael Pavol and Robert Catena

EFFECT OF COMMERCIAL PROSTHETIC FOOT STIFFNESS ON CONTRALATERAL KNEE LOADING AND PROSTHETIC FOOT-ANKLE BIOMECHANICS

Conrad Slater, Elizabeth Halsne, and David Morgenroth

UNEXPECTED UNDERFOOT PERTURBATIONS ELICIT CONSISTENT RESPONSES IN MEDIOLATERAL STABILITY DURING TURNING GAIT

Tyler Ho, Nicholas Kreter, Cameron Jensen, Peter Fino

COGNITIVE-MOTOR FUNCTION DURING JUMP LANDINGS FOLLOWING ANTERIOR CRUCIATE LIGAMENT RECONSTRUCTION

Fatemeh Aflatounian, Ezekiel Barden, James N. Becker, Keith A. Hutchison, Janet E. Simon, Dustin R. Grooms, and Scott M. Monfort

COMPARISON OF SEX-BASED BIOMECHANICAL MODELS TO A DEFAULT MODEL

Abigail R. Brittain, Cristian Sandino, and Tyler N. Brown

EFFECT OF COMMERCIAL PROSTHETIC FOOT STIFFNESS ON CONTRALATERAL KNEE LOADING AND PROSTHETIC FOOT-ANKLE BIOMECHANICS

Slater, C.¹, Halsne, E. G.^{2,3}, Morgenroth, D.C.^{2,3}

¹Hanger Clinic, ²VA RR&D Center for Limb Loss and Mobility (CLiMB), ³University of Washington
Email: conslate13@gmail.com

INTRODUCTION

Individuals with unilateral transtibial amputation (TTA) are at higher risk of osteoarthritis (OA) in their contralateral (non-prosthesis) knee compared to non-amputees [1]. Increased contralateral limb loading is also observed in individuals with TTA [2], which may contribute to the development of knee OA. Previous studies have investigated the effects of prosthetic foot stiffness properties on contralateral limb loading. For example, increased prosthetic forefoot stiffness has been associated with decreased prosthesis push-off power but increased contralateral limb loading [3,4]. However, these studies used experimental prosthetic foot models, which may not be representative of commercial prosthetic feet; thus, the effects of commercial foot stiffness properties remain unclear [5]. The purpose of this study was to assess the association between commercial prosthetic foot stiffness and contralateral knee loading (i.e., knee external adduction moment (EAM)) and prosthetic foot-ankle biomechanics.

METHODS

Participants: 17 males with unilateral TTA were enrolled (age: 49.2±15.3 yrs, height: 176.0±10.4 cm, weight: 89.0±16.3 kg time since amputation: 9.6±12.7 yrs). Most amputations were due to trauma (N=12), followed by dysvascular disease (N=3). Informed consent was obtained from all participants, and all procedures were IRB-approved.

Procedures: Participants trialed three Ossur Variflex feet with varied stiffness categories ('medium' = manufacturer-recommended category based on participant weight and medium activity, 'soft' = -1 category, 'stiff' = +1 category). Participants were initially fit with the medium condition and alignment was optimized, followed by the other two conditions in a randomized order without altering prosthetic alignment. Participants were blinded to foot condition throughout testing.

Data collection and processing: A Vicon MX motion capture system and embedded force plates were used to collect data while participants walked overground for 10m at a fixed speed of 1.3 m/s. Data for a minimum of five clean trials per participant were processed in Vicon Nexus, then filtered with a fourth-order Butterworth filter (6 Hz cutoff frequency). Outcomes were calculated in Matlab, including contralateral knee 1st peak EAM; prosthetic foot-ankle peak push-off power

and work; and prosthetic foot rollover radius. Linear mixed-effects regression was performed in R.

RESULTS AND DISCUSSION

Contralateral knee 1st peak EAM significantly decreased ($p<0.001$) with increasing prosthetic foot stiffness between soft-stiff and medium-stiff foot conditions (Figure 1, Table 1). Prosthetic peak push-off power and work significantly decreased ($p<0.001$, both) between soft-medium, soft-stiff, and medium-stiff conditions (Table 1). Prosthetic foot rollover radius also significantly increased with increasing foot stiffness categories ($p<0.001$) between soft-medium, soft-stiff, and medium-stiff conditions (Table 1).

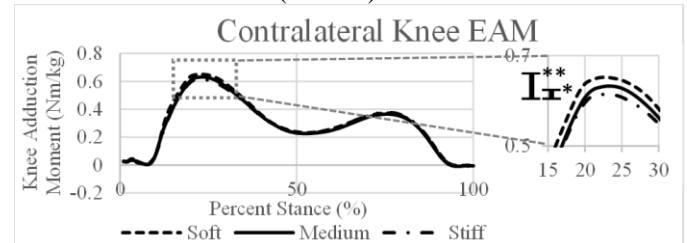


Figure 1: Ensemble averages of contralateral (non-prosthesis) knee EAM. * = significant difference between medium & stiff, ** = significant difference between soft & stiff.

CONCLUSIONS

Walking with a stiffer category prosthetic foot was associated with decreased prosthetic foot-ankle push-off power and work, and decreased contralateral knee peak EAM. With decreasing stiffness, the prosthetic feet demonstrated a reduction in rollover radius suggestive of a “drop-off” effect that might normally be mediated in a clinical setting via prosthetic alignment changes. This “drop-off” effect could lead to increased contralateral limb loading in early stance and thus explain the increased contralateral knee peak EAM.

REFERENCES

1. Struyf, P.A. *Arch Phys Med Rehabil.* **90**, 440-446, 2009.
2. Lloyd C.H. *Gait Posture.* **32**(3), 296-300, 2010.
3. Fey, N. *Clin. Biomech.* **26**, 1025-1032, 2011.
4. Adamczyk, P. *Hum. Mov. Sci.* **54**, 154-171, 2017.
5. Halsne, E.G. *Clin. Biomech.* **80**, 105141, 2020.

Table 1: Means and mean differences on biomechanical outcomes by prosthetic foot stiffness condition. Bolded text represents significant mean differences at the 0.05 level.

	Mean (SE)			Mean differences (SE) [95% CI]			p
	Soft	Medium	Stiff	Soft - Medium	Soft - Stiff	Medium - Stiff	
Contralateral knee peak EAM (Nm/kg)	0.682 (0.033)	0.667 (0.033)	0.627 (0.033)	0.016 (0.013) [-0.015, 0.046]	0.055 (0.013) [0.024, 0.086]	0.040 (0.013) [0.009, 0.070]	3e-04
Prosthetic foot-ankle peak push-off power (W/kg)	3.49 (0.17)	3.32 (0.17)	3.16 (0.17)	0.17 (0.05) [0.03, 0.30]	0.33 (0.05) [0.2, 0.46]	0.16 (0.05) [0.03, 0.30]	4e-06
Prosthetic foot-ankle push-off work (J/kg)	0.250 (0.013)	0.238 (0.013)	0.222 (0.013)	0.012 (0.004) [0.001, 0.022]	0.028 (0.004) [0.018, 0.039]	0.017 (0.004) [0.006, 0.027]	9e-07
Prosthetic foot rollover radius (mm)	254 (10)	270 (10)	286 (10)	-16 (3) [-24, -8]	-32 (3) [-40, -25]	-16 (3) [-24, -9]	6e-11

UNEXPECTED UNDERFOOT PERTURBATIONS ELICIT CONSISTENT RESPONSES IN MEDIOLATERAL STABILITY DURING TURNING GAIT

Ho, TK^{1,2}, Kreter, N¹, Jensen, CB¹ and Fino, PC¹

¹Department of Health and Kinesiology, University of Utah, Salt Lake City, UT USA

²Center for Limb Loss and Mobility, Department of Veterans Affairs, Seattle, WA USA

email: tylerkealii@gmail.com

INTRODUCTION

Humans regularly encounter uneven terrain during everyday walking, which decreases stability [1]. To account for such disturbances, humans make adjustments in their foot placement to ensure forward progression and stability as they walk [2]. While this control strategy has been well described during straight gait, it has not been thoroughly investigated during turning, despite turning making up nearly half of all steps humans take every day [3].

Because turning gait is asymmetrical [4], perturbations to the inside and outside limbs may elicit different recovery responses. The purpose of this study was to investigate how unexpected underfoot perturbations disrupt stability during turning gait, and how individuals alter their foot placement to maintain their stability after such perturbations during turning.

METHODS

Seven healthy adults [age=23.7(2.8)] were recruited from the local community surrounding the University of Utah. Each participant wore a pair of mechanized shoes [5] while completing a series of four 3-minute trials (two clockwise, two counterclockwise) around a circular track (inner radius: 1.2m; outer radius: 1.6m).

During each trial, the left shoe would randomly deploy a small plastic block every 5-9 strides. Retroreflective markers were placed bilaterally on the ASIS, PSIS, iliac crest, heel, 2nd MTP, and 5th MTP, and kinematic data were collected via motion capture (Vicon Nexus ver. 2.12) at a rate of 200 Hz.

Steps were categorized as “inside” or “outside” depending on the walking direction in each trial (i.e. clockwise: left is inside). The mean mediolateral margin of stability (ML MoS) and mean step width (SW) for both inside and outside steps, excluding perturbed steps and the four subsequent steps following each perturbation. The change from the mean of ML MoS and SW was calculated at each perturbed step and the first recovery step.

Linear mixed models were fit for ML MoS and SW with fixed effects of perturbed limb (inside or outside) and perturbation type (eversion or inversion). Significance was assessed at an alpha of 0.05, with a Benjamini-Hochberg correction for multiple comparisons.

RESULTS AND DISCUSSION

Inversion perturbations elicited an increase in ML MoS ($p<0.001$) during the perturbed step, regardless of whether the perturbation was delivered to an inside or outside step. Perturbations to the inside foot also prompted an increase in ML MoS ($p<0.001$) and step width ($p<0.001$) during the first recovery step, regardless of the perturbation type. Perturbations

to the outside foot did not produce a consistent response in either measure during the first recovery step.

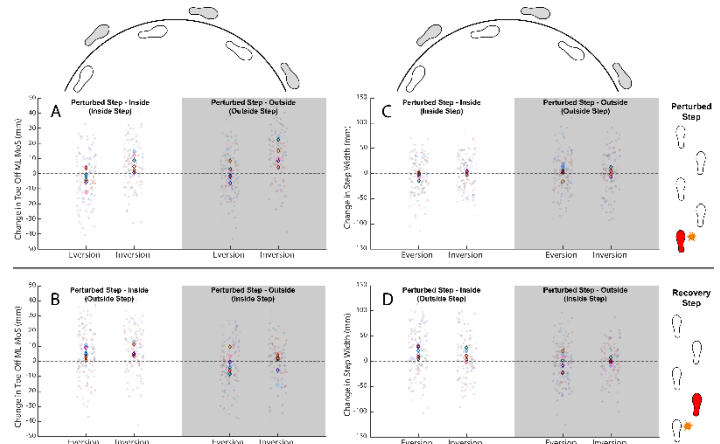


Fig. 1A-D: The change from mean of ML MoS [A,B] and SW [C,D] during perturbed steps [A,C] and the first recovery step post-perturbation [B,D].

The difference in ML MoS between perturbation type is likely because an inversion perturbation directs the body CoM laterally and away from the BoS, while an eversion perturbation redirects the CoM toward the next step. The difference in ML MoS and foot placement during the recovery step indicates that inside and outside steps may serve different purposes during turning. Namely, the outside limb may be primarily for directing the CoM away from the current trajectory, while the inside limb may be used to maintain stability.

CONCLUSIONS

Inversion perturbations appear to be more destabilizing than eversion perturbations during turning. However, only perturbations to the inside limb seem necessitate a recovery response past the initial perturbation.

REFERENCES

1. Marigold, DS and Patla, AE. *J. Neurophysiol.* **94**, 1733-1750, 2005.
2. Bruijn, SM and van Dieën. JH. *J. R. Soc. Interface* **15**, 20170816, 2018.
3. Glaister, BC et al. *Gait Posture* **25**, 289-294, 2007a.
4. Orendurff, MS et al. *Gait Posture* **23**, 106-111, 2006.
5. Kim, H and Ashton-Miller, JA. *J. Biomech.* **45**, 1850-1953, 2012.

ACKNOWLEDGEMENTS

Special thanks to Claire Rogers, Junseop Son, and Jasmine Arreguin for their help on this project.

This project was funded by the National Institute of Health (award no. K12HD073945 to PCF) and the University of Utah's Undergraduate Research Opportunities Program (to TKH).

Cognitive-motor function during jump landings following anterior cruciate ligament reconstruction

Fatemeh Aflatounian¹, Ezekiel Barden¹, James N. Becker¹, Keith A. Hutchison¹, Janet E. Simon²,

Dustin R. Grooms², and Scott M. Monfort¹

¹Montana State University, Bozeman, Montana, USA, ²Ohio University, Athens, Ohio, USA

Email : fatemehaflatounian@montana.edu

INTRODUCTION

Second ACL injury risk remains high following ACL reconstruction (ACLR), indicating a need to improve rehabilitation and return-to-sport (RTS) assessment. Common assessments often do not probe for deficits in cognitive-motor function that can lead to higher-risk biomechanics during sports [1]. The clinical relevance of cognitive-motor function is further emphasized by ACL injuries commonly occurring in sports where athletes need to devote attention externally [2]. Dual-task screening provides a unique chance to detect movement impairments by testing cognitive and motor skills simultaneously [3]. To improve ACLR outcomes, it is crucial to investigate the role of cognitive-motor function in secondary ACL injury risk. This study aimed to evaluate the spectrum of dual-task impairments that persist following ACLR. We hypothesized that adding cognitive tasks would elicit riskier biomechanical predictors of second ACL injuries for ACLR patients compared to matched healthy controls.

METHODS

20 individuals who had undergone primary ACLR surgery and cleared to RTS (AR, 16F/4M, 19.8±1.4 yrs; 1.69±0.10 m; 68.0±14.9 kg, 1.6±0.6 yrs post ACLR; Tegner: 6.9±1.9; Marx: 11.3±4.8) and 20 healthy controls (HC, 16F/4M, 20.0±1.8 yrs; 1.70±0.08 m; 66.0±7.4 kg; Tegner: 6.2±1.6; Marx: 11.2±4.4) who were matched at an individual level on gender, age, dominant limb, BMI, sports activities, Tegner score and Marx activity score participated in this study. Kinematics and ground reaction force data were collected as participants performed a jump landing from a box followed instantly by a secondary jump (up, 45° right, 45° left). We used an inverse kinematics model in Visual 3D to calculate kinematic and kinetic outcomes. Conditions included: Baseline (NAD, anticipated direction, no cognitive task, no visual gaze constraint), Baseline with Visual Constraint (NAF, same as NAD but with looking at the fixation), Visual Unanticipated (VUF, secondary jump direction arrow was presented ~250 msec prior to initial contact with looking at the fixation), Auditory Unanticipated (AUD, secondary jump direction verbal cue played ~250 msec to initial contact), Auditory Unanticipated with Visual Constraint (AUF, same as AUD but with looking at the fixation), and Visual Memory (VAM, anticipated secondary direction with visual working memory task). Dependent variables were second ACL injury predictors [4], including uninvolvement hip rotation net moment impulse (**HM-Impulse** [Nm-s/kg]), limb asymmetry in knee flexor moment at initial contact normalized to the body weight and height (**KFM-IC** [%BW-HT]) and range of knee abduction angle for the involved limb (**KAbA-range** [°]) [4]. We considered age, gender, height, time since surgery, Tegner scale, Marx activity scale, and maximum jump height as potential covariates. Mixed effect statistical models tested for Group*Condition interactions as well as Group differences.

RESULTS AND DISCUSSION

No significant Group*Condition interaction was detected for any of the second ACL injury predictors. Significant Group differences were observed for **KAbA-range** ($p = 0.04$) and **KFM-IC** (**Figure 1**, $p = 0.002$), but not for **HM-Impulse** ($p = 0.069$). Post-hoc analysis showed the AR had riskier knee mechanics compared to HC, as evidenced by increased frontal plane knee motion (**KAbA-range**: 16.4±4.8° for AR and 15.71±4.6° for HC), and more knee extensor moment of uninvolvement relative to involved limb (i.e., decreased **KFM-IC**: $-3.1 \times 10^{-3} \pm 1.0 \times 10^{-3}\%$ for AR and $0.6 \times 10^{-3} \pm 8.4 \times 10^{-3}\%$ for HC), aggregated across conditions. Although the Group*Condition interaction did not reach significance, our preliminary data appear to show clustering of group differences for conditions with anticipated versus unanticipated directional constraints for **KFM-IC** (**Figure 1**), where AR individuals showed the largest deleterious differences compared to HC during unanticipated conditions (Cohen's d range: -0.64 to -0.70) relative to anticipated conditions (Cohen's d range: -0.06 to -0.04). It is noteworthy that data collection is ongoing for this study, highlighting the preliminary findings reported here.

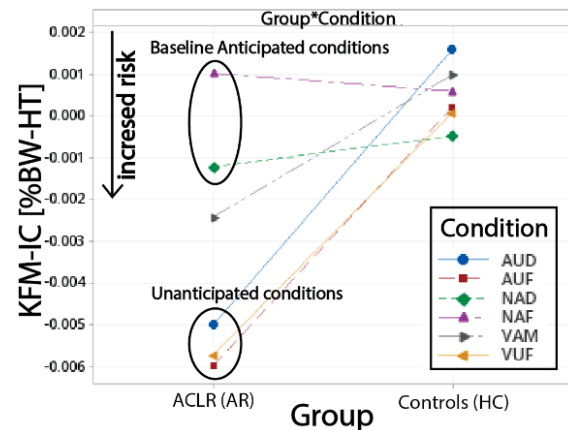


Figure 1: Interaction plot of KFM-IC, Group and Condition

CONCLUSIONS

The study results suggest that individuals with ACL reconstruction exhibit riskier knee mechanics than healthy controls during jump landing movements across scenarios with various additional constraints.

REFERENCES

- [1] Bertozzi et. al. (2023) Sports Health
- [2] Vargas et al. (2023) IJSPT 18(1): 122-131
- [3] Monfort et. al. (2019) Am J Sports Med 47(6):1488–1495
- [4] Paterno et al. (2010) AJSM 38(10)

ACKNOWLEDGEMENTS

Supported by the NIH award R03HD101093.

COMPARISON OF SEX-BASED BIOMECHANICAL MODELS TO A DEFAULT MODEL

Abigail R. Brittain¹, Cristian Sandino, and Tyler N. Brown

¹Biomedical Engineering PhD Program, Boise State University, Boise, Idaho
email: abbybrittain@boisestate.edu

INTRODUCTION

Joint kinetic analysis is dependent on accuracy of link-segment models. These models rely upon segment anthropometric parameters, including segment center of mass, moments of inertia, and geometry, which may not accurately represent participant anatomy. Visual 3D (C-Motion, Rockville, MD) is a biomechanics software commonly used for kinetic analysis that uses default segment anthropometric parameters that do not account for variation between the sexes, potentially producing inaccurate kinetic analyses. It is unknown if using models that include sex-specific segment properties alters joint kinetic output. We hypothesized that a sex-based biomechanical model would produce a significant alteration in ankle, knee, and hip joint moments compared to default Visual 3D model for females, but not males.

METHODS

Thirty-two participants, 14 females (21.2 ± 2.8 yrs., 66.6 ± 13.0 kg; 1.7 ± 0.1 m) and 18 males (21.7 ± 2.8 yrs., 82.9 ± 12.2 kg, 1.8 ± 0.1 cm) had motion captured of their lower-limb gait. Participants ran ($4 \text{ m/s} \pm 5\%$) five trials with a 20 kg body borne load.

A default, male, and female lower limb model, each consisting of 7 segments and 24 DOFs, were created in Visual 3D. The default model was built as described in [1], while the sex-specific models were built with segment properties published in [2]. Specifically, for each sex-based model, segment mass, mass moment of inertia, center of mass, and geometry were modified using male and female anthropometrics. Kinematic and GRF data recorded for each trial were filtered (fourth-order, low-pass Butterworth filter at 12 Hz), and processed in Visual 3D. Models were used to obtain dominant limb stance phase (heel strike to toe off) hip, knee, and ankle joint moments. Peak (both lower and upper bound) of stance hip, knee, and ankle joint moments were submitted to paired *t*-tests to compare joint kinetic data between default and male and female sex-specific models, respectively. Alpha was $p < 0.05$.

RESULTS AND DISCUSSION

Contrary to our hypothesis, the male sex-based model produced a significant alteration in lower limb joint moments compared to default model. At the ankle, the male sex-specific model

produced smaller peak dorsiflexion ($p = 0.007$), plantarflexion ($p = 0.005$), adduction ($p = 0.007$), abduction ($p = 0.023$), and eversion ($p = 0.007$) joint moments. However, it should be noted, compared to the default model, foot inertial properties of the male model differed more than those of the female model. The male sex-specific model also produced smaller knee extension ($p = 0.036$), internal ($p = 0.039$) and external rotation ($p = 0.029$) joint moments, but larger knee adduction ($p = 0.015$) moment. At the hip, male sex-specific model exhibited larger peak flexion ($p < 0.001$), extension ($p < 0.001$), and external rotation ($p = 0.011$) joint moments, and smaller hip abduction ($p = 0.003$) and internal rotation ($p = 0.039$) joint moments compared to the default model.

In agreement with our hypothesis, the female sex-based model did significantly alter lower-extremity joint kinetics compared to the default model. Interestingly, the majority of significant findings were at the knee, a location of high injury prevalence in females. The female sex-based model produced a significantly smaller peak ankle dorsiflexion ($p < 0.001$) joint moment, but significantly higher knee extension ($p < 0.001$), flexion ($p < 0.001$), adduction ($p = 0.049$), abduction ($p = 0.004$), and internal rotation ($p < 0.001$) moments compared to the default model. At the hip, the female sex-specific model produced larger flexion ($p = 0.032$) and external rotation ($p < 0.001$) joint moments.

CONCLUSIONS

Both male and female sex-based models produced significant alterations in hip, knee and ankle joint moments compared to the default Visual 3D model. Alterations are sex, segment, and plane specific. Considered jointly, the current findings support the need for sex-based biomechanical models in research.

REFERENCES

1. Brown et al. (2018), *J Biomech* **69**
2. Dumas et al., (2007), *J Biomech* **40**

ACKNOWLEDGEMENTS

Battelle Energy Alliance/Idaho National Laboratory, Natick Soldier Systems Center and Boise State's IIFTS supported this work.

Table 1: Mean \pm SD peak knee joint moments, reported as magnitudes, for each model.

Joint Moment (Nm)	Male		Female	
	Default	Sex-Based	Default	Sex-Based
Knee Extension	293.82 ± 61.52	208.57 ± 149.54	223.34 ± 37.50	248.85 ± 40.59
Knee Flexion	44.21 ± 14.95	50.27 ± 10.32	34.92 ± 12.22	48.01 ± 9.63
Knee Adduction	6.85 ± 9.96	13.78 ± 13.35	11.40 ± 6.77	17.28 ± 12.89
Knee Abduction	99.57 ± 31.72	76.79 ± 52.16	57.25 ± 22.80	64.65 ± 27.63
Knee Internal Rotation	63.89 ± 19.17	47.56 ± 34.87	47.18 ± 9.20	55.13 ± 8.56
Knee External Rotation	2.47 ± 1.49	7.47 ± 8.74	3.73 ± 1.82	4.68 ± 3.51



MARKERLESS - THE FUTURE OF MOTION CAPTURE

Easy to Use - No subject preparation, allowing you to quickly collect data in natural environments. All data processed automatically.

Validated Solution - Multiple peer reviewed articles showing repeatability, reliability, and accuracy published in the *Journal of Biomechanics*.

Ask New Research Questions - With Theia, you can collect massive amounts of data, and use it to ask new research questions. Collect biomechanics data that is not only descriptive, but also predictive.



HOW DOES THEIA3D WORK?



Record synchronized color video from a multi-camera system.



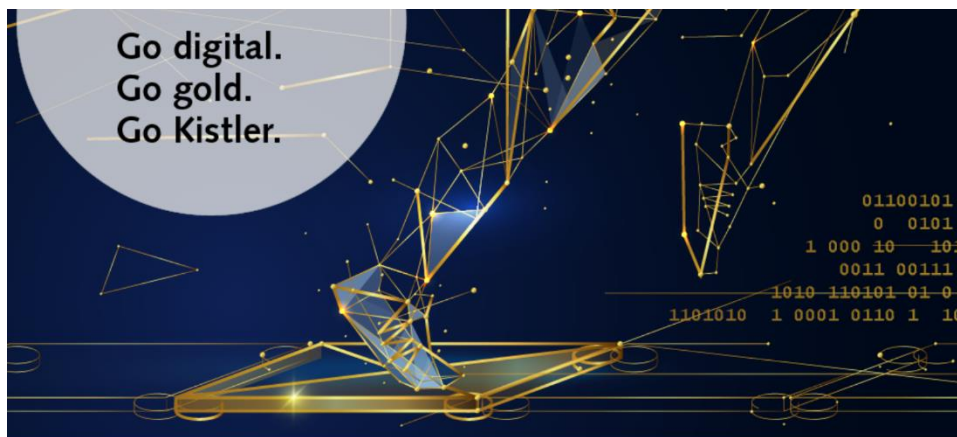
Theia3D's Artificial Intelligence automatically constructs a high-fidelity 3D model from key anatomical features.



Export your 3D model to Visual3D for integrated kinematic and kinetic analysis.



OUR TRUSTED CUSTOMERS



The new gold standard

Kistler unveils the new gold standard in force measurement: triple excellence, with cutting-edge digital technology, a seamless user experience, and superlative service and support.

www.kistler.com/biomechanics

KISTLER
measure. analyze. innovate.

Round-table Discussions

Friday, May 19

3:00 - 3:30 pm

and

Saturday, May 20

2:30 - 3:00 pm

Discussion Topics
<ul style="list-style-type: none">• Managing Work /Life Balance• Choosing Between Academics And Industry• Choosing A Postdoc Position• Tips To Writing A Good Grant• Demystifying The Grant Review Process• Applying For, Securing, And Starting A Faculty Position• Can We Find Alternatives To Lecturing In Biomechanics?• Any Questions You Have

Dinner and Games Friday Night

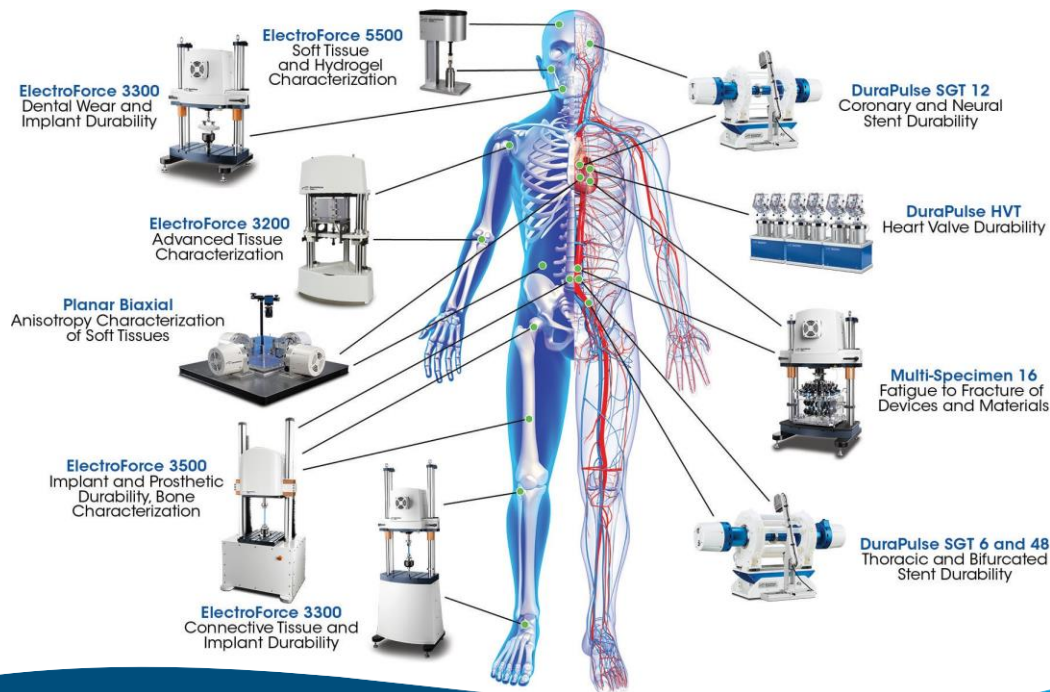
Dinner on Friday night is at HUB Games in the basement of the Husky Union Building (HUB) on campus (see map). There will be bowling, pool tables, table tennis, and video games. This will be an excellent opportunity to make connections and have fun with NWBS colleagues.

WiFi

UW NetID: event0142, Password: C9c8_R7t8_P8z9

Mechanical Test Solutions

Medical Device Fatigue and Tissue Mechanics



Waters™ | TA
Instruments

tainstruments.com

Better Data. Better Decisions.

Better Results.


Tekscan™

- Accurate & reliable pressure data
- Peer accepted & research validated system
- Synchronize with external systems



Objective plantar pressure data for enhanced gait analysis



Advanced intra-joint analysis for improved research outcomes



Ultra-thin sensors

+1.617.464.4281 1.800.248.3669 info@tekscan.com www.tekscan.com/medical

Visit the Tekscan booth for a demonstration!

Poster Session A

*Sponsored by the Mechanical Engineering Department
of the University of Washington*

Friday, May 19th

4:45-5:45 pm

Alder Commons

Poster #	
1	ACUTE SKELETAL MUSCLE FATIGUE REDUCES CELLULAR PASSIVE AND ACTIVE STIFFNESS Grace E. Privett, Austin W. Ricci, Jordan D. Cooper, Damien M. Callahan
2	THE EFFECT OF INCREASED SENSORY FEEDBACK FROM NEUROMODULATION AND EXOSKELETON USE ON ANKLE CO-CONTRACTION IN CHILDREN WITH CEREBRAL PALSY Charlotte D. Caskey, Siddhi Shrivastav, Heather Feldner, Kristie Bjornson, Chet T. Moritz, Katherine M. Steele
3	ESTIMATING CERVICAL VERTEBRAL POSE FROM EXTERNAL MARKERS Ozanich NR, Pascual FG, Vasavada AN
4	MANIPULATING IMPLEMENT WEIGHT DURING WARM UPS TO INCREASE SHOT PUT PERFORMANCE Klein, L. Graham, D. Whitten, J. McKibben, K., and Becker, J.
5	AWARENESS OF VISUAL OFFSET REDUCES BUT DOES NOT ELIMINATE UPPER LIMB MOVEMENT ERRORS IN VIRTUAL REALITY Motoki Sakurai and Andrew Karduna
6	GROUND REACTION FORCE DIFFERENCES BETWEEN CONCRETE AND BARK SURFACES DURING OUTDOOR RUNNING Anya Anand, Rachel Robinson, Michael Hahn
7	QUADRICEPS STEADINESS AND JERKY KNEE MOTION FOR INDIVIDUALS WITH KNEE MUSCULOSKELETAL INJURY AND DISEASE Nicholas L. Hunt, Matthew V. Robinett, Tyler N. Brown
8	SOCCER CLEAT STUD SHAPE AND FATIGUE STATE IMPOSE SEX-SPECIFIC DIFFERENCES IN KNEE MECHANICS Emily Karolidis, Michael E. Hahn

Poster Session A - cont.

9	PEAK TORQUE LIMB COMPARISON AND KINESIOPHOBIA CORRELATION POST-ACLR SURGERY Burr, B, Pollard, CD, Phillips, D, and Hannigan, JJ
10	LOWER EXTREMITY JOINT WORK IN THE NIKE VAPORFLY NEXT% COMPARED TO MINIMALIST FOOTWEAR Reyes, K, Jin, L, Westley, L, and Hannigan, JJ
13	SAGITTAL PLANE TESTING FOR INFANT PRODUCT SAFETY: PROOF OF CONCEPT STUDY Sarah Goldrod, Dr. Erin M Mannen
14	KINEMATICS OF THE FIRST METATARSOPHALANGEAL JOINT: BAREFOOT VS SHOD Eric Thorhauer, William R. Ledoux
15	THE EFFECTS OF SPINAL STIMULATION AND INTERVAL TREADMILL TRAINING ON JOINT KINEMATICS IN CEREBRAL PALSY Avocet Nagle-Christensen, Charlotte D. Caskey, Siddhi Shrivastav, Kristie Bjornson, Chet T. Moritz, Katherine M. Steele
16	THE EFFECTS OF MUSCLE FATIGUE ON LOWER EXTREMITIES BIOMECHANICS DURING LAY-UP AND LANDING IN RECREATIONAL BASKETBALL PLAYERS Brandon Yang, Li Jin
17	CLUSTERING SOCCER ACTIVITIES ASSOCIATED WITH INJURY Shealie Lock, Suliat Yakubu, Wendy Ma, Calvin Kuo
18	EXAMINING HOW MIDSOLE MATERIAL IMPACTS CENTER OF PRESSURE TRAJECTORIES DURING TREADMILL RUNNING Mackenzie N Pitts, Katherine M Steele, Cristine E Agresta
19	IDENTIFICATION OF TISSUE DAMAGE USING FINITE ELEMENT MODELS OF SPINAL CORD INJURY AND MACHINE LEARNING Cesar Jimenez, Mohamad Narimani, and Carolyn Sparrey
20	CADAVERIC SIMULATION OF FLATFOOT AND SURGICAL CORRECTIVE TECHNIQUES: THE EVANS VERSUS THE Z-OSTEOTOMY Corey Wukelic, Grant C. Roush, Eric C. Whittaker, James Meeker, Kelly Apostle, Bruce J. Sangeorzan, William R. Ledoux

Poster Session A - cont.

21	QUANTIFYING THE ACTIVITY LEVELS OF TODDLERS WITH DOWN SYNDROME PLAYING IN A PARTIAL BODY WEIGHT SUPPORT SYSTEM Mia E Hoffman, Reham Abuatiq, Katherine M Steele, and Heather A Feldner
22	THICKNESS OF DUAL-DENSITY METAMATERIALS INFLUENCES 3D-PRINTED INSOLE PROPERTIES Kimberly Nickerson, Ellen Li, Scott Telfer, William Ledoux, Brittney Muir
23	EFFECTS OF SUBMAXIMAL TREADMILL RUNNING ON PLANTAR FASCIA PROPERTIES IN RESOLVED PLANTAR FASCIITIS INDIVIDUALS Lukas Krumpal & Joshua P. Bailey
24	SEX-DIFFERENCES IN THE BIOMECHANICS OF SOFT TISSUE OVER THE HIP: ANALYSIS OF MUSCLE ACTIVATION AND HIP REGION. Fatemeh Khorami ; Carolyn J Sparrey
25	SEEING PROGRESS: AN AUGMENTED REALITY SYSTEM FOR ASSESSING AND VISUALIZING BIOMECHANICS Matthew A. Sielecki, Marianne S. Black
26	NOVEL METHODS TO ASSESS INTERFRAGMENTARY MOTION IN DISTAL FEMUR FRACTURES: COMPUTED TOMOGRAPHY VALIDATION Aerie Grantham, Elmer Vasquez, William D. Lack, William R. Ledoux
27	EFFECTS OF SHOE CUSHIONING ON KNEE LOADING DURING DOWNHILL RUNNING Lachlan Paige, Katie McKibben, Ashlyn Baird, Jim Becker
28	VALIDATION OF BIPLANE FLUOROSCOPY BONE TRACKING Nicholas Entress, Aerie Grantham, Eric Thorhauer, William R. Ledoux
29	THE EFFECTS OF A MEDITATION INTERVENTION ON SELF-REPORTED SUBJECTIVE AND PHYSIOLOGICAL STRESS IN COLLEGE STUDENTS Kara Lau, Sebastian Vargas, Rory McClelland, Katie Butte, Dale Cannavan
30	EFFECTS OF SURFACE STIFFNESS AND MASS ON HEAD IMPACT SEVERITY Omid Vakili, Stephen N. Robinovitch
31	PRELIMINARY DESIGN PROCESS FOR THE DEVELOPMENT OF A NEW ASSISTIVE WALKING DEVICE Kailey Diaz, Kimberly Nickerson, and Brittney C. Muir

Poster Session A - cont.

32	ACUTE FATIGUE MODIFIES MUSCULOTENDINOUS STIFFNESS J D Cooper, A W Ricci, D M Callahan
33	EXPLORING THE EFFECT OF PHYSICAL ACTIVITY ON IN VIVO PASSIVE STIFFNESS IN THE LUMBAR SPINE Chelsea M. Dumasal and Kayla M. Fewster
34	EFFECT OF UNANTICIPATED CONSTRAINT ON LOWER EXTREMITY ENERGY ABSORPTION DURING JUMP LANDINGS FOLLOWING ACL RECONSTRUCTION Brendan P. Silvia, Fatemeh Aflatounian, James N. Becker, Keith A. Hutchinson, Janet E. Simon, Dustin R. Grooms, and Scott M. Monfort
35	OCCUPATIONAL THERAPIST'S PERSPECTIVES ON THE HARMONY EXOSKELETON FOR POST-STROKE REHABILITATION Tiffani Teng, Clairra Geller, Matthew Stutzenberger, Abbey Lacey, Ileana Howard, Brittney C. Muir
36	COMPARING PEAK TIBIAL INTERNAL ROTATIONAL VELOCITY IN RECREATIONAL RUNNERS IN MAXIMAL AND TRADITIONAL SHOES Ory, J, Traut, A, Bartel, L, Phillips, D, Pollard, C, Hannigan, J

ACUTE SKELETAL MUSCLE FATIGUE REDUCES CELLULAR PASSIVE AND ACTIVE STIFFNESS

Privett, GE¹, Ricci, AW¹, Cooper, JD¹, Callahan, DM¹

Department of ¹Human Physiology, University of Oregon, Eugene, Oregon, USA

Web: <https://musclebiology.uoregon.edu/>

INTRODUCTION

Skeletal muscle stiffness, its resistance to deformation under load, is transiently reduced by a single bout of fatiguing exercise[1]–[3]. Because stiffness is related to athletic performance and soft-tissue injury risk, significant efforts have been made to identify and understand chronic modifiers of musculotendinous stiffness (resistance training and aging). However, the mechanisms of acute stiffness reduction by physiological stressors (fatiguing exercise) are poorly understood. Potential intracellular mechanisms may be elucidated by assessment of mechanical measures in single, permeabilized muscle cells (“fibers”). Therefore, the purpose of this study was to compare passive and active stiffness in single skeletal muscle fibers obtained from the fatigued and non-fatigued limbs of young adults.

METHODS

3 male and 6 female volunteers performed one bout of unilateral repeated knee extensions until task failure. Immediately after fatigue, bilateral percutaneous needle biopsies were performed on the fatigued (F) and non-fatigued (NF) Vastus Lateralis muscles. On a later day, single fibers were dissected from muscle samples and mounted between a force transducer and a length motor, enabling measurement of active and passive mechanical properties. To measure passive stiffness, single fibers (88 NF, 83 F) were passively and incrementally stretched (8%/step) to 156% initial sarcomere length (Fig. 1A). Each of the seven stretches was followed by 2 minutes of length-hold to allow for force relaxation. To measure active stiffness, a subset of fibers (65 NF, 56 F) were maximally activated (pCa 4.5) until steady state tension was achieved, whereupon they were quickly (100 ms) shortened by 20 μ m (1.24 \pm 0.44% fiber length) and force at this new length was averaged over 100 ms (Fig. 1B). In both conditions, force and length measures were recorded, allowing for subsequent calculation of stress and strain. Active and passive Young’s Modulus was calculated as $\frac{\Delta \text{Stress}}{\Delta \text{Strain}}$.

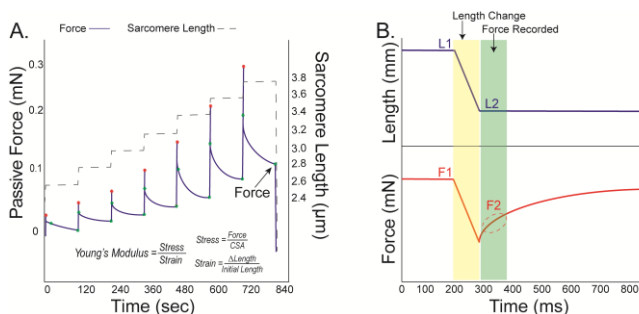


Figure 1: Protocols used to measure passive (A) and active (B) stiffness at the cellular level.

RESULTS AND DISCUSSION

Passive stiffness was higher at baseline in males versus females (34.3 \pm 17.9 vs. 25.3 \pm 9.7 kPa/%Lo, respectively, $p=0.04$, Fig. 2A), and was reduced by fatigue in both groups (NF: 29.10 \pm 14.36 vs. F: 18.25 \pm 8.56 kPa/%Lo, $p<0.01$). Passive stiffness reduction was greater in males versus females ($p=0.018$). Active stiffness at baseline was lower in males versus females (43.5 \pm 14.9 vs. 55.8 \pm 12.6 kPa/%Lo, respectively, $p<0.01$) and was reduced by fatigue (NF: 50.3 \pm 14.9 vs. F: 44.1 \pm 14.0 kPa/%Lo, $p=0.01$, Fig. 2B).

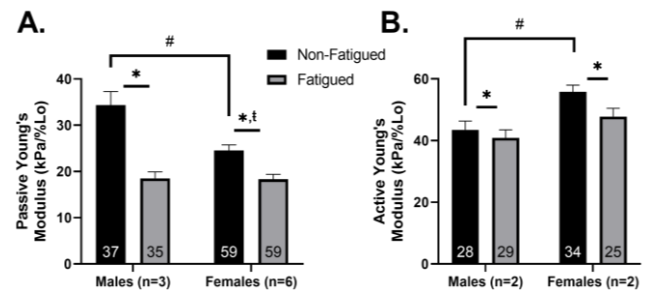


Figure 2: Passive (A) and active (B) Young’s Modulus is reduced at the cellular level by a single bout of fatiguing exercise. Intracellular proteins titin, actin, and myosin may contribute to these reductions. * Fatigue effect, # sex effect, † interaction. $\alpha=0.05$.

CONCLUSIONS

These results suggest acute fatigue reduces passive and active stiffness at the cellular level. The stiffness response to fatigue appears to differ based on biological sex. Stiffness reductions in both active and passive conditions point to multiple cellular mechanisms contributing to fatigue-induced compliance.

REFERENCES

1. E. Chalchat et al., “Changes in the viscoelastic properties of the vastus lateralis muscle with fatigue,” *Frontiers in Physiology*, vol. 11, p. 307, 2020.
2. P. Andonian et al., “Shear-wave elastography assessments of quadriceps stiffness changes prior to, during and after prolonged exercise: a longitudinal study during an extreme mountain ultra-marathon,” *PLoS One*, vol. 11, no. 8, p. e0161855, 2016.
3. J. Siracusa et al., “Resting muscle shear modulus measured with ultrasound shear-wave elastography as an alternative tool to assess muscle fatigue in humans,” *Frontiers in physiology*, vol. 10, p. 626, 2019.

ACKNOWLEDGEMENTS

This work was supported by funds from the Wu Tsai Human Performance Alliance. Many thanks are also due to the research volunteers, who make these studies possible.

THE EFFECT OF INCREASED SENSORY FEEDBACK FROM NEUROMODULATION AND EXOSKELETON USE ON ANKLE CO-CONTRACTION IN CHILDREN WITH CEREBRAL PALSY

Charlotte D. Caskey¹, Siddhi Shrivastav^{2,3}, Heather Feldner², Kristie Bjornson^{2,3}, Chet T. Moritz², Katherine M. Steele¹

Departments of ¹Mechanical Engineering and ²Rehabilitation Medicine, University of Washington, Seattle, WA

³Seattle Children's Research Institute, Seattle, WA

email: cdcasky@uw.edu

INTRODUCTION

Children with cerebral palsy (CP) have a brain injury around the time of birth that impairs motor control, often causing co-contraction of antagonistic muscles which alters movement and increasing energy costs [1]. Increasing sensory feedback prompts greater supraspinal input during tasks and improves control of muscle activity [2-3]. New methods to support and provide sensory feedback may help to reduce co-contraction and improve walking in CP.

Transcutaneous spinal cord stimulation (tSCS) is a novel, non-invasive neuromodulation technique that activates sensory pathways to amplify communication in the nervous system via Ia afferent pathways [4]. In addition, ankle exoskeletons have been shown to alter motor control in CP and may support sensorimotor integration by amplify the sensory feedback during walking [5]. This study sought to evaluate the effect of increased sensory feedback from tSCS and a resistive ankle exoskeleton (Exo) on ankle co-contraction during walking. We hypothesized that ankle co-contraction would decrease when walking with tSCS and the ankle exoskeleton.

METHODS

We quantified co-contraction during walking with (1) no devices, (2) tSCS, (3) Exo, and (4) tSCS and Exo together for five children with CP (10.4±4.5 yrs, GMFCS I-II; 4 male). All walking was performed on a treadmill (Bertec) and totalled 20 minutes at a self-selected speed (91±22 m/s), kept consistent for each child across sessions. Walking tasks were performed on separate days a minimum of five days apart in a convenience randomized order. Electromyography (EMG) data were recorded bilaterally (2000 Hz; Delsys, Inc.) on the soleus and tibialis anterior muscles. EMG data were high-pass filtered (20 Hz), rectified, low-pass filtered (10 Hz), normalized to the 95th percentile, and segmented by gait cycle. Results presented here show the co-contraction of these muscles during stance, defined as the first 60% of the gait cycle, during the final one minute of each session. Co-contraction index (CCI) was calculated as:

$$CCI (\%) = \frac{2I_{ant}}{I_{tot}} \times 100$$

Where I_{ant} is the is antagonistic muscle activity and I_{tot} is the sum of both the agonist and antagonist EMG activity [6].

RESULTS AND DISCUSSION

Children with CP displayed higher levels of co-contraction, 40-80% during baseline walking with no devices compared to prior reports of nondisabled children [1]. Compared to baseline walking, tSCS reduced ankle co-contraction on the less-affected side (Figure 1). Ankle co-contraction increased or stayed the same as baseline during the Exo and Exo+tSCS conditions. These results suggest that tSCS may lead to reduced ankle co-contraction in just one walking session, but that the less-affected side of the body may respond faster than the more-affected side.

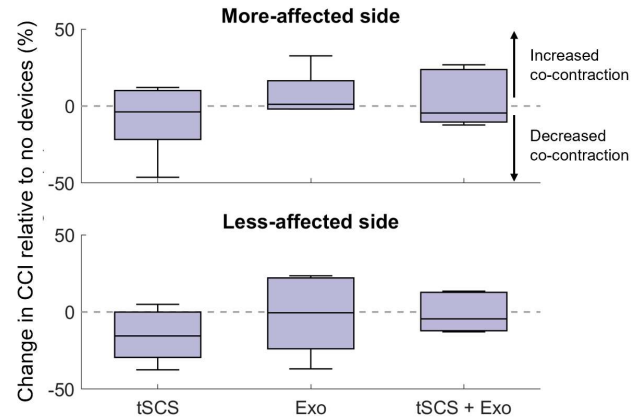


Figure 1: Co-contraction index (CCI) between the soleus and tibialis anterior muscles during walking with no devices (walk), with spinal stimulation (tSCS), with the resistive ankle exoskeleton (Exo), and walking with the tSCS and Exo together (tSCS + Exo).

Gad et al. (2021) also reported a 20% reduction in ankle co-contraction with tSCS applied in a single 30-min session for 9 children with CP [4]. Repeated visits may be needed to reach a response on the more-affected side. The Exo did not have the same effect as tSCS, which may be because the Exo makes the walking task more challenging while increasing sensory feedback. As a results, participants may be fatiguing faster or maintaining high co-contraction to provide extra stability at the ankle. These results also suggests that how the user responds to each device individually may not accurately predict how they respond when devices are used together. Overall, high variability in responses suggests there may be other factors affecting response, such as age, GMFCS level, or mental focus.

CONCLUSIONS

This study demonstrates the potential of combining the Exo and tSCS for treadmill gait training and the effect on coordination of ankle muscle activity for children with CP. We highlight the importance of considering device interactions in rehabilitation and how changes in neuromuscular activity in a single visit may inform long-term, rehabilitative impacts of multimodal device use.

REFERENCES

1. Unnithan et al. *Med Sci Sports Exerc* **28**, 1996.
2. Côté et al. *J Neurosci Res* **24**, 2004.
3. Samejima et al. *PTJ* **103**, 2022.
4. Gad et al. *Neurotherapeutics* **18**, 2021.
5. Conner et al. *Ann Biomed Eng* **48**, 2020.
6. Falconer and Winter *Electromyogr Clin Neurophysiol* **25**, 1985.

ACKNOWLEDGEMENTS

This work is supported by NSF GRFP Award DGE-1762114 and SCH CP Research Pilot Study Fund 2022 Award.

ESTIMATING CERVICAL VERTEBRAL POSE FROM EXTERNAL MARKERS

Ozanich NR¹, Pascual FG², Vasavada AN^{1,3}

¹Voiland School of Chemical Engineering and Bioengineering, ²Department of Mathematics and Statistics

³Department of Integrative Physiology and Neuroscience, Washington State University, Pullman, WA, USA

email: nicholas.ozanich@wsu.edu

INTRODUCTION

Excessive flexion angles of the neck that are intensified by mobile device use are associated with neck pain [1]. The forward position of the head causes an increased gravitational moment [2], resulting in increased spinal loads and muscle fatigue. Musculoskeletal models can be used to predict spinal loads, but previous work has shown that using common assumptions for elucidating the pose of the cervical vertebrae (position and orientation) from external angles does not provide accurate model results compared to using vertebral pose acquired from X-ray images [3]. External marker data is an attractive alternative due to accessibility and the elimination of radiation exposure, but a significant amount of information about the vertebral pose needs to be estimated. Here, we explore a variety of methods aimed at accurately estimating cervical vertebral pose using 5 external markers. We investigated the application of prediction models (linear regression, neural networks) and the feasibility of OpenSim's [4] inverse kinematics (IK) with varying degrees of freedom (DOF). We hypothesized that linear regressions would perform best due to the limited sample size for the neural network to fit on and uncertainty as to how accurate inverse kinematics would be.

METHODS

The data used were collected in an ergonomics study on tablet use [2]. Simultaneous lateral X-ray images and external photos were taken in 5 conditions (postures) for 30 subjects. For all models, predictors were x-y position (cm), relative to the sternal notch, of the canthus, tragus, C7 spinous process, and iliac crest. Predicted variables were the x-y position and angle of C1-C7. To overcome the limited dataset (n=150), we employed a leave-one-subject-out methodology, where we set aside each subject's 5 postures as validation and averaged the error metric of mean absolute error (MAE). We also qualitatively assessed the shape of the predicted cervical spine pose. We used the following models for comparisons: multivariate linear regression (LR), multivariate regression with covariance estimators (MRCE) [5], a shallow neural network (NN), 24 DOF neck model for OpenSim IK (independent rotations at each vertebral level), and a 3 DOF neck model for OpenSim IK (kinematically constrained rotations).

The multivariate linear regression and neural networks were implemented in Python using scikit-learn and Keras from TensorFlow, respectively. The neural network had 3 hidden layers with 64 units each and trained 100 iterations. MRCE was done in R. We used Python to interface with the OpenSim API to run inverse kinematics. We used the Scale Tool in OpenSim

to register the markers, then we locked the movement to only allow cervical vertebral rotation for inverse kinematics.

RESULTS AND DISCUSSION

We found that the linear regression models were the most accurate. MRCE and LR were comparable and outperformed every other model. The NN model commonly predicted nonphysiological neck shapes. The small dataset and the nature of discontinuous static postures likely made it difficult for the NN to properly fit. In addition, this study only evaluated sagittal plane neutral and flexed postures, and the results would be different for continuous three-dimensional postures in a larger range.

OpenSim's inverse kinematics is widely used for human gait. We wanted to explore its use for returning accurate cervical vertebral poses. In terms of MAE, IK resulted in much worse predicted positions and angles. We hypothesize that given 1) time-series data and 2) more markers may allow inverse kinematics solvers and neural networks to perform better.

CONCLUSIONS

Getting accurate inputs to biomechanical models is crucial to receiving accurate outputs from the model. In the case of the neck, the inputs of cervical vertebral pose need to be acquired through X-ray imaging. Accurately predicting these inputs will minimize the cost and risk to individuals and enable ergonomics studies in more natural working environments. Future plans in this project are to use outputs of these predictive models in OpenSim to investigate the effects on spinal loading.

REFERENCES

- [1] Xie, Y., *et al.*, *Applied Ergonomics*, 2017, 59: 132-142
- [2] Vasavada, AN., *et al.*, *Ergonomics*, 2015, 8(6): 990-1004
- [3] Vasavada, AN., *et al.*, *Annals of Biomed Eng*, 2018, 46(11): 1844-1856
- [4] Delp, SL, *et al.*, *IEEE Trans Biomed Eng*, 2007, 54(11):1940-1950
- [5] Rothman, AJ, *et al.*, *J Comput Graph Stat*, 2010, 19(4): 947-962

ACKNOWLEDGEMENTS

We want to thank Ellis Hughes, Rebecca Hsieh, Charles Leahy, John Einsten, and Dr. Xianglong Wang for their contributions to this project. We thank the Office Ergonomics Research Committee for funding support for the subject data collection. This material builds upon work done for the 2021-2022 WSU Bioengineering Senior Capstone.

Table 1: Results from the various prediction models. MAE over all subjects, conditions, and vertebral levels.

	LR	MRCE	NN	24 DOF IK	3 DOF IK
X error (cm)	0.512	0.537	0.765	2.978	3.649
Y error (cm)	0.750	0.703	1.811	1.347	1.442
Angle error (degrees)	5.888	6.155	6.976	12.736	9.072

MANIPULATING IMPLEMENT WEIGHT DURING WARMUPS TO INCREASE SHOT PUT PERFORMANCE

Klein, L. Graham, D. Whitten, J. McKibben, K., and Becker, J.

Department of Health & Human Development, Montana State University, Bozeman MT USA

email: lnklein.msu@gmail.com, www.montana.edu/biomechanics

INTRODUCTION

There is a relatively large body of literature examining methods for improving shotput performance. One topic of recent interest is the application of post-activation potentiation (PAP), a phenomenon whereby a muscles contractile history can increase its ability to generate force in subsequent contractions. Previous research on shot putting shows improved performance benefits from using PAP stimuli such as sprinting, jumping or bench pressing before throwing [1,2]. PAP may also be leveraged through use of overweight implements during warm-ups to improve performance in weight throwing and over the head backwards shot putting [3,4]. However, the impacts of overweight and underweight implement warmups on rotational shot put performance are still unknown. Thus, the goal of this study was to evaluate the impacts overweight and underweight warm up throws have on performance, force development and critical factors of technique in the rotational shot-put.

METHODS

Ten collegiate shot putters (6 males, 4 females) participated in this study. Data was collected on three non-consecutive days. Each day, participants performed three warm-up throws and six maximal effort competition throws. All competition throws were performed using regulation weight implements (men: 7.26 kg, women: 4.00 kg) however warm up throws were randomized to either overweight (men: 8.16 kg, women: 4.53 kg) or underweight (men: 6.35 kg, women: 3.00 kg) on days two and three. Rest time between throws was 3-minutes.

Throwing distance was measured using a tape measure while ground reaction forces were recorded using a custom throwing circle containing two force plates (Accupower, AMTI, Waltham MA, USA). Impulse, peak force, and peak rate of force development from time of foot touch down (either rear foot touch down (RFTD) or front foot touch down (FFTD), respectively) through REL were calculated. Whole body kinematics were recorded using 16-inertial sensors set to export at 120 Hz (IMU, MVN Link System, Xsens Technologies B.V, Enschede, Netherlands). Critical factor kinematics including pelvis-torso separation at RFTD, rear leg hip flexion at RFTD, rear leg knee flexion at RFTD, peak pelvis angular velocity between RFTD and Release were then identified.

Within participants, dependent variables from the three throws in each condition were averaged. A 2 (sex) x 3 (condition) mixed analysis of variance was used to evaluate differences between conditions, with an alpha of .05 to indicate statistical significance. Effect sizes (Cohen's d) were calculated for all pair-wise comparisons, and interpreted in the ranges of <0.2 small, 0.4 0.6 moderate, > 0.8 large.

RESULTS AND DISCUSSION

There was a significant main effect of weight for throw distance ($F_{2,16} = 4.123$, $p = .036$), with participants throwing further in

the PH than the BASE ($p = .002$, $d = .306$, Figure 1). There were no statistically significant differences between conditions for any of the critical factor kinematics or ground reaction force variables.

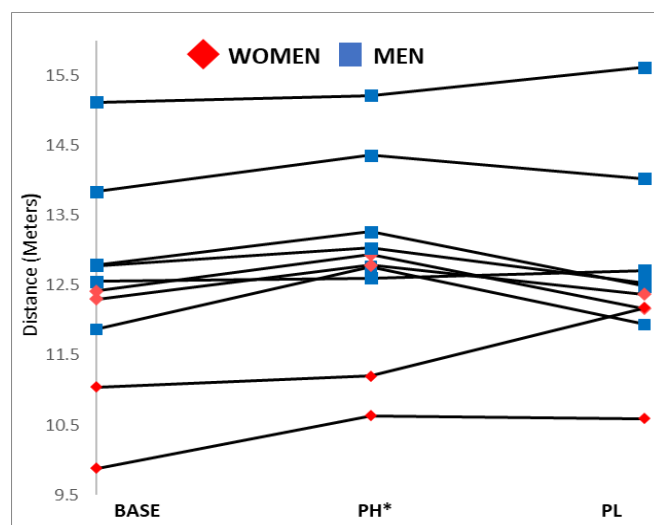


Figure 1: Throwing distance (Meters) vs. Condition; baseline (BASE), Post Heavy (PH) and Post Light (PL).

The lack of differences within measured kinematics and GRF variables between conditions suggests the improved throw distance in the PH condition may be due to other factors such as more optimal projectile release conditions or mechanistic changes in muscle function due to PAP. Clarification of which requires further investigation. However, the lack of differences also means there were no negative changes associated with manipulating implement weight during warmup. Thus, the use of overweight and underweight implements may be useful for periodizing training without negatively impacting technique.

CONCLUSIONS

The use of an overweight implement during warmups improves rotational shot-put throw distance without changing the critical factor kinematics or ground reaction forces of the throw. Since competition rules allow athletes to weigh in heavier implements for warmups, the use of this strategy could be one way for athletes or coaches to improve performance in competitions.

REFERENCES

1. Evetovich et al., 2015. Journal of Strength and Conditioning Research, 29(2),336-342.
2. Terzis et al., 2012. Journal of Strength and Conditioning Research, 26(3), 684-690.
3. Judge et al., 2016. Journal of Strength and Conditioning Research, 30(2), 438-445.
4. Bellar et al., 2012. Journal of Strength and Conditioning Research, 26(6), 1469-1474.

AWARENESS OF VISUAL OFFSET REDUCES BUT DOES NOT ELIMINATE UPPER LIMB MOVEMENT ERRORS IN VIRTUAL REALITY

Motoki Sakurai¹ and Andrew R. Karduna¹

¹Department of Human Physiology, University of Oregon, Eugene OR, USA

email: motokis@uoregon.edu, web: <https://karduna.uoregon.edu/>

INTRODUCTION

While humans integrate vision and proprioception to accurately reach to a target, they generally weigh vision more heavily than proprioception [1]. Additionally, a motor learning study found that visual input could not be disregarded when participants were informed about a visual offset and asked to ignore vision [2]. However, it is not known whether humans can ignore visual input for a reaching task where motor adaption over trials is not involved. In the present study, we investigated the effect of visual offset when participants were instructed to ignore vision during a joint repositioning study. It was hypothesized that 1) induced visual offsets would result in repositioning errors consistent with the direction of the offset, and 2) the same trend in joint repositioning error would be observed when participants were informed about offsets and asked to ignore vision.

METHODS

Twenty-five healthy participants (female/male: 13/12 age: 22.7 ± 5.3 yr, height: 1.7 ± 0.1 m, weight: 71.5 ± 13.6 kg) performed a joint position sense (JPS) test in an immersive virtual reality environment (HTC VIVE, Taoyuan, Taiwan). Auditory cues guided the participants to reach and remember a target shoulder flexion angle (85, 90, 95, or 100°). Participants were then asked to replicate the target angle as accurately as possible, without auditory cues. A black marker represented real-time hand position throughout the trial. Each target was presented three times for a total of 12 trials. There were total of 3 blocks of 12 trials. The first block was a familiarization block, where no visual offset was introduced any of the 12 trials. Following the first block, two offset blocks (OB1 and OB2) were completed, where the task and settings were identical. The only difference between the two offset blocks was that in OB2 block, participants were informed about the visual offset and asked to ignore vision. In the two offset blocks (OB1 and OB2), 4 out of 12 trials did not have a visual offset (0° offset), 4 trials had a -8° vertical offset in the black marker position, and 4 trials had a +8° vertical offset in the black marker position. For all blocks, target angles were presented in a random order (12 trials per block – 3 offset conditions x 4 target angles).

Constant error (CE) was calculated for each condition (-8, 0, +8 offset) by taking the difference between the target angle and replicated angle and averaging across trials. A two-way repeated measures ANOVA was used, with one dependent variable (constant error) and two independent variables (visual offset and block).

Pairwise t-tests with the Bonferroni correction were performed for post-hoc testing when a significant effect or interaction was observed. For all the statistical tests, the alpha level was set at

0.05. All statistical analyses were performed using R 4.2.2 (R Core Team).

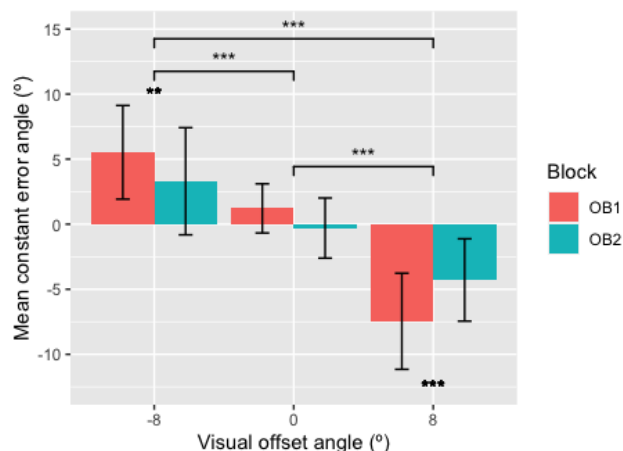


Figure 1: Mean CE with different visual offsets in OB1 and OB2 across participants. ***: $p < .001$, **: $p < .01$.

RESULTS AND DISCUSSION

A significant main effect of visual offset ($p < 0.001$) and an interaction effect ($p < 0.05$) were found. Follow up post-hoc testing revealed that CE was larger in the trials with a visual offset than without a visual offset ($p < 0.001$). CE was also larger in OB1 than OB2 only when a visual offset was introduced ($p < 0.01$). These results support the findings from a previous study in our lab which demonstrated that a visual offset results in an increase in reaching error [1]. It also demonstrated that awareness of visual offset caused smaller reaching errors, though errors were not completely eliminated. These results suggest that humans may integrate vision to some extent for reaching motions regardless of its accuracy when present.

CONCLUSIONS

Our hypotheses were mostly supported that humans weigh vision more heavily than proprioception during a reaching movement, and reaching error still occurs even when they are aware of visual offsets. However, it was not expected that awareness of visual offset would somewhat contribute to reduce JPS error.

REFERENCES

1. Spitzley KA & Karduna AR. *J Motor Behavior*. **54**(1): 92-101, 2022.
2. Morehead JR et al. *J Cognitive Neuroscience*. **29**(6): 1061-107, 2017

GROUND REACTION FORCE DIFFERENCES BETWEEN CONCRETE AND BARK SURFACES DURING OUTDOOR RUNNING

Anand, A¹, Robinson, R¹, Hahn, M¹

¹Neuromechanics Laboratory, Department of Human Physiology, University of Oregon

Email: aanand@uoregon.edu

INTRODUCTION

Ground reaction force (GRF) variables are frequently considered regarding running-related injuries. Previous studies demonstrated associations between higher impact-related GRF variables and risk of common running-related injuries [1]. A common belief amongst runners and clinicians is that softer surfaces assist in reducing running impact. Surfaces with different compliance account for noted changes in joint angles and joint angular velocities [2]. These kinematic differences suggest that there may be GRF differences across surfaces. Other lab-based studies have demonstrated that runners change leg stiffness in response to surface stiffness, minimizing center of mass displacement as well as peak GRF changes [3]. Force-sensing insoles measuring normal forces between the foot and shoe are reliable sensors comparable to force-sensing devices only found in laboratories [4]. Insoles may provide insights to the mechanical demands of outdoor running by profiling the effect of real-world running surfaces on GRF parameters.

The purpose of this study was to determine the outdoor running surface with the least biomechanical load on the body, through measurements of peak normal ground reaction force (pGRF), vertical average loading rate (VALR), average force, and impulse (IMP) on bark and concrete. It was hypothesized that a bark running surface will yield lower GRF values than a concrete running surface.

METHODS

Institutional Review Board approval was obtained prior to data collection and all participants provided informed consent. Fourteen healthy recreational runners (age: 24, height: 173 cm, mass: 64 kg) completed a 5-mile outdoor run which included uphill, downhill, level ground, concrete, and bark path sections. Each runner was equipped with a GPS watch (Garmin, Olathe, KS, USA) and force-sensing insoles (Novel, St. Paul, MN, USA) throughout the run. GPS data were collected at 1Hz, and force-sensing insole data were collected at 100 Hz. All runs were performed at a self-selected pace.

Custom MATLAB programs were employed for analysis. GPS data were utilized to identify level ground sections of the course for each surface condition where participants maintained a constant speed (rounded to the nearest 0.25 m/s) for at least 20 consecutive right footsteps. While speeds varied between participants, the selected bark and concrete sections

within each participant were run at the same speed. The pGRF, average force, IMP, and VALR were calculated for each right footstep. The IMP was calculated as the time integral of GRF. The VALR was calculated as the average slope of the middle 60% of GRF from initial contact to impact peak. The mean and standard deviation of pGRF, VALR, average force, and IMP were calculated for 20 steps of bark and 20 steps of concrete for each participant. A paired t-test was used to determine whether GRF variables differ between surfaces.

RESULTS AND DISCUSSION

Average running speed run amongst all participants was 3.57 m/s (range: 2.75-4.0 m/s). No significant differences in pGRF, VALR, average force, or IMP were detected between bark and concrete surfaces (Table 1). This is consistent with previous lab-based studies that evaluated the effect of surface on peak vertical GRF [3]. These observations further demonstrate that VALR, IMP, and average force are unaffected by surface stiffness in real-world outdoor running as well. This study presents with some limitations. Specifically, type and mileage of footwear wasn't controlled amongst participants. Differences in footwear construction and mileage could impact the results. Additionally, there are inherent errors in GPS measurement, which may affect the accuracy of running speed data. Future studies should consider analyzing GRF parameters on a third running surface: a track running path.

CONCLUSIONS

No significant differences in GRF variables were detected between bark and concrete surfaces in this investigation. While other biomechanical variables may change in response to running surface, these findings indicate that GRF variables do not. Therefore, runners who are seeking to reduce impact loading may choose either running surface, as they will yield relatively similar ground reaction forces.

ACKNOWLEDGEMENTS

This work was supported by the Wu Tsai Human Performance Alliance and the Joe and Clara Tsai Foundation.

REFERENCES

- [1] Johnson et al., *A J Sports Med*, 2020, 48(12)
- [2] Dixon et al., *MSSE*, 2000, 32(11)
- [3] Ferris et al., *Proc Biol Sci*, 1998, 265(1400)
- [4] Renner et al., *Sensors*, 2019, 19(2)

Table 1: Average and standard deviation of four ground reaction force variables for 14 healthy subjects. ($p < 0.05$)

Running Surface	Peak Vertical GRF (BW)	Average Vertical Loading Rate (BW/s)	Average Vertical GRF (BW)	Vertical Impulse (BW*s)
Bark	2.29 ± 0.07	37.01 ± 4.52	1.32 ± 0.05	0.36 ± 0.01
Concrete	2.30 ± 0.06	38.74 ± 4.32	1.32 ± 0.04	0.35 ± 0.01
p-value	0.79	0.34	0.93	0.13

QUADRICEPS STEADINESS AND JERKY KNEE MOTION FOR INDIVIDUALS WITH KNEE MUSCULOSKELETAL INJURY AND DISEASE

Nicholas L. Hunt¹, Matthew V. Robinett², Tyler N. Brown^{1,2}

¹Biomedical Engineering PhD Program, and ²Department of Kinesiology, Boise State University, Boise, ID, USA
email: nichunt@u.boisestate.edu

INTRODUCTION

Knee instability, characterized as joint buckling, shifting, or giving way during weight-bearing activity, is reportedly a pathogenic factor for joint musculoskeletal injury and disease [1]. Adequate quadriceps strength and contraction steadiness may prevent knee instability to mitigate injury and disease development. Although quadriceps steadiness is related to poor physical function, it is unknown if it decreases with knee musculoskeletal injury and disease, or whether it is related to “jerky” knee motion that may characterize joint instability [2]. We hypothesize that individuals with knee injury and disease will exhibit less quadriceps steadiness and jerkier sagittal and frontal plane knee motions, and quadriceps steadiness would exhibit linear relation to jerkiness of knee motion.

METHODS

Four groups (1: adults with confirmed musculoskeletal injury (ACL-R), 2: disease (OA), and sex- and age-matched controls (3: to ACLR and 4: to OA)) participated. Each participant performed three knee extensor maximal voluntary isometric contractions (MVIC) on an isokinetic dynamometer (HUMAC NORM, CSMI, Stoughton, MA, USA) and three walk trials at a self-selected speed through the motion capture volume.

The MVIC trial with highest maximal torque was bandpass filtered (3.9 to 31.2 Hz), linearly detrended, and submitted to a Fast Fourier Transform. Then, quadriceps steadiness measures, including peak power frequency (PPF), defined as frequency with the highest power, and coefficient of variance (CV), defined as the ratio of filtered torque standard deviation by mean of raw torque, were calculated according to [3].

For the walk task, 3D marker trajectories were collected using ten high-speed optical cameras (240 Hz, Vantage, Vicon Motion Systems LTD, Oxford, UK). For each trial, the marker data was lowpass filtered (12 Hz, 4th order Butterworth) and processed in Visual 3D (C-Motion, Rockville, MD) to obtain frontal and sagittal plane jerk cost, according [2].

For statistical analysis, quadriceps steadiness (CV and PPF), and sagittal and frontal plane knee jerk cost during early (0-17%), mid (17-34%), and full stance (0-100%) were submitted to a one-way ANOVA. Correlation analysis determined relation between quadriceps steadiness and knee jerk cost for all participants and each cohort. Alpha level was $p < 0.05$.

RESULTS AND DISCUSSION

Knee injury and disease impacted every quadriceps steadiness and knee jerk measure except CV (all: $p < 0.005$). In partial agreement with our hypothesis, the ACLR cohort exhibited 66% greater PPF ($p = 0.047$), and a 33-42% reduction in sagittal and frontal plane knee jerk cost than matched controls (all: $p < 0.001$); whereas, the OA cohort exhibited no difference in quadriceps steadiness, yet a 34-45% reduction in sagittal and frontal plane jerk cost compared to matched controls (all: $p < 0.001$). Individuals with knee injury and disease may adopt

gait biomechanics to increase joint stability and protect from further soft-tissue degradation, however, it is unclear whether these mechanics compensate for neuromuscular deficits.

Individuals with less steady quadriceps contraction may minimize knee joint motion to provide stability and protect from hazardous soft-tissue loading. Participants exhibited a significant positive relation for CV with midstance sagittal plane jerk cost ($r = 0.482$, $p = 0.011$), and contrary to our hypothesis, a significant moderate, negative relation between PPF to sagittal and frontal plane knee jerk cost during each stance phase (**Figure 1**) (all: $r = -0.440$ to -0.539 , $p < 0.022$). Yet, following knee injury, individuals with less steady quadriceps contraction may exhibit jerkier knee motion when loading the limb in early stance. The ACLR cohort exhibited strong, negative correlations between CV and early stance frontal plane jerk cost ($r = -0.774$, $p = 0.041$), but strong, positive correlation between PPF and early stance frontal plane jerk cost ($r = 0.835$, $p = 0.020$). The OA cohort exhibited strong, positive correlations between PPF and sagittal plane jerk cost during each stance phase ($r = 0.784$ to 0.830 , $p < 0.037$), but further work is needed to determine whether this is a consequence of joint disease or age-related changes to muscle, as OA participants were significantly older than the ACLR cohorts.

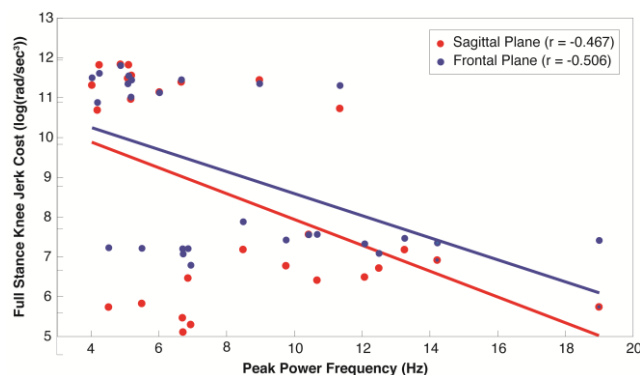


Figure 1: Depicts relation between PPF and full stance sagittal (red) and frontal plane (blue) jerk cost.

CONCLUSIONS

Knee musculoskeletal injury and disease impacted quadriceps steadiness, but lead to a decrease in jerky knee motion. Although individuals with less steady quadriceps contractions may minimize jerky knee motion, and potential soft-tissue loading, future work is needed to determine whether quadriceps neuromuscular deficits contribute to the development and progression of degenerative joint disease.

ACKNOWLEDGEMENTS

NIH NIA (R15AG059655) and NIGMS (2U54GM104944) supported this work.

REFERENCES

1. Blalock et al., *C Med Ins Arth Musc Disord* **8**, 15-23, 2015.
2. Krammer et al., *Gait Posture* **84**, 221-226, 2021.
3. Satam et al., *Clin Biomech* **99**, 105736, 2022

SOCCER CLEAT STUD SHAPE AND FATIGUE STATE IMPOSE SEX-SPECIFIC DIFFERENCES IN KNEE MECHANICS

Karolidis, E¹ and Hahn, ME¹

Department of ¹Human Physiology, University of Oregon

email: ekarolid@uoregon.edu

INTRODUCTION

Anterior cruciate ligament (ACL) injury incidence occurs at a 3-time higher rate in female soccer athletes than in males [1]. This sex-based disparity is associated with differences in neuromuscular control, joint laxity, and anatomical alignment, altering kinetic and kinematic performance profiles [2]. These differences widen with fatigue, furthering the risk of injury in females [3].

Despite mechanical differences between sex, soccer footwear is designed for male users. With known sex differences in movement patterns and joint loading, it should not be assumed that females are able to withstand the same amount of traction as males. High traction footwear may exacerbate female susceptibility to torsional injury mechanisms, such as those of ACL injury, if rotational resistance exceeds ligament loading capacity [4]. Cleat outsole properties, such as stud shape, are moderators of rotational resistance at the shoe-surface interface [4]. However, the effect of stud shape on female mechanics remains unknown. The purpose of this ongoing study is to investigate the influence of soccer cleat stud shape, elliptical and bladed, on the knee mechanics of male and female athletes pre- and post-fatigue.

METHODS

College-aged soccer athletes (n = 20 in progress; 1 male, 1 female reported) performed two data collections. For each visit, cleated footwear of different stud shapes was worn- bladed (adidas Predator .2), or elliptical (adidas Copa Sense .3). Cleat order was randomized for each subject.

Athletes performed sport-specific activities in a turf facility before and after a fatigue protocol. A 19-camera system (Vicon, 100 Hz) collected the trajectories of 28 retroreflective markers, while 4 force platforms (AMTI, 1500 Hz) recorded ground reaction force data. Athletes performed 6 cuts (80% maximum speed to unanticipated 120° cut, 3 trials each direction), representing the pre-fatigue state. A field-based fatigue protocol, developed to challenge aerobic and anaerobic energy systems, was then completed. After, the athlete repeated the cut

tasks, representing the fatigued state. Peak knee valgus angle, internal knee extensor moment at peak knee flexion and anterior tibiofemoral shear force were calculated using inverse dynamics, pre- and post-fatigue, and compared across cleat conditions in male and female athletes. Due to sample size, only descriptive statistics are reported.

RESULTS AND DISCUSSION

Table 1 presents knee mechanics across fatigue states and cleat conditions for the female and male athlete. Preferred landing strategy is marked by a reduction in the listed variables [4]. Initial results indicate the female athlete had greater knee valgus than the male, particularly with the elliptical stud shape. As well, the fatigued state appears to have a detrimental effect on female mechanics, indicated by increased peak valgus angle and knee extensor moment. This is more pronounced in the bladed condition. In contrast, peak knee valgus and knee extensor moment decreased after fatigue for the male athlete, in both footwear conditions.

CONCLUSIONS

Preliminary analyses suggest sex differences in mechanical landing strategy. In the female, the cleat with greater rotational traction (bladed) led to a reduction in knee valgus position, but an increase in shear force, pre- and post-fatigue. Male mechanics appear to be more consistent across cleats and fatigue states. Final analysis of the full study sample should improve our understanding of how cleat design parameters may address female athletes' exposure to knee injury.

REFERENCES

- [1] Waldén et al. *Knee Surg Sport Tr A*, **19**: 3-10, 2010.
- [2] Decker et al. *Clin Biomech*, **18**: 662-669, 2003.
- [3] Kernozek et al. *Am J Sports Med*, **36**: 554-565, 2007.
- [4] Butler et al. *Scan J Med Sci Sport*, **24**: 129-135, 2012.

ACKNOWLEDGEMENTS

This work was supported by the Wu Tsai Human Performance Alliance and the Joe and Clara Tsai Foundation. Footwear was generously donated by adidas.

Table 1: Female and male peak values (mean ± sd) across cleat conditions and fatigue states.

Sex & Cleat Condition		Valgus Angle (°)	Extensor Moment (Nm/kg)	Anterior Shear Force (N/kg)
Female- Bladed Studs	Pre-Fatigue	9.03 ± 2.32	4.75 ± 0.33	11.21 ± 2.45
	Post-Fatigue	12.88 ± 1.94	5.03 ± 0.42	11.53 ± 2.65
Female- Elliptical Studs	Pre-Fatigue	16.99 ± 1.91	4.30 ± 0.57	10.83 ± 1.61
	Post-Fatigue	17.33 ± 3.46	4.57 ± 0.38	10.27 ± 1.82
Male- Bladed Studs	Pre-Fatigue	10.60 ± 1.79	5.77 ± 1.41	15.72 ± 2.72
	Post-Fatigue	10.52 ± 1.99	5.21 ± 0.29	16.17 ± 2.03
Male- Elliptical Studs	Pre-Fatigue	13.18 ± 4.27	6.36 ± 0.74	16.85 ± 3.34
	Post-Fatigue	10.07 ± 4.59	5.99 ± 0.40	15.90 ± 2.28

PEAK TORQUE LIMB COMPARISON AND KINESIOPHOBIA CORRELATION POST-ACLR SURGERY

Burr, B^{1,3}, Pollard, CD^{2,3}, Phillips, D^{1,3} and Hannigan, JJ^{2,3}

Program in ¹Kinesiology and ²Physical Therapy, Oregon State University-Cascades, Bend, OR USA

³School of Biological and Population Health Sciences, Oregon State University, Corvallis, Oregon, USA

email: burrbe@oregonstate.edu

INTRODUCTION

Anterior cruciate ligament (ACL) tears are a commonly occurring knee injury, impacting over 200,000 people each year in the United States alone [1]. ACL reconstruction surgery (ACLR) is the standard treatment of ACL injuries, often followed by 9-12 months of rehabilitation. A recent study has shown that despite the extended rehabilitation protocols occurring post-surgery, fear of re-injury may influence muscle activation and kinematics in side-hopping activities, thought to be a protective mechanism occurring in order to stabilize the knee joint [2]. A recent study in the OSU FORCE Lab demonstrated similar findings, noting avoidance behaviors occurring during cutting trials of post-ACLR participants [3]. In this study, we looked at whether peak torque (PT) and time to peak torque (TTPT) for knee flexion-extension strength testing may also be correlated to fear of re-injury, as this could impact the overall kinematics seen in more dynamic movements.

METHODS

Eight subjects to-date, who were a minimum of 12 months post-ACLR and previously cleared for unrestricted return-to-sport at least 3 months prior to testing, were included in this study.

For the strength testing, PT & TTPT data was collected using an isokinetic dynamometer (Biodex Corp., Shirley, NY). After five practice trials, strength data was collected isokinetically for both extensors and flexors at the knee, on both the involved and uninvolved limb. Five trials were collected at a rate of 60° per second, followed by five trials at a rate of 180° per second. A paired t-test was conducted between the limbs for each variable ($\alpha = 0.05$).

Immediately following strength testing, questionnaire data from the Tampa Scale of Kinesiophobia (TSK) was collected electronically to determine kinesiophobia levels in return-to-sport post-ACLR. A combined scoring approach was used, looking at overall kinesiophobia levels from all 17 questions. A Pearson correlation analysis was then completed between TSK and the involved limb for each strength variable.

RESULTS AND DISCUSSION

No significant differences were found in strength measures between the involved and uninvolved limb ($p > 0.05$, Table 1).

While a moderate correlation was demonstrated between TTPT and TSK at 60° per second for both extension and flexion, it was not found to be statistically significant ($p > 0.05$, Figures 1 & 2).

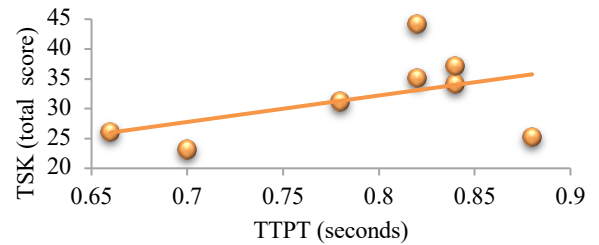


Figure 1: Correlation of TSK scores vs TTPT in the knee extensors at 60°/second ($r = 0.475$, $p = 0.24$).

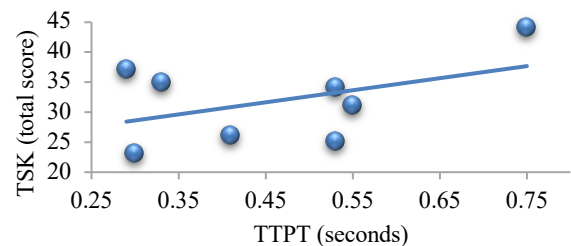


Figure 2: Correlation of TSK scores vs TTPT in the knee flexors at 60°/second ($r = 0.452$, $p = 0.26$).

CONCLUSIONS

We found no significant differences in strength testing (PT or TTPT) between the involved and uninvolved limb. In addition, we did not find a significant correlation between strength testing and kinesiophobia. Therefore, the changes in muscle activation and kinematics witnessed by previous research are likely not a result of these strength-based variables. Further research will need to be completed to confirm these findings.

REFERENCES

1. Musahl, V & Karlsson, J. *N Engl J Med* **380**, 2341–48, 2019.
2. Markström, JL, et al. *Phys Ther* **102**, 2022.
3. Hannigan, JJ, et al. *Proceedings of NACOB 2022*, Ottawa, Canada, Abstract P1-229, 2022.

ACKNOWLEDGEMENTS

This work was funded by the OSU-Cascades Layman Fellowship. We would like to acknowledge Sydney Beck, Breanna Bang, Camille Lopez, Emmanuel Macias, Samantha Noregaard, Lily Bartel and Jordan Ory for their aide in data collection.

Table 1: Peak torque and time to peak torque results averaged for all participants.

	60°/second				180°/second			
	Involved extensors	Uninvolved extensors	Involved flexors	Uninvolved flexors	Involved extensors	Uninvolved extensors	Involved flexors	Uninvolved flexors
PT (Nm/BW)	2.14 ± 0.5	2.29 ± 0.45	1.39 ± 0.21	1.39 ± 0.29	1.17 ± 0.35	1.22 ± 0.46	0.89 ± 0.23	0.90 ± 0.23
TTPT (sec)	0.79 ± 0.08	0.79 ± 0.09	0.46 ± 0.16	0.54 ± 0.18	0.30 ± 0.05	0.31 ± 0.05	0.24 ± 0.07	0.24 ± 0.03

LOWER EXTREMITY JOINT WORK IN THE NIKE VAPORFLY NEXT% COMPARED TO MINIMALIST FOOTWEAR

Reyes, K¹, Jin, L³, Westley, L³, and Hannigan, JJ²

¹Program in Kinesiology, Oregon State University, Corvallis, OR

²Program in Physical Therapy, Oregon State University – Cascades, Bend, OR

³Department of Kinesiology, San José State University, San José, CA

email: kathy.reyes@oregonstate.edu

INTRODUCTION

Footwear companies have altered road racing footwear by increasing midsole cushioning and embedding a carbon fiber plate, potentially influencing ankle, knee, and hip biomechanics, and decreasing the metabolic cost of running [1]. In 2019, Nike released the Nike ZoomX Vaporfly% NEXT% (NP), designed with a combination of increased cushioning, an embedded carbon plate, and polyether block amide (PEBA) foam. The NP increased in popularity after being worn to break the two-hour marathon barrier and has been labeled a “super” shoe. While there is some research on the influence of maximal shoes on injury [2] as well as early versions of “super” shoes on biomechanics [1], there is currently insufficient evidence investigating the effect of more current “super” shoes on lower extremity biomechanics while running. Therefore, the primary purpose of this study was to compare the running biomechanics of the NP with a minimal running shoe, specifically investigating lower extremity joint work and power at the ankle, knee, and hip.

METHODS

Twelve healthy competitive distance runners (men: women 10:2 age: 21.0 ± 2.5 yrs; height: 174.8 ± 10.9 cm; mass: 62.2 ± 7.4 kg) participated in this study. Participants warmed up then completed five successful running trials indoors at their marathon pace wearing the a) Nike Vaporfly NEXT% (NP) and b) New Balance Minimus (NB) shoes in a randomized order. A 16-camera 3D motion capture system (Vicon Motion Systems, Oxford UK) and two force plates (Kistler Instrument Corp., Novi, MI) were used to collect kinematics data at 100Hz and kinetic data at 1000Hz.

Kinetics and kinematics were calculated using Visual3D software (C-Motion, Germantown, MD). Ankle, knee, hip joint power was calculated using an inverse dynamic model coded in Visual 3D (C-Motion, Inc., Germantown, MD) [3]. Positive and negative ankle, knee, and hip joint work were calculated by integrating the joint power data in Visual3D (C-Motion) [3]. Paired t-tests ($\alpha = 0.05$) were used to determine biomechanical differences between shoes.

RESULTS AND DISCUSSION

Negative and positive ankle work as well as negative and positive ankle power were significantly lower in the NP shoe compared to the NB shoe (Figure 1; Table 1). A trending but

non-significant difference was found in positive knee work (NP: 0.70 ± 0.19 J/kg, NB: 0.63 ± 0.19 J/kg, $p = 0.084$). There were no other significant differences in work or power, including negative knee work (NP: -0.55 ± 0.20 J/kg, NB: -0.49 ± 0.25 J/kg, $p = 0.24$), negative knee power (NP: -14.94 ± 5.40 W/kg, NB: -12.88 ± 5.24 W/kg, $p = 0.186$), positive knee power (NP: 13.79 ± 2.97 W/kg, NB: 12.77 ± 3.20 W/kg, $p = 0.179$), negative hip work (NP: -1.38 ± 0.48 J/kg, NB: -1.39 ± 0.38 J/kg, $p = 0.839$), positive hip work (NP: 0.04 ± 0.03 J/kg, NB: 0.03 ± 0.02 J/kg, $p = 0.551$), negative hip power (NP: -21.29 ± 8.47 W/kg, NB: -22.25 ± 6.91 W/kg, $p = 0.331$), or positive hip power (NP: 3.23 ± 2.97 W/kg, NB: 2.10 ± 0.86 W/kg, $p = 0.184$) between shoes. These differences could potentially have implications for energy preservation at the ankle, supporting previous research indicating the reduction of metabolic cost due to the return of energy [2] caused by the increased midsole cushioning, carbon fiber plate and PEBA foam.

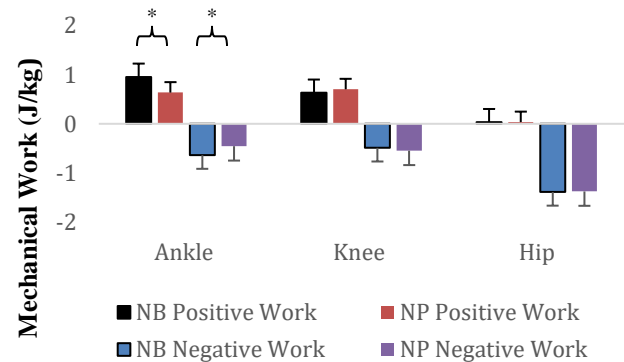


Figure 1: Group average (n=12) ankle, knee, hip joint positive work and negative work between the two shoes (NB & NP).

CONCLUSIONS

Significant differences were found in negative ankle work, positive ankle work, negative ankle power and positive ankle power between shoes. Our findings suggest embedding a carbon fiber plate with increased midsole cushioning and PEBA foam alters ankle joint and power.

REFERENCES

- Hoogkamer et al., *Sports Med* **48**, 133–143, 2019
- Hannigan & Pollard, *J Sci Med Sport* **23**, 15–19, 2020.
- Jin & Hahn. *Human Movement Sci* **58**, 1–9, 2018.

Table 1: Negative and positive ankle joint work and power for both shoe conditions.

Variables	Nike Vaporfly Next%	New Balance Minimus	P-value
Negative ankle work (J/kg)	-0.46 ± 0.18	-0.64 ± 0.18	0.001*
Positive ankle work (J/kg)	0.64 ± 0.19	0.96 ± 0.20	<0.001*
Negative ankle Power (W/kg)	-8.34 ± 3.15	-12.0 ± 3.24	<0.001*
Positive ankle Power (W/kg)	14.46 ± 4.84	21.56 ± 5.20	<0.001*

EVALUATING BETWEEN-LIMB DIFFERENCES IN CUTTING, DROP VERTICAL JUMPING, AND RUNNING BIOMECHANICS POST ACL-RECONSTRUCTION

Dozhier, H.D.^{1,3}, Pollard, C.D.^{2,3}, and Hannigan, JJ^{2,3}

Program in ¹Kinesiology and ²Physical Therapy, Oregon State University-Cascades, Bend, OR USA

³School of Biological and Population Health Sciences, Oregon State University, Corvallis, Oregon, USA.

email: dozhierh@oregonstate.edu, web: <http://osucascades.edu/force-lab>

INTRODUCTION

Anterior Cruciate Ligament (ACL) injuries are prevalent amongst athletes in sports involving dynamic movement, with reconstruction surgery (ACLR) being the most common intervention. Despite the efficacy of this treatment, there is evidence that lower extremity biomechanics are affected even after surgery, specifically bilateral asymmetries [1,2]. It has been proposed that single-leg tasks such as cutting may reveal the most significant asymmetries, making it the best assessment tool for returning to sport (RTS) [3]. Some studies also suggest that asymmetries may exist in drop vertical jumping (DVJ) and running tasks. Therefore, the purpose of this study was to compare cutting, DVJ, and running biomechanics between limbs in both ACLR and healthy participants.

METHODS

Subjects consisted of eight males and nine females (age: 31.9 ± 9.6 yrs) who had torn their ACL, were at least 1-year post-ACLR, and cleared by their orthopedic surgeon to return to full sports activity. Control (CTRL) subjects consisted of eight males and nine females (age: 27.5 ± 7.7 yrs). Prior to participating in this study, all subjects signed an informed consent form approved by Oregon State University.

During data collection, subjects wore a standard New Balance (Boston, MA) running shoe and 21 markers were placed on anatomical landmarks, along with six marker clusters. Three-dimensional kinematics were collected with an eight camera Vicon motion analysis system (Vicon Motion Systems, Oxford UK) sampling at 250 Hz during running, cutting, and DVJ tasks. Two in-ground force plates (AMTI, Watertown MA) sampling at 1000 Hz were used to identify foot-strike and toe-off. Five successful trials of each task were recorded.

Visual3D software (C-Motion, Germantown MD) was used to calculate hip and knee joint kinematics for all tasks. The variables of interest included peak angles for knee and hip flexion, as well as knee and hip flexion excursions. Differences between the ACLR and non-affected limbs as well as between right and left limbs for CTRL participants were calculated using paired t-tests with an alpha-level of 0.05.

RESULTS AND DISCUSSION

For cutting, peak knee flexion (surgical: $44.16 \pm 10.20^\circ$, non-surgical: $48.2 \pm 6.8^\circ$, $p = 0.03$), knee flexion excursion (surgical: $26.88 \pm 6.55^\circ$, non-surgical: $32.1 \pm 5.9^\circ$; $p = 0.00$), peak hip extension (surgical: $11.5 \pm 9.3^\circ$, non-surgical: $16.1 \pm 11.8^\circ$; $p = 0.01$) and hip extension excursion (surgical: $52.8 \pm 11.3^\circ$, non-surgical: $58.7 \pm 9.2^\circ$; $p = 0.03$) were significantly lower in the ACLR limb relative to the non-surgical limb. No significant differences were found between limbs for these measures for CTRL subjects, $p > .05$ (Fig 1).

For DVJ, there were significant differences between limbs in peak hip flexion (surgical: $80.0 \pm 17.4^\circ$, non-surgical: $78.4 \pm 17.6^\circ$; $p = 0.015$) and knee flexion excursion (surgical: 75.6 ± 10.7 , non-surgical: $79.4 \pm 11.0^\circ$; $p = 0.0024$) for ACLR participants. There were also bilateral differences in peak hip flexion in the CTRL group (right: $79.2 \pm 15.6^\circ$, left: $81.7 \pm 15.4^\circ$; $p = 0.012$). No other significant differences were observed ($p > .05$).

For running, there was no significant differences between limbs for either ACLR or CTRL participants, $p > .05$.

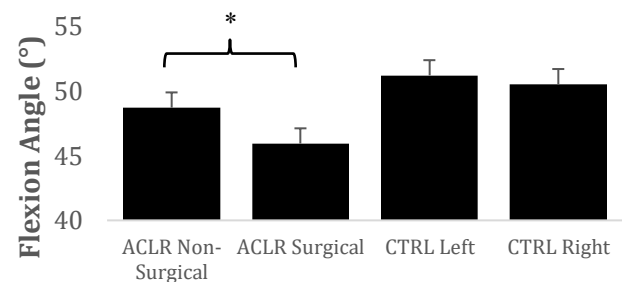


Figure 1: Peak knee flexion averages with bilateral comparison during a cutting task.

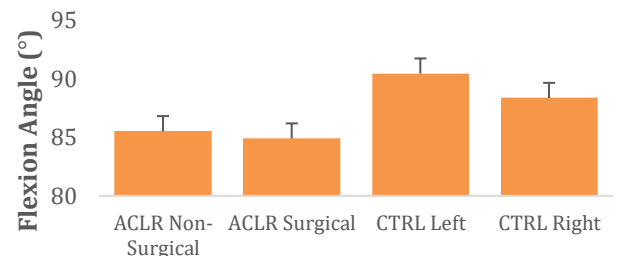


Figure 2: Peak knee flexion averages with bilateral comparison during a DVJ.

CONCLUSIONS

When compared to controls, ACLR individuals demonstrated bilateral asymmetry in cutting and DVJ tasks, but not running, suggesting a hesitancy to demonstrate full ROM in the surgical limb. More significant differences were identified for cutting, and the differences observed in DVJ for peak hip flexion were also present in the control group. This suggests that having ACLR patients complete a cutting task assessment for RTS may be an ideal tool for screening.

REFERENCES

1. Sharafoddin-Shirazi et al. *J Exp Orthop* 7, 2020.
2. Schmitt LC, et al. *Med Sci Sport Exerc.* 47, 1426-1434, 2015.
3. Kotsifaki A, et al. *Orthop J Sports Med.* 10 2022.

QUANTIFYING SPATIAL EXPLORATION OF TODDLERS WITH POWERED MOBILITY

O'Connor, GK¹, Roberts, MJ¹, Zaino, NL^{1,3}, Feldner, HA^{2,3} and Steele, KM^{1,3}

¹Department of Mechanical Engineering, ²Department of Rehabilitation Medicine, and ³Center for Research and Education on Accessible Technology and Experiences, University of Washington, Seattle, WA USA

email: occonnor1@uw.edu, mjr57@uw.edu web: <https://steelelab.me.uw.edu/>

INTRODUCTION

Exploration of space is a crucial part of cognitive development in toddlers. Physical disabilities can limit space exploration and the progression of spatial memorization and adaptation [1]. The use of power mobility devices, such as the Permobil Explorer Mini, can allow for more self-initiated space exploration and increase socio-spatial relationship development [1]. This study's purpose was to quantify how the exploration of space in an Explorer Mini progressed over 12 driving sessions through the percentage of space explored and how it changed with each session. We hypothesized that space explorations would increase throughout sessions as familiarity with driving the Explorer Mini increases.

METHODS

Two children (Table 1) and their parent(s) attended 12 visits over approximately 8 weeks, each including two play sessions approximately 15 minutes long. The play sessions took place in an enriched play environment with 12 Qualisys cameras that tracked 9 reflective markers on the Explorer Mini. We quantified the space explored by dividing the 4 m by 7.5 m space into 0.25 m bins and calculating the percentage of bins that the center of the Explorer Mini entered during the play session.

RESULTS AND DISCUSSION

The participants explored an average of 41.97% of the space (range: 14.17%-79.17%) during the 15-minute play sessions (Figure 1). P3 had a general increase in space exploration over the first 5 sessions but decreasing exploration in the following 3 sessions potentially indicating lack of engagement. P2 had varying spatial exploration over the 12 sessions, which could have been due to various mood factors, but also time spent outside the range of the Qualisys capture system (mocap space). On average participants spent 45.34% of their time (range: 0.17%-87.32%) outside of the mocap space (Figure 1C). The percentage of time spent outside the mocap space is the inverse of area explored in cases of significantly decreased spatial exploration.

Variation between the results for each child can be attributed to the differences in abilities to access the joystick. Driving sessions varied in duration based on the mood and interests of each child, which could affect the percentage of exploration of each individual session while likely not affecting the general trend. The discrepancies that were illustrated could have been because of the age of the participants, variability in mood and excitement of said participants during a particular session, and

interest in playing with the toys over exploring the space. One limitation is that the cameras did not pick up the full extent of exploration play and thus when the participants explored outside of space, there is limited data to quantify where they explored.

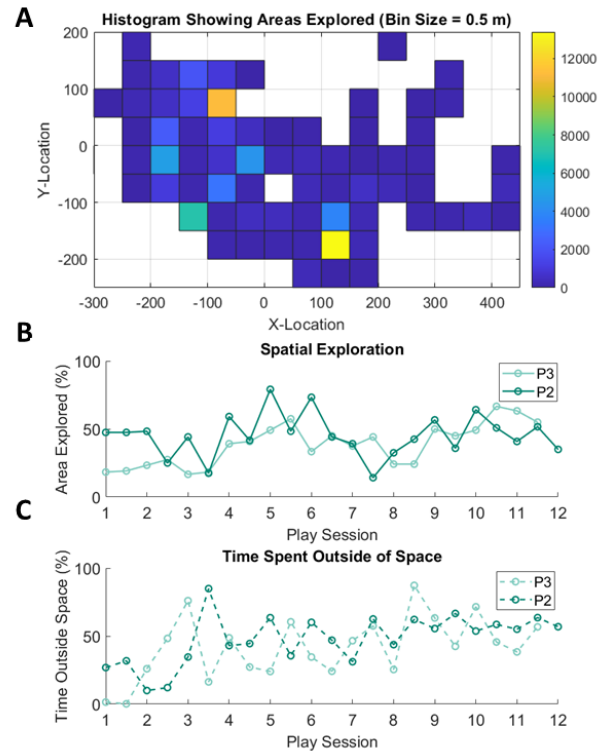


Figure 1: (A) Representative example of histogram showing spatial exploration in x-y plane of P3 play session 5. (B) Percent of space explored over 12 play sessions. (C) Time spent outside the motion capture area over 12 play sessions.

CONCLUSIONS

We were able to quantify spatial exploration for two participants. With more sessions the percentage of exploration did show an overall increasing trend. Future implications of this study will allow for more investigation of space exploration in a larger space to see if area exploration increases and an investigation with multiple participants see if space exploration increases in a social atmosphere.

REFERENCES

1. Aceros J & Lundy M, *Front Pediatr*, **8**, 1541-3144, 2020

Table 1: Demographics of Participants

Participant ID	Age (months)	Weight (lbs)	Sex	Disability Type	Mobility at study entry
P2	14	21.8	M	Neurological	Sitting
P3	16	22.3	M	Orthopedic	Cruising

SAGITTAL PLANE TESTING FOR INFANT PRODUCT SAFETY: PROOF OF CONCEPT STUDY

Sarah M. Goldrod^{1*}, Erin M. Mannen PhD¹

¹Department of Mechanical and Biomedical Engineering, Boise State, Boise, ID, USA

Email: *sarahgoldrod@u.boisestate.edu, web: <https://www.boisestate.edu/coen-babi/>

INTRODUCTION

Approximately 3,400 infants die of sudden unexpected infant death (SUID) each year, and some of these deaths occur in commercial infant products like bouncers or swings when infants are asleep or unattended [1]. To promote safe sleep, the American Academy of Pediatrics (AAP) recommends that caregivers place infants on their backs on a firm sleep surface without soft bedding, and that infants sleep on a non-inclined surface. While a crib is the undisputed safest place for an infant to sleep, commercial infant products like bouncers or swings can provide a contained space for parents to place a baby for attended play. However, many infants are left unattended or fall sleep in commercial products that are not designed for nor adhere to the AAP's safe sleep guidelines. Thus, ensuring that infants are as safe as possible in every infant product is critical.

Previous research has established that head/neck and trunk posture are important for normal breathing. Reiterer et al. found that at 45° of head/neck flexion, the mean lung resistance of the preterm infants increased by 34% compared to a neutral position [3], and extreme head/neck flexion can cause complete airway occlusion in infants lacking head control. Two studies found that slumped sitting significantly decreased lung capacity and expiratory flow [4] as well as ribcage and chest wall motions [5] during breathing compared to a normal sitting position. Clearly, head/neck flexion and trunk flexion are postural characteristics which can negatively influence breathing, yet current regulatory standards governing commercial infant products like a bouncer or swing do little to evaluate infant body posture within products. Two devices currently exist to measure body position – the hinged weight gauge (~\$500) and the CAMI dummy (~\$12,000). The purpose of this proof-of-concept study is to evaluate current test devices and a 4-segment anthropometric device (~1,000) [6], all compared to an actual infant's body position.

METHODS

Testing was divided into two experiments: mechanical testing of with the sagittal plane devices (hinged weight gauge, CAMI dummy, and 4-segment device) and motion capture human subject testing. The Fisher-Price Rock N' Play (Fig. 1) was used for both experiments. This product was chosen because it features a design similar to some bouncers and swings, and our previous research has shown that inclined sleep products result in ~16° of trunk flexion during normal supine lying [7]. Each sagittal plane device was placed in the Rock N' Play in the intended position for a total of three times. We used a Wixey Digital Angle Gauge to measure the segment angles and then computed the difference between segment angles to determine the flexion/extension angles of each hinge/joint. Human testing was conducted on one participant in our IRB approved study (126-MED20-005). We used an eight-camera motion capture system, (Qualisys, Gothenburg, Sweden), to collect data. A marker set of nine retroreflective markers was placed on

the participants to track motion. Each participant was placed supine on a flat surface and in the product for two to three minutes. The flat surface was used to normalize subject data and each trial was trimmed to a single frame for this proof-of-concept study. A custom MATLAB 2022a code was created to process the data and calculate the head/neck and trunk flexion of the infants.

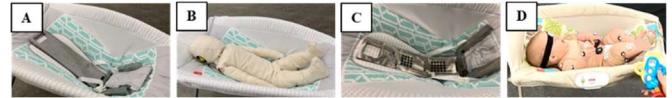


Figure 1: Testing in the Fisher-Price Rock N' Play, (A) hinged weight gauge, (B) CAMI dummy, (C) 4-segment, and (D) participant.

RESULTS AND DISCUSSION

The infant exhibited head/neck flexion of 17° and trunk flexion of 14°. The results revealed several limitations with current testing devices (Fig. 2). The hinged weight gauge cannot model head/neck or trunk flexion angles. The CAMI dummy is ideal for modelling head/neck geometry and flexion but cannot model trunk or hip angles. The 4-segment device was able to measure head-neck, trunk, and hip angles though the head/neck results did not compare well with the infant data. The addition of a pelvis segment to the 4-segment device may facilitate consistent positioning between devices and between tests, and addition of three-dimensional head geometry may improve accuracy of results. A larger data set with more participants and time, with many categories of infant products will provide a more robust comparison on the accuracy of sagittal plane devices. This proof-of-concept study shows that sagittal plane devices can replicate infant body position measurements consistent with *in vivo* data, but that improvements are required to obtain both head/neck flexion and trunk flexion in a single device.

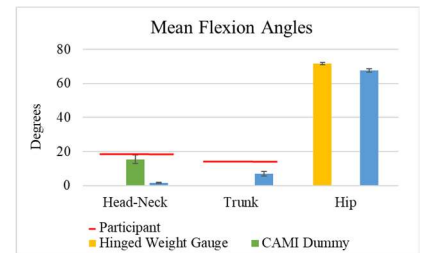


Figure 2: Mean flexion angles of 2-segment infant hinged weight gauge, CAMI dummy, and 4-segment device.

CONCLUSION

Safe body positioning is critical for healthy breathing, and manufacturers would benefit from a simple mechanical device to enable them to measure these parameters in infant products. This study compared three mechanical devices to *in vivo* data from an infant to evaluate accuracy and inform development of improved sagittal plane testing devices.

REFERENCES

1. CPSC 2022.
2. Moon et al. *Ped.*, 2022.
3. Reiterer et al. *Ped. Pulm.*, 1994.
4. Lin et al. *Phys. Med. and Rehab.*, 2006.
5. Lee et al. *Resp. Phys. Neurobio.*, 2010.
6. Mannen et al. *CPSC*, 2022.
7. Wang et al. *J Biomech.*, 2020.

KINEMATICS OF THE FIRST METATARSOPHALANGEAL JOINT: BAREFOOT VS SHOD

Eric D. Thorhauer^{1,3*}, William R. Ledoux^{1,2,3}

Departments of ¹Mechanical Engineering, and ²Orthopaedics and Sports Medicine, University of Washington

³RR&D Center of Excellence, Department of Veterans Affairs, Seattle, WA USA

email: ericthor@uw.edu

INTRODUCTION

With the development of biplanar fluoroscopy systems dedicated to foot and ankle imaging, more precise quantification of first metatarsal phalangeal joint (MTPJ1) kinematics is possible. Among the strengths of biplane systems over conventional motion capture systems are their ability to track bone motion in shoes. This study aims to quantify differences in shod vs barefoot in vivo kinematics.

METHODS

Following IRB approval, subjects underwent bilateral computed tomography scans which were segmented to produce subject-specific first metatarsal and proximal phalanx models (Mimics v20, Materialise, Leuven, Belgium). Bone embedded coordinate systems were defined using the inertial axes of the bone surfaces. Subjects performed both barefoot and shod gait trials at self-selected speeds through the capture volume of a biplane imaging system (ISSI, Painesville, OH, USA) while pulsed X-ray video fluoroscopy sequences (120Hz) were collected. A strain gauge embedded in the X-ray transparent walkway was used to detect the gait cycle events. MTPJ1 bone motion was reconstructed using the model-based method of optimally aligning digitally reconstructed radiographs to the stereo fluoroscopy images in custom software (Figure 1) [1,2]. Kinematic results were smoothed with a second-order Butterworth filter with a cut-off frequency of 20Hz.

RESULTS AND DISCUSSION

Currently the MTPJ1 motion for one subject has been tracked in both conditions. The resultant MTPJ1 dorsiflexion kinematics from late midstance to terminal stance phase were calculated (Figure 2). Between-trials MTPJ1 angles were consistent within conditions. In the shod condition, the MTPJ1 started 15 degrees more dorsiflexed than during barefoot. On average, range of motion was 23.0 degrees for shod and 55.1 degrees for barefoot. Peak dorsiflexion angles were 13.8 degrees higher in barefoot than shod trials on average.

CONCLUSIONS

This study demonstrated the ability to track foot bone motion during shod trials and began quantifying within-subject differences in MTPJ1 kinematics between shod and barefoot gait. Previous studies have found extensive differences between barefoot and shod gait in healthy populations [3,4]. Given that most people spend most of their time in shoes, further research into the kinematics of the foot in these conditions is warranted.

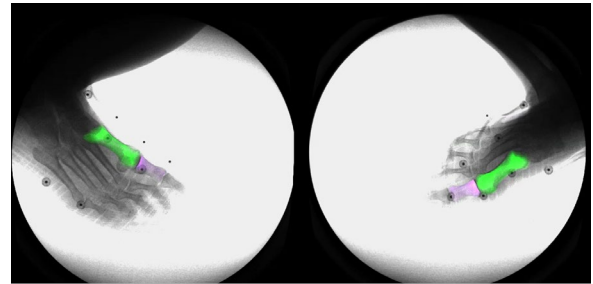


Figure 1: MTPJ1 model-based tracking on biplane fluoroscopy sequences.

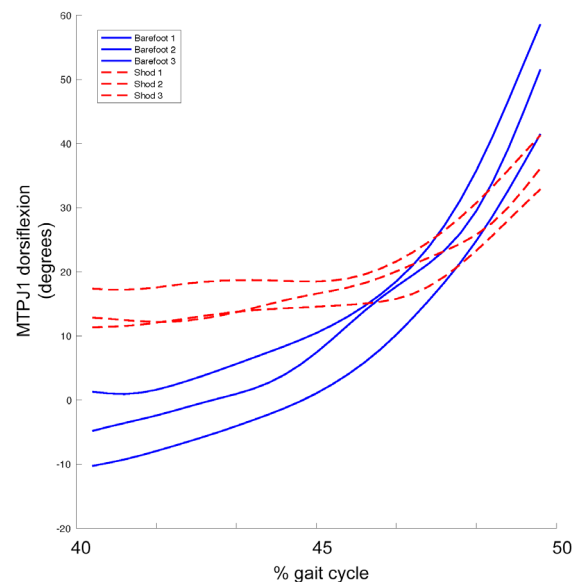


Figure 2: MTPJ1 dorsiflexion angle (degrees) during terminal stance phase for both shod (red dashed lines) and barefoot (solid blue lines) trials.

REFERENCES

1. Iaquineto JM, et al. Preliminary model-based validation of a biplane fluoroscopy system. *J Foot Ankle Res.* 2014.
2. Thorhauer, E., & Ledoux, W. R. (advisor). MS Thesis, Calibration and optimization of a biplane fluoroscopy system for quantifying foot and ankle biomechanics. University of Washington Libraries, 2020.
3. Stone AE, et al. Ankle Fusion and Replacement Gait Similar Post-surgery, But Still Exhibit Differences Versus Controls Regardless of Footwear, *J Orthop Res.* 2021 Jan 17.
4. Keenan GS, et al. Lower limb joint kinetics in walking: the role of industry recommended footwear. *Gait Posture.* 2011;33(3):350-355.

ACKNOWLEDGEMENTS

Supported by VA Rehabilitation Research and Development Grants RX002008 and RX002970.

The Effects of Spinal Stimulation and Interval Treadmill Training on Joint Kinematics in Cerebral Palsy

Avocet Nagle-Christensen¹, Charlotte D. Caskey¹, Siddhi Shrivastav^{1,2}, Kristie Bjornson^{1,2}, Chet T. Moritz¹, Katherine M. Steele¹

¹University of Washington, ²Seattle Children's Research Institute, Seattle, WA USA

Email: avocetnc@uw.edu

INTRODUCTION

Cerebral palsy (CP) is a group of motor disorders caused by a brain injury around the time of birth and manifests in many ways. Children with CP often have a slower preferred walking speed, limited range of motion, and more asymmetry in their gait compared to typically developing children, which can lead to increased energy costs and greater fatigue during walking [2]. Short-burst interval locomotor treadmill training (SBLTT) has shown potential for improving walking function in children with CP, but little is known on its effects on range of motion or gait kinematics [3]. SBLTT consists of 30-minutes of treadmill walking with alternating 30-sec intervals of slow and fast speeds to provide mass practice of speed transitions, more similar to walking in typically developing peers [3]. Non-invasive electrical spinal cord stimulation (Stim) during treadmill training has shown promising potential for motor control and coordination during walking in children with CP [4]. Combining Stim with SBLTT may amplify response to training and lead to improved kinematics and symmetry in children with CP.

The goal of this study is to investigate the effects of SBLTT and Stim on joint kinematics in children with cerebral palsy. We hypothesize that using Stim with SBLTT can improve coordination and joint kinematic range during walking.

METHODS

The study involved a 12-year-old, male GMFCS II, with spastic hemiplegia and a more affected left side. The participant underwent 24 sessions each of SBLTT only and SBLTT + Stim spread across 8-10 weeks with an 8-week washout of no intervention in between. Spinal cord stimulation used an electrical simulator (SpineX Inc, Northridge, CA) with conductive self-adhesive electrodes placed over the T11 and L1 vertebrae. Qualisys motion capture equipment (Qualisys AB, Göteborg, Sweden) was used to record over ground, barefoot walking on a 10-m walkway with a modified Helen Hayes marker set before and after each of the intervention periods and a 2-month follow-up after the study completion.

Joint kinematics over gait cycle in the sagittal plane for the hip, knee, and ankle were calculated using the Inverse Kinematics tool in OpenSim v4.3 (Stanford, Palo Alto, CA) and a custom MATLAB script. The range of joint kinematics was calculated for each joint from the maximum and minimum flexion/extension per gait cycle. Averages and standard deviations were calculated and tested for normality using the Anderson-Darling test. The data were normally distributed, except for the ankle at the end of the washout period, thus a t-test was used to examine the change in kinematic range during walking over each phase of the study to compare the intervention methods (* indicates p-value < 0.05).

RESULTS AND DISCUSSION

SBLTT Only phase led to very minor increases in the ankle kinematic range (right ankle: +1.9°, left ankle: 0.56°), while the SBLTT + Stim increased the ankle and left hip kinematic range

(right ankle: +3.06*, left ankle: +1.12, left hip: +6.97*). This increased ankle kinematic range during gait was due to increased plantarflexion during terminal stance, suggesting a stronger push off. At the ankle, the range increased after both interventions by roughly a degree but comparing Stim + SBLTT to 2-month follow-up we see greater increases in the ankle's kinematic range (right ankle: +15.9°, left ankle: +11.4°). The greatest increase in kinematic range was seen in the knee and ankle of both the left and right sides at two-month follow-up after both interventions (Figure 1). The knee had significant increases in flexion/extension in both sides (right knee: +12.44* with p-value = 1.3 e -8, left knee: +22.5* with p-value = 7.5 e -23) on the left after the end of SBLTT + Stim phase. The improved flexion in the knee during swing indicates better foot clearance.

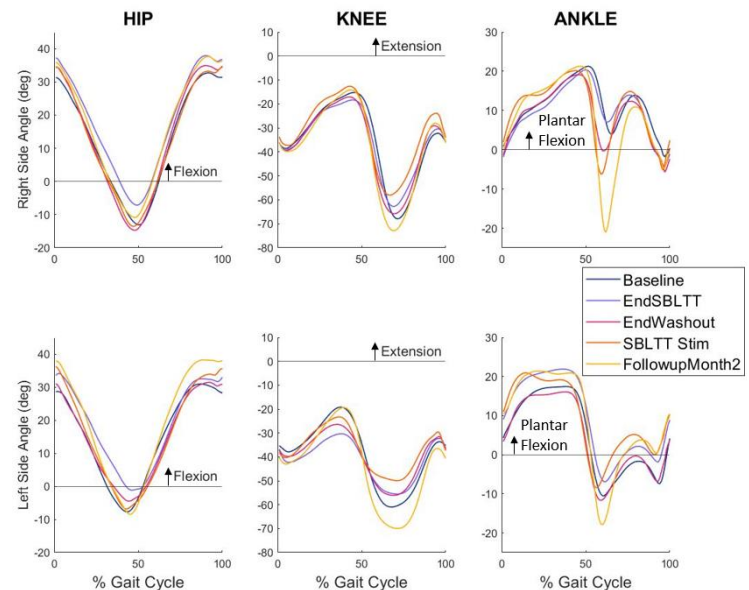


Figure 1: Average joint angles of the left and right hip, knee, and ankle in the sagittal plane over percent gait cycle

CONCLUSION

We observed the greatest changes in kinematics at the knee and ankle from Stim + SBLTT to follow-up. The results are unclear on if the pairing of Stim with SBLTT improves the kinematic range of walking in children with CP. However, it is promising to see drastic improvement of knee and ankle flexion after the two-month follow-up. This data is limited to just one participant, so the findings cannot be generalized about the effects of SBLTT + Stim, but we are able to begin understanding the underlying changes to joint kinematics for these interventions which will better inform us on potential treatments for improving coordination in children with CP.

REFERENCES

- [1] Graham et al., 2016 *Nat. Rev. Disease Prim.*
- [2] Brændvik et al., 2020 *Front Neurol.*
- [3] Bjornson et al., 2019 *Dev. Neurorehabil.*
- [4] Gad et al., 2021 *Neurotherapeutics*

THE EFFECTS OF MUSCLE FATIGUE ON LOWER EXTREMITIES BIOMECHANICS DURING LAY-UP AND LANDING IN RECREATIONAL BASKETBALL PLAYERS

Brandon Yang and Li Jin

Departments of Kinesiology, San José State University, San José, CA USA

email: chengyin.yang@sjsu.edu

INTRODUCTION

Preventing musculoskeletal injuries is crucial in sports and sports medicine research. Muscle fatigue is often experienced during dynamic physical activities. It was found that muscle fatigue could put athletes at risk of injuries [1]. Muscle fatigue usually leads to a reduced maximum force production, decreased reaction time and loss of exercise capacity, which is associated with the risk of sustaining a musculoskeletal injury [2]. Additionally, fatigue produced a smaller knee-abduction angle at initial contact, greater maximum knee-flexion moment, and delayed muscle activation times in semitendinosus, multifidus, gluteus maximum [3]. There are sufficient studies focusing on the knee joint movements under fatigued conditions, however, there are not enough studies being conducted regarding the ankle and hip joint movement under fatigued conditions. Therefore, this study aimed to investigate the effects of fatigue on ankle, knee and hip joint biomechanics during lay-up and landing activities.

METHODS

Two healthy individuals (age: 30 ± 7.1 years, height: 1.73 ± 0.03 m, mass: 63.75 ± 12.37 kg) participated in this study. Participants were asked to perform 3-step approach lay-ups where the take-off leg lands on the force plate. Then the participants performed drop-jumps from a 0.3 m box where they landed on the force plate with the dominant leg. Then the participants went through the fatigue protocol [4]. After going through the fatigue protocol, they repeated the 3-step approach lay-up and drop jump tasks.

36 retro reflective markers were attached bilaterally to lower extremities anatomical landmarks [5]. Kinematics were collected using an 8-camera motion capture system at 100 Hz (Vicon, Oxford, UK). GRF data were collected with two force plates (AMTI, Watertown, MA USA) at 1000 Hz. Paired t-test was used to determine the biomechanical differences between pre- and post-fatigue outcome measures using SPSS software (V26.0, IBM, Armonk, NY, USA).

RESULTS AND DISCUSSION

Table 1: Ground reaction force (GRF) and ankle, knee and hip internal peak joint moment during landing in pre-fatigue and post-fatigue conditions.

Variables	Fatigue Condition, Mean \pm SD, Percentage Change, P-Value			
	Pre-Fatigue	Post-Fatigue	Percentage Difference (%)	P-Value
Peak Vertical GRF (Body Weight, BW)	3.51 ± 0.37	3.46 ± 0.02	1.43	0.430
Peak Ankle Plantar Flexion Moment (Nm/kg)	3.15 ± 0.05	2.85 ± 0.16	10.00	0.451
Peak Knee Extension Moment (Nm/kg)	2.31 ± 0.28	3.56 ± 0.43	42.59	0.027*
Peak Hip Extension Moment (Nm/Kg)	5.99 ± 1.25	6.55 ± 1.94	8.93	0.422

Statistically significant difference was found in the peak knee internal extension moment (pre-fatigue: 2.31 ± 0.28 Nm/Kg, post-fatigue: 3.56 ± 0.43 Nm/Kg, $p = 0.027$) during the landing phase between pre- and post-fatigue. Due to small sample size, no other statistically significant differences were found for the outcome measures between pre-fatigue and post-fatigue conditions. While participants showed a 29.42% increase in peak knee extension moment after the fatigued protocol during the lay-up phase (Figure 1). There was an 8.93% increase in the peak hip extension moment after fatigue (pre-fatigue: 5.99 ± 1.25 Nm/Kg, post-fatigue: 6.55 ± 1.94 Nm/Kg) (Table 1) during the landing phase.

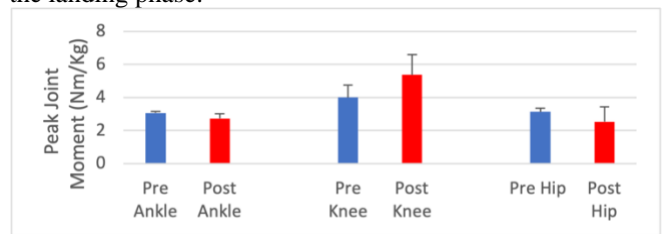


Figure 1: Peak internal ankle, knee and hip joint moment in lay-up between pre- and post-fatigue conditions.

CONCLUSIONS

We found fatigue significantly increased peak knee extension moment during landing. Additionally, fatigue also tend to increase peak hip extension moment during landing, and peak knee extension moment during lay-up. While fatigue also tend to decrease peak ankle plantarflexion moment during landing. Our findings suggest that acute muscle fatigue alters lower extremity joint biomechanical patterns in both landing and lay-up movement activities.

REFERENCES

1. Pappas et al., *J of Sport Sci & Med*, **6(1)**: 77–84, 2007
2. Kim et al., *The Knee*, **24(6)**, 1342–1349, 2017.
3. Haddas et al., *J of Athlete Training*, **50(4)**, 378–384, 2015.
4. Liederbach et al., *Am J Sport Med*, **42(5)**, 1089-95, 2014.
5. Horst et al., *Plos One*, **12(6)**, 2017

CLUSTERING SOCCER ACTIVITIES ASSOCIATED WITH INJURY

Lock, S¹, Yakubu, S¹, Ma, W¹, Kuo, C^{1,2}

¹School of Biomedical Engineering, University of British Columbia

²Centre for Aging SMART, Vancouver Centre for Health Research Innovation.

email: shealock@student.ubc.ca

INTRODUCTION

In 2019, an estimated 13 million girls and women were playing soccer across the globe [1]. Despite being one of the most popular sports, players are susceptible to lower limb injuries. Evidence suggests that 26% to 58% of all soccer injuries are non-contact [2] and female players are at an increased risk for certain non-contact injuries such as Anterior Cruciate Ligament (ACL) tears [5,6]. Such injuries are associated with highly dynamic maneuvers that feature change of direction, rapid deceleration or twisting motions [3,4]. Occurrences of injury are significantly more prevalent during gameplay as opposed to during training sessions [5–9], most notably, during the first and last 15 minutes of play [5].

Many studies considering injury risk rely on post-injury reports [6–9] but modern technology allows for a more proactive approach. Inertial Measurement Units (IMUs) are a type of sensor that make use of accelerometers and gyroscopes to measure linear accelerations and angular velocities. This type of sensor is particularly useful in measuring high-speed change of direction movements often associated with non-contact soccer injuries [2–4, 10]. While IMUs have been previously used to monitor such movement, research is often limited to lab settings and pre-planned movements [10].

METHODS

IMU sensors were deployed to 15 collegiate level female soccer players on a single team throughout the 2022 fall season. Data were collected from all home practices and games. To capture the movement of the torso, the sensors were fixated between their shoulder blades using athletic tape.

The sensors were time-synchronized with two video cameras deployed at each data-collection event. The cameras were placed to provide full coverage of the field. Human raters analyzed activities (Figure 1A) performed by soccer players in the video footage to label IMU data, focusing on dynamic maneuvers that are associated with injury (cutting, etc.).

A one-second window of IMU data was extracted around the video-identified maneuvers (Figure 1B). For each maneuver, we extracted peak kinematics relevant to non-contact injuries (linear accelerations along the superior-inferior and left-right axes, angular velocity about the superior-inferior and anterior-posterior axes). The maneuvers were then clustered based on peak kinematics using K-means clustering in MATLAB.

RESULTS AND DISCUSSION

In pilot analysis, we clustered 26 maneuvers identified from a single player in a game. The clustering algorithm converged to $k = 3$ clusters (Figure 1C). Rather than clustering based on maneuver type (cut, kick, etc.), clusters appeared to form

around the intensity of a maneuver. As seen in Figure 1C, maneuvers with both relatively high accelerations and angular velocities clustered together, while maneuvers with lower accelerations and angular velocities clustered together. The clusters are most distinct when comparing the angular velocities about the vertical and sagittal-horizontal axes. Such motion features are consistent with the change of direction and twisting maneuvers respectively that are associated with non-contact soccer injuries such as ACL tears.

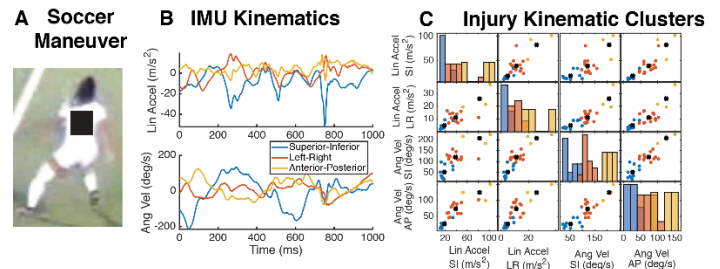


Figure 1: (A) Player performing a cutting maneuver (B) Trace of cutting maneuver captured by IMU (C) Clusters identifying intensities of peak kinematics.

CONCLUSIONS

Clustering suggests that maneuvers are stratified by intensity. This is likely related to what activities were being performed prior to the maneuver (e.g. cutting following a run vs. following a walk), rather than the specific type of maneuver itself (e.g. a cut vs. a jump). Ongoing data analysis will yield more maneuvers for clustering.

REFERENCES

1. FIFA Publications. *Vision Report 2021* [Internet]
2. Junge A and Dvorak J. *Sports Medicine* **34**, 929-938, 2004.
3. da Silva M-V and Pereira B. *Injuries and Health Problems in Football*, 53-64, 2017.
4. Jones PA et al. *Am J Sports Med* **42**, 2095–2102, 2014.
5. Owøye O-A et al. *Sports Med Open* **6**, 1-8, 2020.
6. Östenberg A and Roos H. *Scand J Med Sci Sports* **10**, 279-285, 2000.
7. Morgan BE and Oberlander MA. *Am J Sports Med* **29**, 426-430, 2001.
8. Giza E et al. *Br J Sports Med* **39**, 212-216, 2005.
9. Faude O et al. *Am J Sports Med* **33**, 1694-1700, 2005.
10. Alanen AM et al. *Int J Sports Sci Coach* **16**, 1332-1353, 2021.

ACKNOWLEDGEMENTS

We would like to acknowledge the UBC Women's Soccer team and particularly their coach Jesse Symons for collaborating on this study. We would also like to acknowledge funding sources NSERC Discovery and CFI JELF.

EXAMINING HOW MIDSOLE MATERIAL IMPACTS CENTER OF PRESSURE TRAJECTORIES DURING TREADMILL RUNNING

Pitts, MN¹, Steele, KM¹, and Agresta, CE²

Departments of ¹Mechanical Engineering, and ²Rehabilitation Medicine, University of Washington, Seattle, WA USA
email: mnp0020@uw.edu

INTRODUCTION

The midsole construction in distance running shoes varies across brands and models, and it influences the cushioning system of the shoe. Midsole features like material, density, and thickness affect the cushioning and, in turn, may impact running performance via changes in biomechanics and physiology. However, how to engineer the midsole to optimize performance and minimize injury risk remains an area of open inquiry [1]. Importantly, the midsole is the medium between the foot and the ground, thus, it can alter the stability of the foot during contact [2]. Ankle inversion sprain remains one of the most common injuries in running and may also be influenced by midsole material properties. Prior research has suggested that center of pressure (COP) position and trajectory, especially in the mediolateral direction, may predict risk of inversion sprain [3, 4]. The magnitude of the effect of midsole material properties on COP position, and their potential implications for running performance and injury risk remain unclear. The goal of this study was to evaluate the effect of midsole material on COP trajectories during running. Quantifying COP effects of midsole material properties can provide the foundation to inform footwear design that can improve performance and reduce injury risk.

METHODS

We recruited 20 recreational runners (age: 28.2 ± 7.6 years, sex: 19M/1F, height: 174.0 ± 6.9 cm) to complete 4-6 minute running sessions on an instrumented treadmill (h/p/cosmos, Zebris Medical GmbH, Isny, Germany). Participants ran at a fixed aerobic speed in their native running shoe and four experimental shoes (size 9.5M) in a randomized order, then in a reverse mirrored order. The experimental shoes included two distinct shoe models (A and B). Each model had a midsole material variation (1 or 2), creating four different shoes: A1, A2, B1 and B2. During each run, one minute of plantar pressure data was collected (Noraxon U.S.A., Inc., Scottsdale, AZ, USA). Sample results were calculated for the first 10 participants for this abstract.

A custom MATLAB script was used to evaluate anteroposterior (AP) and mediolateral (ML) COP trajectories normalized to percent of stance and averaged for all left and right steps in each trial for each participant. Variability of a subject's AP and ML trajectories in the experimental shoes were described by the z-score from their respective native running shoe. Average and maximum z-scores were determined for each model.

RESULTS AND DISCUSSION

Changes in midsole material caused deviations in the AP and ML directions (see Figure 1 for sample participant). In the AP direction, all shoes except the A1 design produced positive average z-scores (1.13 ± 1.25 for A2, 1.06 ± 1.37 for B1, and

1.65 ± 1.42 for B2). This outcome suggests that the midsole materials influenced COP movement such that COP trajectories shifted anteriorly compared to the average stride-to-stride variability in COP trajectories in their native running shoes. Midsole material more dominantly affected ML trajectories in model B than in model A. Shoe B1 promoted an average z-score of -1.33 ± 2.26 , and B2 yielded -1.78 ± 2.37 , showcasing more lateral displacement than individuals' native shoes. Conversely, Models A1 and A2 yielded negative z-scores of -0.25 ± 2.58 and -0.26 ± 3.68 , respectively, indicating greater variation between individuals with smaller average impacts on ML COP movement. Maximum deviation from the native shoe occurred at different phases of stance across participants, indicating that the experimental midsoles did not impact a particular phase of stance.

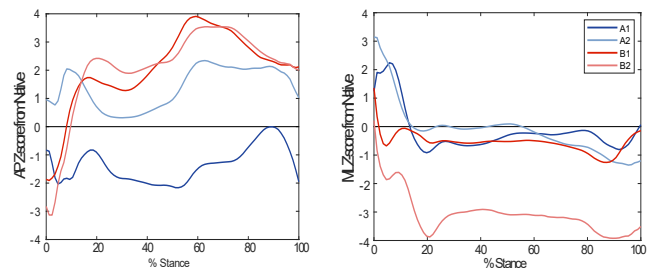


Figure 1: Z-scores for AP (left) and ML (right) trajectories of COP for one participant's left foot in the four experimental shoes.

CONCLUSIONS

The midsole material properties of running shoes influence COP trajectories. Linking these effects to specific material properties, such as stiffness, and physiological outcomes will further support our interpretation of how varying material properties can impact performance and injury risk. Future work should focus on which aspects of the midsole are most influential to changes in COP trajectories, whether runners habituate to this initial response or return to native COP trajectories over time, and the extent to which COP trajectory change relates to foot-ankle injury risk.

REFERENCES

1. Nigg BM, et al. *Footwear Science* **14**, 133-137, 2022.
2. Kozak K, et al. *IEEE EMBC* **13**, 1991.
3. Willems T, et al. *Gait and Posture* **21**, 379-387, 2005.
4. Mousavi SH, et al. *Gait and Posture* **83**, 201-209, 2021.

ACKNOWLEDGEMENTS

Footwear for this project provided by Diadora S.P.A. We also thank Andrew Ba for assistance in collecting data.

Identification of Tissue Damage Using Finite Element Models of Spinal Cord Injury and Machine Learning

Jimenez, C^{1,2}, Narimani, M¹, and Sparrey, CJ^{1,2}

¹Simon Fraser University, School of Mechatronics Systems Engineering, Surrey, Canada

²International Collaboration on Repair Discoveries (ICORD), Vancouver, Canada

email: cjimenez@sfu.ca, website: <https://www.sfu.ca/neurospine.html>

INTRODUCTION

Spinal cord injury (SCI) is often triggered by mechanical loading exerted into the spinal cord tissue [1]. Understanding the relationship between mechanical loading and spinal cord tissue damage in controlled animal experiments is a critical step for developing potential treatments and prevention strategies [2, 3, 4]. Animal finite element (FE) models and post-injury experimental data can provide a high-resolution insight into the distribution of loads in the damaged sections of the spinal cord [3]. However, this information has limited translational value if the correlation between injury mechanics and tissue damage is not properly explored [2, 3]. For instance, the purpose of this study was to use machine learning (ML) algorithms to identify tissue damage based on mechanical outputs of FE models of SCI. Acquired results allowed to compare injury identification in the gray and white matter tissue, evaluate the relevance of included features, and define injury threshold values based on the input data.

METHODS

The sample data of this study was generated from the comparison of histological images taken from SCI experiments in non-human primates [4] and corresponding subject-specific FE models [3]. This data was later divided into three datasets corresponding to gray matter (GM), white matter (WM), and the combination of both tissues. Each dataset included the following mechanical features: min/max principal logarithmic strain (LEP), logarithmic strain in axonal direction (LEAXON), von-Mises stress (MISES), Tresca stress (TRESCA), and strain energy density (ESEDEN).

Each dataset was used for the training and cross-validation of four different ML algorithms. After cross-validation and parameter tuning for each algorithm, the best classifier was selected for each dataset and evaluated with the testing portion of the data. Using inverse prediction, mean values at the 50% probability of injury were requested, as well as the coefficient of importance for each mechanical feature.

RESULTS AND DISCUSSION

Results showed that K-nearest neighbors (KNN) and logistic regression (LR) algorithms performed better at identifying injured elements than support vector machines and decision trees. Additionally, the algorithms' performance changed depending on the evaluated tissue (GM or WM). These results were expected, since previous studies have pointed out the

mechanical differences of GM and WM tissues [3, 5], and different ML algorithms might be more sensitive to the effect of said differences during the identification process.

According to the trained ML models, TRESCA and LEAXON features were the best injury predictors for GM and WM, respectively (Table 1). GM injured elements also showed higher Tresca values (mean 0.428 MPa), suggesting this tissue is susceptible to higher levels of stress than the WM (mean 0.188 MPa). These results agree with the findings in [3], where a similar dataset was used to investigate the correlation between tissue mechanics and injury using logistic regression. However, the mean values at 50% probability of injury reported in [3] were lower by at least 14.1% in most metrics than the ones found in the present study, especially for the GM. Nevertheless, the current study identified and eliminated reported outlier samples in [3] and [4] and considered feature collinearity between the von-Mises and Tresca stresses. These changes are likely one of the contributing factors of the differences between the compared values, remarking the importance of data cleaning before the implementation of tools such as machine learning.

CONCLUSIONS

The implementation of ML can potentially address one of the current limitations of the FE models of SCI by translating mechanical outcomes into clinically relevant information. Based on the presented results, the use of tissue-specific classifiers can improve injury identification and our comprehension of the relationship between mechanical loading and tissue damage in the spinal cord. Moving forward, these findings can help refining injury thresholds based on mechanical features, and improve the clinical relevance of these engineering approaches to study SCI.

REFERENCES

1. Mattucci S, et al. *Clinical Biomechanics* **64**, 69-81, 2019.
2. Sparrey CJ, et al. *J. Neurotrauma* **33**, 1136-1149, 2016.
3. Jannesar S, et al. *J. Neurotrauma* **38**, 698-717, 2021.
4. Salegio EA, et al. *J. Neurotrauma* **33**, 439-459, 2016.
5. Jannesar S, et al. *J. Biomechanical Eng* **138**, 091004, 2016.

ACKNOWLEDGEMENTS

The author would like to acknowledge funding from NSERC, the support provided by WestGrid (www.westgrid.ca) and Compute Canada (www.computeCanada.ca), and the SFU Community Trust Endowment Fund.

Table 1: Mean values at 50% probability of injury and heat map of feature importance (darker color – higher importance)

Spinal cord tissue dataset	Selected ML classifier	Mechanical Feature				
		Min LEP	Max LEP	LEAXON	TRESCA	ESEDEN
GM	KNN	-0.461	0.296	-	0.193	0.043
WM	LR	-0.475	0.310	0.127	0.063	0.069
GM & WM	LR	-0.422	0.290	0.197	0.077	0.021

Cadaveric Simulation of Flatfoot and Surgical Corrective Techniques: the Evans Versus the Z-Osteotomy

Corey Wukelic^{1,2}, Grant C. Roush^{1,2}, Eric C. Whittaker¹, James Meeker³, Kelly Apostle³, Bruce J. Sangeorzan^{1,3}, William R. Ledoux^{1,2,3}

¹RR&D Center for Limb Loss and MoBility (CLiMB), VA Puget Sound, Seattle, WA,
Departments of ²Mechanical Engineering, ³Orthopaedics & Sports Medicine, University of Washington, Seattle, WA
email: cwukelic@uw.edu, web: www.amputation.research.va.gov

INTRODUCTION

Symptomatic flatfoot (pes planus) is a foot condition that is often treated with lateral column lengthening (LCL) procedures such as the Evans LCL. The Z-osteotomy has been proposed as an alternative to the Evans. The purpose of this study is to compare the surgeries statically using radiographs and dynamically using our robotic gait simulator (RGS).

METHODS

Flatfoot was produced in cadaveric specimens by attenuating the ligaments that support the medial arch and cyclic loading through the tibia. Clinical diagnostic measures from X-rays were used to assess foot shape. Each flatfoot was then tested on the RGS with ground reaction forces scaled to 25% of the donor's body weight and the stance phase simulated 6x slower than physiologic gait (4.09s). After flatfoot data collection, one foot in each pair received the Evans LCL while the other received the Z-osteotomy. Post-surgery X-rays were taken, and the feet were again tested on the RGS. Kinematic and kinetic data were collected and compared for both flatfoot and post-surgical trials.

RESULTS AND DISCUSSION

All X-ray parameters were significantly different after the flattening procedure indicating collapse of the arch, forefoot abduction, and hindfoot eversion. The calcaneal pitch angle decreased, though not to the level seen in physiologic flatfoot. Significant changes toward arch restoration were seen in the X-ray parameters after surgeries, but there were no radiographic differences between surgery type (Table 1). Peak pressure under the lateral forefoot significantly increased after both surgeries, but did not differ between procedures. Kinematic data only showed a few differences between the Evans and the Z-osteotomy.

CONCLUSIONS

Radiographic evidence demonstrated that our model produced a mild Stage II flexible flatfoot from neutrally aligned cadaveric specimens, and post-surgical feet showed significant improvement. Few differences between the surgical techniques were seen in the kinematic and kinetic data.

REFERENCES

1. Roush GC, et al. (2011). *Cadaveric Simulation of Flatfoot and Surgical Corrective Techniques: The Evans versus the Z-osteotomy* [Masters dissertation, University of Washington]

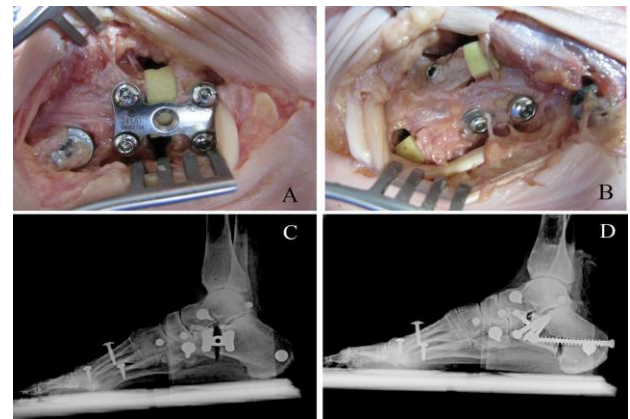


Figure 1: A specimen having received the (A) Evans lateral column lengthening and the (B) Z-osteotomy. The post-surgery M/L radiograph (C, D) is shown below each of the photographs. More screws than typically seen clinically were used to secure the fracture site and plastic wedges were used to maintain bony position. Note that hardware not associated with the fracture site was used to secure the kinematic markers.

Table 1. Mean and standard errors [SE] initial vs. flatfoot differences and flatfoot vs. post-surgery between Evans and Z ($p < 0.05$).

	Mean [SE] change from: Initial→flat/flat→post-surg.	Evans or Z	Mean [SE] change from flat to post-surg.	p-value Initial→flat/flat→post-surg./Evans vs Z
Calcaneal pitch angle (°)	-2.7 [1.1]/+3.6 [1.1]	Evans Z	+2.5 [1.4] +4.7 [1.4]	0.015/0.0014/0.27
Lateral talometatarsal angle (°)	+7.7 [1.0]/-6.0 [1.0]	Evans Z	-4.6 [1.3] -7.4 [1.3]	<0.0001/<0.0001/0.13
Navicular height (mm)	-4.4 [1.3]/+4.7 [1.3]	Evans Z	+4.2 [1.2] +5.2 [1.2]	0.0010/0.0006/0.53
Talonavicular coverage angle (°)	+7.2 [1.3]/-9.2 [1.3]	Evans Z	-8.0 [1.5] -10.3 [1.5]	<0.0001/<0.0001/0.25
Calcaneal eversion distance (mm)	+6.2 [1.6]/-6.9 [1.3]	Evans Z	-7.1 [1.5] -6.6 [1.5]	0.0005/<0.0001/0.79

QUANTIFYING THE ACTIVITY LEVELS OF TODDLERS WITH DOWN SYNDROME PLAYING IN A PARTIAL BODY WEIGHT SUPPORT SYSTEM

Hoffman, ME^{1,3}, Abuatiq R², Steele, KM^{1,3} and Feldner, HA^{2,3}

Departments of ¹Mechanical Engineering, and ²Rehabilitation Medicine, University of Washington,

³Center for Research and Education on Accessible Technology and Experiences (CREATE), University of Washington

email: miahoff@uw.edu, web: <https://miahoffmannnd.github.io/>

INTRODUCTION

Children with Down Syndrome (DS) have delayed motor milestones compared to typically developing peers. Previous work demonstrated that partial body weight supported (PBWS) treadmill training can decrease the time it takes a child with Down Syndrome to learn to walk^{1,2}. However, treadmill training does not adequately mimic the typical activity of a toddler where motor skills are built through nonlinear play and environmental exploration³. In this work, we quantified activity levels of children with DS playing with and without body weight support from a PBWS system in an enriched play environment. We hypothesized that children would increase physical activity (PA) and decrease sedentary (SD) activity when PBWS was provided.

METHODS

Thirteen children (6M:7F, age M: 1.68 yrs) with DS across three sites (University of Washington, University of Puget Sound, and Texas Women's University) were included. All research visits took place in a standardized enriched play environment beneath a 9' x 9' PBWS support structure equipped with toys and platforms to encourage a child to freely move about the space and play at different heights (Figure 1). Children participated in 18, 30-minute play sessions: 9 with subject-



Figure 1. The Research Unicorn playing in the standardized enriched play environment while wearing a harness in the partial body weight support system.

specific PBWS and 9 without PBWS in a randomized crossover order. Data were collected from an Actigraph GT3X+ accelerometer mounted on the mid-trunk of a PBWS harness worn by each child. Vector magnitudes were converted to PA

counts using 15-second epochs and classified as SD, light, or moderate-to-vigorous (MV) PA based on established cut-points^{4,5}. Paired two-tailed t-tests were conducted for each participant comparing PA levels between sessions with and without PBWS.

RESULTS

Body-worn accelerometers detected minimal difference in activity level between play sessions (Figure 2). MV activity was significantly greater ($p<0.05$) in play sessions without PBWS for 8 out of 13 participants. On average, participants spent 7.21-

66.4% of the session in MV activity without PBWS, versus 1.95-60.1% with PBWS. In contrast, SD activity significantly increased ($p<0.05$) for 4/13 participants with PBWS.

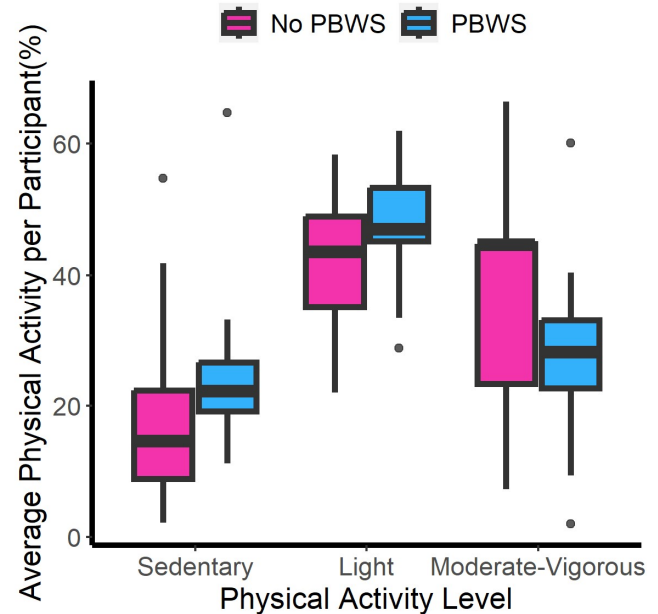


Figure 2. The average percentages in sedentary, light, and moderate-to-vigorous physical activity for each child when

DISCUSSION

Despite being able to freely explore and move, this work shows that playing in a PBWS system may not increase the PA levels of a toddler with DS as measured by an accelerometer. Body-worn accelerometers may not capture critical changes in activity with PBWS, such as body position or loading (e.g., standing vs. sitting). Hence a child standing stationary with weight offset from PBWS may be classified as SD with traditional measures of activity levels from accelerometry but still be supporting important motor development behaviors. Future work using actigraphy with toddlers should look at using cut-point-free PA classification methods and the combination of multiple sensors (e.g., thigh and trunk) to detect changes in body orientation. Other modalities to monitor exploratory play, such as video coding or inclinometers, may be needed to understand how PA levels and engagement change during play sessions with and without PBWS.

REFERENCES

1. Ulrich et al. *Pediatrics* **108**, 2001.
2. Angrulo-Barroso et al. *Gait & Posture* **27**, 2008.
3. Hoch, O'Grady, and Adolph. *Dev. Science* **22**, 2018.
4. Altenburg et al. *J Sport Sciences* **40**, 2022.
5. Trost et al. *Obesity* **20**, 2012.

THICKNESS OF DUAL-DENSITY METAMATERIALS INFLUENCES 3D-PRINTED INSOLE PROPERTIES

Nickerson, KA^{1,2}, Li, EY^{1,2}, Telfer, S^{1,3}, Ledoux, WR^{1,2,3}, Muir, BC^{1,2}

¹RR&D Center for Limb Loss and MoBility (ClimB), Department of Veterans Affairs, Seattle, WA

Departments of ²Mechanical Engineering, and ³Orthopaedics and Sports Medicine, University of Washington, Seattle, WA

email: kanick@uw.edu, web: <https://www.amputation.research.va.gov/>

INTRODUCTION

Individuals with diabetic neuropathy are at high risk for lower limb amputation due to plantar ulcers caused by loss of protective sensation and high plantar pressures [1]. Custom insoles are prescribed to redistribute plantar loads and offload high-pressure regions. These standard of care (SoC) insoles are typically made from multi-layer foams with an accommodative top layer for pressure reduction and a rigid bottom layer for support and pressure redistribution [2]. However, 3D-printed metamaterials may be a more durable and customizable choice for insole fabrication. Previously, our group developed subject-specific 3D-printed insoles that match the full-contact and multilayer design of SoC insoles [3]. One challenge of a full contact design is that the insole may vary in thickness to conform to the shape of a foot. Little is known about the relationship between the thickness of dual-density lattices and their mechanical properties. The purpose of this study was to investigate the influence of thickness on the behavior of dual-density lattices for use in 3D-printed accommodative insoles.

METHODS

Two lattices of differing strut diameters (0.6 mm, 1.03 mm) were designed by Carbon (Carbon Inc., Redwood City, CA) to match the stiffness profiles of bilaminate (accommodative) and EVA (rigid) foams, both are components of a tri-layer foam (Amfit Inc., Vancouver, WA) commonly used for SoC insole fabrication. A third lattice with a uniform strut diameter (0.85 mm) which was the average of the accommodative and rigid lattice struts was also generated. Dual-density lattices with a rigid bottom layer and an accommodative top layer were designed to model the layers of the SoC insole. Pucks of three different compositions were printed with Carbon® Elastomeric Polyurethane (EPU) 41 at thicknesses of 7, 10, and 13 mm, each 30 mm in diameter, to represent insole regions of varying thicknesses [4]. Across puck heights, two types of dual-density lattices and a single-density lattice were printed. The average single-density (ASD) pucks had the average strut diameter lattice across their full thickness. Equal dual-density (EDD) pucks had equal ratios of rigid and accommodative regions across puck thicknesses. Lastly, the consistent dual-density (CDD) puck had an accommodative region kept at 4 mm thick across all puck thicknesses, matching the bilaminate layer (nominally 4 mm) in SoC insoles. Each puck underwent 1000 cycles of compression testing in an E3000 materials testing machine (Instron, Norwood, MA) following the procedures detailed by Hudak et al. [3]. The local stiffnesses at loads equal to plantar pressures of 50, 150, and 250, and the loading curves

for the final loading cycle were compared across puck thicknesses for each configuration (ASD, EDD, CDD).

RESULTS AND DISCUSSION

For ASD pucks, as thickness increased, local stiffness decreased (Table 1), exhibiting behaviors consistent with single-density foam insoles [4]. The stiffness of EDD pucks also decreased as puck thickness increased, suggesting that overall puck thickness and stiffness are inversely related for single and dual-density pucks. In addition to puck thickness, layer thickness impacted the stiffness of dual-density pucks as CDD pucks of all thicknesses had similar stiffness curves for applied pressures less than 250 kPa (Figure 1). The small range of stiffness values across CDD pucks shows that accommodative region thickness may have a more pronounced effect on stiffness for pressures under 250 kPa than total puck thickness. To produce an insole of variable thickness with consistent properties under equal loading, a CDD lattice should be utilized. Although the range in local stiffness values for CDD pucks starts to increase at 250 kPa, a CDD lattice may be sufficient for use in an insole as plantar pressures greater than 200 kPa are considered high-risk for developing ulcers and may require additional offloading [5].

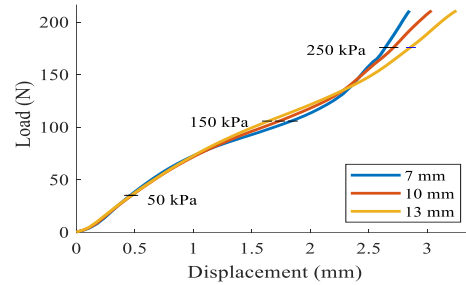


Figure 1: CDD pucks' load-displacement curves for the final cycle of pressure application to 300 kPa

CONCLUSIONS

3D-printed dual-density lattices with constant accommodative and variable rigid region thicknesses may be sufficient for use in accommodative insoles.

REFERENCES

1. Stress R, et al. Diabetes Care **20**(5), 1997.
2. Janisse D and Janisse E, Pro Orth Int **39**(1), 40-47, 2015.
3. Hudak Y, et al. Med Eng & Phys **104**, 2022.
4. Lemmon D, et al. J Biomech **30**(6), 1997.
5. Owings TM, et al. Diabetes Care **33**(5), 2008.

ACKNOWLEDGEMENTS

Funding for this study was provided by VA Award A3539R.

Table 1: Local stiffness values (N/mm) and stiffness range for ASD, EDD, and CDD pucks of multiple thicknesses

		ASD				EDD				CDD			
		7 mm	10 mm	13 mm	Range	7 mm	10 mm	13 mm	Range	7 mm	10 mm	13 mm	Range
Applied Pressure	50 (kPa)	133.80	91.38	69.75	64.05	261.44	129.77	81.69	179.76	87.29	80.40	79.73	7.55
	150 (kPa)	76.16	56.43	46.02	30.14	242.24	91.35	44.77	197.47	42.63	43.92	45.02	2.39
	250 (kPa)	75.54	61.19	44.05	31.49	212.49	86.23	78.02	134.48	151.54	105.74	87.15	64.39

EFFECTS OF SUBMAXIMAL TREADMILL RUNNING ON PLANTAR FASCIA PROPERTIES IN RESOLVED PLANTAR FASCIITIS INDIVIDUALS

Krumpl, L¹, Bailey, JP¹

¹Department of Movement Sciences, University of Idaho, Moscow, ID USA

email: lkrumpl@uidaho.edu

INTRODUCTION

The underlying mechanisms of plantar fasciitis are still unknown. Theories regarding the mechanical sequence of tissue creep suggest that repetitive loading leads to initial plantar fascia (PF) thinning, followed by an inflammatory reparative process. As theorized, PF thickness and stiffness decrease after one running bout, but approximate pre-exercise values after 30 minutes of recovery in individuals without history of plantar fasciitis [1]. Yet, little is known as to whether these PF property mechanics maintain after injury and pain have subsided.

Individuals with plantar fasciitis show increased thickness and decreased stiffness of PF [2,3]. The etiological relationship between these mechanical property differences and the development of plantar fasciitis are however unknown. Additionally, it is unclear how the PF responds once the pain is resolved compared to tissue that has not been previously injured in response to a running stimulus. Thus, the purpose of this study was to evaluate the effects of a 30-minute submaximal treadmill run on PF thickness and stiffness in individuals with resolved plantar fasciitis versus those with no history of plantar fasciitis.

METHODS

Twenty healthy individuals participated in this study. Eight participants had resolved plantar fasciitis (RPF) (4 females; age: 25.1yrs [± 9.8]; mass: 69.4kg [± 12.2], height 180.2cm [± 11.3]). Resolved plantar fasciitis was defined as having had no symptoms for at least one month [4]. Twelve participants had no plantar fasciitis (NPF) history (2 females; age: 23.7yrs [± 5.4]; mass: 70.8kg [± 8.5], height 177.5cm [± 7.1]). Participants performed a maximal effort graded exercise test prior to determine ventilatory threshold 2 (VT2). 80% of the speed at VT2 was used as relative velocity for the 30-minute submaximal run. PF thickness and stiffness were recorded with ultrasonography (LOGIQ S8, GE, Boston, MA, USA) at four time points (before, immediately after, 15 minutes after, and 30 minutes after the run). Thickness was captured via B-mode and stiffness was measured via shear wave elastography. Three live images for each property were taken per time point. Data were analyzed via mixed model (2 group x 4 time) repeated measures ANOVAs, and significant findings were explored with *post-hoc* t-tests. Statistical analyses were completed via SPSS (v.29.0) with alpha levels set at .05.

RESULTS AND DISCUSSION

Analyses showed a significant main effect of time ($p < 0.001$), and a significant main effect of group for PF thickness ($p = 0.042$). Regardless of group, *post-hoc* t-tests revealed that thickness decreased between pre- and post-run ($p < 0.001$; 3.4 to 2.9mm) & increased from post- to 15 min post-run ($p < 0.001$; 2.9 to 3.25mm) and from 15 min post- and 30 min post-run ($p < 0.001$; 3.25 to 3.49mm) (Fig 1). Between groups, *post-hoc* t-tests revealed that the RPF group had a greater PF thickness

compared to the NPF group at the pre-run ($p = 0.016$; 3.84 vs. 3.21mm), the post-run ($p = 0.041$; 3.28 vs. 2.65mm), the 15 min post-run ($p = 0.035$; 3.58 vs. 2.93mm), and the 30 min post-run ($p = 0.045$; 3.81 vs. 3.18) measurements (Fig 1).

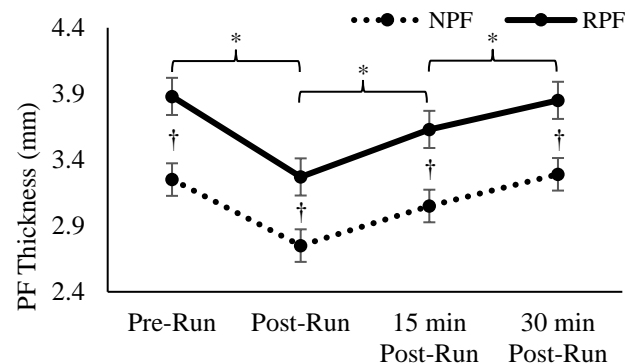


Figure 1: PF Thickness (mm) measurements for the no plantar fasciitis (NPF) and resolved plantar fasciitis groups (RPF).

*Denotes a significant difference between the two adjacent PF measurements regardless of group. #Denotes a significant difference in PF thickness measurements between the two groups.

There was a significant main effect of time ($p < 0.001$) and for group for PF stiffness ($p = 0.018$). Regardless of group, *post-hoc* t-tests revealed that PF stiffness decreased from pre- to post-run ($p < 0.001$; 4.11 to 3.13m/s), increased from post- to 15 min post-run ($p < 0.001$; 3.13 to 3.81m/s) but did not change from 15 min post-run to 30 min post-run measurements. Between groups, *post-hoc* t-tests revealed that the RPF group had a greater PF stiffness compared to the NPF group at the pre-run ($p = 0.03$; 4.54 vs. 3.68m/s) and the 30 min post-run ($p = 0.002$; 4.7 vs 3.62m/s) measurements only.

These findings indicate that the properties of the PF of both asymptomatic and resolved plantar fasciitis individuals behave similarly in response to submaximal treadmill running stimuli. However, mean thickness and stiffness were greater in the RPF group compared to the NPF group for most measurements. This suggests that previous plantar fasciitis alters the morphology of the tissue long term, yet its viscoelastic properties and responses maintain.

CONCLUSIONS

The results highlight that tissue response to mechanical loading, as well as the acute recovery period, do not change with injury history once resolved. This outcome provides essential information for understanding how previously injured PF tissue reacts to mechanical loading, and potentially creates new avenues to evaluate PF injury prevention strategies.

REFERENCES

1. Shiotani H, et al. *J Med & Sc Sports* **30**, 1360-1368, 2020.
2. Baur D, et al. *J Clin Med* **10**, 2351, 2021.
3. Goff JD & Crawford R. *Am Fam Physician* **84**, 76-682, 2011.
4. Wiegand K, et al. *Clin Biomech* **97**, 2022.

SEX-DIFFERENCES IN THE BIOMECHANICS OF SOFT TISSUE OVER THE HIP: ANALYSIS OF MUSCLE ACTIVATION AND HIP REGION.

Khorami, F^{1,2}, Sparrey, C^{1,2}

¹ Department of Mechatronic Systems Engineering, Simon Fraser University, Surrey, BC, V3T 0A3, Canada.

² International Collaboration on Repair Discoveries (ICORD), Vancouver, BC, Canada.

email: csparrey@sfu.ca, web: <https://www.sfu.ca/neurospine.html>

INTRODUCTION

Falls onto hips are one of the main causes of fall-related morbidities [1]. The probability of a hip fracture increases exponentially in females [2]. The soft tissues that cover the hip, function as a natural shock absorber, and disperse the impact forces applied to the bone [3]. It is crucial to comprehend how these forces are distributed by the presence of soft tissues and whether a fall event causes a hip fracture.

Research has shown that sex differences in hip biomechanics and injury risk may potentially be related to variations in muscle activation patterns [4]. Therefore, considering muscle activation is essential when studying sex differences in hip biomechanics and injury risk, as it may provide insights into risk factor analysis and potential strategies for preventative designs.

METHODS

In this research, 40 healthy young people (age = 25.53 ± 3.41 ; 20 males and 20 females) were recruited. EMG and ultrasound imaging were used to record muscle activity and measure soft tissue thickness, respectively. Participants were side lying on a padded massage table with their hips and knees flexed 45 degrees, and the dynamic mechanical indentation test was performed using a precision linear actuator on 6 distinct sites (Figure 1).

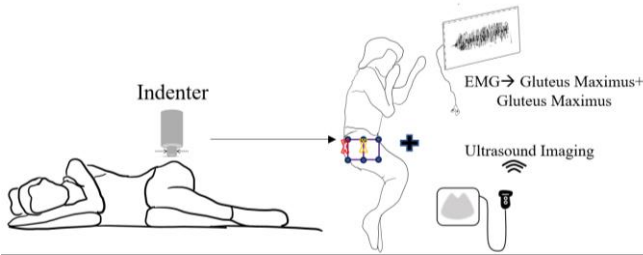


Figure1: The Participants position, indentation, and ultrasound imaging locations on the hip (6 dot grid). Electrode positions on the participant's gluteus medius muscle belly (yellow cross) and gluteus maximus muscle (red cross) are shown.

During the indentation trials, force and displacement were recorded for 6 locations in both passive and active conditions.

Peak force, absorbed energy and stiffnesses were analyzed in sex groups, BMI groups and muscle activation state in all 6 hip sites.

RESULTS AND DISCUSSION

Across the greater trochanter, the soft tissue response was nonlinear, and the unloading response had a pronounced hysteresis. Males experienced a peak force that was 38% greater than females' in passive state ($p=0.005$). When individuals were categorized by BMI, only the obese group ($BMI>30$) showed significant differences in peak force, absorbed energy and stiffness (Table1).

The absorbed energy during contact was 32% greater in the active state than the passive state in all participants ($p = 0.01$). The hip's stiffness varied across different sites, ranging from 0.70 N/m at the posterior gluteal area to 1.20 N/m at the greater trochanter along the femur. We discovered that muscle activation improved energy absorption by up to 32%, indicating that using an active body while falling may be safer.

CONCLUSIONS

Results from the current study can be used for computer model calibrations, fall simulations and the development of more accurate physical test surrogates. The large variability in mechanical tissue properties highlight the need to use targeted properties in models instead of utilizing a single generic model to represent everyone. Sex, muscle activation, and test location all affected observed tissue response with values varying by up to nearly 40 %. Population specific tissue properties may help to better understand injury risk factors for different people.

REFERENCES

1. Empana JP, et al. *J Am Geriatr Soc* 2004.
2. Cummings SR, et al. *Lancet* 2002.
3. Choi WJ, et al. *J Biomech* 2015.
4. Kim SS, et al. *J Mech Behav Biomed Mater* 2023.
5. Anderson RWG, et al. *Nonlinear Dyn* 2009

ACKNOWLEDGEMENTS

This research was supported by NSERC RGPIN-2018-06382 and NSERC RGPAS – 2018 – 522659.

Table 1: Average of peak force, stiffness, and absorbed energy in obese BMI group in muscle passive and active states.

		Passive state	Active state	P-value
BMI>30	Peak force	5.83 ± 2.31	9.47 ± 2.93	0.03
	Stiffness	0.91 ± 0.75	2.02 ± 0.89	0.03
	Energy absorbed	25.19 ± 11.10	43.32 ± 13.18	0.02

Seeing Progress: An Augmented Reality System for Assessing and Visualizing Biomechanics

Matthew A. Sielecki¹ Marianne S. Black¹

¹Department of Mechanical Engineering, University of Victoria

email: msielecki@uvic.ca, marianneblack@uvic.ca

INTRODUCTION

Outside of appointments, most physiotherapy patients don't do their supplemental exercises [1]. Having a device that can assess and provide feedback for tele-physiotherapy could motivate individuals to follow their exercise routines. The overarching goal of this project is to create a device to monitor exercises and correct exercise form. As similar devices already exist, 3D instructional guidance displayed through an augmented reality (AR) headset could be a unique alternative solution.

The main research objective was to display real-time body tracking using the onboard camera stream on an AR headset in conjunction with a mirror.

METHODS

We chose the HoloLens 2 (HL2) headset for the project. The HL2 has a transparent visor, allowing the user to see their real-world surroundings, and displays 3D virtual objects as an overlay. The HL2's front-facing photo/video (PV) camera takes 8-Megapixel frames containing RGB color data (32 bits) [2]. All HoloLens 2 application development was done in Unity.

For pose tracking, we chose OpenPose, a real-time multi-person system to detect the human body, hands, facial and foot joints (keypoints) on single images [3]. We used 2D, single-person body (25 keypoints) detection on a mirror reflecting the user's body. Openpose processed the frames on a computer with the HL2 connected to it via a USB cable.

We developed a custom Unity project to capture PV camera frames as well as send, receive, and display data. Transmission Control Protocol (TCP) sockets connected the Unity project to OpenPose. TCP sockets send data packets between a client and a server. The camera frames are captured by Unity, sent to OpenPose for 25-keypoint body tracking, and 2D vector coordinates are sent back to Unity. Finally, Unity assigned the coordinates to GameObjects displayed on the HL2 (Figure 1).

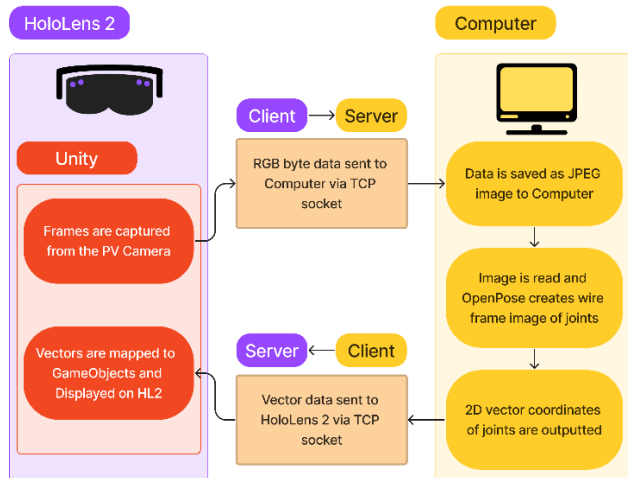


Figure 1: Flow chart of the current data pipeline from sending PV Camera frames to receiving analyzed image data.

While the HL2 only directly connected to Unity, the computer TCP sockets and the OpenPose analysis ran through external python scripts.

RESULTS AND DISCUSSION

We developed the ability to apply OpenPose's 2D, real-time, body tracking from the HL2 camera stream using a full-length mirror (Figure 2).

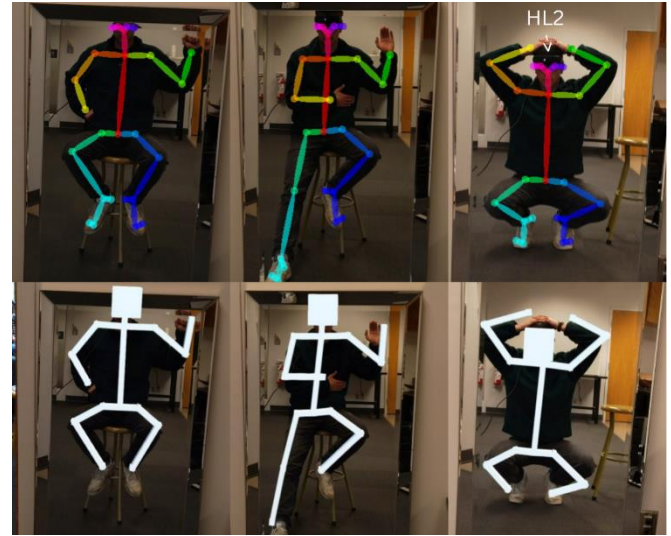


Figure 2: Top row: OpenPose analysis overlaid on photos taken on HL2. Bottom row: Unity GameObjects displayed on the HL2 screen as seen by the user.

The current method of body tracking uses the PV camera, which takes 2D, RGB images. This system could be exported to any headset with an outward-facing camera, such as a Meta Quest or a Magic Leap. Configuring OpenPose with the HL2 depth sensor could produce 3D body tracking results [2,3]. Future work will validate body pose tracking against a motion capture system.

CONCLUSION

We developed a pipeline to use an on-board AR RGB camera with a mirror for 25 keypoint pose tracking and to display the result on the AR device.

REFERENCES

1. R. Campbell, et al. *Journal of Epidemiology & Community Health*, vol. **55**, no. 2, pp. 132-138, 2001.
2. D. Ungureanu, et al. *ArXiv*, vol. **abs/2008.11239**, 2020.
3. Z. Cao, et al. *IEEE Transactions on Pattern Analysis and Machine Intelligence*, 2019.

ACKNOWLEDGEMENTS

Special thanks to EnoxSoftware for their PV Camera Stream binary and Peter Gu for his HoloLens 2 Research binary. Funding was provided by the Canada Research Chairs program and by NSERC USRA.

NOVEL METHODS TO ASSESS INTERFRAGMENTARY MOTION IN DISTAL FEMUR FRACTURES: COMPUTED TOMOGRAPHY VALIDATION

Aerie Grantham¹, Elmer Vasquez², William D. Lack^{1,3}, and William R. Ledoux^{1,3,4}

¹RR&D Center for Limb Loss and MoBility, VA Puget Sound, Seattle, WA, ²School of Medicine and Departments of

³Orthopaedics & Sports Medicine and ⁴Mechanical Engineering, University of Washington, Seattle, WA

email: aerieg@uw.edu web: www.amputation.research.va.gov

INTRODUCTION

Nonunion of distal femur fractures occurs for 32% of these injuries despite nonunion for long bone fractures in general affecting only 5 to 10% of injuries [1-3]. Fracture site motion has been associated with fracture healing rather than the stiffness of the construct used to repair it [4]. However, no previous work has been able to quantify fracture site motion which limits orthopedic surgeons' ability to optimize constructs for fracture healing. In an effort to overcome this obstacle, this study aims to validate different methods of quantifying in vivo fracture motion via a computational modeling, computed tomography (CT), and biplane fluoroscopic assessment. The latter two will use novel bone-based and bead-based tracking processes to quantify fracture site motion. This paper focuses on the current work done on the CT validation aspect.

METHODS

For the CT aspect of this study there is a human subject and cadaveric component. Subjects with distal femur fractures will be recruited from VAPSHCS, UW Medical Center, or Harborview Medical Center. Static stance scans will be captured using a LineUP cone-beam CT scanner (CurveBeam, Hatfield, PA) located at the Center for Limb Loss and MoBility (CLiMB) and are segmented using Mimics medical imaging analysis software (Materialise, Leuven, Belgium).

The human subject static stance data will be used to quantify motion at the fracture site by tracking the position of the proximal and distal femur segments from two scans, one as a non-weight bearing CT (NWBCT) scan and one weight bearing CT (WBCT) scan.

Seven fresh-frozen cadaveric femurs were osteotomized and had a variety of construct configurations (rod and nail as well as lateral locking plate with variable screw placement) affixed to them in order to simulate repairing a distal femur fracture. Stainless steel beads were also implanted in all femurs to allow for bead-based tracking in the CT scans. Prior to hardware implantation, the femurs were scanned at a radiology clinic (Rayus Radiology) with a fan-beam CT scanner (General Electric, Brightspeed). This will be referred to as the 'clinical CT scan'. The specimens were scanned under NWBCT and WBCT conditions in the LineUP scanner by first scanning with just the femur in place, then the femur with increasing weights stacked on top of a femoral head mount (maximum weight of 225.5 N).

Preliminary motion tracking was done by manually aligning the proximal and distal segments from the clinical CT scans to the LineUP scans and picking four points of interest on both segments labeled according to their locations: anteromedial (AM), anterolateral (AL), posteromedial (PM), and

posterolateral (PL). The point-to-point distance was measured for the NWBCT scan and a maximally loaded (225.5N) WBCT scan.

RESULTS & DISCUSSION

The preliminary fracture site motion data (Table 1) shows that as expected, there is less movement on the lateral side in comparison to the medial side. In specimen 6, we see less variation in movement as it is a rod and nail fixation type. As this is preliminary data between two scans per specimen, no statistical analysis has been performed.

The human subject portion presents unique challenges. Each subject's mobility is different and they may not be able to sufficiently load the femur of interest for a WBCT. In addition, the metal constructs in their leg induce metal artifact that make scans difficult and time consuming to segment.

Currently in progress is the development an algorithm that would facilitate bone-based CT registration between clinical and LineUP CT scans. This would allow for measuring fracture site motion much more consistently by minimizing the amount of user input required. This would be utilized for both human subject and cadaver scans. At the same time, work is being done to develop a bead-based tracking methodology to use for the cadaver scans.

Table 1. Point-to-Point displacements of the distal and proximal cadaver segments between 0 N and 225.5 N loading conditions

Specimen	AL (mm)	AM (mm)	PL (mm)	PM (mm)
1	3.83	8.24	-2.29	6.93
2	0.8	2.05	0.72	3
3	4.21	2.76	-0.7	3.14
4	0.45	-0.05	0.68	3.83
5	-0.7	3.93	1.89	7.7
6	-0.3	0.8	0.38	0.79
7	0.47	0.63	4.3	2.06

REFERENCES

1. Lujan, T. J. *et al. Locked Plating of Distal Femur Fractures Leads to Inconsistent and Asymmetric Callus Formation.* www.jorthotrauma.com.
2. Tzioupis, C. & Giannoudis, P. v. *Prevalence of long-bone non-unions.* www.etseven.com/locate/injury (2007).
3. Calori, G., Mazza, E., Colombo, M. & Ripamonti, C. The use of bone-graft substitutes in large bone defects: Any specific needs?
4. Elkins, J. *et al. Motion predicts clinical callus formation.* *Journal of Bone and Joint Surgery - American Volume* **98**, 276-284 (2016).

EFFECTS OF SHOE CUSHIONING ON KNEE LOADING DURING DOWNHILL RUNNING

Paige, L.P., McKibben, K., Baird, A., and Becker, J.

Department of Health & Human Development, Montana State University, Bozeman MT USA

Email: LACHLANPAIGE24@GMAIL.COM, web: <http://www.montana.edu/biomechanics>

INTRODUCTION

Maximally cushioned (MAX) shoes were originally introduced for trail running based on the assumption that they reduce impact loading while running downhill. However, recent studies have shown that compared to traditionally cushioned (TRAD) shoes, MAX shoes increase vertical impact peaks on level terrain and vertical loading rates during downhill running [1,2]. From an injury prevention perspective, the internal loading of tissues is salient, but this is only mildly related to external ground reaction force (GRF) parameters [3], and it remains unknown how MAX shoes influence internal loads at common injury sites during downhill running. Therefore, the purpose of this study was to analyze the impact of MAX and TRAD shoes on patellofemoral and tibiofemoral joint kinetics while running downhill at varying grades (10% and 20%). It was hypothesized that participants wearing MAX shoes would have higher tibiofemoral compressive forces and patellofemoral joint stress, at all grades and that loads would increase with grade.

METHODS

20 healthy adults who run at least 20 miles per month (sex: 5F, 15M; age: 25.89 ± 7.95 years; height: 1.78 ± 0.08 m; mass: 71.69 ± 11.06 kg) were randomly assigned to run in either TRAD or MAX shoes. Participants ran for five minutes in their assigned shoe to become acclimated, and then for five minutes at level, -10%, and -20% grades. Whole body kinematics were recorded at 250 Hz using a 6-camera motion capture system (Motion Analysis, Rohnert Park CA) while ground reaction forces were collected from an instrumented treadmill (Treadmetrix, Park City UT).

At each grade, joint angles, reaction forces, and moments were calculated using Visual 3D for twenty consecutive gait cycles. Tibiofemoral, and patellofemoral kinetics were then calculated using a musculoskeletal model [4,5]. Peak forces, loading rates, impulses, and cumulative impulses per kilometer were then

calculated for all joints. 2x3 mixed ANOVAs were used to evaluate differences in dependent variables across grades and shoe conditions.

RESULTS AND DISCUSSION

To date preliminary results from 10 participants indicate that peak knee flexion ($p < .001$), knee extensor moments ($p < .001$), patellofemoral contact force ($p = .002$) and joint stress ($p = .002$), tibiofemoral compressive ($p = .004$) and shear ($p = .004$) force, and tibiofemoral compressive ($p = .023$) loading rates all displayed main effects of grade, all increasing with higher grades. There were no main effects of shoe for any variable.

These results provide deeper insight about impact loading while running in MAX and TRAD shoes. Although GRF parameters increase while running downhill in MAX shoes [2], our preliminary results show it is mainly the grade and not shoe driving these increases. These findings further support the idea that GRF parameters are only mildly related to internal tissue loading [3] and indicate that MAX shoes may not be different from an injury prevention standpoint than TRAD shoes during downhill trail running.

CONCLUSIONS

Tibiofemoral and patellofemoral kinetics increase with grade but are not affected by shoe type. Future studies could explore how a wider range of grades and speeds influence these differences.

REFERENCES

1. Kulmala JP, et al. *Sci Rep* **8**, 17496, 2018.
2. Chan ZYS, et al. *Eur J Sport Sci* **18**, 1083-1089, 2005.
3. Matijevich, et al. *PLOS One* **14**, 0210000, 2019.
4. Willy et al. *J Orthop Sports Phys Ther* **46**, 664-672, 2016.
5. Willy et al. *J Sports Sci* **34**, 1602-1611, 2016.

Table 1. Mean and standard deviations across grades and shoe type for peak knee flexion (KF), knee extensor moments (KEM), patellofemoral contact forces (PFCF) and joint stress (PFJS), tibiofemoral compressive (TFC) and shear (TFS) forces and loading rates (TFCLR, TFSLR).

	Level		8% downhill		10% downhill	
	Trad	Max	Trad	Max	Trad	Max
KF (°)	33.82 (± 4.15)	33.84 (± 3.03)	37.78 (± 4.94)	37.30 (± 0.57)	41.99 (± 5.96)	39.38 (± 1.37)
KEM (Nm/m*kg)	0.86 (± 0.14)	0.99 (± 0.03)	1.23 (± 0.25)	1.31 (± 0.10)	1.26 (± 0.20)	1.42 (± 0.31)
PFCF (BW)	3.30 (± 0.36)	3.63 (± 0.33)	4.50 (± 1.14)	4.88 (± 0.35)	4.56 (± 0.69)	4.99 (± 0.63)
PFJS (MPa)	4.91 (± 0.59)	4.43 (± 0.41)	6.37 (± 1.18)	5.76 (± 0.25)	6.39 (± 0.78)	6.00 (± 1.04)
TFC (BW)	8.01 (± 0.69)	7.88 (± 1.31)	9.43 (± 0.83)	9.49 (± 0.41)	8.56 (± 1.03)	9.16 (± 0.76)
TFCLR (BW/s)	106.97 (± 19.98)	102.32 (± 32.19)	154.29 (± 54.04)	163.93 (± 95.05)	162.06 (± 43.70)	196.07 (± 139.96)
TFS (BW)	1.47 (± 0.08)	1.37 (± 0.09)	1.66 (± 0.24)	1.53 (± 0.23)	1.56 (± 0.22)	1.66 (± 0.32)
TFSLR (BW/s)	34.26 (± 7.10)	32.52 (± 3.28)	42.72 (± 15.29)	40.39 (± 20.80)	42.72 (± 13.15)	50.91 (± 37.71)

VALIDATION OF BIPLANE FLUOROSCOPY BONE TRACKING

Nicholas Entress^{1,2}, Aerie Grantham¹, Eric Thorhauer^{1,2}, William R. Ledoux^{1,2,3}

¹RR&D Center for Limb Loss and MoBility (CLiMB), VA Puget Sound, Seattle, WA

Departments of ²Mechanical Engineering and ³Orthopaedics& Sports Medicine, University of Washington, Seattle, WA
email: nentress@uw.edu

INTRODUCTION

Traditional methods of tracking bone motion in the foot are limited in precision and practicality. External markers fixed to the skin have limited accuracy, with the skin covering the foot moving relative to the densely packed bones beneath [1]. CT and MRI scans are limited to static representations of the foot [2]. Markers drilled into the bone work well for cadavers, but are not practical for living subjects.

Our proposed solution is to utilize a biplane fluoroscopy system; pairs of X-ray videos captured simultaneously and at a high frame rate are used to track the bones of living subjects during a gait cycle. Similar methods in prior studies have been shown to be an accurate way of measuring bone motion [3]. Before data from this system can be used in various studies, it must first be validated. The purpose of this study, currently in progress, is to determine the accuracy of bone tracking measurements made with our biplane fluoroscopy system.

In addition to validation of our bone tracking, another goal of this study is to develop a methodology for testing cadaveric specimens in our biplane system. Such a process has the potential to be used for a variety of future studies.

METHODS

Normal human limb gait kinematics and ground reaction forces have been captured in the CLiMB gait lab. Ankle muscle forces are needed for ankle plantarflexion, dorsiflexion, inversion, and eversion. These forces were taken from existing literature. The kinematics, ground reaction forces, and muscle forces were used to generate a simulated standard gait trajectory. This trajectory was fed into our simVITRO system, consisting of a Kuka robotic arm, a force plate, and four tendon actuators.

To run our trials, a cadaveric foot and a portion of the tibia and fibula is mounted to the robotic arm. Tendons connected to the four muscle groups described earlier are attached to the four actuators. An optimization procedure iteratively alters the superior, anterior, and medial positions of the foot, as well as the ankle plantarflexion force, until the ground reaction forces match those of the desired trajectory. The rotational position of the tibia is not altered during the optimization process.

The robotic gait simulation will next be run under biplane fluoroscopy. Metal beads implanted into the bones of the foot will be tracked using a previously validated bead tracking tool. This will provide us with accurate measurements of the position of each bone in the global coordinate system.

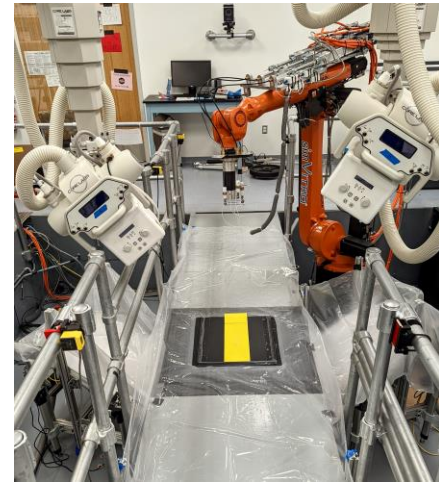


Figure 1: The Kuka robot in the Biplane Lab positioned to mount a cadaveric specimen.

The same bones will then be directly tracked under fluoroscopy using our in-house bone-tracking software. This software, called DRACO, determines bone pose and position. The results can then be compared (bone-based vs. bead-based) to examine the accuracy and repeatability of fluoroscopy bone tracking during a gait cycle.

CURRENT STATUS

Several cadaveric feet have been attached to the Kuka robot and run through trajectories at varying speeds. The fastest stable trajectory that we have been able to run goes from heel strike to toe-off in ten seconds. We are in the process of fine tuning the robot controller to achieve a smooth motion at faster speeds. The bone tracking software is still in development.

REFERENCES

1. Nester, et al. (2007). Foot kinematics during walking measured using bone and surface mounted markers. *Journal of Biomechanics*, 40(15), 3412–3423.
2. Marquez-Barrientos et al. (2012). Correlation between anatomic foot and ankle movement measured with MRI and with a motion analysis system. *Gait and Posture*, 36(3), 389–393.
3. Anderst, et al. (2009). Validation of three-dimensional model-based tibio-femoral tracking during running. *Medical Engineering and Physics*, 31(1), 10–16.

ACKNOWLEDGEMENTS

Will Lin assisted in creating the trajectories used on the Kuka robot. Eric Thorhauer and Dennis Knippel developed the bone tracking software being validated in this study.

The effects of a meditation intervention on self-reported subjective and physiological stress in college students

Vargas, SA, Lau, KY, McClelland, R, Butte, K, Cannavan, D
Health and Human Performance, Seattle Pacific University, Seattle, WA USA
Email: lauk3@spu.edu [Exercise Science](http://ExerciseScience.com) | [Seattle Pacific University \(spu.edu\)](http://SeattlePacificUniversity.com)

INTRODUCTION

Stress negatively impacts college students' mental health [6]. Although previous studies show meditation practices to improve perceived stress over a prolonged period [4][5], research has yet to find an effective short-term method to reduce momentary stress and quantify it physiologically. Respiratory Exchange Ratio is a common measure of resting metabolism that determines the body's fuel-substrate utilization during resting [3]. Typically, fat is the primary source of fuel under resting conditions (RER of 0.8) and increases during physical activity or intense exercise [1]. When the body is under stress, the body is sympathetically driven to release free glucose in the bloodstream becoming readily available for metabolism [2]. Hence, it can be hypothesized that RER may be used to physiologically quantify stress. Thus, the purpose of this randomized, crossover experimental study was to examine the effect of a meditation intervention using the CALM APP on self-reported momentary stress and RER in moderately stressed college students.

METHODS

Participants (N=12; M_{age} 20.92±1.31) attended the laboratory on two occasions. During these sessions, levels of momentary stress were assessed via a questionnaire and resting RER was measured (metabolic cart; premeasures). Participants were then randomly allocated after the premeasures (momentary stress and RER) to either a 10-min meditation intervention using the CALM APP, or a 10-min control group (were participants lay on the testing bed). Immediately after either time matched condition, momentary stress and RER were remeasured (post measures). They returned one week later (at the same time of day) to complete the other condition. Paired sample t-tests were used to compare the conditions and time points for perceived stress and RER.

RESULTS AND DISCUSSION

Paired sample t-tests showed no difference between RER and MSS score at baseline for momentary stress and RER ($p>0.05$), showing similar baseline values for each session that are not found to be statistically significant as a pre-measurement. There was a significant improvement in momentary stress after both the 10-minute CALM APP intervention ($p<0.05$) and control condition ($p<0.05$) and for RER for the intervention ($p<0.05$) and control ($p<0.05$). Further, there was a significantly greater improvement in the pre-post RER differences in the intervention condition compared to the control condition ($p<0.05$) but not for momentary stress ($p>0.05$; Table 1).

These results demonstrate that the CALM APP meditation was effective at reducing RER. This suggests that meditation alters fuel use as RER values changed from a mean of .85 to a mean of .78. With a mean of .85, the results show that the average participant was working more anaerobically under resting conditions. However, after the intervention, the mean of .78 shows a shift from using carbohydrates as a fuel source to using fat (with a healthy RER of under .8) meaning that the average participant was working more aerobically after the intervention. The intervention was more effective in lowering RER than the control condition. Statistical significance also supported both our intervention and our control protocol were effective in lowering momentary stress

in our participants, however, there was no significant difference between the two interventions. The 10-minute CALM APP meditation protocol showed to be effective in reducing momentary perceived stress and RER in moderately stressed college individuals. Future studies should examine the effects of meditation practices on RER over prolonged intervention periods as well as investigate its relationship with perceived stress.

Table 1. Means ((SD)) of Data Analysis: Paired T-Tests

	Mean (SD)	p-value
RER Pre-Intervention	.85 (.07)	.001*
RER Post-Intervention	.78 (.06)	
RER Pre-Control	.82 (.07)	.033*
RER Post-Control	.80 (.06)	
RER Difference Intervention	.07 (.06)	.002*
RER Difference Control	.03 (.04)	
MSS Pre-Intervention	6.50 (4.34)	.003*
MSS Post-Intervention	3.50 (4.85)	
MSS Pre-Control	5.50 (4.03)	.004*
MSS Post-Control	2.08 (2.94)	
MSS Difference Intervention	3.00 (2.98)	.230
MSS Difference Control	3.42 (3.70)	

* $p<0.05$; RER: Respiratory Exchange Ratio; MSS: Momentary Stress Scale

CONCLUSIONS

College students who undergo very stressful situations should incorporate short meditation practices on a regular basis to help relieve stress and improve their overall physiologic and mental health.

REFERENCES

1. Brooks GA. *Journal of Applied Physiology*. 1994;76(6).
2. Chu B. Physiology, Stress Reaction. PubMed. Published September 18, 2021.
3. Delsoglio M. *Journal of Clinical Medicine*. 2019;8(9):1387.
4. Gorvine MM. *Health Psychology and Behavioral Medicine*. 2019;7(1):385-395
5. Huberty J. *JMIR mHealth and uHealth*. 2019;7(6):e14273.
6. Pedrelli P. *Academic Psychiatry*. 2014;39(5):503-511.

ACKNOWLEDGEMENTS

We give special thank to DR. Butte and Dr. Cannavan for mentorship, support, and for providing the lab equipment. Also, special thanks to our lab tech, Mr. Hubbell, for administering the lab equipment and our subjects for participating in our study.

EFFECTS OF SURFACE STIFFNESS AND MASS ON HEAD IMPACT SEVERITY

Vakili, O¹ and Robinovitch, SN¹

¹ Department of Biomedical Physiology and Kinesiology, Simon Fraser University, Burnaby, Canada

email: ovakili@sfu.ca , web: www.sfu.ca/IPML

INTRODUCTION

Traumatic brain injuries (TBIs) are most often caused by a direct blow to the head [1]. The risk for TBI depends on the peak head acceleration during impact, which in turn depends on the impact velocity, and the stiffness and mass of the object that impacts the head [2]. In this project, we conducted experiments with a Hybrid-III head-form to examine how peak head acceleration depends on the stiffness and mass of the object that the head impacts.

METHODS

We conducted experiments with a Hybrid-III head (containing nine accelerometers) and neck secured to an impact pendulum that struck a surface with two different impact velocities of 2.55 ± 0.06 and 3.31 ± 0.03 m/s (Figure 1). We systematically modified the mass and stiffness of the impact surface by placing a metal plate above, below or between layers of soft and hard polymeric foam. We conducted three repeated trials in each condition and used ANOVA to compare peak translational head accelerations between conditions.

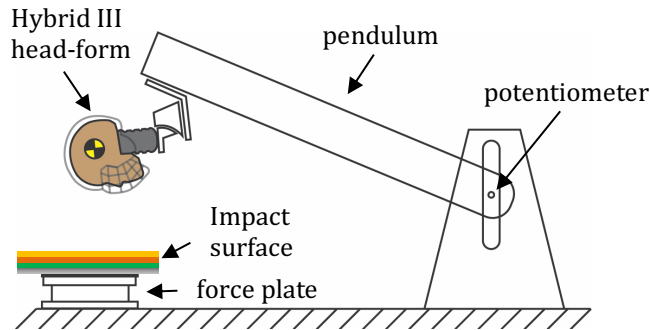


Figure 1. Hybrid III impact pendulum setup. The impact surface consisted of varying layers of foam and a metal plate.

RESULTS AND DISCUSSION

The addition of mass to the impact surface increased peak head accelerations, in a manner that depended on the location of the mass relative to the impact surface, and the stiffness of the foam above and below the mass. In the low velocity impacts, when the mass was located closest to the surface, the peak acceleration increased 30.2% (from 18.9 ± 1.8 to 24.8 ± 1.8 g; $p < 0.0001$) relative to the zero mass condition. In the high velocity impacts, when the mass was located below a hard foam layer, the peak acceleration increased 17.2% (from 31.4 ± 0.4 g to 26.8 ± 0.3 ; $p = 0.0010$). When the mass was located below a soft foam layer, the peak acceleration was no different for the zero mass condition ($p = 0.2416$ and 0.7791).

CONCLUSIONS

The stiffness and mass of the impacting surface influenced head impact accelerations. The effect of mass was mitigated by a variable stiffness medium having a low-stiffness top layer. By clarifying how peak head accelerations depend on the stiffness and mass of the impact surface, our results can inform the design of helmets and padding to reduce the risk for TBI in high-risk activities and environments.

REFERENCES

1. Hutchison MG, et al. *Br J Sports Med* **49**(8), 552–555, 2015.
2. de Grau S, et al. *Proc IMechE Part P: J Sports Engineering and Technology* **234**(1), 98-106, 2020.
3. Yan EB, et al. *Neuroscience* **248**, 17–29, 2013

ACKNOWLEDGEMENTS

Supported by NSERC (RGPIN/04065-2015), the (CSA) Group and the (ASTM) International.

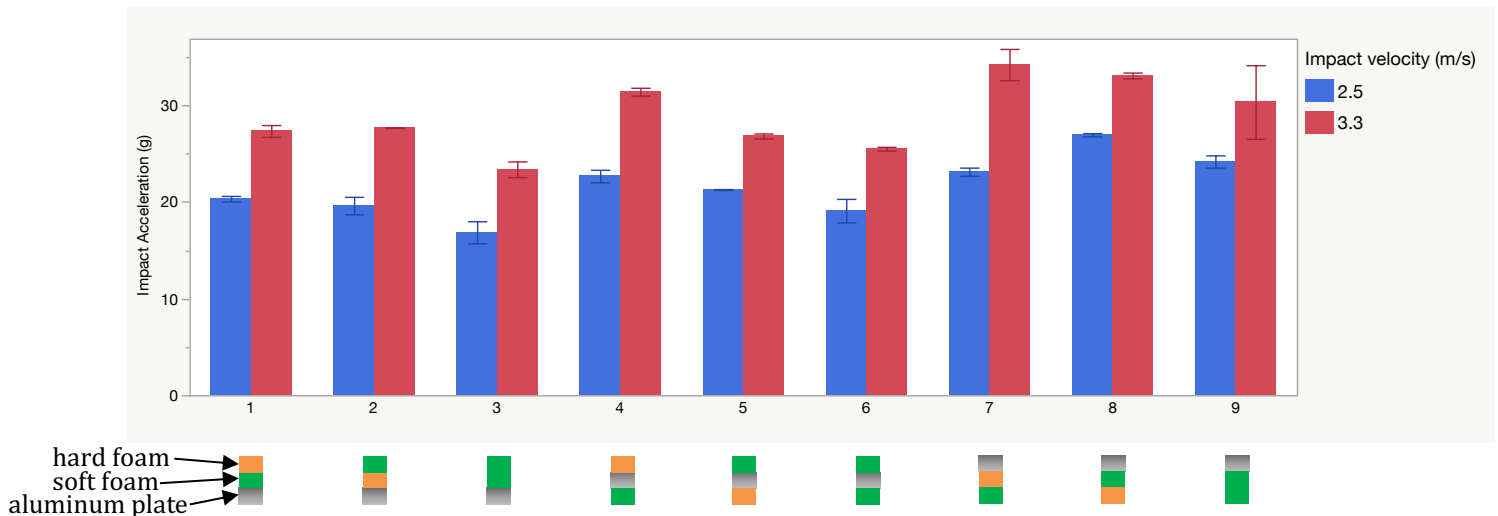


Figure 2. Mean peak resultant translational head acceleration for each impact condition. Error bars are showing standard deviation. Conditions 1-3 involve no mass, conditions 4-6 involve mass sandwiched between foam layers, and conditions 7-9 involve mass at the top, closest to the head.

PRELIMINARY DESIGN PROCESS FOR THE DEVELOPMENT OF A NEW ASSISTIVE WALKING DEVICE

Diaz, K.^{1,2}, Nickerson, K.^{1,2}, and Muir, B.C.^{1,2}

¹Department of Mechanical Engineering, University of Washington

²RR&D Center for Limb Loss and MoBility (CLiMB), VA Puget Sound, Seattle, WA USA

email: kdiaz10@uw.edu, web: <https://amputation.research.va.gov>

INTRODUCTION

Walkers are commonly prescribed mobility aids to reduce falls in older adults [1]. While walkers theoretically increase stability by widening the user's base of support, studies have found no significant improvement in fall incidence rates for walker users compared to non-users with the same demographic and medical backgrounds [2]. In previous work, we analyzed common fall circumstances among older adult wheeled walker users in long-term care facilities and found that sideways and backward falls are the most prevalent fall directions for users. Deficiencies in the maneuverability, lateral stability, and velocity control of current walkers contributed to falls, indicating that device redesign is needed [3]. The purpose of this project is to present the preliminary design process for the development of a novel assistive walking device that addresses the current deficiencies of existing walker designs.

METHODS

Market research was conducted to identify and analyze existing walker designs. The design specifications (cost, weight, etc.) of 12 walkers were evaluated. Additionally, we performed a stakeholder analysis by reviewing existing literature on assistive technology deficits, including interviews with clinicians and users. Based on this background and the previously identified areas of deficiency, we established lists of core functions, customer requirements, and engineering specifications to be used as a benchmark for preliminary concept generation.

RESULTS AND DISCUSSION

Market Research: General specifications for two common walker designs, the two-wheeled walker and rollator, are listed in Table 1. Two-wheeled walkers are primarily used by patients who require weight-bearing support. With fixed front-wheels, the user must pick up the device to turn. For patients with increased mobility or poor endurance, rollators are more maneuverable and have an integrated seat. Most rollators are equipped with cable loop brakes which are difficult to engage for users with low grip strength [4].

Table 1: Most Common Walker Designs on Market

	Two-Wheeled	Rollator
		
Cost	\$30-\$100	\$100-\$800
Weight	5-10 lbs	15-22 lbs
Brakes	No	Yes
Wheel rotation	Rear: N/A Front: Fixed	Rear: Fixed Front: 360°

Stakeholder Analysis: We have identified users, clinicians, and health insurance companies as the top beneficiaries of a new walker design since these groups currently face the most challenges with existing walkers. For example, users may fall and sustain injury whilst using a walker [2] so they seek a device which increases their safety and locomotor independence. Clinicians struggle with improper device use among patients [5] and seek a device that requires less demanding training and promotes natural gait patterns. Insurance companies face complex and expensive claims and seek a device that reduces upfront cost and medical bills from injury.

Core Functions and Requirements: For a walker to satisfy the stakeholder needs, the walker must be 1) stable during basic locomotion (walking, turning, sitting, and standing), 2) maneuverable in home, in-patient, and outdoor environments, 3) transportable, 4) easy to operate (low physical and cognitive load), and 5) adjustable throughout disease progression. Other lower-level requirements are low cost, durability, and comfort.

Engineering Specifications: To drive the design of a new walker, measurable specifications are listed in Table 2.

Table 2: Critical-to-Quality Specifications

Cost	≤ \$350	Weight Capacity	≥ 300 lbs
Width	22 – 26"	Wheel # and Diameter	4 ≥ 8"
Height	32 – 39"	Handle Grip Width	17 – 18"
Weight	≤ 15 lbs	Required Brake Force	≤ 18.2 kg

Concept Generation: Concepts targeting stability during locomotor activities include adjustable wheel resistance to control device velocity and developing new, easier-to-use mechanisms to engage and lock the brakes. For optimal maneuverability, a new rollator will have front wheels with only 180° of lateral rotation. Other concepts include a flip-up seat to promote appropriate body position within the device during gait, detachable weights to improve transportability without sacrificing stability, and adjustable width and seat heights to increase user customization.

CONCLUSIONS

The next steps in the design process are to select concepts, develop prototypes, and conduct benchmark testing. Additional investigation of clinician perspectives on new mobility device designs is needed to increase likelihood of device translation to the clinical field.

REFERENCES

1. Stel VS, et al. *Age and Aging*, **33**(1), 2004.
2. Gell NM, et al. *JAGS*, **63**(5), 2015.
3. Nickerson KA, et al. *J. Assist. Technol.*, under review.
4. Einbinder E, *US Patent 7708120B2*, 2010.
5. Clarke P, et al. *JAH*, **21**(4), 2009.

Acute Fatigue Modifies Musculotendinous Stiffness

J. D. Cooper¹, A. W. Ricci¹, D. M. Callahan¹

Department of ¹Human Physiology, University of Oregon,
Eugene, Oregon

INTRODUCTION

Musculotendinous stiffness affects tension generation and flexibility, making it an important contributor to athletic performance. Musculotendinous stiffness may also predict soft-tissue injury risk. Recent studies [1-3] have demonstrated acute reductions in whole skeletal muscle stiffness following a single bout of fatiguing exercise. Fatigue-induced stiffness reduction may contribute to increased injury risk at fatigue, especially in female athletes [4,5]. However, previous studies were conducted in almost exclusively males, and it is unclear whether the stiffness response to fatigue differs in males versus females. Furthermore, previous studies assessed resting muscle stiffness, and the effect of fatiguing exercise on active skeletal muscle stiffness remains unclear. Therefore, the purpose of this study is to investigate the changes in active musculotendinous stiffness in the Patellar Tendon (PT) and Vastus Lateralis (VL) after a single bout of fatiguing exercise in young adult males and females.

METHODS

20 young, highly trained male (11) and female (9) volunteers performed three maximum voluntary isometric contractions (MVIC) of the knee extensors (KE). Maximum strength and rate of torque development (RTD) were assessed. Active stiffness was measured at the vastus lateralis muscle (VL) and patellar tendon (PT) via ultrasound at 50% of MVIC during ramped isometric contractions. Volunteers then performed repeated, isotonic KE at 30% MVIC until task failure. Active stiffness measures were repeated immediately following the fatiguing exercise. Active stiffness values were calculated as absolute change in force divided by the absolute change in length. Differences in stiffness were assessed by two factor (sex/fatigue) repeated measures ANOVA with pairwise comparisons. Sex differences in strength and morphology were assessed by unpaired t-test.

RESULTS AND DISCUSSION

There was no main effect of fatigue on VL ($p=0.23$) or PT ($p=0.90$) active stiffness. However, there was a fatigue by sex interaction ($p=0.02$) on PT stiffness, and trends suggesting fatigue decreased PT stiffness in males ($p=0.08$) and increased PT stiffness in females ($p=0.13$). PT stiffness was significantly higher in males versus females at baseline ($p=0.02$) but did not differ after fatigue ($p=0.96$). There was a strong main effect of sex on active VL stiffness ($p<0.01$).

CONCLUSIONS

Fatigue induces PT compliance during contraction in males but not in females, suggesting a possible mechanism for enhanced injury risk.

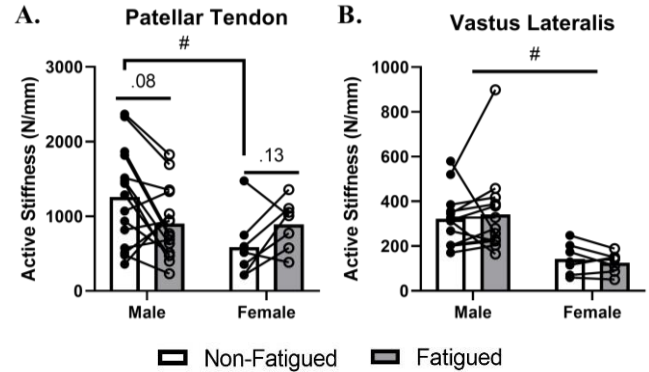


Figure 1. Active stiffness in the PT (A) and VL (B) of males and females before and after fatiguing exercise. # indicates sex effect, $\alpha = 0.05$.

REFERENCES

- [1] P. Andonian et al., "Shear-wave elastography assessments of quadriceps stiffness changes prior to, during and after prolonged exercise: a longitudinal study during an extreme mountain ultramarathon," *PLoS One*, vol. 11, no. 8, p. e0161855, 2016.
- [2] E. Chalchat et al., "Changes in the viscoelastic properties of the vastus lateralis muscle with fatigue," *Frontiers in Physiology*, vol. 11, p. 307, 2020.
- [3] J. Siracusa et al., "Resting muscle shear modulus measured with ultrasound shear-wave elastography as an alternative tool to assess muscle fatigue in humans," *Frontiers in physiology*, vol. 10, p. 626, 2019.
- [4] E. A. Arendt, J. Agel, and R. Dick, "Anterior Cruciate Ligament Injury Patterns Among Collegiate Men and Women," *J Athl Train*, vol. 34, no. 2, pp. 86–92, 1999.
- [5] J. R. Deitch et al., "Injury Risk in Professional Basketball Players: A Comparison of Women's National Basketball Association and National Basketball Association Athletes," *Am J Sports Med*, vol. 34, no. 7, pp. 1077–1083, Jul. 2006

ACKNOWLEDGEMENTS

This work was supported by the Wu Tsai Human Performance Alliance. Many thanks are also due to the study volunteers, who make these studies possible.

Muscle Function and Morphology						
Sex	Relative Peak Torque (Nm/cm)*	Rate of Torque Development (%MVIC/s)	Peak Power (W)*	Time to Fatigue (s)	Muscle Thickness (cm)*	Echogenicity (AU)*
Males	127.8 ± 31.8	6.7 ± 1.9	683.1 ± 179.4	75.4 ± 19.2	2.5 ± 0.40	28.6 ± 17.1
Females	83.8 ± 27.9	6.2 ± 2.1	383.9 ± 129.6	95.9 ± 51.6	2.2 ± 0.34	64.0 ± 20.1

EXPLORING THE EFFECT OF PHYSICAL ACTIVITY ON IN VIVO PASSIVE STIFFNESS IN THE LUMBAR SPINE

Chelsea M. Dumasal^{1*} & Kayla Fewster¹

¹School of Kinesiology, University of British Columbia, Vancouver, BC, Canada

*Corresponding author's email: cdumasal@student.ubc.ca

INTRODUCTION

Passive stiffness in the lumbar spine is an indicator of lumbar spine health, as passive stiffness properties contribute to spinal stability [1,2]. Deviations in baseline passive stiffness may provide insights into lumbar spine injury mechanisms or pain reporting, as changes in lumbar spine stiffness have been linked to factors such as chronic low back pain reporting [3], rear-end automobile collisions [4], and prolonged sitting [5]. As such, more recent findings have advocated for switching between postures for lumbar spine health, as opposed to static postures [6, 7]. Despite this potential for movement to positively influence the lumbar spine, one limitation common to the passive studies is that physical activity (PA) lifestyle behaviours across participants is not controlled for. To address this gap, the purpose of the current investigation was to determine the effect of PA lifestyle on flexion passive stiffness in the lumbar spine. It was hypothesized that differences in passive stiffness would emerge across participants classified as having either an active (ACT) or sedentary (SED) lifestyle.

METHODS

9 participants (5 ACT, 4 SED) were recruited. To measure PA lifestyle, participants completed the International PA

Questionnaire - Short Form to quantify their activity and of which types [8]. Participants were classified as SED if they routinely completed less than 150 minutes of moderate-to-vigorous aerobic activity and less than 2 sessions of total-body strengthening activities per week over the past year. Likewise, participants fell into the ACT group if they met aerobic and strength activity thresholds. During passive stiffness testing, participants laid on their left side on a customized frictionless jig. The legs, pelvis and arms were secured in a fixed position, while the torso was permitted to move through the full range of flexion motion. The experimenter then pulled the participant into maximum flexion. Throughout testing, motion capture tracked motion of the trunk and pelvis (Optotrak Certus, NDI, Waterloo, Canada) at a rate of 20 Hz. A load cell (Model MLP-100, Transducer Techniques Inc., Temecula, CA) was attached in series to the top of the upper body cradle to measure the force applied by the experimenter. Surface EMG (2000 Hz, Noraxon, USA Inc., Scottsdale, Arizona, USA) monitored the lumbar erector spinae and rectus abdominus bilaterally to ensure they remained below 5% MVC. Applied moment was calculated by measuring the moment arm between the point of force application and the location of the L4-L5 intervertebral disc. From passive trials, moment-angle curves were generated to quantify differences in passive stiffness. Moment-angle curves were partitioned into 3 linear regions (low, transition and high stiffness) for flexion [9]. Differences in the shapes of the passive moment-angle curves (slopes of each region, moment-angle breakpoints) were quantified. A one-way ANOVA assessed the influence of Activity Level on Passive Stiffness parameters.

RESULTS AND DISCUSSION

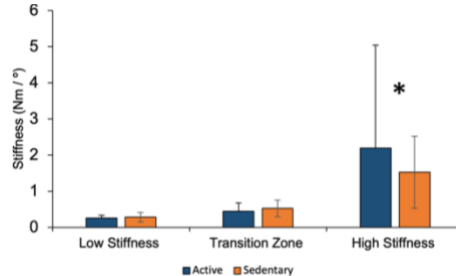


Figure 1: Mean stiffnesses of the ACT group from the low stiffness, transition, and high stiffness zones were 0.26 ± 0.07 , 0.45 ± 0.23 , and 2.20 ± 2.85 Nm/° respectively. Mean stiffnesses of the SED group from the low stiffness, transition, and high stiffness zones were 0.28 ± 0.13 , 0.53 ± 0.23 , and 1.53 ± 1.00 Nm/° respectively. Statistically significant differences are identified with an asterisk.

A significant effect of Activity Level on Passive Stiffness in Lumbar Flexion was observed for the high stiffness slope ($p = 0.020$), indicating that ACT individuals have higher measures of passive stiffness in comparison to SED individuals. No other significant differences were seen across the low stiffness ($p = 0.286$) and transition zone slopes ($p = 0.596$) between groups. Although not significantly different, trends were observed in the low and high moment-angle breakpoints (% maximum flexion), such that the breakpoints of ACT individuals occurred at a greater percentage of their maximum range of lumbar flexion. Mean low moment-angle breakpoints of ACT and SED individuals were $43 \pm 6\%$ and $34 \pm 12\%$ respectively. Mean high moment-angle breakpoints of ACT and SED individuals were $79 \pm 7\%$ and $74 \pm 11\%$ respectively.

CONCLUSIONS

The current investigation demonstrated differences in *in vivo* passive stiffness in the lumbar spine between individuals with a physically active versus sedentary lifestyle. The findings of the study may have implications for injury risk to the lumbar spine. Further studies are warranted to investigate sex-based differences and different types of physical activity.

REFERENCES

1. Panjabi MM, et al. *Spine* **14**, 1111-1115, 1989.
2. Panjabi MM, et al. *J Biomech* **38**, 1694-1701, 2005.
3. Gombatto KM, et al. *Clin Biomech* **23**, 986-995, 2008.
4. Fewster KM, et al. *Clin Biomech* **90**, 105507-105507, 2021.
5. Beach TAC, et al. *TSJ* **5**, 145-154, 2005.
6. Sorensen CJ, et al. *Man Ther* **20**, 553-557, 2015.
7. Fewster KM, et al. *HMS* **66**, 84-90, 2019.
8. Craig CL, et al. *Med & Sci* **35**, 1381-1395, 2003.
9. Barrett JM, et al. *HMS* **76**, 102765-102765, 2021.

ACKNOWLEDGEMENTS

This research was funded by Natural Sciences and Engineering Research Council of Canada.

EFFECT OF UNANTICIPATED CONSTRAINT ON LOWER EXTREMITY ENERGY ABSORPTION DURING JUMP LANDINGS FOLLOWING ACL RECONSTRUCTION

Brendan P. Silvia¹, Fatemeh Aflatounian¹, James N. Becker¹, Keith A. Hutchinson¹, Janet E. Simon², Dustin R. Grooms², and Scott M. Monfort¹

¹Montana State University, Bozeman, MT, USA, ²Ohio University, Athens, Ohio, USA
Email: scott.monfort@montana.edu

INTRODUCTION

Nearly a quarter of athletes younger than 25 years old who have undergone anterior cruciate ligament reconstruction (ACLR) suffer a second ACL injury [1]. Athletes who have undergone ACLR demonstrate altered patterns of bilateral energy absorption in the joints of the lower limbs through greater hip extension and ankle plantar flexion [2]. Return to sport (RTS) tests have found that although limb symmetry in single leg hop distance may be >90%, it is achieved through compensation from the hip and ankle of the injured limb [3]. Additionally, it is unknown how these compensations might change when individuals are subjected to sport-like constraints, such as rapid decision making [4]. The purpose of this study was to examine the differences in energy absorption across each joint of the lower body during unanticipated jump landings. Specifically, this study investigated how an unanticipated directional cue influenced the relative proportion of negative work performed at the ankle, knee, and hip joints during a jump landing. We hypothesized that, due to compensatory mechanisms following ACLR, added cognitive challenge during a jump landing task would cause a decrease in the negative work done at the injured knee during landing.

METHODS

36 participants (10M/26F; 19.8 ± 1.76 yr; 69.57 ± 12.81 kg; 1.71 ± 0.10 m; 1.46 ± 0.62 years since surgery, Tegner: 6.8 ± 1.8) with prior ACLR and having been cleared for RTS performed a series of jump-land-jump trials from a 30 cm box set at half the participants' height from the force plates. Participants were instructed to jump as high as they could upon landing from the initial jump. This abstract focuses on a subset of data from a larger study. Specifically, we focused this analysis on baseline (BL) and unanticipated conditions (UA – a visual cue given ~250 msec prior to the initial landing of which a secondary direction to jump was given: up, 45° left, 45° right). The average of 5 successful conditions for the secondary jump direction of straight up for both the BL and UA were used for the analysis. Lower extremity kinematics and kinetics were estimated, and then negative work for each lower extremity joint for both limbs were calculated for the initial landing by integrating the sagittal plane joint power curves. Percent of negative work at each joint was used as the dependent variable, with the primary analysis focusing on the percent of negative work at the involved knee. Mixed effects models were used to test for differences between conditions (BL vs. UA), with participants as random factors and covariates of age, gender, mass, and time since surgery also included in the statistical models.

RESULTS & DISCUSSION

Consistent with prior studies, the uninvolved knee and limb absorbed more energy compared to the involved knee and limb (both $p < 0.001$) [3]. The tendency to use the uninvolved limb more to absorb energy during jump landings may highlight maladaptive landing techniques following ACLR considering the increased

risk of a second ACL injury on the uninvolved limb after passing RTS criteria [2, 5]. However, our hypothesis was not supported as there was not a significant change in energy absorption at the involved or uninvolved knee due to changing conditions ($p = 0.908$ and $p = 0.392$, respectively). When expanding analysis to include other joints, the hip (involved: $p = 0.001$; uninvolved: $p = 0.024$) and ankles (involved: $p = 0.007$; uninvolved: $p < 0.001$) experienced significant differences between conditions, **Figure 1**. For the UA trials, ankles demonstrated an increase in relative energy absorption, while the involved hip demonstrated a decrease in energy absorption. The increase in relative energy absorption at the ankle requires greater involvement from the ankle plantar flexors, which has previously been correlated to an increased loading of the ACL through the action of the gastrocnemius [6,7].

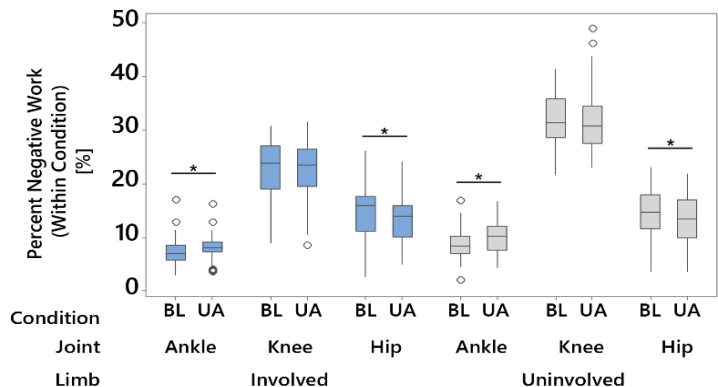


Figure 1. Distribution of negative joint work at each joint (bilaterally) for anticipated (BL) and unanticipated (UA) conditions. Significant differences between conditions are indicated with an *.

Longer time since surgery was associated with greater energy absorption by the involved knee ($p = 0.015$). The increase of energy absorption in the involved knee with increased time since surgery suggests that as this time increases, so does the tendency for patients to involve the surgical knee during jump landings.

CONCLUSIONS

Participants shifted the relative energy absorption from the hip to the ankles when faced with an unanticipated jump landing constraint. These findings highlight how sport scenarios can elicit ACL-injury relevant shifts in energy absorption.

REFERENCES

- [1] Wiggins et al. (2016) AJSM 44(7).
- [2] Decker et al. (2002) MSSE 34(9).
- [3] Kotsifaki et al. (2022) BJSM 56(5).
- [4] Mohammad et al. (2021) IJATT 26(3).
- [5] Webster et al. (2019) SM (49)6.
- [6] Romanchuk et al. (2020) JB 113.
- [7] Navacchia et al. (2019) ABE 47(12).

ACKNOWLEDGEMENTS

This research was supported by the NIH award R03HD101093.

OCCUPATIONAL THERAPIST'S PERSPECTIVES ON THE HARMONY EXOSKELETON FOR POST-STROKE REHABILITATION

Tiffani Teng¹, Clairia Geller², Matthew Stutzenberger², Abbey Lacey², Ileana Howard^{1,3}, Brittney C. Muir^{3,4}

Departments of ¹Rehabilitation Medicine and ³Mechanical Engineering University of Washington; ²Rehabilitation Care Services and

⁴RR&D Center for Limb Loss and MoBility (CLiMB), Department of Veterans Affairs, Seattle, WA USA

Corresponding author email: bcmuir@uw.edu

INTRODUCTION

Stroke is a major health concern worldwide, with millions of new cases diagnosed each year. In the United States alone, hundreds of thousands of people experience a stroke annually, making it the leading cause of neurological long-term disability [1]. Occupational therapy plays a significant role in improving patient's regain in function and engagement in activities that are meaningful to them. Electromechanical and robot-assisted therapy devices have emerged as a promising technology for stroke rehabilitation [2]. Upper-limb rehabilitation robotics offer intensive and repetitive training to promote recovery of upper-limb function in stroke survivors. The Harmony exoskeleton is one of these devices (Figure 1).

In this paper, we aim to explore the perspectives and experiences of occupational therapists who have facilitated robot-assisted therapy using Harmony and examine the advantages and challenges of integrating this therapy into an inpatient rehabilitation program. By gathering this information, we hope to improve the implementation and utilization of robotic therapy in stroke rehabilitation and ultimately enhance patient outcomes.

METHODS

The study team conducted a literature review to develop a set of questions to facilitate the discussion regarding the study clinicians' experiences using the Harmony exoskeleton with stroke survivors.



Figure 1: Harmony Exoskeleton can provide bilateral upper-body training in stroke survivors.

During the discussion, the study teams clinicians were asked to share their perspectives on the strengths and weaknesses of the technology, its ease of use, and highlighted areas for improvement. They also were asked to share their views based upon experience with Harmony on how robotic technology can be utilized in stroke rehabilitation, such as selecting appropriate patients, improving patient engagement, best practices, and obstacles to incorporating its usage in stroke rehabilitation.

RESULTS AND DISCUSSION

Overall, the clinicians felt that the Harmony exoskeleton is a promising tool for upper extremity rehabilitation that can be used in conjunction with traditional therapies to enhance rehabilitation outcomes. Clinicians reported 1) positive results with the use of the Harmony exoskeleton in helping patients gain strength and function in their upper extremities, 2) High patient engagement due to the technological features of the device, and 3) the robot's range of motion provides therapists

with the freedom to devise creative interventions and treatments that are beneficial and motivational for patients. Clinicians also emphasized that the Harmony exoskeleton's ability to provide objective assessment of motor activities is a significant advantage during the rehabilitation process. The adjunctive role of the robot is also highlighted as a supplementary tool that boosts rehabilitation, especially due to the increased number of repetitions that the Harmony exoskeleton can facilitate in comparison to a human with physical limitations.

While robotic therapy offers significant advantages, it also has potential drawbacks and limitations that need to be addressed. These drawbacks, noted by clinicians, include 1) physical limitations of the current device as the research prototype lacked flexibility, 2) technical difficulties relating to the software function related to the prototype nature, and 3) no method for the robot to provide real time advanced quantitative feedback and data regarding quality of movements, range of motion, and the amount of support needed by the user.

Clinician's opinions on the Harmony exoskeleton is consistent with previous studies on clinician attitudes towards robotic-assisted technology and rehabilitation [3]. Therapists have expressed positive views on the use of robotic-assisted technology in rehabilitation, but they have also expressed concerns about the device's functionality and patient suitability. The challenges associated with adoption and implementation of robotic-assisted technology suggest areas for improvement in future versions of the technology and plans for introducing it in clinical settings

CONCLUSIONS

Clinicians who worked with the Harmony exoskeleton expressed enthusiasm for its benefits in stroke rehabilitation. The device's technological features provide high patient engagement, objective assessment, and adjunctive support for therapists. However, limitations such as physical constraints, technical difficulties, and a desire for quantitative feedback were identified. Continued research and development of the Harmony exoskeleton incorporating feedback from clinicians is necessary to fully realize robotic-assisted technology in stroke rehabilitation.

REFERENCES

1. Tsao CW, et al. *Heart Disease and Stroke Statistics—2022 Update: A Report From the American Heart Association*.
2. Chien, Wai Tong, et al. "Robot-assisted Therapy for Upper-limb Rehabilitation in Subacute Stroke Patients: A Systematic Review and Meta-analysis." *Brain and Behavior* **10**, no. 8 (2020).
3. Mashizume, Y., et al. "Occupational therapists' perceptions of robotics use for patients with chronic stroke." *The American Journal of Occupational Therapy*, **75**(6) (202

COMPARING PEAK TIBIAL INTERNAL ROTATIONAL VELOCITY IN RECREATIONAL RUNNERS IN MAXIMAL AND TRADITIONAL SHOES

Ory, J¹, Traut, A^{1,3}, Bartel, L¹, Phillips, D¹, Pollard, C^{1,2} and Hannigan, J^{1,2}

Program in ¹Kinesiology and ²Physical Therapy, Oregon State University-Cascades, Bend, OR USA

³School of Biological and Population Health Sciences, Oregon State University, Corvallis, Oregon, USA.

email: oryj@oregonstate.edu

INTRODUCTION

Rearfoot eversion during running gait has been associated with developing a running-related injury (RRI) [1]. Differences have been found in eversion mechanics between runners wearing maximal and traditional running shoes, which may increase RRI risk. Historically, rearfoot eversion kinematic data has been obtained using three-dimensional motion capture systems which are expensive, time-consuming to set up, and relatively immobile [1,2,3]. In comparison, wearable sensors such as inertial measurement units (IMUs) are compact, wireless, less expensive, and capable of providing kinematic data such as peak internal tibial rotational velocity (ITRV). Excessive tibial internal rotation is also associated with common RRIs and may be related to eversion mechanics [4]. Therefore, the purpose of this study was to compare peak ITRV of recreational runners wearing maximal running shoes and traditional running shoes using an IMU.

METHODS

41 (21 female, 20 male) recreational runners (ran >10 miles/week) between 18 to 55 years old and that were injury free within the past 6 months participated. Each participant was fitted with a Delsys Trigno® Research+ System wireless sensor that was adhered to the skin at the distal medial tibia with double-sided tape and 3M™ Coban™ reinforcement. Each participant ran 20 meters at a consistent self-selected pace and completed five trials while wearing each of the following shoes: (1) maximal, HOKA Bondi (stack height: rearfoot 37mm, forefoot 33mm), and (2) traditional, New Balance 880 (stack height: rearfoot 32mm, forefoot 22mm).

Gyroscopic data was analyzed and processed with Visual3D software. The peak ITRV was averaged across all trials for each participant for each shoe. Then, the mean peak ITRV was calculated for the participant cohort for each shoe. Paired t-tests ($\alpha = .05$) compared peak ITRV between shoes, and effect sizes were calculated using Cohen's d .

RESULTS AND DISCUSSION

The average peak ITRV for the maximal shoe was 502 ± 101 degrees/second, while the traditional shoe was higher at 538 ± 103 degrees/second ($p < 0.001$, Cohen's $d = 0.35$).

The difference in peak ITRV between shoe type can possibly be attributed to the difference in material and cushioning, as maximal shoes typically have more cushion or 'give' than a traditional running shoe. The extra cushion in a maximal shoe may reduce the ITRV by force absorption during foot landing. In contrast the traditional shoe has a stiffer composition, which may have caused eversion with a 'slap' motion, as opposed to a 'roll' motion with a more cushioned maximal shoe. The slap motion can be characterized as the tibial segment internally rotating

from the beginning to the end of foot landing at a quick rate, whereas the rolling motion would be a more gradual internal rotation and, thus, occurring at a slower rate.

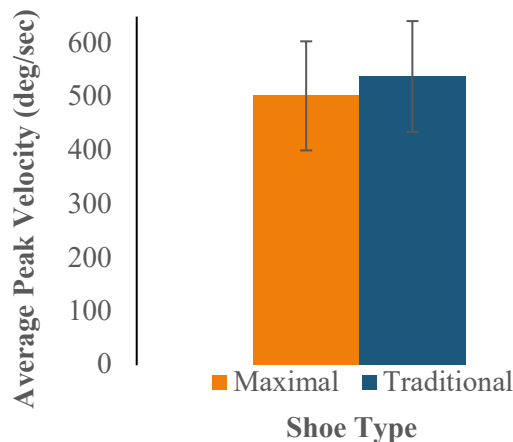


Figure 1: The average peak ITRV for maximal and traditional shoes with standard deviations.

CONCLUSIONS

We conclude that peak ITRV is significantly higher in recreational runners wearing traditional shoes versus maximal shoes. The data from this study indicates that there is a lower peak ITRV of runners in maximal shoes, which may also result in a slower peak rearfoot eversion velocity. Given rearfoot eversion's association with RRIs, more research should be done to evaluate the relationships with rearfoot eversion velocity and ITRV between various shoe types. This may provide additional insight regarding how shoe type relates to injury risk.

REFERENCES

1. Pollard et al. *Orthopedic Journal of Sports Med* **6**, 2018.
2. Farina and Hahn. *Biology* **11**, 2018.
3. Williams et al. *Journal of Athletic Training* **49**, 290-296, 2014.
4. Fischer et al. *Gait & Posture* **51**, 188-193, 2017.

ACKNOWLEDGEMENTS

We would like to thank the OSU Cascades Layman Fellowship program, made possible by Doug and Daisy Layman, for funding this research. Additionally, we appreciate the support and contributions to this research from the OSU Cascades FORCE Lab, Bethany Burr, and Rian Ory, M.S.

The **Zeno Walkway System** powered by **PKMAS Software** collects and analyzes temporal, spatial and pressure data for overground gait and movement research, education and clinical applications.

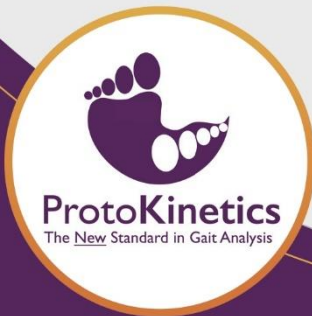


Features:

- Durable 2 or 3 layer configuration
- Portable roll up design
- No equipment placed on subject
- Sizes to fit your needs

Our platform delivers clinically relevant, scientifically valid, and repeatable data for:

- Gait protocols
- Standing balance
- Jumping and hopping
- Transitional movements
- Running
- And More



www.protokinetics.com



BERTEC

Poster Session B

*Sponsored by
The College of Engineering at
the University of Washington*

Saturday, May 20th

10:00-11:00 am

Poster #		Alder Commons
1	KINEMATIC SEQUENCE DIFFERENCES BETWEEN TRAINED BASEBALL PLAYERS AND UNTRAINED ADOLESCENT INDIVIDUALS Wukelic, CP, Machak, S, Gromeier, M, and Shultz, SP	
2	A ROBOTIC GAIT SIMULATOR USING A 6-DOF ROTOPOD CONTROLLED WITH SIMVITRO SOFTWARE FOR TESTING PROSTHETIC AND CADAVERIC FEET William Lin, William R. Ledoux	
3	QUANTIFYING TENSION IN A VERTEBRAL BODY TETHERING SYSTEM FOR SCOLIOSIS TREATMENT Phoebe Cain, Christy Farnsworth, Jason Caffrey, Tony Olmert, Erin Mannen, and Salil Upasani.	
4	TRANSPORT DYNAMICS IN THE RAT ACHILLES TENDON DEPEND ON PARTICLE SIZE Forer, JM, Pacheco, YC, Link, K, Hahn, ME, Willett, NJ	
5	QUANTIFYING FACET JOINT CAPSULE STRAIN IN THE CERVICAL SPINE Isabel D. Evans, Jeff M. Barrett, Kayla M. Fewster	
6	EFFECT OF SPEED ON LOWER LIMB JOINT STIFFNESS DURING DECLINE RUNNING Lee S., Robinson R., Chebbi A., Hahn M.	
7	VALIDITY AND RELIABILITY OF A SMARTPHONE IN MEASURING POSTURAL STABILITY Lovekin, Emily; Lugade, Vipul; Davis, April; San Juan, Jun	
8	EFFECTS OF PRIOR ACLR AND COGNITIVE CHALLENGE ON POSTURAL CONTROL FOLLOWING A MEDIAL SIDE HOP Kaylan J Wait, Fatemah Aflatounian, Janet E Simon, Dustin R Grooms, James N Becker, Keith A Hutchison, Scott M Monfort	

Poster Session B - cont.

9	EXPLORING CLINICIAN PERSPECTIVE ON STANDARD OF CARE AND 3D-PRINTED ACCOMMODATIVE INSOLES Leo Gagnon, Kimberly Nickerson, Christina Carranza, Brittney Muir
10	QUANTITATIVE EVALUATION OF NOVEL HYBRID ANKLE FOOT ORTHOTIC DESIGN Gagnon, L, Muir, B, Klute, G, Cyr, K, Walling, K and Rogers, E
11	EFFECTS OF MANUAL MOBILIZATIONS ON FOOT KINEMATICS AND MUSCLE ACTIVITY Riley Hagger, Jackson Golden, James Becker, Forest Allan, Lachlan Paige
12	RELIABILITY OF LOW- AND HIGH-TECH METHODS TO QUANTIFY RUNNING FOOTWEAR FEATURES OF AN ERGOGENIC SHOE: A PRELIMINARY ANALYSIS Katie Landwehr, Sarah Shultz, Cristine Agresta
13	THE EFFECT OF SPEED ON ANKLE JOINT MECHANICS DURING INCLINE TREADMILL RUNNING Hidetaka Hayashi, Rachel Robinson, Seth Donahue, Aida Chebbi, Michael Hahn
14	DOES SUTURE TYPE OR CONFIGURATION MATTER IN PERCUTANEOUS ACHILLES TENDON REPAIR? Hana Keller, Scott Telfer, Kenneth Chin, Nate Benner, Grant Branam
15	INFANT CARRIAGE STRATEGIES UTILIZED BY NULLIPAROUS WOMEN WHILE NEGOTIATING STAIRS Holly Olvera, Abigail R. Brittain, Erin M. Mannen, Safeer F. Siddicky
16	NEUROFENCING: STUDY OF BRAIN, HEART AND MUSCLE NEURON ACTION POTENTIALS TO IMPROVE FENCER PERFORMANCE Supriya Nair
17	EFFECT OF 3-D PRINTED CUSTOM ACCOMMODATIVE INSOLES ON BALANCE DURING WALKING Mathew Sunil Varre, Patrick Aubin, Jing-Sheng Li, Brittney C. Muir
18	THREE-DIMENSIONAL ANALYSIS OF WINDLASS MECHANISM USING WEIGHTBEARING COMPUTED TOMOGRAPHY IN PATIENTS WITH HALLUX RIGIDUS AND HEALTHY VOLUNTEERS Takumi Kihara

Poster Session B - cont.

19	DEVELOPING COMPUTATIONAL MODELS OF UNILATERAL CERVICAL CONTUSIONS IN RATS TO QUANTIFY INJURY BIOMECHANICS Dexter L. Zamora, Cesar Jimenez, Shawn Liu, Carolyn J. Sparrey
20	LOWER-LIMB MUSCLE CO-ACTIVATION DOES NOT DIFFER BY AGE DURING DISTRACTED WALKING OVER CHALLENGING SURFACES Matthew V. Robinett, Nicholas L. Hunt, Amy E. Holcomb, Clare K. Fitzpatrick, and Tyler N. Brown
21	MORPHOLOGICAL PROPERTIES OF THE PLANTAR FASCIA: INTERVAL VS. CONTINUOUS RUNNING Margaret A. Lewis, Lukas Kruppl, Joshua P. Bailey
22	EVALUATING EFFICACY OF A FORCE-AMPLIFYING IMPLANTABLE MECHANISM IN A LIVE RABBIT FOREARM MODEL USING ELECTRICAL STIMULATION TO GENERATE MUSCLE TWITCHES Gabiella I Justen, Hantao Ling, Leah Streb, Jennifer Sargent, and Ravi Balasubramanian
23	MYTH OR SCIENCE: INCREASED GLUTEUS MAXIMUS ACTIVATION IMPROVES RUNNING ECONOMY Ricardo Sanchez, Carlos Hernandez, Justus Ortega
24	EFFECTS OF A TOTAL MOTION RELEASE (TMR®) INTERVENTION ON ASYMMETRICAL MOVEMENT PATTERNS Nickolai Martonick, Joshua Bailey
25	EVALUATING FRICTIONAL FORCES AT THE TENDON-IMPLANT INTERFACE WITH AND WITHOUT A LUBRICIOUS NON-FOULING COATING Ajay Zubin Ratty, Hantao Ling, Ravi Balasubramanian
26	EVALUATING THE BIOMECHANICAL EFFICACY OF AN ORTHOPEDIC IMPLANT IN AN IN-VIVO RABBIT MODEL Mockel, Stayce A; Bestel, Hans A; Balasubramanian, Ravi
27	MEASURING NATURAL DIVING KINEMATICS Alex Liu, Hayden Sidney-Phillips, Jean-Sébastien Blouin, Peter Cripton, Gunter Siegmund
28	MECHANICAL CHARACTERIZATION OF PAVLIK HARNESS STRAPS Sabrina L Mead, Erin M Mannen

Poster Session B - cont.

29	EFFECTS OF SIDE LOAD CARRIAGE ON LIMB LOADING AND UNLOADING IN TRANSTIBIAL AMPUTEES Satria Ardiuanauri, Krista M. Cyr, Glenn K. Klute, Richard R. Neptune
30	SURFACE, BUT NOT AGE IMPACT LOWER LIMB JOINT WORK DURING WALK AND STAIR ASCENT Thomas A. Wenzel, Nicholas L. Hunt, Amy E. Holcomb, Clare K. Fitzpatrick, Tyler N. Brown
31	EFFECTS OF CHANGING HIP POSITION ON SCAPULAR KINEMATICS Sarah Schlittler, Dave Suprak, Lorrie Brilla, Jun San Juan
32	EVALUATING EXISTING TRANSTIBIAL AMPUTEE MUSCULOSKELETAL MODELS FOR USE ON FEMALE POPULATIONS: A SYSTEMATIC REVIEW Tess M.R. Carswell, Misha Hasan, and Joshua W. Giles
33	STUDYING SEX DIFFERENCES IN THE PROSTHETIC NEEDS AND PRIORITIES OF LOWER LIMB AMPUTEES BY ADAPTING THE PROSTHESIS EVALUATION QUESTIONNAIRE Tess M.R. Carswell, Helen Monkman, and Joshua W. Giles
34	ACUTE EFFECTS OF A NON-EXHAUSTIVE LONG RUN ON METATARSAL BONE LOADS Kaitlyn McKibben, Megan Peach, and James Becker
35	MEASURING PLANTAR TISSUE STIFFNESS WITH THE ULTRASHOE (AN ULTRASOUND EMBEDDED SANDAL) Ellen Y. Li, Scott Telfer, Brittney Muir, William R. Ledoux
36	MACHINE LEARNING METHODS FOR FACILITATING ANALYSIS OF KANGAROO RAT HOPPING Ozanich NR, Tamakloe VT, McGowan CP, and Lin DC

Kinematic Sequence Differences Between Trained Baseball Players and Untrained Adolescent Individuals

Wukelic, CP^{1,2}, Machak, S^{1,3}, Gromeier, M^{4,5}, and Shultz, SP^{1,6}

¹Kinesiology Department, Seattle University, ²Center for Limb Loss and MoBility, VA Puget Sound, Seattle WA, USA, ³University of Canterbury, Canterbury, England, UK, ⁴Faculty of Psychology and Sports Science, Department of Sport Science, Bielefeld University, Bielefeld, Germany, ⁵Neurocognition and Action-Biomechanics – Research Group, Bielefeld University, Bielefeld, Germany, ⁶Marjorie K Unterberg School of Nursing and Health Studies, Monmouth University, NJ, USA
email: wukelicc@seattleu.edu, web: <https://www.seattleu.edu/artsci/kinesiology/ms/>

INTRODUCTION

An overhead throwing motion is a common gross motor skill often taught in early childhood. Studies have found that fundamental motor competency (e.g. object control) is positively correlated with physical activity and cardio-respiratory fitness in children and adolescents [1,2]. Research investigating motor efficiency in overhead throw often focuses on improving performance in trained individuals. This project compares kinematic sequencing between trained and untrained youth.

METHODS

After a brief warm-up, untrained high school students (N=9) and trained high school and college students (N=10) threw a weighted tennis ball for accuracy (N=10 throws). Upper extremity angular velocities were collected using three-dimensional inertial sensor motion capture. Kinematic sequencing of joints (pelvis, trunk, shoulder, elbow, wrist) was assessed using Kruskal-Wallis test; Friedman and Wilcoxon tests identified group differences between sequences.

RESULTS AND DISCUSSION

Ten independent kinematic sequences were identified (N=3 unique trained; N=6 unique untrained; N=1 shared). The most common kinematic sequence (Figure 1) was the ideal proximal-to-distal sequencing when throwing overhead (pelvis → trunk → shoulder → elbow → wrist). The rankings for the trained group maintained a consistent pattern with only elbow and wrist joints producing similar rankings (Table 1). The untrained group lacked that consistency with similar rankings of elbow vs wrist, trunk vs shoulder, and pelvis vs shoulder.

CONCLUSIONS

Trained individuals threw with a more efficient distal-to-proximal sequencing pattern than the untrained participants, specifically at the trunk and shoulder. Continuous training of gross motor skills beyond initial skill development is necessary to maintain motor proficiency.

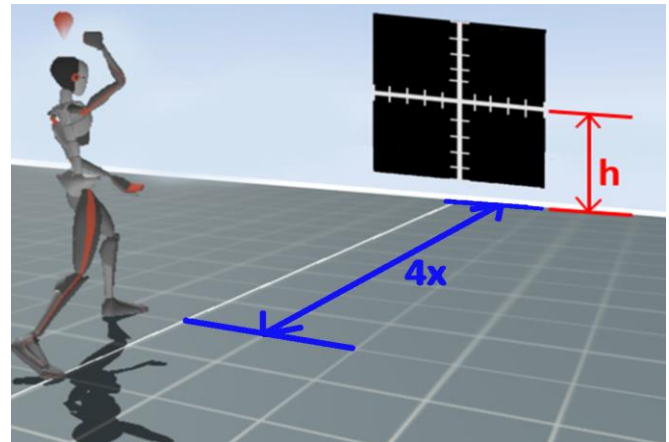


Figure 1. Virtual Representation of the experimental setup of the motor testing and movement analysis. Note: x = body height; h = shoulder height.

REFERENCES

1. Lubans, D. R., Morgan, P. J., Cliff, D. P., Barnett, L. M., Okely, A. D. (2010). Fundamental Movement Skills in Children and Adolescents. *Sports medicine* 40(12), 1019–1035.
2. Yu, J. J., Capio, C. M., Abernethy, B., & Sit, C. (2021). Moderate-to-vigorous physical activity and sedentary behavior in children with and without developmental coordination disorder: Associations with fundamental movement skills. *Research in developmental disabilities*, 118, 104070.

ACKNOWLEDGEMENTS

I would like to thank Eve Kerschenbaum for helping with data collections. Also thank you to Donny Harrel and Carter Capps from the Seattle University baseball team as well as local Seattle high schools and select teams to allow us access to their players for this study.

Table 1. Means \pm SD for time to peak total magnitude of angular velocity (Frames; 120Hz) and mean rank within the sequence.

	Wrist	Elbow	Shoulder	Trunk	Pelvis
Trained	108.05 \pm 10.13 (4.50)	109.30 \pm 11.07 (4.50)	105.06 \pm 9.84 (2.85)	102.62 \pm 10.86 (2.15) *	100.63 \pm 11.16 (1.00)
Untrained	61.10 \pm 8.55 (4.61)	61.01 \pm 8.33 (4.28)	55.56 \pm 13.08 (2.22)	55.92 \pm 7.34 (2.56) *	52.12 \pm 6.18 (1.33)

Note. Mean rank is presented in parentheses. * indicates significant differences ($p < 0.05$) between groups in joint ranking. Bold font indicates significant differences ($p < 0.05$) in sequencing within the same group.

A ROBOTIC GAIT SIMULATOR USING A 6-DOF ROTOPOD CONTROLLED WITH SIMVITRO SOFTWARE FOR TESTING PROSTHETIC AND CADAVERIC FEET

William Lin¹ and William R. Ledoux^{1,2,3}

¹RR&D Center for Limb Loss and MoBility (CLiMB), VA Puget Sound, Seattle, WA,

Departments of ²Mechanical Engineering, ³Orthopaedics & Sports Medicine, University of Washington, Seattle, WA

Email: willdlin@uw.edu

INTRODUCTION

Measuring the effects of a surgical technique on foot bone motion or joint stress during gait poses challenges from measurement methods to subject variability. Therefore, cadaveric gait simulations have been used in the past to analyze motion in the foot and ankle to better understand normal and pathological function [1]. Compared to trials on living subjects, cadaveric studies allow for more controlled, repeatable gait cycles and use of invasive tracking methods and surgical techniques.

The Center for Limb Loss and MoBility (CLiMB) has been developing a robotic gait simulator (RGS) to simulate *in vivo* foot kinematics and kinetics during gait stance phase. The goal of this abstract is to present the current capabilities of the RGS and the next steps to better simulate *in vivo* conditions.

METHODS

The RGS is built around a 6-DOF Mikrolar R3100 rotopod. A Kistler force plate is fixed to the moving platform of the rotopod and a tibial shaft is rigidly mounted above it. In this way, the RGS inversely simulates gait trajectories by moving a force plate, acting as the ground, relative to a fixed tibia, similar to CLiMB's original RGS [2]. An OptiTrack motion capture system with eight cameras tracks bone kinematics, linear actuators can control up to nine tendons, and a novel pliance mat records plantar pressure distribution.

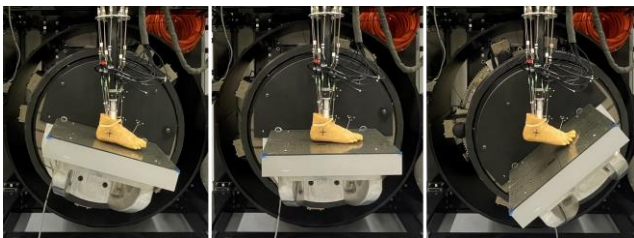


Figure 1: Robotic gait simulator in three phases of stance: (left to right) heel strike, foot flat, and toe off.

Kinematic and kinetic gait trajectories are controlled through simVITRO, a software built by the BioRobotics team at the Cleveland Clinic. A user specifies proportional-integral-derivative (PID), feedforward (FF), and deadband (DB) control gains to achieve desired positions and forces throughout stance, and iterative compensation schemes can further improve the ability to reach desired trajectories.

Our typical trajectory controls three kinematic rotations and three GRFs with nine extrinsic tendons active throughout stance. From heel strike to midstance, the system is in force control. From midstance to toe-off, superior translation is position controlled and the superior GRF is controlled by the Achilles tendon force.

RESULTS AND DISCUSSION

The RGS has run 50 second gait cycles at 25% body weight. The ground reaction forces (GRF, anterior, medial, superior) from one such trial had root mean square errors of 11.4, 2.54, 10.5 N, respectively (Figure 2). Tendon forces for the Achilles, tibialis anterior, and tibialis posterior were tracked (Figure 3).

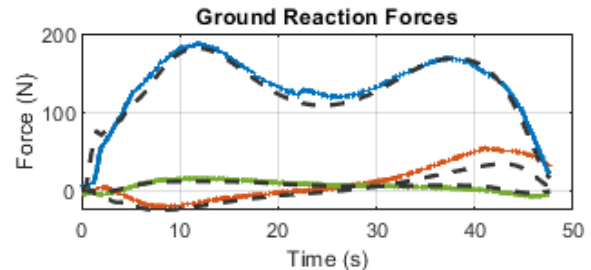


Figure 2: GRF desired (dotted, black) vs actual (color) from a 25% BW, 50 second trajectory.

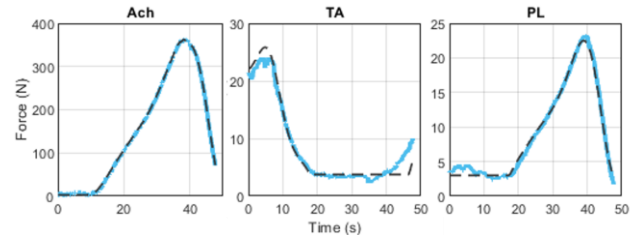


Figure 3: Achilles, tibialis anterior, peroneus longus (dotted, black) vs actual (color) tendon forces from a 25% BW, 50 second trajectory.

These curves were generated with user-specified control gains, so while they generally match the desired curves, they are not optimized. Using simVITRO's compensation scheme, which iteratively changes controls to better match the desired curves, will improve simulation accuracy.

CONCLUSIONS

The RGS is still in development, but initial testing has been promising. The RGS can theoretically complete trajectories at full bodyweight and gait speed, but incremental testing is necessary to safely reach those targets. However, once completed, the RGS will be instrumental in kinematic and kinetic foot testing with applications in studying joint motion, fracture mechanics, or surgical techniques.

REFERENCES

1. Wang, D, et al., *Proceedings of the Institution of Mechanical Engineers, Part H*, **234**(10):1070-1082, 2020.
2. Aubin P, et al. *IEEE Transactions on Robotics*, **28**(1):246-55, 2012.

ACKNOWLEDGEMENTS

Funded by NIH grant AR076475

QUANTIFYING TENSION IN A VERTEBRAL BODY TETHERING SYSTEM FOR SCOLIOSIS TREATMENT

Cain, P¹, Farnsworth CL², Caffrey JP², Olmert T³, Mannen EM¹, Upasani, VV^{2,3}

¹Mechanical & Biomedical Engineering, Boise State University, Boise, ID; ²Rady Children's Hospital, San Diego, CA; and

³University of California San Diego, San Diego, CA.

Email: phoebecain@u.boisestate.edu

INTRODUCTION

The gold standard surgical treatment for children with adolescent idiopathic scoliosis is deformity correction with spinal instrumentation and fusion. However, there is associated significant, long-term morbidity in fusing multiple motion segments in a child. Pain, inflexibility, and degenerative arthritis are often sequelae of the surgery due to fusion sites being immobile [1], and longevity of the metal rods and screws is a long-term concern. However, an innovative approach, vertebral body tethering (VBT), was recently approved by the FDA and has since provided an alternate treatment option. VBT takes advantage of the natural growth of a child's spine to modulate spinal growth and correct the deformity over time without spinal fusion. A flexible polyethylene tether is affixed to multiple spinal segments to apply compressive forces on the vertebral growth plates. Using a tensioner device, the amount of tension in the tether at each vertebral level is controlled, eventually correcting spinal curvature as the patient grows. Recent data shows 74% of patients treated with VBT achieve clinical success [2]. The tensioner device has tension settings of 0 to 5, though no data is available to correlate with the amount of tension generated in the tether at each setting. Furthermore, there are two different tensioner device designs that can be used in this medical device set (methods A and B), and it is unknown whether these different tensioners produce similar tension. Therefore, the purpose of this study was to quantify the forces generated with the two tensioner methods (A and B) at six categorical tension levels using current VBT instrumentation.

METHODS

We created mechanical fixtures (Figure A) with two bone screws inserted into polyethylene blocks to mimic implantation into cortical bone. The screws were set apart at a distance of 45 mm. These fixtures were rigidly mounted to a mechanical testing frame to allow uniaxial force measures through the tether at each tensioner setting. Each tensioned tether was affixed to both bone screws with set screws. Eight orthopedic surgeons tested two tensioner methods (A and B), each at the six different settings (0 to 5) in a randomized order and held for 2 minutes each. Force through the tether at the end of each trial was recorded. Tension mean and standard deviation were computed at each tensioner setting for all surgeons, as well as linear regressions across all tensioner settings for both tensioner methods (A and B).

RESULTS AND DISCUSSION

The mean tensions for both tensioning methods A and B ranged from 30 to 350 N (Figure C). Most standard deviations were within 10% of the means. We found that both tensioner methods A and B exhibited linear relationships of the tension and setting number, with high coefficients of determination ($r^2 > 0.95$). The method B tensioner consistently produced higher forces in the tether with 64.5 N/tension level, compared to the method A tensioner with 52.1 N/tension level. In the future, we will add

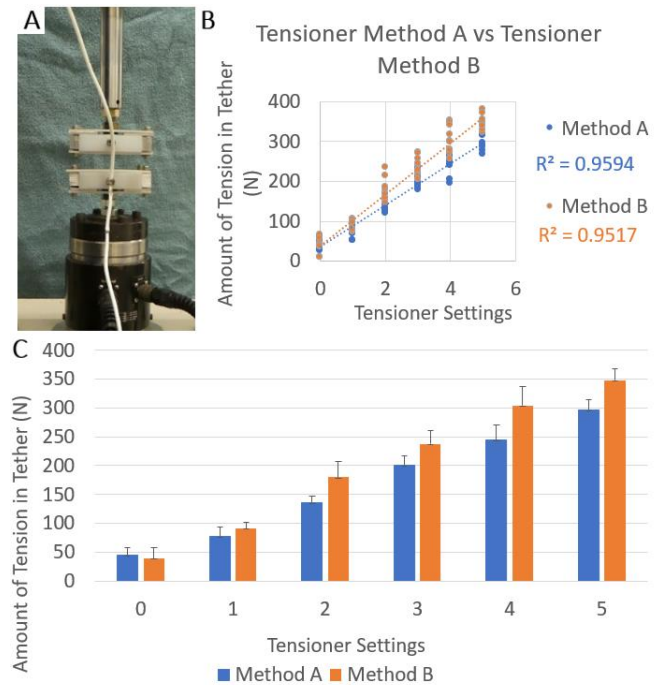


Figure 1. (A) Photo of mechanical testing setup. (B, C) Tension [N] at each Tensioner Setting [0-5] for both methods [A, B] with linear regression r^2 values. Error bars mean \pm SD.

inter- and intra-rater reliability and statistical comparisons of the two methods to this novel data set.

CONCLUSIONS

We quantified the tension in the tether of the VBT at each tension setting (0 to 5), finding that the relationship between tension and setting is linear for both tensioner methods. The method B tensioner results in greater force generation compared to method A in the tether at each setting, which was unexpected since the settings (0 to 5) for each method were not different. This research will allow us to better understand and interpret clinical outcome data of vertebral tethering surgery by relating device setting levels to actual force at each vertebral level. This research will provide analytical data that may inform surgeons on how to specify VBT loads for each spinal segment and potentially allow patient specific VBT loading. This may ultimately result in improved outcomes of VBT as an innovative surgical option for patients with scoliosis.

REFERENCES

1. Hoernschemeyer DG et al. J Bone Joint Surg Am. 2020 Jul 1;102(13):1169-1176.
2. Newton PO et al. Spine Deform. 2022 May;10(3):553-561.

ACKNOWLEDGEMENTS

The Scoliosis Research Society Biedermann Innovation Award supported this research. We thank ZimVie for use of the set.

TRANSPORT DYNAMICS IN THE RAT ACHILLES TENDON DEPEND ON PARTICLE SIZE

Forer, JM^{1,2}, Pacheco, YC¹, Link, K¹, Hahn, ME², Willett, NJ¹

¹Phil and Penny Knight Campus for Accelerating Scientific Impact, University of Oregon, Eugene, Oregon, USA

²Bowerman Sports Science Center, Department of Human Physiology, University of Oregon, Eugene, Oregon, USA
email: jforer@uoregon.edu

INTRODUCTION

The lymphatic system's capacity for clearing and recycling waste entities is essential in all aspects and stages of life. Near-infrared (NIR) imaging has been shown to accurately report lymphatic and vasculature fluid flow in an effort to better understand disease progression [1]. However, little is known about the *in vivo* drainage of tendons, especially Achilles tendons. Describing the size-dependent nature of drainage out of a region of interest is an essential first step in understanding the overall phenomenon of fluid transport, as shown previously in the rat knee joint [2]. This is exciting as previous work has demonstrated lymphangiogenesis to occur after injury to the Achilles tendon [3], meaning that a better knowledge of the mechanics at play can lead to future interventions in the healing process. We use an *in vivo* NIR imaging setup to compare the period in which the rat Achilles tendon clears out a lymphatic draining 20kDa PEG (Poly(ethylene glycol)) conjugated NIR dye, whose size prevents entry into blood vessels, to the drainage of NIR dye alone through the vasculature.

METHODS

Female Sprague-Dawley rats (Charles River Labs, 3-12 months old) received a 15 μ L intratendinous injection of either 20 kDa PEG conjugated with IR dye (n=5, 3 animals euthanized after 24 hours) or the IR dye alone (LI-COR, n=3) in one hind limb Achilles tendon. Subjects in which the injection occurred outside of the targeted region were excluded. While under anesthesia, the subjects were imaged using an IVIS Spectrum (PerkinElmer) machine to measure the intensity of dye in the Achilles tendon region. At progressive timepoints after the injection (1, 3, 6, 24, 48, 72, and 96 hours), the subjects were once again anesthetized and imaged using the same settings to measure the intensity of dye remaining in the target region. The average radiance was calculated for an automatically generated freeform region of interest using the Living Image Software program (PerkinElmer) with a 4% threshold for all images. The radiance values were then normalized to the dye intensity at 1 hour to account for variation in fluorescent intensity between subjects. Calculations and data analyses were done in Prism (GraphPad).

RESULTS AND DISCUSSION

Normalized average radiance (the intensity of the dye remaining in the tendon space) is shown as a function of time after injection as both visualized and plotted data (Figure 1). A decrease in average radiance over time implies that the injected fluorescent dye is evacuating from the measured region. The half-lives of the exponential fit lines to the data are 2.98 hours for the conjugated dye, and 2.19 hours for the dye alone. This demonstrates that clearance of particles in the Achilles tendon space depends on particle size. Future studies involving histology of tissues and biodistribution of the dye are necessary.

Experiments are also planned to observe the effects that exercise post-injection may have on the tendon space drainage kinematics in line with literature studying other regions [2]. Furthermore, preclinical tendon injury or disease models will help describe how natural lymphangiogenesis within the region might change the fluid transport properties. One other area of future research will be in understanding how therapies that alter vessel properties (such as contractility) affect drainage.

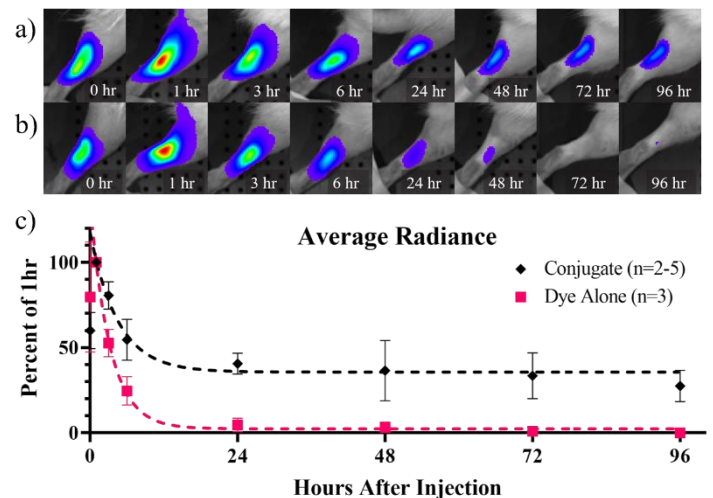


Figure 1: (a) Conjugate dye and (b) dye alone intensity decreasing over time in IVIS captures. (c) Average radiance of the two groups over time normalized to the value at 1 hour post injection. Single phase exponential decay fits are plotted with dotted lines. Results are shown as mean \pm SD.

CONCLUSIONS

In this study, we showed the rate and size dependency of biotransport within the rat Achilles tendon. Fluid and particle transport of tendon tissue is a limited scientific space and the procedure and initial findings described here help lay the groundwork for future discoveries. Defining the kinematics of fluid transport is an essential first step to understanding the regenerative dynamics of tendons and potential interventions.

REFERENCES

1. Weiler M et al. *J Biomed Optics* **17**: 066019, 2012.
2. Bernard F et al. *J Biomed Optics* **26**: 126001, 2021.
3. Tempfer H et al. *Histochem and Cell Bio* **143**: 411-19, 2015.

ACKNOWLEDGEMENTS

This material is based upon work supported by the National Science Foundation Graduate Research Fellowship under Grant No. 2022335756. The research is also supported by the Wu Tsai Human Performance Alliance and the Joe and Clara Tsai Foundation

QUANTIFYING FACET JOINT CAPSULE STRAIN IN THE CERVICAL SPINE

Isabel D. Evans¹, Jeff M. Barrett², Kayla M. Fewster

¹School of Kinesiology, University of British Columbia

²ICORD Orthopaedic & Biomechanics Group, Vancouver, BC, Canada

email: isabel.d.evans@gmail.com

INTRODUCTION

The facet joint capsule (FJC) ligament is a structure in the cervical spine that constrains motions of the vertebrae. It is innervated by mechanically sensitive neurons that respond to stretch. Many researchers have identified a link between chronic neck pain and FJC strain [1]. Some investigations have examined FJC strain during shear loading [2] and determined that soft tissue spinal injuries are load-rate dependent [3,4]. Despite this evidence, there has been no investigation into cervical spine FJC strain under physiological loading conditions across loading rates. Therefore, this study aimed to quantify peak FJC principal strains across various loading rates during anterior and posterior shear. It was hypothesized that peak FJC strain would decrease as rate increased.

METHODS

One human cadaver C6-C7 functional spinal unit (36-year-old, Caucasian, male, 183cm height, 64kg weight) underwent non-destructive shear range of motion (ROM) testing. ROM testing was completed at displacement rates of 1, 10, and 100 mm/s (i.e. low, medium and high rates of loading) until reaching a shear force threshold of approximately 200N. ROM testing was completed in both the anterior and posterior shear directions. Throughout ROM testing the specimen was held in the neutral posture. Shear displacement data was then input into an existing cervical spine model in OpenSim [5], to estimate the peak principal strain experienced in the FJC ligament across the tested loading rates and directions. All strain data estimated from the model were then represented as a function of measured shear force.

RESULTS AND DISCUSSION

During anterior shear ROM testing the maximum FJC strain was estimated to be -10.1%, -9.9%, and -7.8% during low, medium, and high-rate loading, respectively (Table 1, Figure 1). During posterior shear ROM testing, the maximum strain was estimated to be 24.0%, 24.6%, and 23.6% during low, medium, and high-rate loading, respectively (Table 1, Figure 2). Anterior ROM testing results supported our hypothesis that peak FJC strain was inversely related to load-rate. However, posterior ROM testing showed an increase in peak strain from low to medium loading rate but an ultimate decrease during the high-rate loading.

It is important to note that overall greater magnitudes of peak FJC strain were experienced during posterior shear ROM testing. This is likely due to the anatomical positioning of the FJC which allows for greater ligament stretch during posterior shear, as the facets are separating. The estimated peak strain values, across all ROM testing, do not reach the approximate 45% and 47.2% strain thresholds associated with after discharge and nociception [6], respectively.

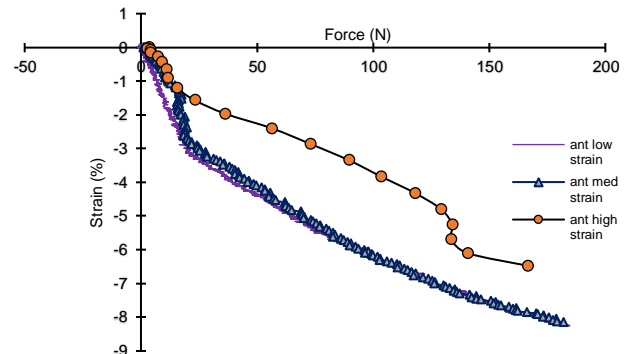


Figure 1: Capsular ligament strain during anterior shear loading.

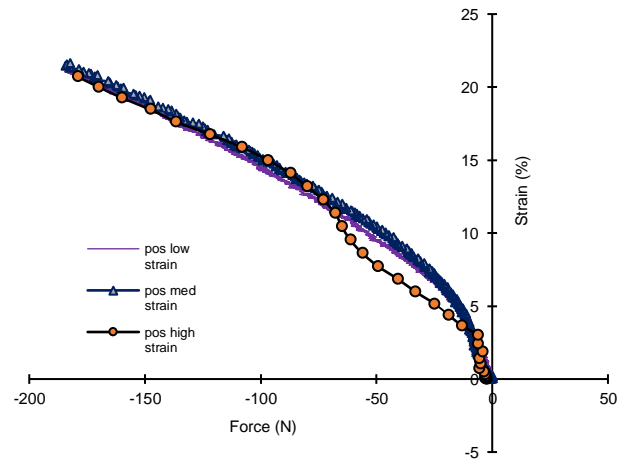


Figure 2: Capsular ligament strain during posterior shear loading.

Table 1: Peak Capsular Ligament Strain During Anterior and Posterior Loading at Varying Rates.

	Anterior	Posterior
	Peak Strain %	Peak Strain %
Low (1 mm/s)	-10.1%	24.0%
Medium (10 mm/s)	-9.9%	24.6%
High (100 mm/s)	-7.8%	23.6%

REFERENCES

1. Cavanaugh, J. M., et al. *JBJS*, **88(suppl_2)**, 63-67, 2006.
2. Zehr, J. D., et al. *The Spine Journal*, **20(3)**, 475-487, 2020.
3. Cripton, P. *Proceedings of the Symposium on Injury Prevention Through Biomechanics*, Detroit, MI, 1995.
4. Mattucci, S. F., et al. *Journal of the mechanical behavior of biomedical materials*, **10**, 216-226, 2012.
5. Barrett, J., et al. *Journal of Applied Biomechanics*, **37(5)**, 481-493, 2021.
6. Lu, Y., et al. *Stapp Car Crash Journal*, **49**, 49, 2005.

EFFECT OF SPEED ON LOWER LIMB JOINT STIFFNESS DURING DECLINE RUNNING

Lee, S¹, Robinson, R¹, Chebbi, A¹ and Hahn, M¹

¹Department of Human Physiology, University of Oregon

Eugene, OR USA

email: slee20@uoregon.edu

INTRODUCTION

Joint stiffness can be defined as a given joint's resistance to angular displacement under mechanical loading expressed as moment of force [1]. Increased joint stiffness is associated with a decrease in range of motion, as well as the inability to adequately attenuate shock throughout the body; all of which are associated with running related injuries [2]. Because joint stiffness is correlated with variables like range of motion and shock attenuation, understanding the factors that influence stiffness has potential application in injury prevention and rehabilitation, such as determining optimal exercises to reduce running related overuse injuries [2]. Across the literature, increases in running speed have been correlated with increased measures of joint stiffness [4]. However, this relationship has only been examined during level ground running. Running at grades other than level ground is a common challenge that distance runners encounter in the real-world, but is an area that remains relatively unexplored [1]. The purpose of this study is to examine the effect of speed on joint stiffness and quantify differences in stiffness between the hip, knee and ankle during decline running.

METHODS

Approval from the Institutional Review Board was obtained, and all participants provided informed consent prior to data collection. Four healthy female participants (age: 25 years, height: 162 cm, mass: 56 kg) performed four 30s running trials on a 7.5° declined treadmill at three speeds, ranging from 3.35-3.83 m/s. Kinetic data were collected at 1000 Hz (Bertec, Columbus, OH) and kinematic data were collected at 200 Hz (Motion Analysis, Santa Rosa CA). Sagittal plane joint angles and internal moments of the hip, knee, and ankle were calculated using a custom pipeline in Visual 3D software (C-motion, Inc., Germantown, MD). Joint stiffness was quantified by the equation: $K_{joint} = \frac{\Delta M_{joint}}{\Delta \theta_{joint}}$ where ΔM_{joint} is the change in sagittal joint moment, and $\Delta \theta_{joint}$ is the change in sagittal angular displacement over the first half of stance phase [3]. A two-way ANOVA was performed to determine the effect of speed and joint type on joint stiffness. Post hoc pairwise t-tests were run in the case of a significant main effect for significant trials.

RESULTS AND DISCUSSION

The average stiffness of the hip, knee and ankle across increasing speeds are displayed in Figure 1. A significant main effect was detected for joint type ($p < 0.001$), however no main effect for speed ($p = 0.87$) or interaction effect ($p = 0.88$) between joint type and speed were detected. A significant difference was detected between ankle and knee joints across all speeds, however no significant difference was detected between hip and ankle, or hip and knee joints. Across speeds,

joint stiffness was highest at the ankle, followed by the hip and knee. This differs from previous studies on the effect of speed on joint stiffness across level ground running, where joint stiffness was reported to increase with speed, with the hip having the highest stiffness, followed by the ankle and the knee. Thus, the effect of speed on joint stiffness appears to differ depending on grade. Future studies should analyze the interaction effects of speed and grade on joint stiffness including various grades of decline running to more thoroughly understand joint stiffness patterns.

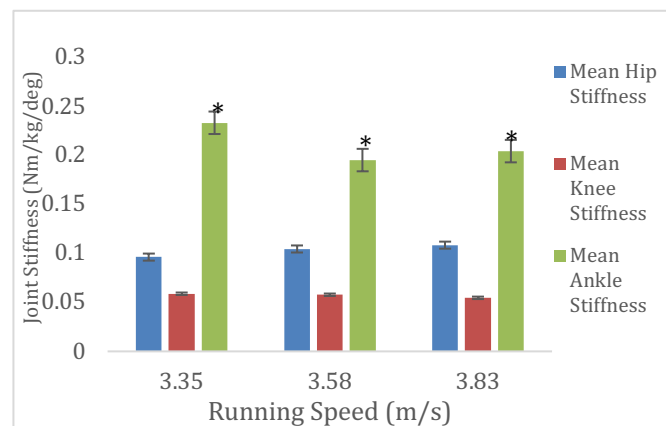


Figure 1: Mean joint stiffness of the hip, knee, and ankle across speeds during decline running. Significant difference between knee and ankle is noted by (*).

CONCLUSIONS

A significant main effect was detected for joint type on joint stiffness, but there was not an effect of speed on joint stiffness. While joint stiffness differs between the hip, knee and ankle while running on a decline surface, stiffness does not appear to change in response to speed. This suggests that decline running is the primary factor affecting joint stiffness, and should be further considered when developing optimal training programs to reduce running related overuse injuries. Since only one decline grade was observed, future studies should investigate the effect of decline grade magnitude on joint stiffness.

REFERENCES

1. Davis JJ and Gruber AH. *OJSM*, **9(5)** 2021.
2. Brughelli M and Cronin J. *Sports Med*, **38**, 647-657 2008.
3. Li J and Hahn M. *J Biomech*, **2**, 441-452, 2022.
4. Li J and Hahn M. *Hum Mov Sci*, **58**, 2018.

ACKNOWLEDGEMENTS

This work was supported by the Wu Tsai Human Performance Alliance and the Joe and Clara Tsai Foundation

VALIDITY AND RELIABILITY OF A SMARTPHONE IN MEASURING POSTURAL STABILITY

Lovekin, E¹, Lugade, V², Davis, A¹, and San Juan, JG¹

¹Department of Health and Human Development, Western Washington University

²Division of Physical Therapy, Binghamton University, Binghamton, NY

email: lovekie@wwu.edu, web: <https://wp.wwu.edu/biomechanicslab/>

INTRODUCTION

Postural sway is often observed in clinical settings, as it can provide important context in determining mortality, injury and re-injury risk of the lower extremity, and cognitive status [1,2]. Smartphone apps have demonstrated good validity and reliability in assessing balance [3]. However, many of these studies have entailed subjects wearing smartphones directly attached to the body, most commonly around the approximate COM of the subject. As users do not attach their smartphone at the location of the COM, but rather in the pocket, assessment of the COP movement in this location warrants further investigation.. Therefore, the purpose of this study is to assess the validity and reliability of a smartphone-based tri-axial accelerometer in measuring human balance during quiet standing in both a home and lab environment. We hypothesized that usage of a custom smartphone app to assess balance during quiet standing in the lab and at home would result in valid and reliable measurements across all.

METHODS

A total of 16 healthy participants, 9 Females, (age = 28.1 ± 10.3 years; height = 1.68 ± 5.5 m; mass = 77.0 ± 22.1 kg) were included in this study. All participants possessed an Apple iPhone 6S or newer that had an operating system of iOS13 or newer. Participants were given a code to download IMPROVE custom app for free in the Apple App store. A force plate (AMTI Inc., Watertown, MA) captured ground reaction forces and center of pressure (COP) data at 1000 Hz. During each trial, two iPhones using the IMPROVE app collected tri-axial acceleration (100 Hz) and automatically calculated sway. One was placed in a smartphone belt on the lower back around the waist, at the level of the L3 lumbar spine. The other iPhone was placed in the participant's right front pocket. During the quiet standing balance trial, participants were asked to stand barefoot with their feet positioned on a foam pad placed on top of the force plate for a total of 45 seconds. The foot placement was self-selected, marked, and measured to ensure that the same position was achieved for each data collection session. Three sessions were held within 7 days. Sessions 1 and 3 were held in the lab using both iPhones. Session 2 was completed at the participant's home using just the iPhone placed in their front pocket. To assess the concurrent validity of the smartphone with

the force plate, a Pearson Product moment correlation was utilized. The Intra-class Correlation (ICC_{2,1}) was used to evaluate inter-day reliability. A paired t-test was used to examine the difference between smartphones on the waist and in the pocket. The alpha level was set to 0.05 and SPSS v28 was used to calculate the statistical analysis. ICC values below 0.5 indicate poor reliability, 0.5 – 0.75 moderate reliability, 0.75 – 0.9 good reliability, and above 0.9 exceptional reliability [4].

RESULTS AND DISCUSSION

Most of the smartphone acceleration sway measurements were significantly correlated to the COP measures of sway using the force plate. Only the RMS and Range A-P showed no significant correlation (Table 1). Overall, the smartphone in the pocket and force plate showed moderate to good test-retest reliability ($r = 0.63$ to 0.81). Only Range A-P showed poor reliability ($r = 0.39$ and 0.46). Other than sway area ($p = 0.04$), no significant differences were found between the smartphone on the waist and in the pocket in measuring the trajectory measures ($p > 0.05$). The result of the current study showed that smartphones with a custom app are a reliable and valid measurement for assessing static postural stability. Also, smartphones used to measure postural stability can be placed in the front pocket instead of using a smartphone belt placed around the waist.

CONCLUSIONS

The current study can provide clinicians and patients with the ability to improve intervention and assessment of static postural stability. The smartphone with the custom app is a valid and reliable tool to measure static postural stability and can be deployed in a safe, and easy-to-use manner.

REFERENCES

1. Wingert JR, et al (2014). *Arch Phys Med Rehab*. 95(2).
2. Leach JM, et al (2018). *Front. Aging Neurosci*. 10
3. Fiems C et al (2018). *NeuroRehabilitation*. 43(2).
4. Koo & Li My (2016), *J Chiropr Med* 15(2).

ACKNOWLEDGEMENTS

We would like to thank Dr. Barbara Lehman for her assistance with the statistical analysis.

Table 1. Concurrent validity of the Smartphone in measuring static postural stability.

Trajectory Measures	Force Plate (m)		Smartphone in Pocket (m/s ²)		Correlation	
	Mean	SD	Mean	SD	r	p
Distance	0.010	0.002	0.011	0.003	0.53	0.04
RMS	0.011	0.002	0.013	0.004	0.49	0.06
Path	0.792	0.202	1.495	0.474	0.69	0.003
Range A-P	0.030	0.010	0.054	0.021	0.40	0.13
Range M-L	0.051	0.013	0.050	0.013	0.82	< 0.001
Range	0.052	0.012	0.070	0.019	0.51	0.04
Sway Area (m ² /s; m ² /s ²)	9.1 x 10⁻⁵	4.0 x 10⁻⁵	2.1 x 10⁻⁴	1.1 x 10⁻⁴	0.75	< 0.001

Effects of Prior ACLR and Cognitive Challenge on Postural Control following a Medial Side Hop

Kaylan J. Wait;¹ Fatemeh Aflatounian;¹ Janet E. Simon;² Dustin R. Grooms;² James N. Becker;¹ Keith A. Hutchison;¹ Scott M. Monfort¹

¹Montana State University, Bozeman, MT; ²Ohio University, Athens, OH.
Email: kaylanwait@gmail.com

Introduction

Altered postural control following anterior cruciate ligament reconstruction (ACLR) has been identified as a risk factor for a second injury [1]. High reinjury rates, approaching 26% for athletes 25 years of age, following ACLR may indicate gaps in current RTS testing [2, 3]. The medial side hop jump task (MSH) provides potential insight on the differences between healthy and injured limbs and is commonly utilized in return-to-sport (RTS) testing [4]. Adding a cognitive task to existing RTS tests, such as the MSH, may enhance the ability for these tests to reveal unresolved cognitive-motor deficits that may contribute to the high reinjury rate. Novel measures characterizing rapid stabilization may also be relevant given the short timeframe where ACL injuries occur (~100 msec after landing). However, results can vary by balance task, which motivates the need for further investigation to understand potential therapeutic targets to improve ACLR outcomes. The purpose of this study was to determine how postural stability compares between ACLR and uninjured limbs after landing from a medial side hop (MSH) test with added cognitive task. We hypothesized that traditional and transient measures will reveal a lack of ACLR stability compared to the healthy limb when in the presence of a cognitive task.

Methods

32 ACLR adults cleared for unrestricted activity (8 m / 24 f; 19.8 ± 1.8 years, 1.71 ± 0.10 m, 69.7 ± 12.8 kg, 1.5 ± 0.6 years since surgery, Tegner: 6.8 ± 1.9) performed the MSH task and maintained single-limb stance for 30 seconds upon landing [5]. Participants performed the task using both the ACLR involved and uninjured limb. The MSH was performed under single task (ST; MSH only) and dual task (DT; MSH + cognitive task) conditions. The cognitive task was a visual working memory task: a series of letters flashed on a screen, participants were asked to recall a letter at a specific location, the task repeated for the 30 seconds after landing [5]. Center of pressure characterized postural sway using 95% confidence ellipse area (EA). Whole trial estimate (EA_{wt}) and time-varying analysis (ΔEA ; first 5 sec after landing to last 5 sec of standing balance) were dependent variables, with natural logarithms used to improve normality of model residuals. ΔEA quantified how much participants reduced sway over time. Mixed effects models tested for Limb (ACLR vs. uninjured), Condition (ST vs. DT), and Limb*Condition fixed effects, with a covariate of MSH distance.

Results and Discussion

Condition ($p=0.002$) and Limb ($p=0.043$) were significant for EA_{wt} . EA_{wt} was smaller (less sway) for DT than ST (ST: 7.64 ± 0.32 vs. DT: 7.54 ± 0.32 ln(mm), Cohen's $d = -0.31$) and for ACLR limb compared with uninjured limb (uninvolved: 7.62 ± 0.30 vs. ACLR: 7.55 ± 0.35 ln(mm), Cohen's $d = -0.21$). Condition remained significant with the inclusion of MSH distance ($\beta_{std} = 0.10$; $p=0.016$), but Limb did not ($p=0.095$). For ΔEA , MSH distance was a significant covariate ($\beta_{std} = 0.11$;

$p=0.046$) along with a trending effect of Limb ($p=0.065$, Cohen's $d = 0.26$), with more relative early-stance sway for the ACLR limb. Adding a cognitive task resulted in decreased overall postural sway after landing from a maximal effort medial side hop and trended toward an increase in transient response (i.e., change in sway over time). The decreased sway on the ACLR limb may be related to an increase in perceived postural threat on the surgical limb that could have elicited a tighter control approach to maintaining balance for the ACLR limb and in the presence of the added cognitive challenge [6].

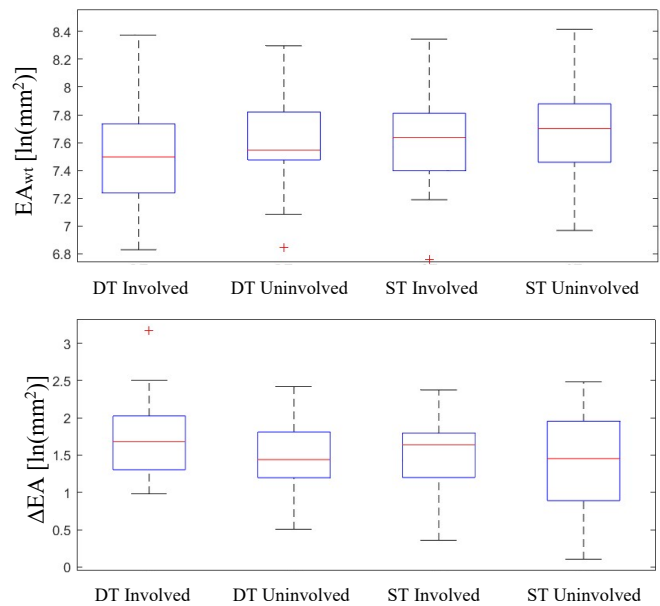


Figure 1: Box plots for whole trial (top) and transient measures (bottom) across conditions (DT and ST) and limb Involved (ACLR) and Uninvolved.

Conclusions

Our results indicate that the addition of a cognitive task revealed disparities between healthy and injured limbs. However, contrary to our hypothesis, we observed that the ACLR limb experienced less sway in the presence of a dual task, and less overall sway than the healthy limb.

Acknowledgments

Supported by: NIH Awards P20GM103474 and R03HD101093

References

- [1] Paterno *JAT* (2015) 1097-9
- [2] Barber-Westin and Noyes *Sports Health* (2020) 587-597
- [3] Unverzagt et al. *Int J Sports Phys Ther* (2021), 1168-77
- [4] Ebert et al. *Int J Sports Phys Ther* (2021) 393-403
- [5] Farraye et al. *Phys Ther Sport* (2022) 40-45
- [6] Monfort et al. *Gait & Posture* (2022) 109-114

EXPLORING CLINICIAN PERSPECTIVE ON STANDARD OF CARE AND 3D-PRINTED ACCOMMODATIVE INSOLES

Gagnon, L¹, Nickerson, KA^{1,2}, Carranza, C¹ Muir, BC^{1,2}

¹RR&D Center for Limb Loss and MoBility (CLiMB), Department of Veterans Affairs, Seattle, WA

²Department of Mechanical Engineering, University of Washington, Seattle, WA

email: leo.gagnon@va.gov, web: <https://www.amputation.research.va.gov/>

INTRODUCTION

In the United States, complications due to diabetes are a leading cause of amputation, with over 100,000 amputations occurring yearly as a result [1]. Patients with diabetes mellitus are at an increased risk for developing foot wounds, and ulcers, and when those fail to heal, amputation is often the only solution. Common clinical preventative measures include daily skin checks, wearing appropriate fitting shoes, and foam insoles that aim to reduce and redistribute plantar pressures [2]. These insoles are the standard of care (SoC) and are traditionally created from a seated foam crush box impression capturing the individual's feet.

Recent research focused on additive manufacturing has demonstrated the use of 3D-printed metamaterials to fabricate patient-specific insoles (3DP) [3]. The production steps include a scan of the foam crush box impression used for SoC fabrication, and an in-shoe pressure assessment to identify areas of high pressure. From the pressure assessment, reliefs to offload the regions of high pressure are incorporated into the insole design (Figure 1) [4].

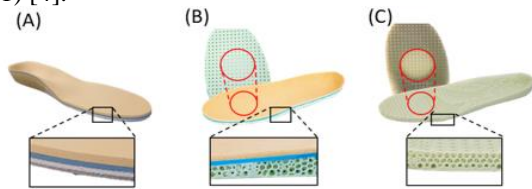


Figure 1: Insoles (a) SoC, (b) 3DP with bilaminate top layer, (c) full 3DP. Offloading regions indicated in red.

The feasibility of incorporating this novel workflow for 3DP insole fabrication into clinics has yet to be investigated. The purpose of this study was to obtain clinician perspective on the advantages and disadvantages of SoC and two versions of the novel 3DP insoles, ideas for improvement, and practical hurdles experienced in clinical settings.

METHODS

Five (3 male, 2 female, age: 39.8 ± 12 ,) Veteran's Affairs (VA) Orthotic and Prosthetic Clinicians (4 certified orthotist prosthetists, 1 certified prosthetist, years of practice: 13.8 ± 11) participated in an open forum focus group. Two sessions were held, with an average length of 35 minutes. During each focus group session, clinicians were shown three orthotics (Figure 1) and prompted with a series of standardized questions. Focus group sessions were audio-recorded and transcribed, from which main themes pertaining to each question category (Table 1) were extracted.

RESULTS AND DISCUSSION

Both focus groups discussed similar themes for the disadvantages of SoC and 3DP insoles. SoC disadvantages were durability and individualized customization of the design. SoC insoles pack out quickly, requiring timely replacement which if neglected results

in insufficient cushioning and pressure relief. Previous work comparing SoC and 3DP materials demonstrates increased durability of the 3DP design and a less frequent need for replacement [3]. Furthermore, 3DP insoles may have more customized surface geometry corresponding to a patient's foot as clinicians described the 3DP insoles as having more arch support than the SoC. One disadvantage of the 3DP design noted by clinicians is the limited ability to make in-clinic adjustments through traditional methods such as grinding. However, improved conformity of the design to the foot and shoe shape may eliminate the need for most post-manufacturing adjustments. Another concern with the 3DP design is the perforated top surface being unhygienic, and/or debris getting trapped. Methods to clean the latticed insole and their effects on device lifespan should be a focus of future work. A hybrid design (Fig 1b) with a bottom layer of the 3DP material and SoC top layer was quantitatively tested without significant improvement compared to SoC, and in the focus groups the top layer, for ease of cleaning, was liked but preferred thinner. The main concern with implementation into the clinic was insurance coverage. However, clinicians thought that the addition of the in-shoe walking pressures assessment would be feasible in current appointment timeframes with the appropriate availability and bandwidth of the technologies.

Table 1: Key Themes from focus groups, sorted by category, an underline indicates a theme that was discussed in both sessions.

Category	Theme
SoC Disadvantages	<u>Poor durability</u> Edge pressure around reliefs <u>Poor customization</u>
SoC Advantages	Quick manufacturing time Easily modifiable by clinicians
3DP Disadvantages	<u>Perforated top surface</u> <u>Limited ability to make adjustments and modify</u>
3DP Advantages	Support in the arch
3DP workflow application in the clinic	<u>Insurance guidelines</u> Addition of walking pressures to appointment Bandwidth of software

CONCLUSIONS

Applying a clinical perspective to the design of novel foot orthotics may increase the likelihood of translating these devices into use, thus improving patient outcomes.

REFERENCES

- Walicka M, et al. *J Diabetes Res* **2021**, 2021.
- Janisse D and Janisse E, *Pro Orth Int* **39(1)**, 40-47, 2015.
- Hudak Y, et al. *Med Eng & Phys* **104**, 2022.
- Muir BC, et al. *Clin Biomech* **98**, 2022.

Acknowledgments

Funding for this study was provided by VA Award A3539R.

Quantitative Evaluation of Novel Hybrid Ankle Foot Orthotic Design

Gagnon, L¹, Muir, BC^{1,2}, Klute, G¹, Cyr, K¹, Walling, K and Rogers, E

¹RR&D Center for Limb Loss and MoBility (CLiMB), Department of Veterans Affairs, Seattle, WA

²Department of Mechanical Engineering, University of Washington, Seattle, WA

email: leo.gagnon@va.gov, web: <https://www.amputation.research.va.gov/>

INTRODUCTION

The American Spinal Cord Injury Association (ASIA) Impairment Scale defines a “D” classification as motor function being preserved below the neurological level, and at least half of the key muscles below neurological level having a manual muscle score of 3 or more [1]. However, presentation of an incomplete spinal cord injury (SCI) can vary drastically between individuals.

A 57-year-old rural veteran, sustained a T11 ASIA D injury 26 years ago and maintained independence since recovery. Due to bilateral lower extremity weakness since initial SCI, the Veteran utilized bilateral ankle-foot-orthotics (AFOs) for daily ambulation. Since 2012, the veteran has utilized DynamicBracingSolutions (DBS) style AFOs (Figure 1A) in place of a traditional solid ankle AFOs or posterior dynamic element carbon fiber AFOs, for self-perceived increase in independence, and decrease in reported falls (currently 4-5 times/week with DBS AFOs).

While trialing a new Hybrid AFO design (Figure 1B) with a split toe, thin non-adjustable proximal shell, and two carbon, energy storage clever bones the veteran showed promising results in qualitative testing with a more normalized gait pattern and increased patient satisfaction with regards to ground compliance, stability, proprioception, and overall ease and function.

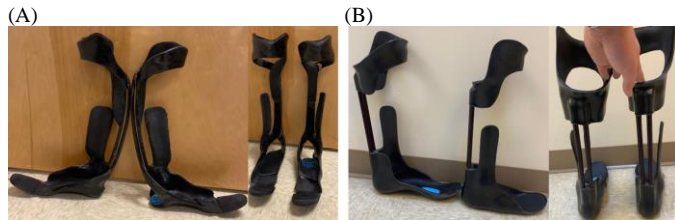


Figure 1. Sagittal and coronal views of AFOs (a) DBS AFOs, (b) Hybrid AFOs.

This case study aimed to quantitatively evaluate the Hybrid AFOs against the DBS AFOs, and unbraced gait, to determine if the Hybrid AFOs provide a biomechanical benefit to the Veteran to account for the perceived improvements.

METHODS

One veteran (male, age 57, T11 ASIA D classification) completed three trials of overground walking at Self-Selected Walking (SSW) and Fast-Walking (FSW) with each the DBS and Hybrid AFOs. Kinematics (Vicon) and kinetics (AMTI) were collected with video recording to aid in the analysis and interpretation of the data.

RESULTS AND DISCUSSION

Ankle data comparisons of AFO style across SSW and FSW were almost exact replicas, this is likely a result of the AFO, as both styles restrict anatomical ankle motion, using a 1/2" solid ankle cushion heel and a toe plate rocker to facilitate forward progression. The DBS and Hybrid AFOs demonstrated an almost parallel pattern across gait cycle (GC) with the Hybrid AFOs values translated down the vertical axis. This may be due to a variation of built-in plantar flexion angle between AFO styles. In normal walking, maximum knee flexion angle is 60° [2]. Maximum knee flexion achieved with the DBS AFOs ranged from 67° to 75° (R SSW to L FSW respectively), while in the Hybrid AFO values were between 62°-67° (L SSW and R FSW respectively).

In knee flexion, peak knee power in the DBS AFOs was 1.54W/kg (SSW) and 1.76W/kg (FSW) with the L and R side averaged together, following the same procedure peak knee power in the Hybrid AFOs was 1.33W/kg (SSW) and 1.35W/kg (FSW) at 59% of GC. Peak knee flexor power in both conditions is slightly higher than the 1.2 W/kg observed in normal walking during knee flexion (approximately 59% of GC) [2].

Hip angle in the DBS and Hybrid AFOs across SSW were within 4° of normal, however for the FSW trials data were near identical until 75% of the GC (start of mid-swing, with a normal peak hip angle: 25°) when flexion in the Hybrid AFOs stayed within 4° of normal, but hip flexion in the DBS AFOs increased nearly 8°.

Normal peak hip power (1.14W/kg) was achieved with both the DBS and Hybrid AFOs at pre-swing for all trials and conditions except for the R DBS SSW trial where the max hip power was only 0.66W/kg [2].

CONCLUSIONS

Walking in the Hybrid AFOs resulted in values closer to normal gait than in the DBS AFOs for maximum knee flexion, peak knee power during flexion, and peak hip power, which may be indicative of biomechanical benefit from the Hybrid AFOs for users with lower extremity weakness secondary to a SCI but further research is still needed.

Evaluating and comparing AFOs and their impact on joint segments up the body with quantitative measures, helps broaden the understanding of AFOs and the benefits they can provide users which may ultimately help clinician choose the most appropriate intervention for their patients and goals.

REFERENCES

1. Roberts, T. Clin Orthop Relat Res. 475(5), 1499-1504, 2017.
2. Perry J, Burnfield J. *Gait Analysis* (2), 51-160, 2010.
3. Podsiadlo D, Richardson S. J Am Geriatric Societies 1991.

EFFECTS OF MANUAL MOBILIZATIONS ON FOOT KINEMATICS AND MUSCLE ACTIVITY

Hagger, R.¹, Golden, J.¹, Paige, L.¹, Allen, F.², and Becker, J.¹.

¹Department of Health & Human Development, Montana State University, Bozeman MT USA

²ProChiropractic LLC, Bozeman MT USA

email: riley.hagger@student.montana.edu, web: <http://www.montana.edu/biomechanics>

INTRODUCTION

Mobilization through manual therapy can increase the range of motion (ROM) at the tibiofibular, talocrural, subtalar, and midtarsal joints to restore normal arthrokinematic function to the ankle and foot joints [1]. While the acute effects of manual therapy in clinical patients is well known, it is unclear whether mobilizations may provide similar benefits to foot and ankle function in an otherwise healthy individual [2,3,4]. Therefore, the purpose of this case study was to identify the effects of manual therapy mobilizations on foot kinematics, muscle activation, and plantar pressures during walking in a healthy individual. It was hypothesized that mobilizations would increase joint ROM, increase activation at the adductor hallucis (AbH), and increase peak pressures under the metatarsal heads.

METHODS

One 21-year-old male (1.80 m, 80kg) participated in this case-study. Foot kinematics were recorded using a 10-camera motion capture system, EMG from miniature sensors placed on the belly of the AbH muscle, and plantar pressures from a pressure mat located in the middle of the walkway. Data was recorded for five walking trials before (PRE) and after (POST) foot mobilizations. Extremity joint mobilizations were applied by a licensed chiropractor and included mid-tarsal dorsiflexion and subtalar eversion manipulations to increase ROM through the midtarsal and subtalar joints. ROM for the talocrural, subtalar, transverse tarsal, and 1st metatarsophalangeal joints were calculated using the Rizzoli foot model in Visual 3D. Peak root mean squared amplitudes were used to quantify AbH activity. Plantar pressure maps were segmented into ten regions and peak pressures were determined for each metatarsal head. Differences between PRE and POST conditions were evaluated using paired t-tests, with effect sizes (Cohen's d) calculated to aid in interpretation of results.

RESULTS AND DISCUSSION

PRE and POST sagittal plane ROM measurements were not significantly different for talocrural ($p = .093$, $d = 0.88$), subtalar ($p = 0.35$, $d = 0.70$), transverse tarsal ($p = 0.47$, $d = 0.42$), 1st MPJ ($p = 0.82$, $d = 0.19$), and tarsometatarsal joints ($p = 0.14$, $d = 1.18$). AbH EMG activation was greater for POST (.36 mV) than for the PRE trial (.16 mV). PRE and POST plantar pressures were not significantly different for any section of the foot including the M1 ($p = 0.73$, $d = 0.25$) and M2 areas ($p = 0.91$, $d = 0.06$).

Previous literature shows mobilizations result in acute increases in ROM in clinical populations. However, most patients that have suffered from chronic injury lack mobility and directly benefit from improving ROM [5]. Our participant had normal ROM pre-treatment which may have created a ceiling effect on ROM improvements. The increased activation of AbH, with lack of changes in joint kinematics may be due to the focus of cueing different muscles which was provided

during the mobilizations. This cueing may have resulted in the participant inadvertently recruiting the muscles more during gait following the mobilization.

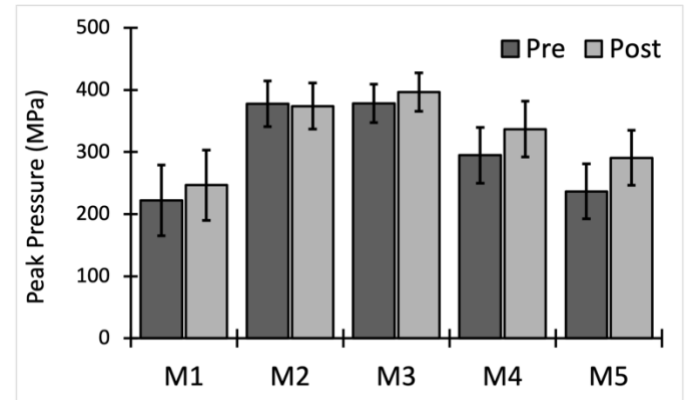


Figure 1: Peak pressures under metatarsal heads pre and post mobilizations.

Table 1. Mean and standard deviations for foot kinematics pre and post mobilization. TC: talocrural, ST: subtalar, TT: transverse tarsal, Tmet: tarsometatarsal, MPJ: metatarsophalangeal joints. Sag: sagittal, Front: frontal, Trans: transverse plane range of motion.

Joint/Plane	Pre	Post
TC Sag	27.84 ± 1.69	29.65 ± 2.40
ST_Front	6.21 ± 2.27	4.97 ± 1.30
TT_Sag	15.70 ± 1.76	16.3 ± 1.09
TT_Front	5.01 ± 0.76	5.99 ± 0.67
TT_Trans	9.73 ± 0.58	10.12 ± 0.60
Tmet_Sag	7.11 ± 0.73	8.00 ± 0.79
Tmet_Front	8.81 ± 0.68	7.94 ± 1.14
Tmet_Trans	2.51 ± 0.71	3.04 ± 0.72
1 st MPJ	37.40 ± 2.72	38.09 ± 4.46

CONCLUSION

Manual therapy mobilization on a healthy individual appears to have no acute effect on joint ROM or plantar pressures but may increase muscle activation in the adductor hallucis.

REFERENCES

1. Loudon JK, et al, J Athl Train (1996) 31(2):173-178.
2. Cruz-Díaz, D., et al.(2015). Rehab, 37(7), 601–610
3. Gogate, N., et al.(2021). Sports Med, 48, 91–100.
4. Izaola-Azkona, L., et al. (2021). Phys Ther, 101(8), 111–.
5. Teixeira, L. M., et al.(2013). J Manip and Physio Therapeutics, 36(6), 369–375.

RELIABILITY OF LOW- AND HIGH-TECH METHODS TO QUANTIFY RUNNING FOOTWEAR FEATURES OF AN ERGOGENIC SHOE: A PRELIMINARY ANALYSIS

Katie Landwehr¹, Sarah Shultz¹, Cristine Agresta²

¹ Department of Kinesiology, Seattle University, Seattle, WA, United States ² Department of Rehabilitation Medicine, University of Washington, Seattle, WA, United States

email: klandwehr@seattleu.edu, web: <https://www.seattleu.edu/artsci/kinesiology/research/>

INTRODUCTION

The impact of footwear features on running performance is being increasingly studied in the literature [1,2]. However, methods to measure footwear features lack standardization. Lack of standardization for measuring or reporting limits generalization, and comparison or synthesis across studies. Additionally, World Athletics amended their policy that restricts distance running shoes from ‘must not be constructed so as to give athletes any unfair assistance or advantage’ to ‘must not exceed a maximum thickness of 40mm’ [3].

Of key interest are shoe mass and midsole stack height because of their demonstrated or *perceived* connection to performance [1,2,4]. Recent tools like the Minimalist Index [5], the Footwear Assessment Tool [6], and the Total Asymmetry Score Tool [7] have begun to standardize feature measuring and reporting but still lack the sufficient precision and functionality to quantify continuous measures of footwear features.

Since the reliability of shoe mass and midsole stack height measurements has not yet been established, the purpose of our study was to determine the inter-shoe reliability of these key running footwear features for a well-known ergogenic shoe.

METHODS

A single rater took low- and high-tech measures from 6 pairs of the same model (Nike ZoomX Vaporfly Next % 2) from a local running store. Low-tech measurements were collected using digital calipers and a digital scale. We collected shoe mass, shoe length, and three rearfoot stack height measures (Figure 1) based to match anecdotal and regulatory procedures [3]. High-tech measurements were captured using a high-resolution 3D surface scanner and associated software (Creaform, AMETEK, Inc., Levis, Canada). Ethical approval was not required because there were no human participants.

Means and standard deviations (SD) were calculated for all footwear feature measurements. Intraclass correlation coefficients (ICC) and 95% confidence intervals (CI_{95%}) were calculated to assess the reliability between left and right shoes

of the same pair. Analyses were performed using IBM SPSS 28.0 (IBM Corp., Armonk, NY, USA).

RESULTS AND DISCUSSION

Reliability values of low- and high-tech measurements are listed in Table 1. Inter-shoe reliability was excellent for shoe mass, shoe length, internal stack height, central and medial rearfoot stack height via both measures. Surprisingly, the reliability for high-tech measures were not much higher than manual methods with some falling below low-tech method values. This suggests that while high-resolution tools allow one to capture more precise measures, processing, and point selection to calculate measurements may introduce more error than simple low-tech methods. Efforts to standardize point selection and calculations from high-resolution scans are necessary to improve reliability and utility.

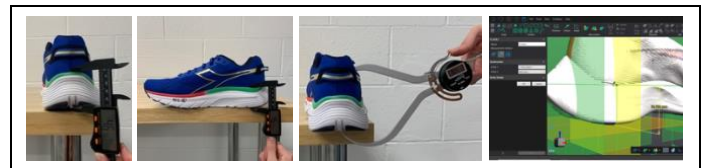


Figure 1: Illustration of low- and high-tech rearfoot stack height measurements.

REFERENCES

1. Hoitz et al., *Footwear Science*, **12**, 2020.
2. Sun et al., *Journal of Sports Science and Medicine*, **19**, 2020.
3. World Athletics, *Press Release*, 2020.
4. Frederick, *Footwear Science*, **12**, 2020.
5. Esculier et al., *Journal of Foot and Ankle Research*, **8**, 2015.
6. Barton et al., *Journal of Foot and Ankle Research*, **2**, 2009.
7. Ramsey et al., *Footwear Science*, **10**, 2018.

ACKNOWLEDGEMENTS

We'd like to thank Super Jock n' Jill in Seattle, WA for access to their inventory and John Meier for his assistance with data collection.

Table 1. Reliability for manual and digital measurements.

	Low-Tech Measures		High-Tech Measures	
	ICC (2,1)	(CI _{95%})	ICC (2,1)	(CI _{95%})
Shoe Mass (g)	0.988	(0.929 - 0.998)	-	-
Shoe Length (mm)	-	-	0.980	(0.701 - 0.997)
Rearfoot Stack Height: Central Heel (mm)	0.926	(0.582 - 0.989)	0.820	(0.268 - 0.972)
Rearfoot Stack Height: Medial Heel (mm)	0.790	(0.075 - 0.968)	0.819	(0.230 - 0.972)
Rearfoot Stack Height: Internal - Central (mm)	0.823	(0.126 - 0.974)	0.815	(0.079 - 0.973)

THE EFFECT OF SPEED ON ANKLE JOINT MECHANICS DURING INCLINE TREADMILL RUNNING

Hidetaka Hayashi¹, Rachel Robinson¹, Seth Donahue², Aida Chebbi¹, Michael Hahn¹

¹ Department of Human Physiology, University of Oregon, Eugene, USA.

² Northwestern University Prosthetics-Orthotics Center, Northwestern University, Chicago, USA

email: hhayash7@uoregon.edu

INTRODUCTION

Uphill running is characterized by an increased demand for work performed and is often incorporated in a runner's training regimen. Previous studies have reported an increase in ankle joint work and power with grade during stance phase, while joint moment remained unchanged [1,2]. This suggests that an increase in joint angular velocity is the source of increased power, and thus increased work. Indeed, it has been shown that the shortening velocity of the gastrocnemius muscle-tendon unit (MTU) increases with grade [3], leading to an effective increase in joint angular velocity. While the effect of grade has been well documented, the role of speed on the mechanical properties of the ankle joint is still unclear. Therefore, the purpose of this study was to clarify the effect of speed on ankle joint mechanics during incline treadmill running.

METHODS

Seven healthy, recreational runners (2M, 5F; age: 24.5 years, height: 176.8 cm, mass: 67.7 kg) completed 30s running trials at 4 speeds with a grade of 7.5° incline on a force-instrumented treadmill (Bertec). Speeds were relative to each participant's self-reported 5k pace (Speed 4), where Speeds 1, 2, and 3 were 1:30, 1:00, and 0:30 min/mile slower, respectively. Kinematic data were collected using an 8-camera motion capture system at 200 Hz (Motion Analysis Corp.), and force data were collected at 1 kHz. Peak plantar flexion (PF) and dorsiflexion (DF) angular velocity was calculated from joint kinematic data. Ankle joint power was calculated using an inverse dynamics approach in Visual3D (C-motion), and work was defined as the time-integral of power (Figure 1). The effect of speed on dependent variables was assessed with a one-way repeated measures ANOVA using SPSS (IBM Corp.). Sphericity was assessed via Mauchly's Test with Greenhouse-Geisser correction used when violated.

RESULTS AND DISCUSSION

Both peak positive and negative power increased with speed ($p < .001$), while there was no significant effect of speed on net work ($p = .235$). Peak PF and DF angular velocity increased with speed ($p < .001$; $p = .022$, respectively). Post-hoc pairwise

comparisons with Bonferroni correction are summarized in Table 1.

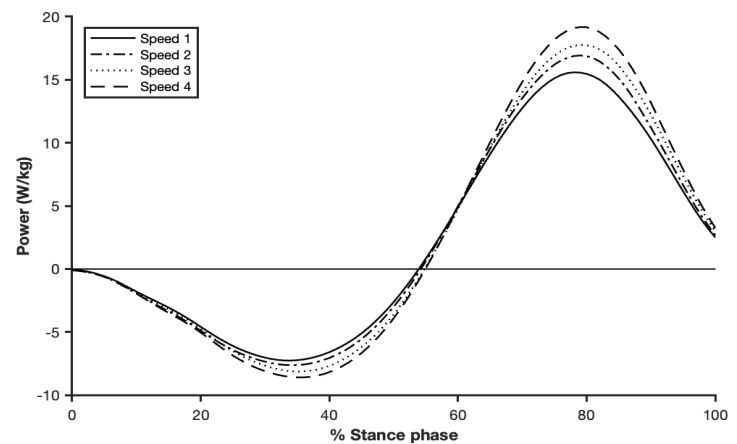


Figure 1 Ankle joint power (W/kg) during stance (average of 7 subjects).

CONCLUSIONS

No change in ankle joint net work was observed, while peak positive and negative power increased. This increase in power may be attributed to the observed increase in joint angular velocity, suggesting greater stretch and recoil of tendinous tissue. Future work should clarify further the contribution of the whole MTU to joint power at different running speeds, specifically about the ankle joint.

REFERENCES

1. Roberts & Belliveau *J Exp Biol* **208**: 1963-70, 2005
2. Nuckols et al. *PLoS One* **15**(8): e0231996, 2020
3. Lichtwark & Wilson *J Exp Biol* **209**: 4379-88, 2006

ACKNOWLEDGEMENTS

This work was supported by the Wu Tsai Human Performance Alliance and the Joe and Clara Tsai Foundation.

Table 1. Average values of ankle joint work, power, and angular velocity across 4 speeds (n = 7)

	Speed 1	Speed 2	Speed 3	Speed 4	p-value
Net work (J/kg)	0.54 ± 0.13	0.56 ± 0.15	0.57 ± 0.12	0.59 ± 0.14	p = .235
Peak positive power (W/kg)	15.83 ± 1.37	17.15 ± 1.92	18.01 ± 1.84 ^a	19.40 ± 1.66 ^{a,b,c}	p < .001
Peak negative power (W/kg)	-7.49 ± 1.8	-7.82 ± 1.63	-8.29 ± 1.85 ^a	-8.82 ± 1.84 ^{a,c}	p < .001
Peak PF velocity (°/sec)	-612.68 ± 43.74	-642.64 ± 50.24 ^a	-666.45 ± 49.07 ^{a,b}	-690.60 ± 46.86 ^{a,b,c}	p < .001
Peak DF velocity (°/sec)	242.71 ± 47.23	249.53 ± 40.82	254.63 ± 40.15	259.78 ± 35.86	p = .022

Values are mean ± SD. a: difference between Speed 1; b: difference between Speed 2; c: difference between Speed 3.

DOES SUTURE TYPE OR CONFIGURATION MATTER IN PERCUTANEOUS ACHILLES TENDON REPAIRS?

Keller, H¹, Benner, N², Branam, G², Chin, K², Telfer, S²

¹Elson S. Floyd College of Medicine, Washington State University

Department of ²Orthopaedics and Sports Medicine, University of Washington

email: hana.keller@wsu.edu

INTRODUCTION

The human Achilles tendon is functionally important for dynamic activities and is a common site of tendon rupture, resulting in pain, weakness, and removal from sport. While treatment options vary and the opinions regarding optimal management are not uniform, percutaneous repair techniques through commercially available guides is one option that has been used widely [1]. The purpose of this study was to test the mechanical properties of four different suture permutations.

METHODS

This biomechanical study used Porcine toe flexor tendons as an analogue for the human Achilles tendon. Simulated rupture was performed and tendons repaired using a percutaneous guide. Technique was uniform with pre-determined allotment into one of four groups based on suture configuration (single or double locked) and type (round or flat) with a total of 10 specimens in each group. Specimens then underwent a static creep test, a dynamic load creep test, and finally a load to failure test. Analysis of variance was performed, followed by pairwise comparisons using independent t-tests to assess inter-group differences if significant effects were found, adjusted for multiple comparisons.

RESULTS AND DISCUSSION

The suture configuration used was determined to have a significant effect on the maximum load to failure of the constructs ($p = 0.018$). Pairwise comparisons showed that Double Tape had a significantly greater load to failure than Single Tape and Single Round conditions. No significant differences were found between the Double Tape and Double Round techniques, nor the Double Round and either of the Single techniques.

The suture configuration also had a significant effect on the maximum stress in the construct during the load to failure test ($p = 0.019$). Pairwise comparisons showed that the Double Tape repair reached greater stresses before failure compared to the Single Tape and Single Round conditions. No significant differences were found between the double tape and double round techniques, nor the Double Round and either of the Single techniques.

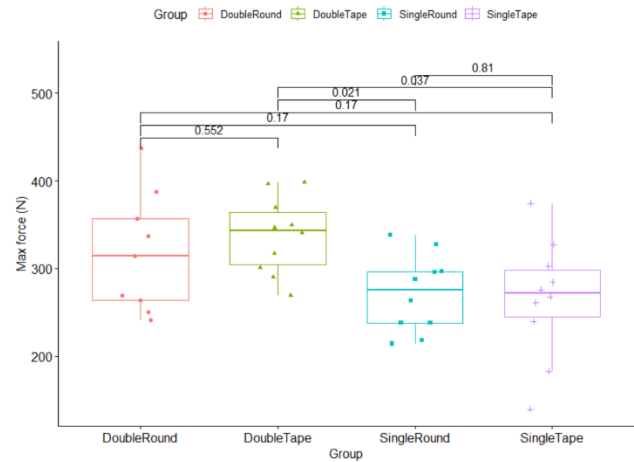


Figure 1: Max load force to failure by group. P-values between groups noted above.

CONCLUSIONS

Currently, there is no compelling data to support surgical over non-surgical management of Achilles tendon ruptures [2]. However, by patient or surgeon preference, many patients undergo operative intervention, and repair through a percutaneous guide is a popular technique [3]. The results of this study, using a porcine model to simulate a minimally invasive technique for Achilles tendon repairs, suggest that the use of a double locked tape or round suture configuration leads to a stronger overall construct.

REFERENCES

1. Soroceanu A, Sidhwa F, Aarabi S, Kaufman A, Glazebrook M. Surgical versus nonsurgical treatment of acute Achilles tendon rupture: a meta-analysis of randomized trials. *J Bone Joint Surg Am.* 2012;94(23):2136-2143..
2. Willits K, Amendola A, Bryant D, et al. Operative versus nonoperative treatment of acute Achilles tendon ruptures: a multicenter randomized trial using accelerated functional rehabilitation. *J Bone Joint Surg Am.* 2010;92(17):2767-2775.
3. Hsu AR, Jones CP, Cohen BE, Davis WH, Ellington JK, Anderson RB. Clinical Outcomes and Complications of Percutaneous Achilles Repair System Versus Open Technique for Acute Achilles Tendon Ruptures. *Foot Ankle Int.* 2015;36(11):1279-1286.

Table 1: Comparison of maximum load force and maximum stress depending on suture configuration group.

	Double Round	Double Tape	Single Round	Single Tape
Maximum Load Force (N)	317 ± 64	337 ± 41	271 ± 41	265 ± 64
Maximum Stress (N/mm ²)	0.450 ± 0.093	0.468 ± 0.087	0.396 ± 0.099	0.412 ± 0.124

INFANT CARRIAGE STRATEGIES UTILIZED BY NULLIPAROUS WOMEN WHILE NEGOTIATING STAIRS

Holly Olvera^{1*}, Abigail R. Brittain¹, Erin M. Mannen¹, Safeer F. Siddicky^{1,2}

¹Mechanical and Biomedical Engineering, Boise State University, Boise, ID

²Kinesiology and Health Education, The University of Texas at Austin, Austin, TX

*Corresponding author's email: hollyolvera@u.boisestate.edu

INTRODUCTION

For the first year of life, infants rely heavily on their caregivers to transport them. While some infant carriage strategies such as carrying infants in arms, in wraps, and in baby carriers on a parent's body have been prevalent through history, modern infant product design has introduced alternative methods including car seats and strollers. However, it is unclear how these different carrying methods may impact caregivers' biomechanics or injury risk. The objective of this pilot study is to identify the strategies utilized by nulliparous women when negotiating stairs while carrying an infant manikin.

METHODS

Ten healthy females (age: 22.3 ± 1.4 years; height: 65.2 ± 2.5 inches; weight: 142.7 ± 17 lbs.) participated in this study. All participants were injury and pain free. No participant was a mother or had been previously pregnant. Participants carried an infant manikin in a body-worn baby carrier, car seat, stroller, and in arms while negotiating stairs in an outdoor setting. Each carrying method was completed six times, three times ascending stairs and three times descending. High-speed video cameras filmed each trial. Three investigators analyzed 50 randomly selected trials to identify movement strategies for each carrying condition. A total of 480 trials were collected. Twenty-two trials were excluded due to equipment malfunction.

RESULTS AND DISCUSSION

Of the 458 trials completed by participants, 112 were in arms, 114 in a baby carrier, 115 in a car seat, and 117 in a stroller. Some common strategies are demonstrated in Fig. 1, and all observed strategies and their frequencies of utilization presented in Fig. 2. When carrying the infant manikin in arms, five main strategies were identified: cradling and carrying on the hip with a single arm (dominant or non-dominant) with and without support from the second arm. When carrying the manikin in a baby carrier, three main strategies were observed: arms hanging freely, arms wrapped around the baby carrier providing additional support, and arms resting on the baby carrier providing little to no support. Six strategies were identified in the car seat condition: carrying the car seat at the elbow (dominant and nondominant) with and without support from the second arm (support), a mixed grip, and a single arm "lock" grip. Five strategies were identified in the stroller condition: a forward push, a backwards pull, a front wheel pop, carrying, and a step-by-step carry. A "switch" and an "other" category was added to each condition for cases when a participant transferred between strategies or used a strategy not defined above. For the in arms condition, participants preferred to carry the manikin on the dominant hip and with the dominant arm while the non-dominant arm provided support (41/112 trials). This was an unexpected observation since a left sided bias exists when carrying infants and inanimate objects alike [1], and 9/10 of our participants were right-dominant. The most

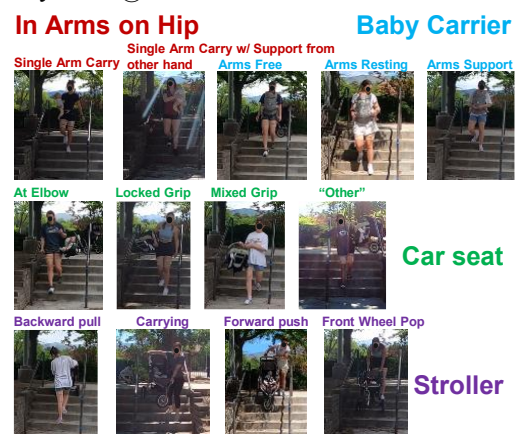


Figure 1: Photos of some distinct carrying strategies.

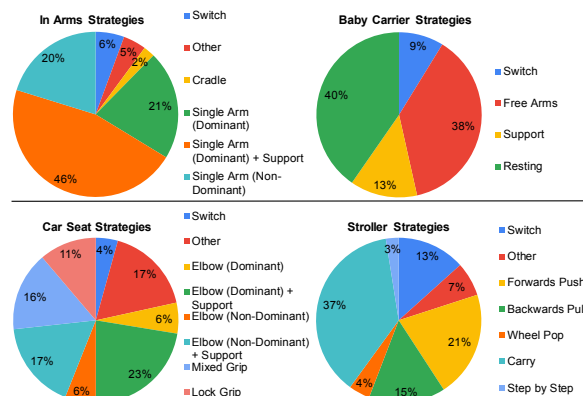


Figure 2: Frequency of all carrying strategies.

employed strategy when carrying the manikin in baby carriers was resting the hands on the carrier (46/114 trials), followed closely by free hanging arms (43/114 trials). This observation is well aligned with recent findings [2] that indicate that caregivers primarily utilize babywearing for the ability to be "hands free". The most common strategy for carrying the car seat was carrying at the elbow (dominant) with support from the non-dominant arm (26/116 trials). Carrying the stroller was the most common strategy used in the stroller condition (45/117 trials). Carrying the manikin in car seats and strollers showed more variability in carrying strategies chosen, compared to the in arms or carrier conditions. This may be attributed to a relative lack of infant care experience in the participants. Car seats and strollers are also fairly heavy carrying devices which may have contributed to participants altering their carrying strategies.

CONCLUSIONS

This feasibility study provides the basis for a full experimental exploration of the impact of various common infant transport methods on caregivers' biomechanics in real-world scenarios.

REFERENCES

1. Ellis et al. (2013), 37:231-44, *J Nonverbal Behav.*
2. Havens et al. (2022), 46:25-34, *J Wom Health Phys Therapy.*

NEUROFENCING 3.0

IMPACT OF WARM UP ON BIOMECHANICS OF FENCERS MOVEMENT & NEURON ACTION POTENTIAL.

Supriya Nair

Freshman, Stanford Online High School, USA Fencing (Id: 100208472), Society for Neuroscience SfN (Id: C-035007)

email: supriya@neurofencing.com, Website: [Neurofencing](https://neurofencing.com)

INTRODUCTION

I am a USA Fencing competitive all weapon (Foil, Epee, Saber) fencer from Northwest. In fencing, it is a common practice to do warm-ups prior to a fencing bout. But does this practice actually help performance? To answer this question, we study "Neurofencing", the intersection of Neuroscience & Fencing. Neurofencing analyzes neuron action potentials, muscle movement time during a fencing lunge with and without a 15-minute warm up. It helps us understand the biomechanics of a fencer's lunge and quantifies the physiological impact of warm-up. After a 15-minute warm-up, I expect the brain to transition from relaxed to aware, heart from rest to active and improve muscle movement time for a 6ft lunge to target by 10%.

The Mount Sinai IRB approved study STUDY-22-01661 was conducted with multiple fencers at Abilities Research Lab, Mount Sinai Hospital in New York in March 2023. This poster presents a preliminary analysis about the impact of warmup on the biomechanics of a fencer's movement.

METHODS

Several active USA Fencing members were recruited to participate for an hour each on two different days, one of which was randomly selected for warm up of 15 minutes. On warm up day (WD), the fencers EEG & EKG recordings were recorded for 2min upon arrival, followed by a set of warm-up exercises for 15min. Post warm-up EEG & EKG recordings were taken. The fencer then conducted 10 lunges towards a fixed target 6ft away and their EMG & IMU signals were recorded from six sensors in their dominant Bicep, Tricep, Forearm, Thigh, Hamstring & Calf and with two sensors from non-dominant hand and leg. On non-warm-up day (NWD) they recorded EMG & IMU signals for their 10 lunges along with EKG & EEG recordings before & after the lunges.

DATA ACQUISITION

An individual fencer generates time series data $(2 \times 10 \times 8) = 160$ EMG signals and $2 \times 10 \times 8 \times 3 (x, y, z) = 480$ Accelerometer IMU signals, $2 \times 10 \times 8 \times 3 (x, y, z) = 480$ Gyroscope IMU signals in addition to 5 EEG and 5 EKG data streams. Every fencer completed 20 lunges, 10 each pre & post warm up on different days. Data analysis includes 25 EKG, 25 EEG and 100 EMG recordings.

RESULTS AND DISCUSSION

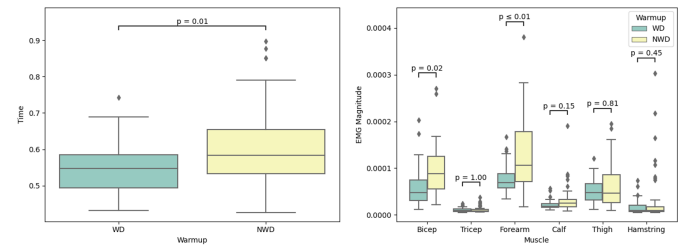


Figure 1: Improvement in Fencer muscle movement time 9.4 percent (reduction from 604ms to 547ms) for a lunge towards a fixed target 6ft away. Significant reduction in magnitude of muscle action potential (EMG magnitude) post warm up especially in fencer's dominant Forearm and Bicep. Fencers are 10-14yrs old, each box plot represents $4 \times 10 = 40$ lunges.

First in muscle movement time, we observed a 9.4% improvement on the warm up day ($p=0.01$). Warm up increases blood flow making it easier for muscles to activate and contract efficiently, resulting in a smoother and less forceful contraction. Second, there is significant reduction in the magnitude of the EMG spike in the forearm ($p<0.01$) and bicep ($p=0.02$). Better coordination between nervous system and muscles yields controlled, precise movements, potentially reducing the need for large, forceful contractions with larger EMG spikes. EKG analysis shows minimum heart rate (HR min) post lunge w/ warm up to be significantly higher vs non warmup day ($p<0.01$). It also shows significant reduction in (HRV PNN50) proportion of time that the interval between heart beats is greater than 50ms ($p=0.03$). When relaxing post lunge, preliminary EEG analysis of C3 & C4 channels (Motor Cortex) shows band power for delta waves post lunge w/ warm up to be significantly higher vs non warmup day ($p<0.01$).

CONCLUSIONS

Fencer muscle movement time improves with warm up and it takes less effort to innervate them.

REFERENCES

De Luca Foundation. (n.d.).

<https://www.delucafoundation.org/download/bibliography/de-luca/078.pdf>

ACKNOWLEDGEMENTS

Team Mount Sinai - Dr Mariam Zakhary & Dr David Putrino, Mackenzie Doerstling, Bradley Hamilton, Jamie Wood, Abby Sawyer & Megan Shepherd from Delsys.

EFFECT OF 3-D PRINTED CUSTOM ACCOMMODATIVE INSOLES ON BALANCE DURING WALKING

Mathew Sunil Varre^{1,2*}, Patrick Aubin², Jing-Sheng Li², Brittney C. Muir^{1,2}

¹Center for Limb Loss and Mobility, Veterans Affairs Health Care System, Puget Sound, ²Department of Mechanical Engineering, University of Washington, Seattle
email: msvarre@uw.edu

INTRODUCTION

Individuals with diabetes mellitus (DM) are often prescribed custom accommodative insoles to prevent high plantar pressure (PP) and subsequent foot ulcers [1]. The standard of care accommodative insoles (SoC) are soft, collapsible, and conform over time. Our group has recently developed a 3D printed pressure-based custom accommodative insoles (PBI) [2]. Although SoC and PBI have been shown to reduce PP [1,3], the effects of accommodative insoles on balance in persons with DM is limited to a single study [4]. Balance is especially critical in this population as many older adults with DM have sensory deficits and deteriorated balance [3]. In this study, we examined the effect of PBI and SoC compared to a no insole (NOI) condition on dynamic balance in individuals with DM and healthy controls. We expect the COP parameters to significantly differ in DM participants compared to healthy persons in PBI and SoC conditions over the NOI condition during shod walking.

METHODS

Six participants (three healthy males [66 (9) years; 1.8 (0.1) m;88 (15) Kg] and three males diagnosed with DM [67(9) years; 1.8 (0.2) m;100 (27) Kg]) were recruited for this study. Foot impressions and in-shoe PP measurements (Novel, DE) while walking in a standardized research shoe (Dr. Comfort, USA) were collected during a baseline visit and were used to design SoC and PBI [5]. During a follow-up visit, in-shoe PP measurements during walking were recorded in the NOI, SoC, and PBI conditions. The data were processed to compute within step center of pressure (COP) measures (mean, variability, range, and velocity along medial-lateral (ML) and anterior-posterior (AP) directions) (Fig 1) [6]. Average, standard deviation, and percentage differences of the PBI and SoC compared to the NOI condition for each group are presented.

RESULTS AND DISCUSSION

Mean COP amplitudes were larger in DM compared to healthy controls. No differences were identified in mean COP amplitudes across conditions in AP and ML directions for both groups. In the DM group, when compared to the NOI condition, COP range, variability, and velocity increased in ML for both PBI (2-12%) and SoC conditions (12-17%; Table 1). In healthy controls, these variables varied by 1-8% in both AP and ML

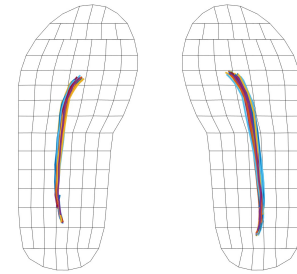


Figure 1: COP trajectories of a DM participant in NOI condition during shod walking

(Table 1). Overall, a pattern of larger deviations in COP measures range, variability, and velocity in ML was found in both groups. The changes observed in various COP measures, in the ML direction, specifically in the DM group, indicates a possible lateral instability induced by custom accommodative insoles (PBI and SoC) leading to more adjustments of COP to maintain balance.

CONCLUSIONS

The preliminary findings of this study demonstrate that custom accommodative insoles could potentially alter the lateral balance in individuals with DM during shod walking. Future studies with larger sample sizes are needed to clearly establish the alterations in both static and dynamic balance due to custom accommodative insoles in individuals with DM. Such an assessment would be useful in developing custom accommodative insoles that would not compromise balance while reducing the risk for foot ulcers in persons with DM.

REFERENCES

1. Bus et al (2020), *Diabetes Metab Res Rev*, 32(1).
2. Hudak et al (2022), *Med Eng Phys* 104.
3. Muir et al (2022), *Clin Biomech*, 98.
4. Hijmans et al (2007), *Gait Posture* 25(2).
5. Paton et al (2016), *J Foot Ankle Res* 9(40).
6. Quijoux et al (2021), *Physiol Rep*, 9(22).

ACKNOWLEDGEMENTS

Funding for this study was provided by VA award A3539R.

Table 1: Average (SD) and percentage change (%) of COP Measures

		Mean (cm)		Range (cm)		Variability (cm)		Velocity (cm/s)	
		ML	AP	ML	AP	ML	AP	ML	AP
Healthy	NOI	4.5(4.0)	7.7(6.6)	1.3(0.4)	14.5(1.6)	0.4(0.1)	4.7(0.5)	4.1(2.1)	46.4(15.7)
	PBI	4.5(4.0) 0%	7.8(6.7) 2%	1.3(0.4) -2%	13.7(0.6) -6%	0.4(0.1) 1%	4.5 (0.1) -5%	4.4(2.9) 6%	45.8(17.5) -1%
	SoC	4.5(3.9) 0%	7.7(6.4) 0%	1.4(0.3) 4%	14.6(0.6) 0%	0.4(0.1) 8%	4.7(0.3) 0%	4.4(2.4) 6%	46.5(17.1) 0%
DM	NOI	6.7(0.2)	12.2(2.2)	1.5(0.2)	13.0 (1.9)	0.5(0.1)	4.3(0.8)	3.4 (1.8)	33.0(20.4)
	PBI	6.7(0.2) 1%	12.1(2.0) -1%	1.6(0.4) 4%	13.0(1.8) 1%	0.5(0.1) 2%	4.4(0.8)1%	3.8(2.4) 12%	33.8(20.0) 2%
	SoC	6.7(0.1) 0%	12.3(1.8) 0%	1.7(0.3) 14%	13.1(2.0) -1%	0.5(0.1) 12%	4.3(0.8)0%	4.0(2.1)17%	32.7(19.5) 1%

THREE-DIMENSIONAL ANALYSIS OF WINDLASS MECHANISM USING WEIGHTBEARING COMPUTED TOMOGRAPHY IN PATIENTS WITH HALLUX RIGIDUS AND HEALTHY VOLUNTEERS

Takumi K^{1,2,3}, Tadashi K¹, Mitsuru S¹, Naoki S², Asaki H², Makoto K¹

¹Department of Orthopaedic Surgery, ²Institute for High Dimensional Medical Imaging, The Jikei University School of Medicine, Tokyo, Japan, ³RR&D Center for Limb Loss and MoBility (CLiMB), VA Puget Sound Health Care System, Seattle,

Washington, USA

email: takumi.kihara@jikei.ac.jp

INTRODUCTION

The windlass mechanism (WM) increases the height of the longitudinal arch of the foot by tensing the plantar aponeurosis during dorsiflexion of the metatarsophalangeal (MTP) joint [1]. We speculated that this mechanism may be deeply involved in the pathogenesis of forefoot diseases such as hallux rigidus (HR) and hallux valgus (HV) [2]. These conditions are three-dimensional (3D) deformities including rotational deformity, but the role of the WM has been evaluated only two-dimensionally by measuring the height of the navicular on lateral plain radiographs [3]. The purpose of this study was to analyze in detail the WM of normal and HR feet in 3D.

METHODS

Participants were 14 patients with HR (5 men and 9 women; 17 feet) and 13 healthy volunteers (6 men and 7 women; 21 feet), with mean ages of 55.7 (33–66) and 67.2 (44–79) years, respectively. The healthy volunteers had no history of foot disease or trauma, whereas the patients with HR had Hattrup and Johnson classification I or II. Computed tomography (CT) of the foot with a load equivalent to the participant's body weight was performed. Imaging was performed with the 1st MTP joint in the neutral position (toe touching the floor) and dorsiflexed 30 degrees.

From the obtained CT images, each bone was segmented and 3D models were created using the image processing software Mimics. Next, we used the iterative closest point (ICP) algorithm, which allows 3D objects to be superimposed without specifying anatomical feature points. Then, we performed 3D measurements of (1) the amount of rotation of each bone in the MLA with respect to the tibia, (2) the amount of rotation of the distal bone with respect to the proximal bone in each joint of the MLA, and (3) changes in the height of the geometric center of the navicular from the sole of the foot.

RESULTS AND DISCUSSION

At the calcaneus and navicular, the HR group showed less inversion and adduction than healthy group ($P<0.05$) (Figure1). At the talonavicular joint, the navicular was inverted 3.7° and adducted 2.9° in the healthy group and inverted 2.4° and adducted 1.3° adduction in the HR group. At the talocalcaneal joint, the calcaneus was inverted 1.7° and adducted 1.5° in the healthy group and inverted 0.9° and adducted 0.6° in the HR group. In the talonavicular and talocalcaneal joint, the HR group showed less inversion and adduction than control ($P<0.05$) (Figure2).

Figure 1 The amount of rotation of each bone in the MLA

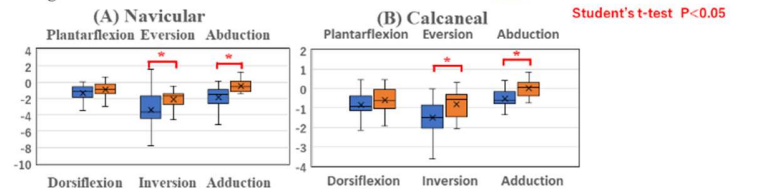
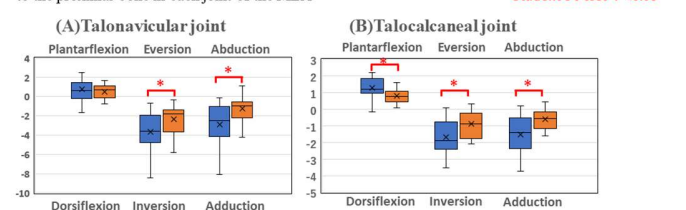


Figure 2 The amount of rotation of the distal bone with respect to the proximal bone in each joint of the MLA



With dorsiflexion of the hallux, the height of the navicular increased by 2.1 mm in the healthy group and 1.3 mm in the HR group. There was a significant difference ($P<0.05$) between the two groups. In this study, we used the ICP algorithm to analyze 3D CT images, which enabled us to directly and precisely measure the bone dynamics of the first ray with respect to the WM, with a low mean error of 0.6 mm.

In the healthy foot, the height of the navicular was increased by the effect of the WM. This was caused by the gradual plantarflexion of each joint from the talonavicular joint to the first tarsometatarsal joint, which increased the arch height.

The calcaneus and navicular moved not only in the sagittal plane but also in the frontal plane. These changes were similar in the HR group, but the movement of the talonavicular and talocalcaneal joints and the change in height of the navicular were significantly reduced compared with the healthy group.

CONCLUSIONS

In the HR group, the motion of the midfoot and hindfoot during dorsiflexion of the hallux was limited, suggesting that the function of the WM was impaired.

REFERENCES

1. Hicks, J.H., The mechanics of the foot. I. The joints. *J Anat*, 1953. 87(4): p. 345-57.
2. Maceira, E. and M. Monteagudo, Functional hallux rigidus and the Achilles-calcaneus-plantar system. *Foot Ankle Clin*, 2014. 19(4): p. 669-699.
3. Gelber, J.R., et al., Windlass mechanism in individuals with diabetes mellitus, peripheral neuropathy, and low medial longitudinal arch height. *Foot Ankle Int*, 2014. 35(8): p. 816-824.

DEVELOPING COMPUTATIONAL MODELS OF UNILATERAL CERVICAL CONTUSIONS IN RATS TO QUANTIFY INJURY BIOMECHANICS

Zamora, DL^{1,2}, Jimenez, C^{1,2}, Liu, S¹ and Sparrey, CJ^{1,2}

Department of ¹Mechatronics Systems Engineering, Simon Fraser University, Surrey, BC CA

²International Collaboration on Repair Discoveries (ICORD), University of British Columbia, Vancouver, BC, CA

email: csparrey@sfu.ca, web: <https://www.sfu.ca/neurospine.html>

INTRODUCTION

Computational spinal cord injury (SCI) models are being used alongside *in vivo* studies to examine and quantify injury biomechanics. We previously developed a non-human primate (NHP) model that captures *in vivo* contusion experiments using smoothed particle hydrodynamics (SPH) and an inhomogeneous cord [1]. Leveraging these advances, our objective was to develop a rat SCI model employing similar approaches to the NHP models to quantify tissue-level biomechanical differences in controlled contusion (Infinite Horizon – IH) and weight drop (WD) injury models.

METHODS

Unilateral cervical contusions of rat SCI were simulated using finite element (FE) methods with material properties and rat morphology from previous studies [1], [2]. The IH model used the averaged displacement from 357 experiments from the ODC-SCI database [3] as input and validated the simulated peak reaction force against the experimental average. The WD models used reported impact velocities and drop mass for two drop heights (6.25 mm and 12.5 mm) as inputs and compared the resulting cord compressions for validation [2].

Spinal cord stress and strain distributions were compared in the validated models to quantify the mechanistic differences between IH and WD injuries. Calculated stresses and strains were compared to values representing the 50% probability of tissue injury [1] using the same peak displacements.

RESULTS AND DISCUSSION

The displacements of the validated computational models (Figure 1) showed varying profiles for the same peak displacement. The WD model sustained higher initial velocity at a shorter time than the IH.

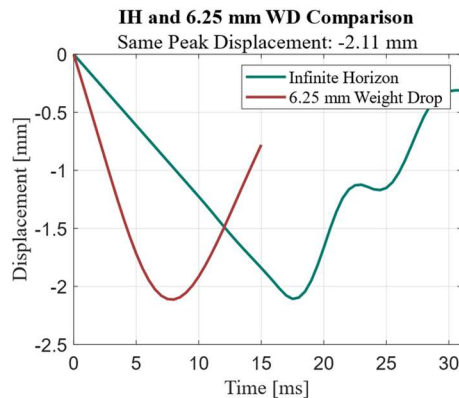


Figure 1: Simulated impactor displacement time histories

Most of the stresses and strains looked similar between the IH and WD model at the same displacement. However, some stress

distributions of the gray matter (GM) and white matter (WM) (Figure 2) showed that the WD model had larger ipsilateral regions to the contusions above the injury probability compared to the IH model. These highlighted differences were in the GM ventral horns and WM lateral columns.

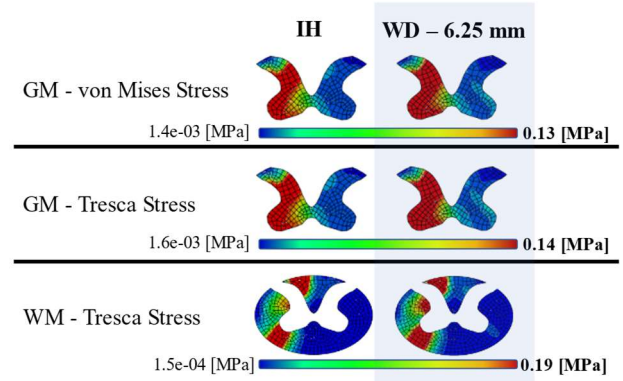


Figure 2: Transverse cross-sections at the injury epicenter of gray matter (GM) and white matter (WM). Note that the bolded values represent the 50% probability of tissue injury.

The differences between the IH and WD models' injury locations at these tissue levels show that the two injury mechanisms affect different regions. This discrepancy could result in different effects on motor functions assessed in behavioral tests. Some possible factors contributing to this discrepancy are impact velocities and exposure time differences that could affect the resulting stress and strain outcomes.

CONCLUSIONS

This study developed rat cervical SCI computational models validated through *in vivo* experiments. The computational models highlighted differences in locations of possible tissue injuries between injury mechanisms. These models provide the opportunity to assess ways to quantitatively compare injuries and aid in consolidating results across studies by more accurately quantifying the injury exposure.

REFERENCES

1. Jannesar S, Salegio EA, Beattie MS, Bresnahan JC, Sparrey CJ. *J. Neurotrauma* **38**, 698-717, 2021
2. Gensel JC, Tovar CA, Hamers, FPT, Deibert RJ, Beattie MS, Bresnahan JC. *J. Neurotrauma* **23**, 36-45, 2006
3. "odc-sci" <https://odc-sci.org/> (accessed Mar. 07, 2023)

ACKNOWLEDGEMENTS

The authors would like to acknowledge the Natural Sciences and Engineering Research Council of Canada (NSERC), supported by the Digital Research Alliance of Canada (www.computecanada.ca)

LOWER LIMB MUSCLE CO-ACTIVATION DOES NOT DIFFER BY AGE DURING DISTRACTED WALKING OVER CHALLENGING SURFACES.

Matthew V. Robinett¹, Nicholas L. Hunt¹, Amy E. Holcomb¹, Clare K. Fitzpatrick¹, and Tyler N. Brown¹

¹Boise State University

email: matthewrobinett@u.boisestate.edu

INTRODUCTION

To compensate for loss of muscle mass, older adults (over 65 years) increase lower limb muscle co-activation to provide joint stability and decrease fall risk when walking [1]. Older adults commonly fall when walking over a challenging, i.e. slick or uneven, surface as it reportedly requires greater lower limb co-activation to provide the stability necessary to mitigate the fall. Yet, it is unknown whether a cognitive distraction further exacerbates the lower limb co-activation to safely walk over a challenging surface – particularly for older adults. We hypothesize that lower limb co-activation, quantified using a Vector Coding Technique, will be greater for older adults, and further increase on a challenging surface and when distracted.

METHODS

16 young (18 to 25 years) and 13 older (> 65 years) adults participated. Each participant had lower limb muscle activity quantified while walking at a self-selected speed over a normal, slick and uneven surfaces, and with and without a cognitive distraction. The slick and uneven surfaces consisted of a wood panel fixed atop a force platform, and covered by either smooth, plastic material or nine wooden blocks of differing heights. The cognitive distraction required participants perform a serial subtraction task by verbally subtracting by three from a random number presented at the beginning of each walk trial. Participants performed three successful walk trials for each condition.

During each trial, surface EMG electrodes (Trigno, Delsys Inc., Boston, MA) recorded participants vastus lateralis (VL), lateral hamstring (LH), and lateral gastrocnemius (LG) muscle activity. The EMG data was bandpass filtered (20-450 Hz, 4th order Butterworth filter) to remove noise, before being rectified and low pass filtered at 25 Hz to create a linear envelope. The linear envelope was normalized to the maximum value recorded during the walk trials, and then, VL:LH and VL:LG co-activation was quantified during weight acceptance (1%-50% of stance phase) using a Vector Coding Technique according to [2, 3]. The co-activation index, calculated by the number of frames the muscle pairs were in- or anti-phase divided by the total number of frames of interest, was quantified for analysis.

The co-activation index for VL:LH and VL:LG muscle pairs were submitted to statistical analysis. Each dependent variable was submitted to two-way mixed model ANOVAs to test main effects and interaction between age (young and older adults) and surface (normal, slick, and uneven), and age and distraction (with and without) on each surface. Alpha level was < 0.05.

RESULTS AND DISCUSSION

Contrary to our hypothesis and existing experimental evidence, older adults did not walk with greater lower limb co-activation than their younger counterparts. There was no main effect of age ($p > 0.05$) for either VL:LH or VL:LG contraction with or without the cognitive distraction. Yet, surface only impacted VL:LG co-activation when the participant was distracted ($p = 0.008$). When distracted, participants increased VL:LG co-

activation on the slick compared to the uneven ($p = 0.013$), but not normal surface ($p > 0.99$) (Figure A). The decreased friction of the slick surface provides a challenge that may require increased lower limb muscle co-activation during weight acceptance to prevent an accidental slip or fall.

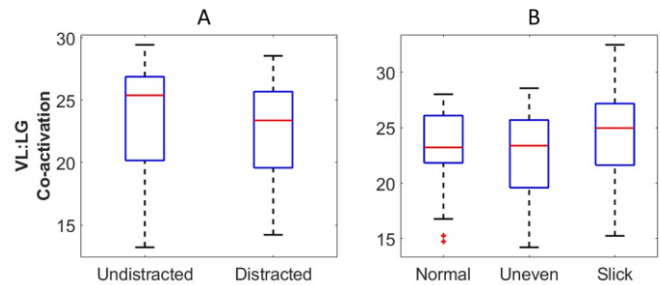


Fig 1. Boxplot of VL:LG co-activation on the uneven surface with and without distraction (A) and for each surface (B).

The cognitive distraction only impacted VL:LG co-activation when walking over the uneven surface ($p = 0.040$). Contrary to our hypothesis, participants exhibited a 6% decrease in co-activation while walking with the cognitive task on the uneven surface compared to the slick surface (Figure B). While the reason for the discrepancy with existing literature is not immediately evident, using VCT to quantify muscle co-activation may improve estimates of simultaneous agonist / antagonist activation, as it performs well with various degrees of Signal-to-Noise Ratio and higher cut-off frequencies [3]. Regardless, further study is needed to determine if the cognitive distraction required participants to focus less on their stability to walk over the uneven surface.

CONCLUSIONS

Older adults neither walked with greater lower limb co-activation than their younger counterparts, nor exhibited greater increases in co-activation than young adults when navigating a challenging surface or when distracted. All participants, however, increased VL:LG co-activation on the slick surface, but decreased VL:LG co-activation with the addition of the cognitive distraction on the uneven surface. Further research is warranted to determine whether improved treatment of noisy EMG data with VCT quantification of muscle co-activation contributes to the discrepancy with existing experimental evidence.

ACKNOWLEDGMENTS

NIH Institute on Aging (R15AG059655) provided support.

REFERENCES

- [1] Cruz-Jimenez, *Clinics of North America*, **28**, 2017
- [2] Yoo et al., *J Mech Science and Technology*, **30**, 2016
- [3] Rinaldi et al., *J Electromyography and Kines.*, **14**, 2018

MORPHOLOGICAL PROPERTIES OF THE PLANTAR FASCIA: INTERVAL VS. CONTINUOUS RUNNING

Margaret A. Lewis^{1*}, Lukas Kruppl¹, Joshua P. Bailey¹

¹Department of Movement Sciences, University of Idaho, Moscow, ID, USA

email: *lewi6014@vandals.uidaho.edu

INTRODUCTION

The plantar fascia (PF) is a band of connective tissue that supports the medial longitudinal arch of the foot. The viscoelasticity of the PF allows the tissue to lengthen during running and then recoil when tension is removed [1]. PF thickness of the tissue has implications for plantar fasciitis and can be used as clinical diagnostic tools [2]. Literature has shown that long distance running induces a decrease in PF thickness due to continuous mechanical loading [1,3], but the effects of higher intensity interval running bouts are uncertain. Thus, the purpose of this study was to assess PF thickness response to maximum effort 400-meter intervals and 5k run. It was hypothesized that the 5k would elicit a greater decrease in PF thickness seen in post run measurements when compared to those of the 400 m intervals.

METHODS

Sixteen healthy individuals participated in the present study (9 Females, 7 Males; Age: 28.6 yrs (\pm 8.9), Height: 171.6 cm (\pm 7.5), Mass: 66.3 kg (\pm 8.7)). All participants were considered physically active according to ACSM. Participants were asked to refrain from physical activity, caffeine, and alcohol consumption 24 hours prior to data collection for both running stents. A minimum of seven days were allotted between the 400 m intervals and 5k run. All participants completed the 400 m first, and then 5k run second after said 7-day period. Participants wore their own shoes and exercise clothing for both protocols. The 400-meter interval guidelines stated that all participants had to do at least 5 maximal effort laps (with a 1:1 work to rest ratio), followed by additional laps until a 5% performance fatigue threshold was reached. As with the interval runs, the 5k run was also completed at a maximal effort. PF thickness was measured via ultrasound pre, immediately post, and 30-minutes post run. Ultrasound measurements for thickness were taken using B-mode imaging. For these measurements, the participant laid in a prone position with their bilateral lower limbs in full extension and bare feet over the edge of the table. The dependent variable, PF thickness, was analyzed using a two-way (2 run x 3 time) repeated measures ANOVA. Interaction effects were followed up by simple main effects and pairwise comparisons using Bonferroni corrections. The alpha was set at $\alpha = 0.05$, and IBM SPSS Statistics (v.28) was used to perform the statistical analyses.

RESULTS AND DISCUSSION

There was a significant interaction effect between run and time for PF thickness ($F[2,30] = 3.911$, $p = 0.031$, $\eta_p^2 = 0.207$). Follow up simple main effects analyses showed a significant effect of time for the interval ($F[2, 30] = 24.239$, $p < 0.001$, $\eta_p^2 = 0.618$) and the 5k run ($F[2, 30] = 22.789$, $p < 0.001$, $\eta_p^2 = 0.603$). Pairwise comparisons found a significant decrease in PF

thickness from pre- to post-run for the interval runs ($p < 0.001$; 3.29 to 2.86 mm) and the 5k ($p = 0.001$; 3.13 to 2.81 mm), and a significant increase from post-run to 30 minutes post-run for the interval runs ($p = 0.003$; 2.86 to 3.14 mm) and the 5k ($p < 0.001$; 2.81 to 3.22 mm) (Fig 1).

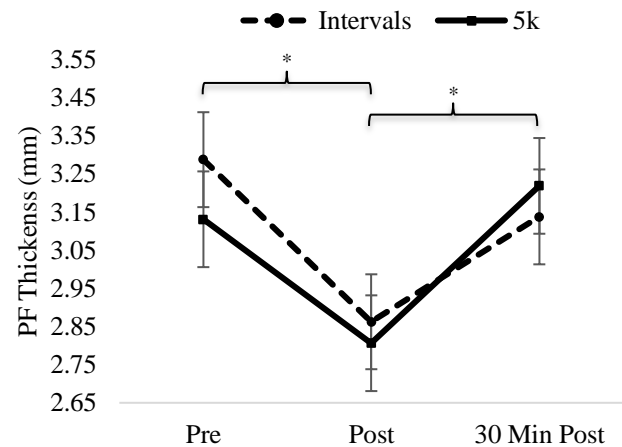


Figure 1: Mean PF thickness at pre-, post-, & 30 min post-run for the interval run and the 5k sessions. *Indicate a significant difference between measurements for both runs.

Data analysis revealed that both the high intensity track intervals and the maximal effort 5k run acutely decreased PF thickness. Thus, based upon this finding, we reject the initial hypothesis. This suggests that both running protocols, interval running and long distance running, had a similar effect on PF thickness. However, PF thickness decreased by a greater margin after the interval runs ($\Delta -0.43$ mm), compared to the 5k run ($\Delta -0.33$ mm). After 30 minutes of recovery, PF thickness appeared to recover more efficiently following the 5k run ($\Delta 0.41$ mm), compared to the interval runs ($\Delta 0.28$ mm).

CONCLUSIONS

The present findings indicate that two different maximal effort running protocols elicit similar responses to the morphology of the PF. However, the greater decrease and slower recovery of PF thickness in response to the interval runs compared to the 5k warrant further investigation. Thus, future research should study the influence of kinematic factors such as stride rate, frequency, and length, or kinetic factors such as vertical impact forces on PF properties to better understand response to imposed mechanical demands.

REFERENCES

1. Shiotani H. *Scand J Med Sc Sports*, **30**, 1360–1368, 2020.
2. Wall JR. *Foot & Ankle*, **14**, 465–470, 1993.
3. Taunton JE. *Br J Sports Med*, **36**, 95–101, 2002.

EVALUATING EFFICACY OF A FORCE-AMPLIFYING IMPLANTABLE MECHANISM IN A LIVE RABBIT FOREARM MODEL USING ELECTRICAL STIMULATION TO GENERATE MUSCLE TWITCHES

Gabriella I Justen, Hantao Ling, Leah Streb, Jennifer Sargent, and Ravi Balasubramanian
Oregon State University, Corvallis, OR
email: justeng@oregonstate.edu

INTRODUCTION

In the United States, 58.7% of the 17,700 spinal cord injuries that occur each year result in some degree of tetraplegia¹, which leads to reduced control of upper limb muscles. Tendon transfer surgeries are often necessary to restore upper limb functions and decrease an individual's dependence on caregivers and family members². To restore thumb key pinch grip, a brachioradialis (BR) to flexor pollicis longus (FPL) tendon transfer surgery is often conducted. We propose the use of a novel modification to the standard tendon transfer procedure by introducing a pulley-like implant between the BR and FPL tendons that amplifies the force transferred from the BR muscle to the FPL tendon by up to 2X. The trade-off for the force amplification effect is a proportional increase in the muscle contraction length to create the same output tendon excursion. In this work, we electrically stimulate the common digital extensor (CDE) muscle in an analogous BR tendon transfer procedure in a live New Zealand white rabbit forearm model. Specifically, the purpose of this study is to evaluate the efficacy of such a force-amplifying implant by generating muscle twitch forces in a standard and implant-modified tendon transfer surgery at varying tendon lengths while measuring output tendon forces.

METHODS

The right forelimb of a single New Zealand white rabbit (n=1) was used in this preliminary study, and both tendon transfer surgeries were conducted in the same leg of the anesthetized rabbit. After the implant-modified surgery was first conducted, the forelimb was fixed at the elbow and wrist joints in a custom testbed, and fine-wire electrodes were inserted into the CDE muscle. A load cell attached to a micrometer head was then connected to the distal end of the pulley implant via Kevlar string to measure the force of the output tendon. The custom testbed enabled muscle length adjustments within 0.01 mm. The CDE muscle was initially set to 0.25 N of passive tension, and 5 muscle twitches were generated at 1 second intervals using electrical stimulation (3 mA, 40 Hz). The muscle length was incrementally increased by 0.25 mm and stimulated again using the same protocol until there was an equal number of data points on either side of the estimated active muscle force curve plot. During data collection, custom MATLAB code was used to actively calculate active muscle forces from raw data and fit an active muscle force-length curve³ onto the raw data. Following data collection, the surgery was modified to a standard tendon transfer procedure. The CDE muscle was initially set to 0.125 N of passive tension and the output tendon length was increased by 0.50 mm between muscle twitches to account for the change in force-amplification effect and output tendon excursion lengths between the two surgeries.

RESULTS AND DISCUSSION

The force-length curves for the implant-modified and standard tendon transfer surgeries were aligned on the horizontal axis

using the estimated optimal muscle length and can be seen in Figure 1. The peak muscle twitch force for the implant-modified surgery was 1.51 N while the peak force in the standard surgery was 0.86 N. However, the curve for the implant-modified procedure is noticeably narrower than the standard procedure.

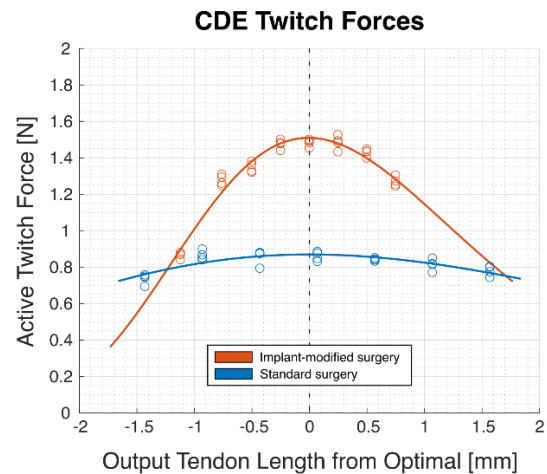


Figure 1: CDE muscle twitch forces from a rabbit forearm in an implant-modified and standard tendon transfer surgery.

The objective of this study was to explore the efficacy of force-amplifying implant in a live rabbit model across varying muscle lengths. When compared to the standard surgery, the implant-modified surgery produced a peak force 1.74X times greater but this force amplification diminishes as you move away from the optimal muscle length. This is due to the narrower force-length curve for the implant-modified surgery, which is caused by the difference in excursion transmission between the two surgeries. This study is limited by having a sample size of one. A larger sample size is needed to validate the results that were achieved.

CONCLUSIONS

This study demonstrates some of the characteristics of a force-amplifying implant used in tendon transfer surgeries. While the implant has the potential to improve functional strength of tendon transfer surgery, the force amplification may not be constant over the joint range of motion. Using the implant will ultimately require more precise tendon tensioning during surgery but has the potential to drastically improve outcomes for spinal cord injury patients.

ACKNOWLEDGEMENTS

We would like to thank LARC and RAIL staff for transporting and taking care of the animal and cleaning the space we used.

REFERENCES

- [1] National Spinal Cord Injury Statistical Center 2018, *UAB*.
- [2] Smaby et al. 2004, *J Rehabil Res Dev*.
- [3] Kaufman et al. 1989, *J Biomechanics*.

MYTH OR SCIENCE: INCREASED GLUTEUS MAXIMUS ACTIVATION IMPROVES RUNNING ECONOMY

Sanchez, R¹, Hernandez, C¹, and Ortega, J¹

Department of ¹ Kinesiology, California State Polytechnic University, Humboldt
email: rs120@humboldt.edu; ch216@humboldt.edu

INTRODUCTION

Within the running community, there are methods that a trainer will utilize to improve the performance of an athlete. Many of these methods have limited evidence to show that the specific training method is responsible for improving an athlete's running performance. One such training method suggests that increasing Gluteus Maximus (GM) muscle activation improves the efficiency of runners. To date, the relationship between GM muscle activation and running economy (RE) has not been examined. The primary purpose of this study was (1) to examine the relationship between GM activation and RE and (2) to examine the relationship between GM activation and running kinematics. A secondary purpose of this study was (1) to examine the relationship between other leg muscles and RE, and (2) to examine the relationship between leg muscle activation running kinematics.

METHODS

Seven male and three female recreational runners (27±8 yrs) ran on a treadmill at 11 km/h. For each trial, we quantified running economy as metabolic power (Watt/kg) using indirect calorimetry (ParvoMedic), muscle activation (2000 Hz; Delsys Trigno) of the Rectus Femoris (RF), Biceps Femoris (BF), Soleus (SOL), Tibialis Anterior (TA) muscles and leg kinematics data (200 Hz; Vicon Nexus) were collected in the last two minutes of each five-minute trial. Pearson product correlations were used to determine the strength of the relationship between muscle activation and RE and the relationship between muscle activation and kinematic variables.

RESULTS AND DISCUSSION

There was no significant relation between GM activation and metabolic cost at 11km/hr ($r = -.08$, $p = .817$, Figure 1). When examining secondary lower extremity muscles, none of the muscles had a correlation with metabolic cost (Table 1). Similar studies examining metabolic cost and muscle activation found similar trends in which GM was reported to be one of the lower activating muscles at slower speeds [1].

When examining the relationship between muscle activation and kinematic variables, none of the lower extremity muscles examined were correlated with peak joint angles and spatio-temporal kinematics. This lack of a relationship between muscle activation and running metabolic cost may be related to the Spring-Mass mechanics of running in which elastic energy is stored

in the muscle-tendon units during the first half of the stance phase (absorption) of the gait cycle and transferred into kinetic energy during the second half of the stance phase (propulsion), thus reducing the amount of work performed and energy consumed by the muscles. [2, 3].

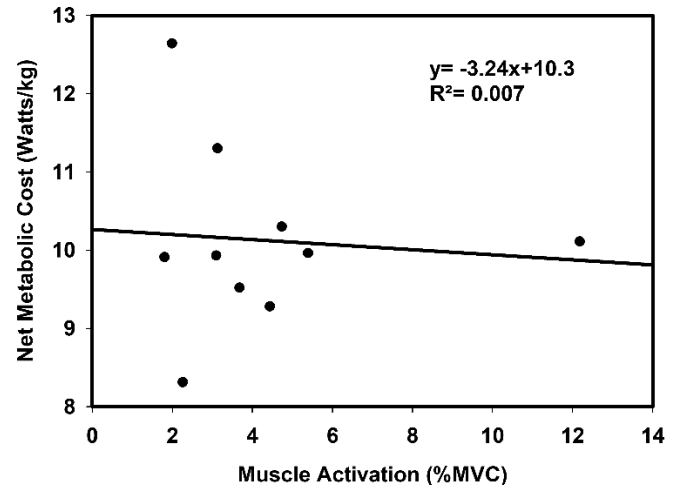


Figure 1: Relationship between gluteus maximus activation and net metabolic cost at 11km/hr. (n=10).

CONCLUSIONS

GM activation does not correlate with metabolic cost or kinematic variables at intermediate running speeds. Based on these limited results, training of the GM should not be considered when focusing on improving metabolic performance at moderate running speeds. The results of this study will be beneficial to coaches and athletes in developing a training program to improve running performance.

REFERENCES

1. Yokozawa, T., Fujii, N., & Ae, M. (2007). Muscle activities of the lower limb during level and uphill running. *Journal of Biomechanics*, 40(15), 3467–3475.
2. Farley, C. T., Glasheen, J., & McMahon, T. A. (1993). Running Springs: Speed and Animal Size. *Journal of Experimental Biology*, 185(1), 71–86.
3. Alexander, R. M. (1991). Energy-saving mechanisms in walking and running. *The Journal of Experimental Biology*, 160, 55–69.

Table 1: Correlation matrix between muscle activation (integrated EMG) and net metabolic cost at 11km/hr.

Variable	n	M	SD	1	2	3	4	5	6
1. Net Metabolic Cost (Watts/kg)	10	10.13	1.17	-					
2. Biceps Femoris (% MVC)	10	5.05%	2.65%	0.59	-				
3. Gluteus Maximus (% MVC)	10	4.27%	3.03%	-0.08	-0.29	-			
4. Rectus Femoris (% MVC)	10	4.04%	3.20%	0.08	-0.14	0.29	-		
5. Soleus (% MVC)	10	10.95%	6.23%	-0.17	-0.21	-0.10	0.02	-	
6. Tibialis Anterior (% MVC)	10	6.05%	2.47%	0.12	-0.355	-0.13	0.41	0.31	-

Effects of a Total Motion Release (TMR®) Intervention on Asymmetrical Movement Patterns

Martonick, NJP¹ and Bailey, JP¹

¹Department of Movement Sciences, University of Idaho, Moscow, ID USA

email: nmartonick@uidaho.edu

INTRODUCTION

Injuries and their corresponding symptoms (e.g., pain, tightness) have the potential to limit single leg squat (SLS) depth, which may result in a discrepancy between sides [1]. However, the relationship between self-identified factors related to injury and movement symmetry remains unclear. Total Motion Release® (TMR®) is a rehabilitation protocol designed to identify movement asymmetries during a SLS by self-identifying a preferred and non-preferred side through a rating scale for factors such as pain and tightness [2]. The protocol is also theorized to correct imbalances by performing movements on the side contralateral to the symptomatic limb (i.e., the preferred side) [2]. A kinematic and kinetic analysis of the TMR® protocol could provide implications for the importance of symmetrical movement patterns as they relate to symptoms of injury. The purpose of our study was to investigate whether self-identified asymmetries during a SLS corresponded with asymmetrical movement patterns, and whether improving symptoms affected mechanical asymmetries.

METHODS

Twenty participants qualified for the study (10 female, 10 male; age = 24.1 ± 3.5 years; height = 173.8 ± 10.8 cm; mass = 72.0 ± 14.4 kg). Participants were included if they had imbalances between legs ≥ 10 for self-identified ratings on a 0-100-point scale. The leg that had a lower rating was considered the preferred leg. Ratings, and mechanical variables were analyzed at baseline, post treatment, and after a 10-minute wash-out period. Sagittal plane kinematics and internal joint moments at the hip, knee, and ankle were collected with an eight-camera motion capture system (200 Hz) and a force platform (1000 Hz). Eight baseline SLSs were collected on each leg prior to the intervention. The intervention consisted of performing sets of 10 SLSs on the preferred leg. After each participants rated each leg again. Sets were performed until the score equalized between legs or until 4 sets were performed without a resolution of symptoms (difference between legs > 0). Eight more SLSs were collected immediately following the intervention and then 10 minutes after. Separate (2 leg x 3 time) repeated measures ANOVAs were used to assess TMR® scores (traditional ANOVA) and mechanical variables (Statistical Parametric Mapping [SPM] ANOVAs). Significant main effects were followed up with *post hoc* paired *t*-tests and single subject (SS) analyses for the mechanical variables. The significance level was set *a priori* to $\alpha = 0.05$.

RESULTS AND DISCUSSION

Bilateral differences for movement patterns are often masked at the group level due to intraparticipant variability [3]. Using a TMR® scoring protocol, both group and SS analyses found a bilateral difference ($p < 0.01$) for knee flexion (Figure 1), indicating that using objective measures of movement perception successfully dichotomized legs when bilateral differences were present. Following the intervention, TMR®

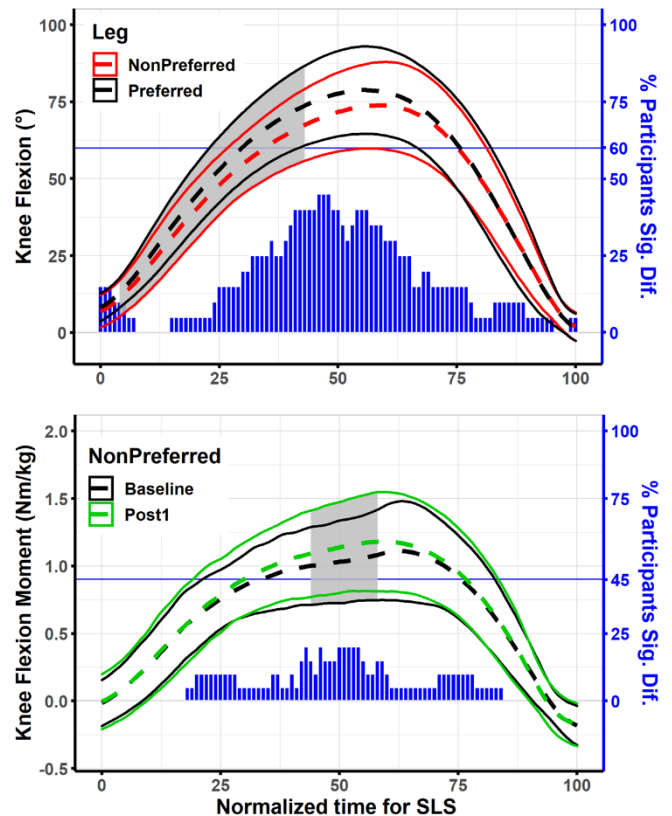


Figure 1: SPM paired *t*-test comparing preferred and non-preferred legs (above) and Baseline-Post1 analyses for the non-preferred leg (below). Shaded gray area indicates where the group waveforms were statistically different. Vertical blue bars indicate the results of the single subjects analyses and percentage of participants with a significant difference at each percentage of the squat. The horizontal blue line indicates the overall percentage of participants with a significant difference for more than 10% of the squat.

scores decreased on the non-preferred leg ($\Delta 15.0$, $p < 0.01$); however bilateral differences were still observed and there was no effect of time for kinematics. However, increased knee flexion moments were found on the non-preferred leg following the intervention ($p < 0.01$, Figure 1). Thus, reducing symptoms allowed participants to perform the SLS using a movement pattern that increased knee joint moments without increasing knee flexion.

CONCLUSIONS

A TMR® intervention could benefit rehabilitation protocols by reducing symptoms related to injury and increasing the ability of patients to load the symptomatic knee. Further investigations are necessary to elucidate the importance of asymmetrical movement patterns.

REFERENCES

1. Houston A, et al. *Clin Biomech* **90**, 238-244, 2021.
2. Miley E, et al. *J Sport Rehabil* **30**, 961-964, 2020.
3. Martonick, et al. *Int J Sport Phys Ther* **17**, 1271-1281, 2022.

EVALUATING FRICTIONAL FORCES AT THE TENDON-IMPLANT INTERFACE WITH AND WITHOUT A LUBRICIOUS NON-FOULING COATING

Ajay Zubin Ratty, Hantao Ling, Ravi Balasubramanian
Oregon State University, Corvallis, OR
ratty@oregonstate.edu

INTRODUCTION

Injury to the cervical spinal cord can lead to incomplete tetraplegia, which can affect various functions in the body's extremities¹. To restore this loss of function, tendon transfer surgeries are commonly conducted. One exemplar procedure used to restore thumb key pinch grasp is the brachioradialis (BR) to flexor pollicis longus (FPL) tendon transfer surgery, which sutures the two tendons together to restore the grasp. However, this procedure only restores 2 kg-f of grasp strength compared to the 9 kg-f produced in a healthy population^{2,3}. With the recent development of novel force-amplifying implants that take advantage of mechanics principles to passively increase force⁴, it is important to consider the physiological reactions the body has to these implants. In this study, we evaluate the frictional forces at the tendon-implant interface between an analogous rabbit forearm tendon and three different surfaces of medical-grade titanium rods, including one uncoated and two coated rods. These non-fouling coatings are designed to improve foreign body integration in biological systems while also adding lubriciousness due to their hydrophobic properties. The two coatings are molecularly identical but are applied to the surface using two different processes. We hypothesize that the two coated rods will see reduced resistance forces and coefficients of friction compared to the uncoated rod.

METHODS

Both extensor digitorum communis (EDC) tendons from a single New Zealand white rabbit ($n = 2$) were excised for use in this study. Each tendon was clamped on either end to Kevlar string and a 5lb Futek load cell and routed through a series of pulleys mounted on a custom testbed developed to measure the frictional forces between the tendon and a titanium rod. One end of the tendon is attached to a precision Faulhaber motor while the other end is connected to a weight that maintains a constant tension in the system. This methodology is based on previous work that utilizes the theoretical relationship between arc of contact, cable tension, and coefficient of friction defined by wrapping a cable around a mechanical pulley⁵. Specifically, the coefficient of friction, μ , is calculated using: $\mu = \ln(F_2/F_1)/\phi$, where F_2 is the tension of the cable pulled away from the pulley, F_1 is the tension of the cable pulled toward the pulley, and ϕ is the arc of contact. The EDC tendon is routed under a titanium rod ($L = 25.4\text{mm}$, $\phi = 3.175\text{mm}$) that imitates the surface of the force-amplifying implant, and the motor was programmed to jog the tendon 10mm at a rate of 1mm/s.

In total each tendon was jogged back-and-forth four times across four loading conditions ($120^\circ+200\text{g}$; $120^\circ+500\text{g}$; $160^\circ+200\text{g}$; $160^\circ+500\text{g}$) and all three titanium rods (Uncoated, Coating 1, Coating 2), for a total of 48 excursions per tendon. The loading conditions are unique combinations of two different arc of contacts with two tension weights that were chosen to imitate best- and worst-case tendon-implant

configurations. Resistance forces are defined as the difference in force readings between the load cells on either side of the tendon and coefficients of friction are calculated using the aforementioned equation.

RESULTS AND DISCUSSION

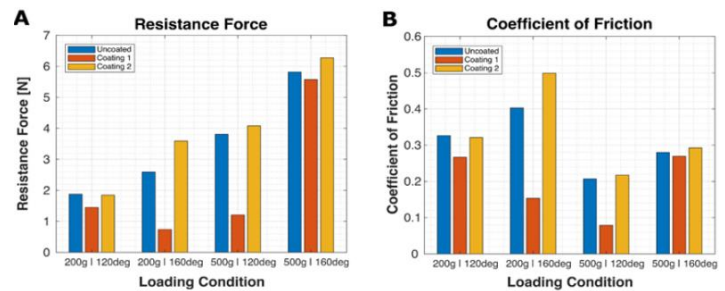


Figure 1: Calculated (A) resistance forces (B) and coefficients of friction for the interaction between rabbit tendon and uncoated and coated titanium rods.

As seen in Figure 1A, resistance force generally increased as loading increased. Coating 1 (0.74N–5.5N) consistently drastically outperformed the Uncoated (1.87N–5.82N) and Coating 2 (1.85N–6.27N) rods in the middle two loading conditions (200g+160° and 500g+120°) and only marginally outperformed the other two conditions at the extreme loading conditions (200g+120° and 500g+160°). In Figure 1B, there was no apparent trend in coefficient of friction as loading increased. However, the same trend appeared comparing the Coating 1 (0.08–0.27) rod with the Uncoated (0.21–0.40) and Coating 2 (0.22–0.50) rods where the Coating 1 rod outperformed the other two conditions marginally in the extreme loading conditions and drastically in the middle two loading conditions. There did not appear to be a significant difference in either resistance force or coefficient of friction between the Uncoated and Coating 2 rods. From this pilot study, Coating 1 always performed either marginally or significantly better in reducing friction compared to both Uncoated and Coating 2 rods. The application process used for Coating 2 appears to hinder the lubriciousness of the coating.

CONCLUSIONS

The friction at the tendon-implant interface plays a significant role in tendon abrasion and the efficacy of a force-amplifying implant. By fully understanding this interaction, we enhance the capabilities of a force-amplifying implant that can advance the field of tendon transfer surgery and improve functional outcomes for patients of spinal cord injury.

REFERENCES

- [1] NIH. (n.d.). *Spinal Cord Injury*, [2] Hamou et al. 2009, JHS; [3] Mathiowetz et al. 1985, APMR, [4] Ling et al. 2019, ORS, [5] Uchiyama et al. 1995, J. Bone Jt. Surg

EVALUATING THE BIOMECHANICAL EFFICACY OF AN ORTHOPEDIC IMPLANT IN AN IN-VIVO RABBIT MODEL

Mockel, Stayce A¹, Bestel, Hans A¹, Balasubramanian, Ravi¹

¹Oregon State University, Corvallis, OR

email: mockels@oregonstate.edu

INTRODUCTION

Our lab has developed an orthopedic implant for individuals who have suffered a C5-C8 spinal cord injury. The implant, when used in tendon-transfer surgery, improves hand function by modifying the transmission of forces. The implant is passive and creates a differential (swiveling) mechanism which enables the distribution of movement from one muscle across multiple output tendons, even as the fingers driven by the output tendons adapt to external contact constraints during grasping [1]. As with any implant, there will be a foreign body response. This foreign body response could encapsulate the implant, tendons, and surrounding tissues in scar tissue. This in turn may limit the implant's functionality. To determine our implant's efficacy in the presence of a foreign body response, we conducted a three-week live animal survival trial, implanting the implant between tendons I/II and III/IV of the extensor digitorum communis (EDC) tendon bundle of the New Zealand white rabbit with varying suture protocols [2]. Prior work had shown one suture loop per implant suture hole to be unreliable, with the suture failing in previous trials. Following the implantation period, we validated the efficacy of the implant-tendon construct to create differential action by comparing it against the non-implanted contralateral leg.

METHODS

A pilot study was conducted with n=2 rabbits implanted with the implant. For rabbit 1, the implant was secured to tendons with one suture loop through each available suture hole on the implant. Rabbit 2 had two suture loops through each of the suture holes. The rabbits were implanted for three weeks. Throughout the first week, the rabbits had bandage changes daily and were maintained in their cages. During the second week, the rabbits no longer received bandages and were allowed some time daily to move about in a larger pen. In the third week, the rabbits participated in daily passive range of motion exercises and continued to exercise in the larger pen. Following euthanasia, a biomechanical test was performed using a custom test bed to quantify the efficacy of the implant (Figure 1). The test bed measures force and displacement of the EDC tendons for translational and rotational movements. Translational movement was achieved using springs on both distal tendon bundles while weight was applied proximally to the EDC muscle with a preload of 0.57 N then in the following increments: five 0.2 N, three 0.5 N, three 1.0 N, and one 2.0 N. Rotational movement was achieved using a spring on just one tendon bundle and again applying weight proximally with a preload of 0.57 N then in the following increments: five 0.2 N, three 0.5 N, and two 1.0 N. Three trials were conducted each for translation and rotation for the implanted and contralateral limb of each rabbit. Data from the implanted leg was then compared to the contralateral.

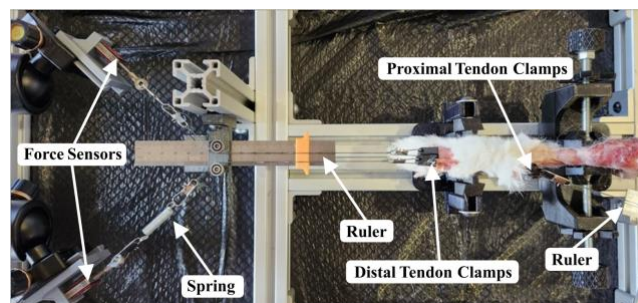


Figure 1: Biomechanical test bed used to quantify the efficacy of the implant with key features labeled. Test bed is currently shown in the rotation configuration, with a spring on one distal tendon pair.

RESULTS AND DISCUSSION

Results from the pilot study found that the implant had remained secured to the EDC tendons successfully and fibrosis had formed around the implant site in both rabbits. The amount of fibrosis was seen to be larger in rabbit 2, with the increase in suture eliciting a larger foreign body response. For rabbits 1 and 2, there was no significant difference in the force to create movement between the implanted and contralateral leg. For rabbit 1, the force ratio between tendon bundles I/II and III/IV was found to be 37% higher in the implanted case until 1 N of added weight and 26% higher overall across all weight increments. This shows that the implant increased the force balance between the tendon bundles during rotation. In rabbit 1, the implanted case was found to have an 113% improvement in the differential action between tendon bundles. For rabbit 2, the force ratio between the tendon bundles was negligible and the implanted case was found to have a 19% improvement in the differential action between tendon bundles. This difference in rabbit 2 was likely due to the increased foreign body response inhibiting implant functionality.

SIGNIFICANCE

These preclinical trials continue to advance the development of an orthopedic implant that will allow for improved hand function for individuals experiencing C5-C8 spinal cord injuries. This work develops the New Zealand white rabbit model for research applications, specifically with tendons. Additionally, this work expands on rehabilitation practices and surgical methods in the rabbit model.

REFERENCES

- [1] Mardula KL, et al. *HAND*. 2015;10(1):116-122.
- [2] Lindsay EJ, et al. *J Hand Surg Glob Online*. 2022;4(1): 32-39

MEASURING NATURAL DIVING KINEMATICS

Liu, A¹, Phillips HS¹, Jean-Sébastien Blouin¹, Crompton, PA², Siegmund, GP^{1,3}

Schools of ¹Kinesiology, and ²Biomedical Engineering, University of British Columbia, Vancouver, BC, Canada

³MEA Forensic Engineers & Scientists, Richmond, BC, Canada

Email: alexllz@student.ubc.ca, web: <https://kin.educ.ubc.ca/>

INTRODUCTION

Diving headfirst into a body of water is a popular recreational activity with a high risk of catastrophic injury if the water is too shallow. Indeed, spinal injuries from diving accidents account for over 75% of recreation-related acute spinal cord lesions¹. The most common site of injury includes the C5-C7 vertebrae, with teardrop and burst fractures, subluxation, and unilateral or bilateral facet dislocation of cervical vertebrae^{2,3}. Severe diving injuries can result in quadriplegia⁴ and come with significant social and economic costs².

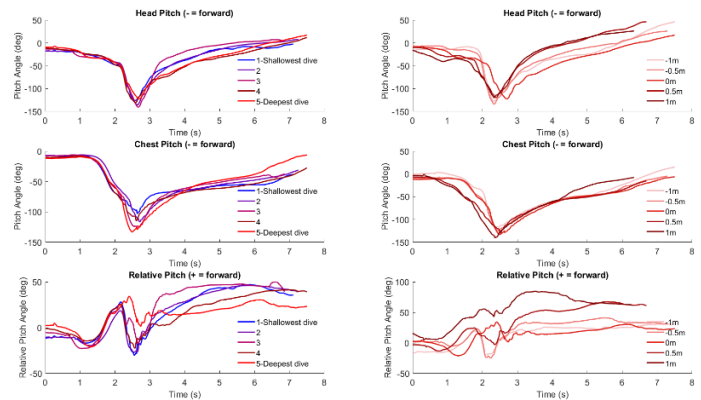
Currently there are few studies that quantify human diving motion² and no studies that quantify head-neck alignment at various dive depths across a wide range of dive trajectories. In this preliminary study, we sought to measure the 2D kinematics of recreational divers and quantified head, neck, and body postures over a range of dives (from shallow to deep dives) initiated from different initial heights relative to the water surface.

METHODS

The diving study was approved by UBC's Clinical Research Ethics Board and was conducted in a deep-water dive tank for participant safety. Three high-speed video cameras filming at 120 fps were situated above (one camera) and below (two cameras) the water to capture right lateral views of the dives. The two underwater cameras were mounted on custom-machined frames and they were 2.2 meters deep and 2.6 meters apart. The above water camera was located 2.2 meters lateral to the dive platform. Together the cameras have – amount of field of view and was able to capture a dive spanning 7m from the highest starting height (1m).

Two IMUs recording at 120 Hz were placed under the external occipital protuberance and over the midpoint of the sternum to capture head and torso motion. Circular marker with a diameter of 18 mm were drawn directly on the participants' skin and on their swim cap using skin-safe, waterproof markers for video digitization and kinematics analysis. The markers were located over the bony landmarks of head, torso, shoulder, wrist, elbow, hip, knee, and ankle. Participants performed 10 dives at each of 5 different heights (total 50 dives), starting from -1m (hip deep in water) increasing in 0.5 m increments to 1m above water. Participants were instructed to start with their shallowest dive and incrementally increase dive angle to almost vertical across 5 dives, then decrease dive angle from vertical for the next 5 dives.

RESULTS AND DISCUSSION



Left figure illustrates the head and chest angle across different dives at deck level (0m). Head angles are relatively unchanged, but chest forward pitch increased as dive angle increased. Right figure shows the head and chest angles of the deepest dives across various starting heights. Head angle is relatively consistent, and chest forward pitch increased as starting height increased.

Complete data analysis in the near future will examine head and torso velocities along with angles at i) water entry, and ii) depths where diving injuries occur as a function of dive angles together with starting heights. Depth-dependent impact conditions can be estimated, and predicting impact kinematics from initial dive conditions becomes possible with this data.

CONCLUSION

This study will provide a comprehensive dataset from which the complex relationship between dive speed and dive depth can be developed. These data can be used to provide better evidence-based recommendations regarding safe water depths for swimming pools and can also provide key posture and kinematic data for developing computation models to better catastrophic spinal injuries during diving, and ultimately prevention of them.

REFERENCES

1. Blanksby BA, et al. *Sports Medicine*, 23(4), 228-246, 1997
2. Boriis PY, et al. *European Spine Journal*, 19(4), 552-557, 2010.
3. Aito S, et al. *Spinal cord*, 43(2), 109-116, 2005
4. Stuhler M, et al. *Injury*, 2023

ACKNOWLEDGEMENTS

The authors thank Mr. Jeff Nickel and Mr. Mircea Oala-Florescu for building the dive platform and calibration rig, and for assisting with data collection and digitizing.

MECHANICAL CHARACTERIZATION OF PAVLIK HARNESS STRAPS

Mead, SL¹, Mannen, EM¹

¹Department of Mechanical and Biomedical Engineering, Boise State University, Boise, ID

Email: sabrinamead@u.boisestate.edu

INTRODUCTION

The Pavlik Harness is the most used treatment for developmental dysplasia of the hip (DDH) in infants. The harness holds the infant's hips and knees in flexion and the hips in abduction, it is believed that this position encourages hip reduction in dislocated or subluxated hips. The reported success rates range from 45% to 100% [1]. When failures in treatment occurred, it was found that the most common cause was improper fitting by the orthopedist or by using poor-quality construction, or both [2]. Due to inconsistent success rates, the absence of modern and repeated experimental methods, and a lack of application procedure, there is a clear need to further investigate the infant body positioning in the harness and the impact that has on DDH treatment. To investigate further we plan to develop a Pavlik Harness that is integrated with various sensors that will be able to measure data such as: kicking force, kicking frequency, strap strain, leg and hip positioning, etc. There is a need to define material properties of the harness to be able to select the appropriate sensitivity of the integrated sensors. Strain data collected from the stirrups will require an understanding of the basic mechanical properties of the strap.



Figure 1: Infant wearing Pavlik Harness

METHODS

To investigate the mechanical properties a cyclic tensile test was performed on the anterior stirrup strap. The strap was prepared by cutting it free from a large sized Pavlik harness. The initial length and width of the strap was 232mm and 21mm respectively. The testing setup consisted of an Instron 5542 test frame equipped with a 500N load cell. The strap was clamped at both ends using Instron 2710-004 Screw Side Action Grips (Fig. 2). The grip was chosen to ensure clamping force was evenly distributed along the width of the strap. The strap was subjected to a 5N tensile preload and then cyclically loaded at a rate of 0.5mm/sec until a maximum load was achieved followed by unloading at the same rate for 100 cycles. Three different conditions were tested based on the hook and loop setting of the harness: (i) the shortest setting, (ii) the intermediate setting, and (iii) the longest setting. The three conditions were pulled 100 cycles each and then the max load was increased by increments of 10N. The max loading increments were: 10N, 20N, 30N, and 40N. These conditions were tested consecutively on a single strap at room temperature. The force and displacement data were recorded during testing and was analyzed using a custom MATLAB program. The program analyzed the data to compare the creep behavior of the strap under these three conditions. The creep

displacement was calculated as the difference between displacement at the end of each cycle and the creep rate was calculated as the ratio of creep displacement to the time interval of each cycle.

RESULTS AND DISCUSSION

The testing does show that the straps do experience a small amount of creep during the initial loading cycles, however 90% of the total creep was achieved in less than 25 cycles regardless of the maximum force being applied. This suggests that the straps experience a “pre-conditioning” period and then stop creeping. The overall creep experienced by the strap ranged from 1.5mm to 8mm (the smallest creep corresponding to the smallest max load). This produces strain values 0.64% to 3.45%. These values are very small and measuring the strains experienced by the stirrup straps will require somewhat sensitive sensors that can expand to approximately 10cm. It was also found that the straps do not experience strictly linear-elastic deformation while in tension. Characterizing this non-linear behavior is important for data analysis of the sensor data in the future.

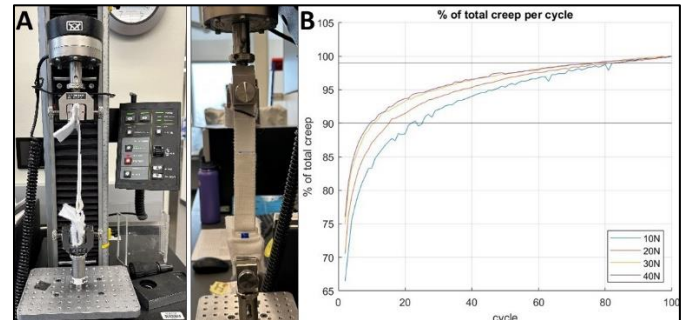


Figure 2: (A) Cyclic tensile test setup using Instron testing frame. (B) 90% and 99% of total creep compared for four max loading conditions. Pre-Conditioning of 25 cycles accounts for at least 90% of total creep deformation in strap.

CONCLUSIONS

The straps of the Pavlik Harness do not experience large quantities of creep, but do exhibit an initial stretching pre-conditioning period of about 20 cycles. The strains produced from testing were less than 5% but had a max stretch of 8mm. This criterion will be used to select appropriate sensors to embed in a smart Pavlik Harness. The straps exhibit consistent non-linear elastic behavior, this should be noted for data analysis in the future. While this testing was beneficial for selection of a strain sensor a multitude of other material properties should be investigated to aide in the design and selection of sensors for a smart Pavlik harness.

REFERENCES

1. Gargan K, et al. *Journal of Children's Orthopaedics*, (2016), 289-293, 10(4).
2. Mubarak S, et al. *Journal of Bone and Joint Surgery – Series A*, 1239-1248, 63(8), 1981.

EFFECTS OF SIDE LOAD CARRIAGE ON LIMB LOADING AND UNLOADING IN TRANSTIBIAL AMPUTEES

Ardianuari, S^{1,2}, Cyr, KM², Neptune, RR³ and Klute, GK^{1,2}

¹Department of Mechanical Engineering, University of Washington, Seattle, WA

²Center for Limb Loss and MoBility, Department of Veterans Affairs, Seattle, WA

³Walker Department of Mechanical Engineering, The University of Texas at Austin, Austin, TX

email: satria@uw.edu

INTRODUCTION

Lower limb amputees are at elevated risk of developing musculoskeletal injuries in their intact limb due to increased limb loading while walking [1] and running [2]. Transtibial amputee (TTA) fallers demonstrate a larger intact limb unloading rate, exposing the prosthetic limb to higher forces during single support [3]. In general, TTAs often experience increased anteroposterior and vertical ground reaction forces (vGRF) in their intact limb compared to the prosthetic limb [4]. Carrying a load during TTA gait may exacerbate the asymmetrical limb loading and unloading, depending on which side, prosthetic or intact, the load is carried.

The aim of this study was to examine the limb loading rates (LR) and unloading rates (ULR) in TTAs while carrying a side load. It was hypothesized that TTAs would exhibit significant differences between LR_{int} (intact limb) and LR_{pro} (prosthetic limb), and between ULR_{int} and ULR_{pro} within each condition. (i.e., no load, intact side load, prosthetic side load). A second hypothesis was that there would be a significant difference in LR_{int}, LR_{pro}, ULR_{int}, and ULR_{pro} between load conditions.

METHODS

Twelve TTAs (2 female), aged 46±15 yr, weighing 96.3±16.7 kg, and with an average height of 1.8±0.1 m, provided informed consent to participate in this institutional review board-approved study. Subjects wore a study provided, passive-elastic prosthetic foot (Sierra; Freedom Innovations, Irvine, CA) and carried a load of 13.6 kg (30 lbs) for the side load conditions.

Each subject walked overground at their self-selected speed with no load, load on their prosthetic side, and load on their intact side across 5 embedded force plates (AMTI, Watertown, MA). A motion capture system (Vicon, Oxford, GBR) recorded ground reaction force (GRF) data at 1,200 Hz.

The GRF data included peak anteroposterior braking (BkF) and propulsion (PrF) forces, and vGRF. The leading limb vGRF were analyzed using MATLAB software (Mathworks, Natick, MA) to calculate LR and ULR (Fig.1). All data were normalized by subject's bodyweight (all conditions) and side load (intact and prosthetic side load conditions). Statistics were analyzed in R (RStudio, Boston, MA), by performing the *t*-test/Wilcoxon test, and mixed-effects linear regressions.

RESULTS AND DISCUSSION

No significant differences were observed between LR_{int} and LR_{pro}, or between ULR_{int} and ULR_{pro} within each load condition. Further, LR_{int}, LR_{pro}, ULR_{int}, and ULR_{pro} were each not significantly different between load conditions. Our null results led to a secondary analysis of other GRF data (i.e., BkF and PrF), and we found that compared to the prosthetic limb,

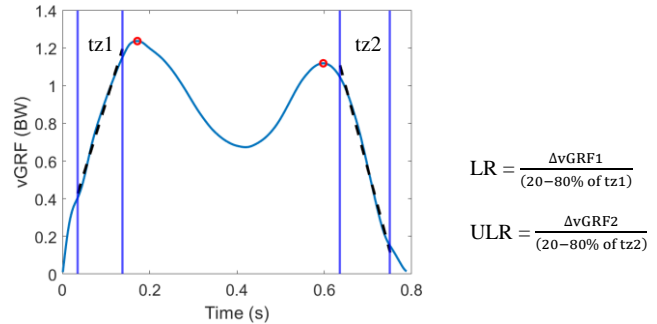


Fig. 1: Loading period (tz1) occurs from heel strike to the 1st peak vGRF (0-100% tz1). LR is the slope of vGRF over a 20-80% time window of tz1. Unloading period (tz2) occurs from the 2nd peak vGRF to toe-off (0-100% tz2). ULR is the slope of vGRF over a 20-80% time window of tz2.

subjects exhibited higher BkF_{int} and PrF_{int} within each load condition while no significant differences were found between load conditions (Fig.2). No change in LR or ULR whether carrying no load, an intact-side, or a prosthetic-side load suggests that TTAs quickly adapted their gait to accommodate the loads without altering their limb loading. Our results suggest that side load carriage may have an insignificant effect on limb loading and unloading distribution.

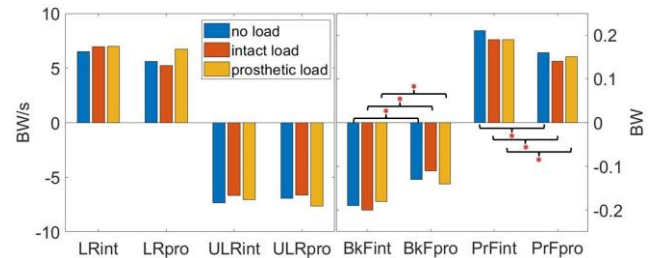


Fig. 2: Left: LR and ULR (BW/s), and Right: BkF and PrF (BW) for each limb and load condition. *Significant difference between limbs (int vs. pro) within each load condition ($p < 0.05$).

CONCLUSIONS

Despite the peak braking and propulsive force being significantly higher in the intact limb compared to the prosthetic limb, carrying a side load did not appear to exacerbate the asymmetrical limb loading and unloading rates in TTAs.

REFERENCES

- Esposito et al. *Clin. Biomech* **30**, 1049-1055, 2015.
- Hobara et al. *Gait Posture* **39**, 386-390, 2014.
- Vanicek et al. *POI*, **34**, 399-410, 2010.
- Sanderson et al. *Gait Posture* **6**, 126-36, 1997.

ACKNOWLEDGEMENTS

Funding from the VA-RR&D Service (RX003138&RX002974) and a 2022 OPERF Fellowship.

SURFACE, BUT NOT AGE IMPACT LOWER LIMB JOINT WORK DURING WALK AND STAIR ASCENT

Wenzel, TA¹, Hunt, NL¹, Holcomb, AE², Fitzpatrick, CK², Brown, TN¹

Departments of ¹Kinesiology, and ²Mechanical and Biomedical Engineering, Boise State University, Boise, ID, USA

email: thomaswenzel@u.boisestate.edu

INTRODUCTION

Older adults (> 65 years) often fall when navigating a challenging slick or uneven surface [1]. During locomotor activities, such as walk or stair ascent, older adults exhibit unfavorable lower limb biomechanical changes, including diminished joint torque and power, and proximal mechanical work redistribution that may increase their fall risk [2,3]. Yet, it is currently unknown whether traversing a challenging slick or uneven surface exacerbates older adults' unfavorable lower limb work and power changes. We hypothesize that older adults will produce less limb and joint work, but greater proximal contribution to walk and ascend stairs; while all participants (young and older) will increase proximal joint work contribution when navigating a challenging surface.

METHODS

Twelve young (18 to 25 years) and 12 older (> 65 years) adults performed a walk and stair ascent task on a normal, slick, and uneven surface. Participants either walked through the motion capture volume or stepped up a set of stairs (18.5 cm rise) at a self-selected pace striking the force platform or target stair with their dominant limb. The slick surface consisted of a wood panel covered by a smooth, plastic material fixed atop of the force platform or stairs, while the uneven surface consisted of a wood panel composed of nine painted wooden blocks of differing heights fixed atop the force platform or stairs. Participants performed three walk and stair ascent trials over each surface.

For each walk and stair ascent trial, synchronous 3D marker trajectories and GRF data were collected using ten high-speed optical cameras (240 Hz, Vantage, Vicon Motion Systems LTD, Oxford, UK) and a single force platform (2400 Hz, OR6, AMTI, Watertown, MA). For each trial, the marker and GRF data were lowpass filtered (12 Hz, 4th order Butterworth), and processed in Visual 3D (C-Motion, Rockville, MD) to obtain lower limb sagittal plane joint power. Then, limb, and hip, knee and ankle positive mechanical work and each joint's percent of contribution to total limb work (joint work divided by limb work and multiplied by 100) were determined.

Stance phase positive limb and joint work, and relative joint work were submitted to statistical analysis. Two-way mixed model ANOVAs tested main effects and interaction between age (young and older adults) and task (walk and stair ascent), age and surface (normal, slick, and uneven) for each task. Alpha level was < 0.05.

RESULTS AND DISCUSSION

Ascending the stairs required greater positive limb, and hip, knee, and ankle work than walking (all: $p < 0.001$; Fig. 1). Participants increased hip contribution 37% to total positive work during the walk ($p < 0.001$), and knee contribution 48% during the stair ascent ($p < 0.001$). This increased contribution

by the knee musculature to lift the center of mass up during the ascent task may accelerate muscular fatigue and increase likelihood of a fall, particularly for the older adults.

In partial agreement with our hypotheses, surface, but surprisingly not age, impacted positive limb work. When walking over a challenging surface, limb ($p < 0.001$), hip ($p = 0.010$), and knee ($p < 0.001$) positive work increased. Specifically, limb and knee work increased on the uneven, and hip work increased on the uneven and slick surfaces. Hip ($p = 0.015$), knee ($p < 0.001$), and ankle ($p = 0.010$) work increased when navigating the challenging surfaces during the stair ascent. Hip and ankle work were greater on the slick surface, while knee work increased when ascending stairs with an uneven surface. The instability of the challenging surfaces may require greater contribution from large hip and knee musculature to maintain stability, and forward or vertical propulsion. In fact, navigating the challenging surfaces lead to approximate 9% and 4% decrease in percent ankle contribution to total work during the walk and stair ascent; but, an approximate 4% increase in hip during walk and a 6% increase in knee contribution during the stair ascent and both tasks.

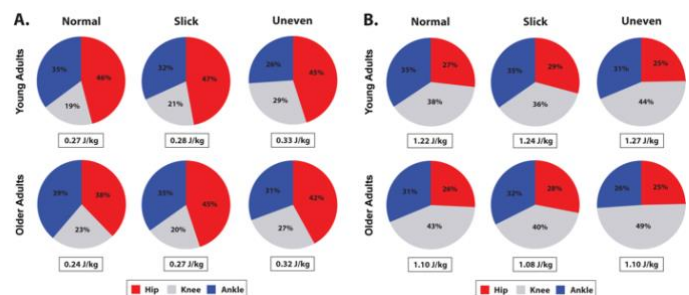


Fig. 1. Limb positive work (J/kg), and hip (red), knee (gray), and ankle (blue) contribution to total limb work for young and older adults during the walk (A) and stair ascent (B) task on each surface (normal, slick, uneven).

CONCLUSIONS

Ascending stairs required more positive work than the walk, particularly from the knee, which may increase fall risk. Yet, both walking and ascending stairs over a challenging surface required more, proximally distributed work. The increased contribution from the large proximal musculature may be necessary to maintain stability on the challenging slick and uneven surfaces but may accelerate fatigue, increasing fall risk.

REFERENCES

1. Li et al. *Am J Public Health* **96**, 2006.
2. DeVita et al. *J Appl Physiol* **88**, 2000.
3. Franz et al. *Gait Posture* **39**, 2014.

ACKNOWLEDGEMENTS

NIH Institute on Aging (R15AG059655) supported this work.

EFFECTS OF CHANGING HIP POSITION ON SCAPULAR KINEMATICS

Schlittler, S^{1,2}, Suprak, D¹, Brilla, L¹, San Juan, J¹

¹Department of Health and Human Development, Kinesiology, Western Washington University

²email: pines2@wwu.edu, web: <https://chss.wwu.edu/health-human-development/pines2>

INTRODUCTION

Seated versus standing posture is known to affect scapular kinematics, activation of the rotator cuff muscles is known to affect the function of the glenohumeral joint, and fascia is known to affect force production [1-5]. However, the effects of these attributes have yet to be directly applied to shoulder function as a result of hip position. Therefore, the purpose of this study is to determine the effect of ipsilateral and contralateral hip position on scapular kinematics.

METHODS

The study population includes 24 college-aged males (n=12) and females (n=12) with an average height of 170.94 ± 8.84 cm and an average mass of 73.55 ± 11.61 kg. The subjects were physically active with an average activity level of 2.40 ± 2.09 days per week of strength training and 2.76 ± 2.14 days per week of cardiovascular training. Subjects were recruited via flyer and word of mouth. Following a screening questionnaire and informed consent signing, subjects were included in the study. Exclusion criteria included individuals experiencing pain or who had current or recent shoulder or hip injury and those with tight hip flexors.

Scapular kinematics, of the dominant arm were measured using the Polhemus FasTrak electromagnetic tracking system collecting at 40 Hz, in conjunction with a custom LabVIEW script. Polhemus sensors were placed on the thorax, the upper arm (deltoid tuberosity), and the scapular spine of the dominant arm.

Subjects' shoulders were placed in the scapular plane (30-40 degrees from the frontal plane) and a rod was used to ensure the subject maintained this motion within the scapular plane. For each condition, the subject was asked to elevate the arm to approximately 180° and back down to neutral (arm at the side) for three repetitions. The four study conditions were pre-randomized: (1) bilateral hip extension (standing) (2) bilateral hip flexion (seated), (3) seated unilateral hip flexion- the subject performed a lunge (such that the ischial tuberosity of the ipsilateral hip was on the chair); and (4) seated unilateral hip flexion- the subject performed a lunge (such that the ischial tuberosity of the contralateral hip was on the chair).

Two-way ANOVAs were used to evaluate effects of shoulder elevation and condition on scapular upward rotation (UR), posterior tilt (PT), and external rotation (ER).

RESULTS AND DISCUSSION

For ER, there was no significant interaction ($F[60, 1380] = 0.889, p = .714$) and no main effect of elevation ($F[1.207, 27.751] = 0.320, p = .618$) or condition ($F[3,69] = 1.019, p =$

.390). For PT (Fig. 1), there was no significant interaction ($F[60,1380] = 0.899, p = .693$), but significant main effects of

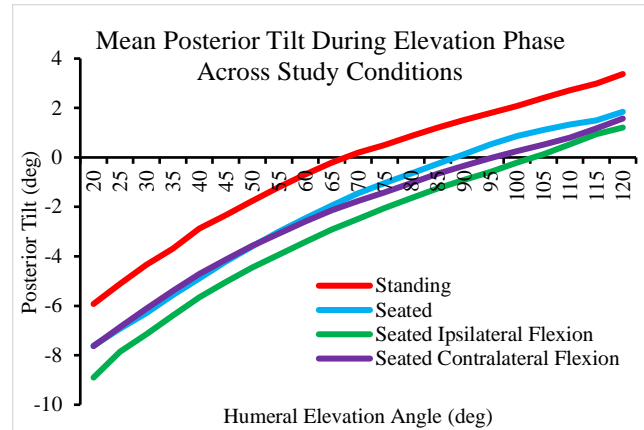


Figure 1: Mean posterior tilt (measured in degrees, deg), during arm elevation (measured in degrees, deg), for all four study conditions.

elevation ($F[1.367,31.439] = 45.45, p < .001$) and condition ($F[3,69] = 7.779, p < .001$), with the greatest PT in standing. For UR, there was no significant interaction ($F[60,1380] = 0.896, p = .698$), a significant main effect of elevation ($F[1.534,35.293] = 657.614, p < .001$), and no significant effect of condition ($F[3,69] = 0.439, p = .726$).

REFERENCES

1. Kanlayanaphotporn, R. Changes in sitting posture affect shoulder range of motion. *Journal of Bodywork and Movement Therapies*, **18**(2), 239-243, 2014. doi:10.1016/j.jbmt.2013.09.008
2. Schleip, R., Klingler, W., & Lehmann-Horn, F. Active fascial contractility: fascia may be able to contract in a smooth muscle-like manner and thereby influence musculoskeletal dynamics. *Medical hypotheses*, **65**(2), 273-277, 2005. doi:10.1016/j.mehy.2005.03.005
3. Thigpen, CA, et al. Head and shoulder posture affect scapular mechanics and muscle activity in overhead tasks. *Journal of Electromyography and Kinesiology*, **20**(4), 701-709, 2010.
4. Terry, GC, and Chopp, TM. Functional anatomy of the shoulder. *Journal of athletic training*, **35**(3), 248, 2000.
5. Yucesoy, CA, et al. Effects of inter-and extramuscular myofascial force transmission on adjacent synergistic muscles: assessment by experiments and finite-element modeling. *Journal of biomechanics*, **36**(12), 1797-1811, 2003. doi:10.1016/S0021-9290(03)00230-6

EVALUATING EXISTING TRANSTIBIAL AMPUTEE MUSCULOSKELETAL MODELS FOR USE ON FEMALE POPULATIONS: A SYSTEMATIC REVIEW

Carswell, TMR¹, Hasan, M¹ and Giles, JW¹

¹Department of Mechanical Engineering, University of Victoria, Victoria, BC Canada
email: tmrc@uvic.ca, web: <https://gileslab.wixsite.com/uvicbiomech>

INTRODUCTION

Transtibial amputees (TTAs) have become a population of interest in the computational musculoskeletal (MSk) modeling community [1]. Most studies use a generic MSk model linearly scaled to match the subject's anthropometrics [2]. Despite their prevalence, generic models can neglect innate variations between distinct groups. For example, while sex differences exist in MSk geometry and musculotendon parameters [3], most generic models were developed using predominantly male data [4,5], affecting their validity to study female populations. Therefore, when choosing a model, it is important researchers are aware of the data used to develop and validate it. This work presents a systematic review of existing open-source TTA models, aiming to help guide researchers when choosing an MSk model. Existing models were also evaluated to determine the model most representative and capable of reproducing female TTA biomechanics. This model will be used in future work studying sex differences in amputees.

METHODS

A systematic search of 10 key terms was performed on three online databases (PubMed, Scopus, Web of Science). Eligible studies were retained for review if they presented an open-source, 3D, human MSk model representing a TTA with a generic non-osseointegrated (OI) prosthetic. A database was created based on data detailing the development and validation of the eligible models. The database was then used to evaluate the models on their capability of representing female TTAs based on predefined weighted criteria (Table 1) with scoring scales. Criterion 1 assesses how representative the model development data are of female TTAs. Criterion 2 determines how comprehensive the model's validation was as defined by the MSk Modelling Grand Challenge [6]. Criteria 3 and 5 assess the functionality and motions the model and its prosthesis can accommodate. Criterion 4 evaluates how transparent the model development process was in each study.

RESULTS AND DISCUSSION

The systematic search yielded 352 results. Upon consideration against eligibility criteria, three studies remained: LaPrè et al., Willson et al., and Miller & Esposito [1,7,8]. The database created compiles data for the three models, providing a detailed account of how and with what data each was developed and validated. However, through further investigation of the Miller & Esposito model, it was found to represent an OI prosthetic, making it ineligible for further analyses. Upon evaluation of the two remaining models, the Willson model scored higher against all criteria except Criterion 5. For this criterion, the LaPrè model was able to accommodate more motions than that of the Willson.

CONCLUSIONS

This work presents a systematic review and evaluation of existing open-source TTA models. Data on three models was compiled into a database resource for researchers in future modeling studies. Upon evaluating eligible models, the Willson model was determined the most representative and capable of reproducing female TTA biomechanics. This model will be used in future work studying sex differences in amputees.

REFERENCES

1. Willson AM, et al. *Comp Meth Biomech Biomed Eng* 1-12 2022.
2. Akhundov R, et al. *PLoS One* **17**, 1-16, 2022.
3. Haizlip KM, et al. *Physiology* **30**, 30-39, 2015.
4. Klein Horsman MD, et al. *Clin Biomech* **22**, 239-247, 2007.
5. Hoy MG, et al. *J Biomech* **23**, 157-169, 1990.
6. Fregly BJ, et al. *J Orthop Res* **30**, 503-513, 2011.
7. LaPrè AK, et al. *Int J Num Meth Biomed Eng* **34**, e2936, 2017.
8. Miller RH, and Esposito ER. *PLoS One* **13**, e0191310, 2018.

ACKNOWLEDGEMENTS

Graduate funding for TMRC was provided by NSERC Canada Graduate Scholarships – Doctoral (CGSD).

Table 1: Criteria and weightings used to evaluate eligible models for selection.

Evaluation Criteria	Guiding Questions	Weight (%)
1. Representative of desired population	What were the demographics of subjects used to develop the model?	25
2. Experimentally validated	Was the model validated and if so, how?	25
3. Functionality of prosthesis model	What degrees of freedom and ranges of motion does the prosthetic allow?	12.5
4. Transparency of model development	Were the developers transparent in how they developed the model?	12.5
5. Functionality of overall model	What motion was the model validated for and what motions does it allow?	25

STUDYING SEX DIFFERENCES IN THE PROSTHETIC NEEDS AND PRIORITIES OF LOWER LIMB AMPUTEES BY ADAPTING THE PROSTHESIS EVALUATION QUESTIONNAIRE

Carswell, TMR¹, Monkman, H² and Giles, JW¹

¹Department of Mechanical Engineering, University of Victoria, Victoria, BC, Canada

²School of Health Information Science, University of Victoria, Victoria, BC, Canada

email: tmrc@uvic.ca, web: <https://gileslab.wixsite.com/uvicbiomech>

INTRODUCTION

Despite ~30% of lower limb amputees (LLAs) being female [1], the majority of LLA and prosthetics research is focused on males [2]. Female LLAs also experience different challenges than males, including having a higher risk of osteoarthritis, lower functional abilities, higher prosthesis rejection rates, and greater overall dissatisfaction [3]. A key aspect of early-stage medical device research is consulting with users to understand their specific needs [4]. Therefore, studying sex differences in the prosthetic priorities of LLAs through survey methods may improve understanding of female-specific needs as well as inform the design of sex-specific prosthetics. However, as females have been historically underrepresented or overlooked, most prosthesis questionnaires neglect what may make them different. To this end, we took a user-centered design (UCD) approach to adapting the Prosthesis Evaluation Questionnaire (PEQ) [5] to better capture and assess sex differences in LLA prosthetic needs and priorities.

METHODS

A committee of 5 female LLAs (i.e., prosthesis users) was formed to engage them in developing a modified questionnaire. We met with these users to assess and adapt the original PEQ. In doing so, they contributed to the creation of a modified instrument targeting technical and personal aspects of a user's prosthesis, and sex and gender related topics. In the adapted questionnaire, 7 of the 9 validated PEQ subscales were retained and new questions were added to better target the study's objectives. Closed questions were scored on Likert scales from 1 (negative) to 10 (positive). Results were analyzed using Mann-Whitney U tests in SPSS.

RESULTS AND DISCUSSION

The questionnaire was completed by 18 LLAs (9 female, 9 male). No statistically significant sex differences (i.e., $p < 0.05$) were found in participant demographics, making these good comparative groups. Although no significant sex differences

were found in the validated PEQ subscales, differences were found in individual questions on mobility and psychosocial factors (Table 1). Females expressed a significantly poorer ability to ambulate up or down a steep hill, potentially linking to their prosthetic and functional challenges presented in literature [3]. Additionally, sex-specific challenges related to mobility have major implications for the design of sex-specific prosthetics, particularly in aspects of ankle adjustability and range of motion. Such challenges, among many others, can further impact psychosocial aspects of an amputee's life and can affect males and females differently. For instance, compared to male participants, females were significantly less interested in having children because of their amputation. We plan to explore links between such psychosocial aspects and mobility challenges by triangulating questionnaire findings with those from planned follow-up interviews.

CONCLUSIONS

A UCD approach was taken to modify the PEQ and assess sex differences in LLA prosthetic needs. Female participants expressed poorer ambulation capabilities with their prosthetic compared with males. Sex-specific challenges with LLA mobility emphasize the need for further research addressing sex differences in physical and psychosocial aspects. Such differences have major implications for and can ultimately guide design of sex-specific prosthetics.

REFERENCES

1. Imam B, et al. *Can J Pub Heal* **108**, e374-e380, 2017.
2. Sagawa Y, et al. *Gait Posture* **33**, 511-526, 2011.
3. Randolph BJ, et al. *Mil Med* **181**, 66-68, 2016.
4. Gherardini F, et al. *Int J Adv Man Tech* **91**, 5-8, 2017.
5. Legro MW, et al. *Arch Phy Med Reh* **79**, 931-938, 1998.

ACKNOWLEDGEMENTS

Graduate funding for TMRC was provided by NSERC Canada Graduate Scholarships – Doctoral (CGSD).

Table 1: Select questionnaire results for male and female participants showing 25th percentile, median, and 75th percentile values.

Source	Subscale/Question	Female (n = 9)			Male (n = 9)			p-value
		P25	Median	P75	P25	Median	P75	
PEQ	Ambulation Subscale – overall ambulation ability	4.9	6.0	7.9	6.0	7.6	8.6	$p = 0.171$
PEQ	Ambulation ability up steep hill using prosthetic	2.0	5.0	7.0	5.0	8.0	9.5	$p = 0.033$
PEQ	Ambulation ability down steep hill using prosthetic	1.5	3.0	6.5	4.5	5.0	8.0	$p = 0.045$
New	Effect of amputation on interest in having children	4.0	8.0	10	10	10	10	$p = 0.012$

ACUTE EFFECTS OF A NON-EXHAUSTIVE LONG RUN ON METATARSAL BONE LOADS

McKibben, K, Peach, M, and Becker, J

Department of Health and Human Development, Montana State University
email: katiemckibben1@gmail.com, web: <https://www.montana.edu/biomechanics>

INTRODUCTION

Running is popular activity associated with a high incidence of overuse injury and long-distance runners are especially susceptible. An estimated 79% of long-distance runners will experience an overuse injury in a given year and those who run more than 20 miles per week are at greater risk of a lower extremity injury [1]. In particular, metatarsal stress fractures make up almost 9% of these injuries and runners who experience larger volumes of bone loading may be at a higher risk for developing stress injuries [2]. While the influence of footwear and footstrike pattern on metatarsal loading have been previously reported, it remains unclear how run duration influences metatarsal loads. Therefore, the purpose of this study was to compare changes in metatarsal bone loading at the beginning and end of a long-distance run. We hypothesize that peak plantar stress, peak dorsal stress, and peak midshaft bending moments will increase after completing a long-distance run.

METHODS

Nineteen runners (sex: 12F, 7M; age: 21.57 ± 3.53 years; mass: 70.01 ± 10.79 kg) who average at least 25 miles per week ran a distance equivalent to 25% of their weekly mileage at a self-selected pace on an instrumented treadmill (Treadmetrix, Park City, UT). Whole body kinematics were recorded with a 6-camera motion capture system (Motion Analysis Corp., Santa Rosa, CA), with foot kinematics quantified using a multisegment foot model [3]. Pressure insoles (Tekscan, Boston, MA) were used to quantify forces beneath each metatarsal head. Kinematics, ground reaction forces and plantar pressure measurements were recorded pre and post run.

Metatarsal loads including plantar stresses, dorsal stresses, and midshaft bending moments were calculated using a musculoskeletal model of the metatarsals [4,5]. Variables were assessed for normality using Shapiro-Wilk tests. Paired t-tests were used to compare mean peak loads between the beginning and end of the run.

RESULTS AND DISCUSSION

Post run, peak plantar stresses increased 8% in the second ($p < 0.001$, $d = 0.248$) and 7% in the third ($p < 0.001$, $d = 0.182$)

Table 1. Mean (\pm standard deviation) for measures of metatarsal loading pre and post long-distance run for each metatarsal (met). Negative stress values represent compressive stress. Positive stress values represent tensile stress. * indicates statistically significant difference from pre to post run.

	Peak Plantar Stress (MPa)		Peak Dorsal Stress (MPa)		Peak Bending Moment (Nm)	
	Pre	Post	Pre	Post	Pre	Post
1 st met	101.25 (\pm 33.49)	101.04 (\pm 31.56)	-106.13 (\pm 35.20)	-109.75 (\pm 39.62)	6.74 (\pm 2.23)	6.71 (\pm 2.10)
2 nd met	213.99 (\pm 69.49)	231.99 (\pm 72.42)*	-215.31 (\pm 67.19)	-226.77 (\pm 75.89)*	4.65 (\pm 1.45)	5.02 (\pm 1.56)*
3 rd met	286.39 (\pm 113.31)	308.07 (\pm 124.72)*	-287.42 (\pm 112.91)	-303.66 (\pm 128.09)*	4.93 (\pm 1.94)	5.30 (\pm 2.14)*
4 th met	178.09 (\pm 53.04)	186.82 (\pm 58.12)	-178.56 (\pm 52.87)	-188.25 (\pm 59.03)	3.38 (\pm 1.00)	3.55 (\pm 1.10)
5 th met	111.85 (\pm 37.57)	108.72 (\pm 35.63)	-112.29 (\pm 37.91)	-110.36 (\pm 36.42)	2.91 (\pm 0.98)	2.83 (\pm 0.93)

metatarsals. Peak dorsal stresses increased 5% in the second ($p = 0.029$, $d = 0.160$) and third ($p = 0.012$, $d = 0.135$) metatarsals. Peak midshaft bending moments also increased 8% in the second ($p < 0.001$, $d = 0.245$) and 7% in the third ($p < 0.001$, $d = 0.180$) metatarsals after the run. Mean peak midshaft bending moments, mean peak plantar stresses, and mean peak dorsal stresses were within one standard deviation of previously reported values for these parameters (Table 1) [4,5].

A long-distance run equivalent to many runners weekly long run increases plantar stress, dorsal stress, and midshaft bending moments in the second and third metatarsals. This may be detrimental as the second and third metatarsals are more susceptible to stress fracture in comparison to other metatarsals due to their slim shape and the amount of load experienced during a run [2]. Additionally, the largest increases in stress seen post run were in plantar values. During the stance phase of running gait, the plantar side of the bone is in tension and the dorsal side is in compression. Because cortical bone is weaker in tension than compression [6], a greater increase in plantar stress may be a further indicator of increased bone stress injury risk.

CONCLUSIONS

A non-exhaustive weekly long run can increase metatarsal bone loading parameters in the second and third metatarsals, potentially increasing injury risk.

REFERENCES

1. van Gent et al. *Br J Sports Med* **41**, 469-480, 2007.
2. Chuckpaiwong et al. *Br J Sports Med* **41**, 510-514, 2007.
3. Bishop et al. *Gait Posture* **37**, 552-557, 2013.
4. Gross & Bunch *Am J Sports Med* **17**, 669-674, 1989.
5. Ellison et al. *J. Biomech* **105**, 2020.
6. Hart et al. *J Musculoskelet Neuronal Interact* **17**, 114-139, 2017.

ACKNOWLEDGEMENTS

This study was funded by the Ellen Kreighbaum Movement Science Lab Endowment at Montana State University.

MEASURING PLANTAR TISSUE STIFFNESS WITH THE ULTRASHOE (AN ULTRASOUND EMBEDDED SANDAL)

Ellen Y. Li^{1*}, Scott Telfer^{1,2,3}, Brittney Muir^{1,3}, William R. Ledoux^{1,2,3}

¹RR&D Center for Limb Loss and MoBility (CLiMB), VA Puget Sound, Seattle, WA

Departments of ²Orthopaedics & Sports Medicine, ³Mechanical Engineering, University of Washington, Seattle, WA
email: eli17@uw.edu

INTRODUCTION

Individuals with diabetes mellitus are often at a higher risk for plantar tissue ulceration and subsequently lower limb amputation. Some researchers hypothesize that increased risk is related to changes in plantar tissue properties, leading to increases in plantar tissue stiffness and pressure. Measuring plantar tissue stiffness requires identifying the amount of load applied to a region and subsequent tissue compression. Previous studies that simultaneously measured plantar pressure and compression used either fluoroscopy during gait trials [1], exposing subjects ionizing radiation, or ultrasound but in static conditions by applying a known load to the foot through indentation tests [2]. One study embedded an ultrasound probe into shoes and captured plantar pressure and tissue compression dynamically [3], but pressure sensors covered a large surface area, minimizing the accuracy of the load measurements. The goal of this study was to develop a novel sandal (Ultrashoe) that embeds an ultrasound probe with load cells below it to safely and accurately measure plantar tissue stiffness during gait.

METHODS

A sandal sole was casted with liquid polyurethane plastic (Smooth-On Simpact 60A) in a 3D printed mold. It was designed to contain a forefoot and heel cut-out to hold load cells and an ultrasound probe below the second or third metatarsal head and the calcaneus, respectively (Fig 1A). Adjustable Velcro straps and Dacron padding were incorporated to maximize adherence between the foot and the sandal surface, and to reduce skin irritation (Fig 1B). Four load cells (Model 13, Honeywell) were placed in the forefoot cut-out under an uncased ultrasound probe (SLH20-6, Aixplorer), secured with custom 3D printed parts. A layer of Dacron was used as a thin insole padding and a 0.5mm thick ultrasound gel pad was placed on top of the ultrasound probe and case cover to allow for a consistent imaging interface with the plantar surface (Fig 1C). The ultrasound (SuperSonic Imagine's Aixplorer) was set to its maximum frame rate, 45 Hz, and load cell data was collected through LabVIEW software (National Instruments) at 100 Hz.



Figure 1: Ultrashoe design. (A) Polyurethane molded shoe and straps. (B) Prosthetic foot secured for visual. (C) Ultrashoe with load cells, ultrasound probe, insole liner, and gel pad.

Preliminary data were collected from a male subject with diabetes mellitus. The subject was fitted with a size 11 men's Ultrashoe with an ultrasound probe centered on the second

metatarsal head. An AMTI split-belt treadmill was used for data collection and the speed was set to 0.4 m/s, comparable to his measured unassisted overground walking speed. Once the treadmill reached its target speed, Ultrashoe data were collected for 30 seconds, which included a deceleration phase during the last 5 seconds. Data were synchronized during post-processing and plantar thickness was semi-automatically tracked using a custom script in MATLAB (MathWorks). Plantar tissue force-deformation data were calculated by averaging the loading curves, with the first and last two steps removed. Subsequently, plantar tissue stiffness was determined with a linear regression in the last 30% of the loading curve.

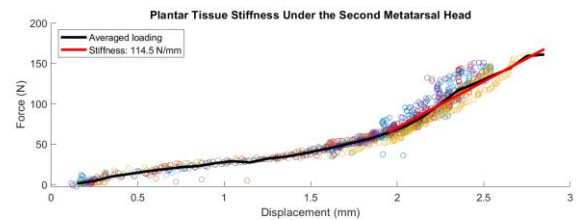


Figure 2: Plantar tissue stiffness under the second metatarsal head.

Loading curves from 11 steps are plotted as unfilled, colored circles with displacement (mm) and force (N) along the x- and y-axis, respectively. Solid lines are used to represent the average loading curve (black) and plantar tissue stiffness within the final 30% of strain (red).

RESULTS AND DISCUSSION

One 30 second walking trial was analysed, and 11 of the 13 steps were used to estimate plantar stiffness (Fig 2). Without filtering, the raw data estimates a plantar stiffness of 114.5 N/mm and elastic modulus of 2.9 MPa. The forefoot stiffness and elastic modulus measured are higher than those reported in other studies [2]. Other studies often used low applied forces (<10N) during indentation tests [2], which would lead to the analysis of only the toe region of loading curve and lower predicted moduli. Additionally, our study may include an initial compression due to shoe strapping, lowering the maximum compressive strain recorded.

CONCLUSIONS

The Ultrashoe allows researchers to measure plantar tissue properties across dynamic gait trials, providing insight on plantar tissue stiffness and strain rate across individuals with or without pathologies affecting plantar tissues.

REFERENCES

1. Wearing, CS, et al., Clin Biomech, 24:397-402, 2009.
2. Klaesner, JW, et al., Arch. Phys. M. 83(12):1796-1801, 2002.
3. Telfer, S, et al., Gait & posture 39(1): 328-332, 2014.

ACKNOWLEDGEMENTS

Funding for this study was provided by NIH grant AR072216-01 and VA award A3539R. Preliminary research was conducted by Tony Huynh.

MACHINE LEARNING METHODS FOR FACILITATING ANALYSIS OF KANGAROO RAT HOPPING

Ozanich, NR¹, Tamakloe, VT¹, McGowan, CP³ and Lin, DC^{1,2}

¹Voiland School of Chemical Engineering and Bioengineering; ²Department of Integrative Physiology and Neuroscience Washington State University, Pullman, WA; ³Dept. of Integrative Anatomical Sciences, University of Southern California
email: nicholas.ozanich@wsu.edu

INTRODUCTION

Markerless pose estimation software (e.g., DeepLabCut [1]) has made extracting kinematics from video much faster than manual labeling. We have successfully extracted kinematics from videos of kangaroo rats hopping and we are interested in ways to automatically label the gait cycle to facilitate our research questions. Here, we explore using B-SOiD [2] for unsupervised clustering and classification of kangaroo rat hopping kinematics obtained from our trained DeepLabCut neural network.

METHODS

Previously, we collected videos of kangaroo rat hopping on a custom designed circular treadmill on which we can use different substrates and obstacles (e.g., sand and rocks) [3]. We employed DeepLabCut to train a neural network (MobileNet v2_1.0 with average test error of 4.14 pixels with a p-cutoff of 0.6) to track anatomical landmarks on the kangaroo rats. The videos were collected in short timeframes where kangaroo rats were hopping.

We used the B-SOiD Streamlit interface to fit the random forest classifier on multiple videos from a single kangaroo rat hopping. Another video of a different animal was used to validate performance. We used body markers and the first three tail markers to detect the hop cycle (Figure 1). The output labels, corresponding to the low-dimensional clusters (Figure 2), were qualitatively interpreted by the authors. Videos were manually labeled to track the frames where key events (takeoff, landing) or behaviors (bipedal, quadrupedal gait) occurred. This allowed for a quantitative assessment of how accurate B-SOiD was at assigning each frame to a cluster that clearly represented the identified behavior.

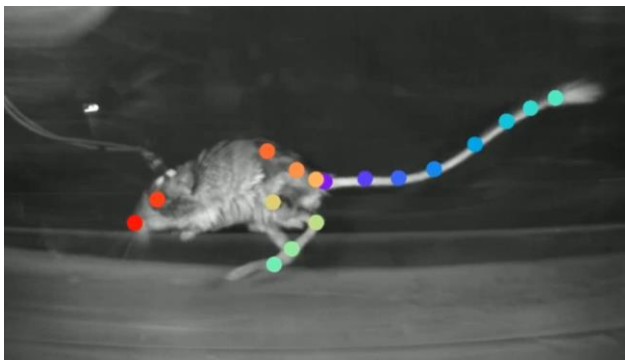


Figure 1: Screenshot from a video generated using DeepLabCut. Predicted locations of various body parts are superimposed on top of the input video.

RESULTS AND DISCUSSION

From our preliminary analysis of using B-SOiD, we found that several clusters often represented the same behavior. More analysis needs to be done to determine if this is an artifact of

clustering cyclic data, or perhaps is representative of a spatial, temporal, or behavioral feature that was overlooked during our qualitative analysis. We grouped together clusters that solely represented takeoff and landing, respectively. We found that takeoff was correctly clustered for 95% of occurrences for the video that the classifier was fit on and 78% for the video that the classifier was not fit on. Landing was correctly clustered 93% of occurrences for the video that the classifier was fit on and 98% for the video that the classifier was not fit on. We are currently analyzing more data and determining if B-SOiD can distinguish bipedal and quadrupedal gait as well as hopping on flat terrain versus variable terrain. Additionally, we will compare performance of B-SOiD to supervised methods.

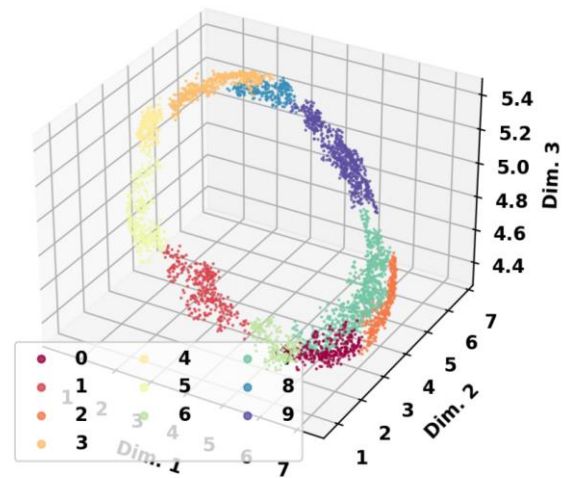


Figure 2: Generated in B-SOiD Streamlit app. Shown are all kinematic data from one kangaroo rat in a reduced dimension space (Note: the lower dimensional space was 6D, 3D is shown for interpretability). Cluster assignment from HDBSCAN and the labels are shown. Takeoff clusters are 5,4,1. Landing clusters are 9,7,2. Other clusters represent stance and swing phases.

CONCLUSIONS

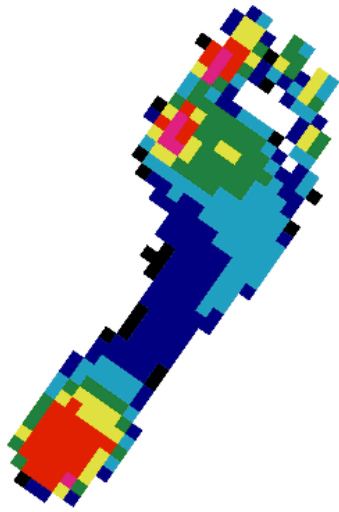
Advancements in the capabilities of machine learning and computer vision research have enabled new methods for automating processes to facilitate large-scale analysis. Extracting context from kinematics is an active research field that we explore here.

REFERENCES

1. A. Mathis et al., *Nature Neuroscience*, 21(9), 2018.
2. AI. Hsu and EA. Yttri, *Nature Communications*, 12(1), 2021
3. Hall et al., *Royal Society Open Sci*, 9(2), 2022.

ACKNOWLEDGEMENTS

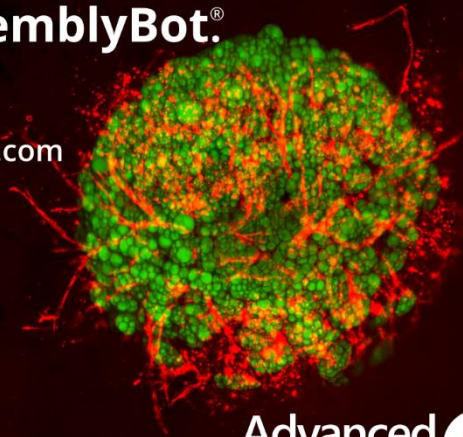
Work supported by NSF grant #2128545.



novel

Unleash the investigative power of
3D Biology through automation
with **BioAssemblyBot®**.

learn more:
AdvancedSolutions.com



Advanced
SOLUTIONS 